

Modeling of Organic Solvent Nanofiltration: A Study of the Parameters which Affect Permeation Properties

Dissertation

zur Erlangung des akademischen Grades
Doktor der Ingenieurwissenschaften
(Dr.-Ing.)
der Technischen Fakultät
der Christian-Albrechts-Universität zu Kiel

Daniel Fierro

Kiel
2009

1. Gutachter: Prof. Volker Abetz

2. Gutachter: Prof. Jörn Mosler

3. Gutachter: Prof. Klaus Rätzke

Datum der mündlichen Prüfung: 11.11.2009

Table of Contents

Table of Contents	i
List of Tables	v
List of Figures	vii
List of Symbols	xiii
Latin letters	xiii
Greek letters	xvii
Subscripts	xviii
Chapter 1. Introduction	1
Chapter 2. Theoretical Background	5
2.1 Physical properties	5
2.1.1 Volumetric properties	5
2.1.2 Flory-Huggins-Staverman phase equilibria solution theory	7
2.1.2 Activity coefficients	11
2.2 Free volume theory	14
2.2.1 Diffusion of small molecules through polymers	15
2.3 Membrane separation process	26
2.3.1 Polymer membranes	26
2.3.2 Pore-flow model	32
2.3.3 Solution-diffusion model	34
2.3.4 Solution-diffusion with imperfections model	38

Table of Contents

2.3.5 Stefan–Maxwell multicomponent diffusion transport equation	39
2.4 References	40
Chapter 3. Experimental Part	47
3.1 Materials	47
3.2 Measurements	50
3.2.1 Scanning electron microscopy (SEM)	50
3.2.2 Differential scanning calorimetry (DSC)	51
3.2.3 Tracer-diffusion measurements	51
3.2.4 Swelling experiments	53
3.2.5 Solution concentration	54
3.2.6 Gas permeation	56
3.2.7 Nanofiltration	56
3.3 References	58
Chapter 4. Results and Discussion	61
4.1 Physical properties	61
4.1.1 Interaction parameters	61
4.1.2 Interaction parameters as a function of temperature	62
4.1.3 Swelling experiments	64
4.1.4 Polymer crosslinking parameters	66
4.1.5 Interaction parameters as a function of concentration	69
4.2 Diffusion coefficients	72

4.2.1 Self-diffusion coefficients	72
4.3 Nanofiltration	83
4.3.1 Permeation experiments	83
4.3.2 Concentration inside the membrane	88
4.3.3 Mutual diffusion coefficients	89
4.3.4 Modeling of organic solvent nanofiltration	91
Chapter 5. Summary and Conclusions	99
Chapter 6. Acknowledgments	103
Appendix 1. Organic solvent nanofiltration of Hexane/Polyisobutylene and Hexane/Sunflower Oil systems	105
References	109
Appendix 2. ActDF software	111
Appendix 3. GKSS-NSRM program	115
Appendix 4. Modeling example	117
A4.1 Estimation of tracer diffusion coefficients	118
A4.2 Estimation of the concentration of the permeants inside the membrane	152
A4.3 Estimation of thermodynamic diffusion coefficients	163

List of Tables

Table 2.1. Group contribution of van der Waals volume in cm ³ /mol.	6
Table 2.2. Group contribution for the zero point molar volume cm ³ /mol.	7
Table 2.3. Polymer free volume parameters.	18
Table 3.1. Chemical structure and physical properties of the used substances.	48
Table 3.2. Solvent densities as a function of the temperature.	49
Table 3.3. Solvent viscosities as a function of temperature.	50
Table 4.1. Van der Waals volume and zero point molar volume for the polymer and employed solvents.	61
Table 4.2. Solubility parameters of polymer and solvents as a function of temperature.	63
Table 4.3. Enthalpic interaction parameter of the mixtures estimated with solubility parameters.	63
Table 4.4. Weight fraction (%) from polymer swelling experiments as a function of solute concentration of binary mixtures.	65
Table 4.5. Volume fraction (%) from polymer swelling experiments as a function of solute concentration of binary mixtures.	66
Table 4.6. PDMS (thermally crosslinked) crosslink parameters for binary systems.	67
Table 4.7. Enthalpic interaction parameter of the mixtures estimated by the Flory-Huggins-Staverman solution theory.	71
Table 4.8. Measured solvents self-diffusion coefficients at 25 °C with PFG-NMR.	73
Table 4.9. Diffusion and free-volume parameters calculated from the Vrentas & Duda diffusion theory.	75
Table 4.10. Tracer diffusion coefficients for binary solvent-polymer systems and ternary solvent-solvent-polymer systems as a function of EGDME concentrations.	77

List of Tables

Table 4.11. Critical molar volume ratio between jumping units in a binary mixture.	78
Table 4.12. Critical molar volume ratio between jumping units in a binary mixture.	82
Table 4.13. Concentration inside the membrane for the MEK/TEGDME system at different experimental conditions.	89
Table 4.14. Regressed parameters from the solution-diffusion with imperfections model: membrane thickness (l), partial viscous permeability of the membrane (K) and compaction factor as a function of different feed concentrations (α).	93
Table A1.1. Chemical structure and molecular weight of the used substances.	106

List of Figures

Figure 1.1. Scheme of this doctoral thesis.	3
Figure 2.1. Schematic representation of the Flory-Huggins-Staverman cubic lattice model for binary systems: a) low molar mass components; b) polymer solutions; and c) polymer blends.	8
Figure 2.2. Schematic representation of a membrane separation module.	26
Figure 2.3. Schematic representation of four basic types of membranes. a) Isotropic porous membrane b) Integral anisotropic porous membrane c) Isotropic dense membrane d) Composite anisotropic membrane	28
Figure 2.4. Volume of an amorphous polymer as a function of temperature.	29
Figure 2.5. Application range of different liquid filtration processes	30
Figure 2.6. Pressure-driven permeation process through a membrane, according to the pore–flow transport model.	33
Figure 2.7. Schema of the different parameters which affect the behavior of microporous membranes. a) Cross section of porous membranes with different tortuosity. b) Surface view of porous membranes with same porosity and different pore diameters.	34
Figure 2.8. Pressure-driven permeation process through a membrane according to the solution-diffusion model.	35
Figure 2.9. Pressure-driven permeation process through a membrane according to the solution-diffusion model without constant pressure consideration.	37
Figure 3.1. Scanning electron micrograph of a PDMS composite membrane.	47
Figure 3.2. Schematic representation of spin-echo sequence in PFG-NMR measurements.	52
Figure 3.3. GPC calibration to estimate the mixtures concentration.	55
Figure 3.4. Schematic representation of the gas permeation set-up.	56

Figure 3.5. Schematic representation of the nanofiltration equipment. Left-hand side: 1) supply vessel, 2) pump, 3) membrane cell, a) feed solution sample, b) permeate solution sample, c) retentate solution sample. Right-hand side: 3D representation of the equipment.

57

Figure 4.1. Polymer swelling degree as a function of solute (TEGDME or PEGDME) concentration in binary mixtures. \diamond MEK / TEGDME, \circ MEK / PEGDME, \triangle DEK / TEGDME, \square DEK / PEGDME.

64

Figure 4.2. DSC second heating scans for the PDMS samples, crosslinked: (a) chemically; (b) chemically and by radiation.

68

Figure 4.3. Schematic representation of the differences between swelling experiments and membrane separation process. The points represent the place where the solvent/solute average concentration inside the polymer is considered.

69

Figure 4.4. Activities of binary solvent mixtures, as a function of solute weight concentration. For each mixture, solvent and solute are represented by filled and open symbols respectively. \blacklozenge MEK / TEGDME, \bullet MEK / PEGDME, \blacktriangle DEK / TEGDME, \blacksquare DEK / PEGDME, \star MEK / TEG.

70

Figure 4.5. Self-diffusion coefficients for \blacktriangledown MEK, \ast DEK, \triangleleft TEGDME, \triangleright PEGDME, \blacklozenge TEG as a function of temperature.

73

Figure 4.6. Solvent viscosity as a function of temperature. The broken lines correspond to simulated data and the symbols represent experimental data with the following identification: \blacktriangledown MEK, \ast DEK, \triangleleft TEGDME, \triangleright PEGDME, \blacklozenge TEG.

74

Figure 4.7. TEG viscosity as a function of temperature. The symbol \blacklozenge corresponds to viscosity data estimated by ASPEN Properties, the solid line represents the estimation by curve fitting and the dashed line corresponds to the non-linear regression.

76

Figure 4.8. Correlation between experimental PFG-NMR diffusion data and simulated data from the Vrentas & Duda diffusion theory for crosslinked polymers (the insert corresponds to non-crosslinked polymers).

80

Figure 4.9. Correlation between experimental PFG-NMR diffusion data (measured diffusivities) and simulated data from the Wesselingh & Bollen diffusion model (modeled diffusivities). 80

Figure 4.10. Correlation between experimental PFG-NMR diffusion data and simulated data from the Wesselingh & Bollen diffusion model. The filled, struck and open symbols correspond to $\lambda = 1.0$, $\lambda = 0.69$ and $\lambda = 0.5$, respectively. 81

Figure 4.11. Correlation between experimental PFG-NMR diffusion data and simulated data from the Wesselingh & Bollen diffusion model when the free volume overlap factor is regressed from experimental ternary diffusivities. 83

Figure 4.12. Experimental permeation fluxes at 25 °C for a MEK/TEGDME system as a function of the absolute applied pressure for different TEGDME feed concentrations. The filled symbols represent the fluxes of MEK, whereas the open symbols correspond to TEGDME fluxes. 84

Figure 4.13. Experimental permeation fluxes at 25 °C for a MEK/PEGDME system as a function of absolute applied pressure for different PEGDME feed concentrations. The filled symbols represent the fluxes of MEK, whereas the open symbols correspond to PEGDME fluxes. 84

Figure 4.14. Experimental permeation fluxes at 25 °C for a DEK/TEGDME system as a function of absolute applied pressure for different TEGDME feed concentrations. The filled symbols represent the fluxes of DEK, whereas the open symbols correspond to TEGDME fluxes. 85

Figure 4.15. Experimental permeation fluxes at 25 °C for a MEK/TEG system as a function of absolute applied pressure for different TEG feed concentrations. The filled symbols represent the fluxes of MEK, whereas the open symbols correspond to TEG fluxes. 86

Figure 4.16. Experimental permeation fluxes at 20 °C for a MEK/TEGDME system as a function of absolute applied pressure for different TEGDME feed concentrations. The filled symbols represent the fluxes of MEK, whereas the open symbols correspond to TEGDME fluxes. 87

Figure 4.17. Experimental permeation fluxes at 30 °C for a MEK/TEGDME system as a function of absolute applied pressure for different TEGDME feed concentrations. The filled symbols represent the fluxes of MEK, whereas the open symbols correspond to TEGDME fluxes. 87

Figure 4.18. Scheme of different calculation methods for the estimation of mutual diffusion coefficients. 90

Figure 4.19. Correlation between measured MEK/TEGDME permeation fluxes and simulated data calculated by the solution-diffusion with imperfections model. The filled symbols represent the fluxes of MEK, whereas the open symbols correspond to TEGDME fluxes. 91

Figure 4.20. Correlation between measured MEK/PEGDME permeation fluxes and simulated data calculated by the solution-diffusion with imperfections model. The filled symbols represent the fluxes of MEK, whereas the open symbols correspond to PEGDME fluxes. 92

Figure 4.21. Correlation between measured DEK/TEGDME permeation fluxes and simulated data calculated by the solution-diffusion with imperfections model. The filled symbols represent the fluxes of DEK, whereas the open symbols correspond to TEGDME fluxes. 92

Figure 4.22. Correlation between measured MEK/TEGME permeation fluxes and simulated data calculated by the solution-diffusion with imperfections model, with permeant concentrations estimated by interaction parameters from binary systems. The filled symbols represent the fluxes of MEK, whereas the open symbols correspond to TEGDME fluxes. 94

Figure 4.23. Correlation between measured MEK/TEG permeation fluxes and simulated data calculated by the solution-diffusion with imperfections model. The filled symbols represent the fluxes of MEK, whereas the open symbols correspond to TEG fluxes. 95

- Figure A1.1.** Permeation fluxes of hexane/sunflower oil and hexane/PIB 1300 systems (8 wt%) as a function of the applied pressure. The symbols correspond to experimental values and the lines correspond to simulated data. The filled symbols represent the hexane fluxes, whereas the open symbols correspond to solute fluxes. ★ Pure hexane, ▲ hexane/PIB 1300, ● hexane/sunflower oil. 107
- Figure A2.1.** Screenshot of the main window of the program ActDF. 112
- Figure A2.2.** Screenshot of the result window of the program ActDF. 112
- Figure A2.3.** Screenshot of the graphic window of the program ActDF. 113
- Figure A3.1.** Screenshot of the main windows of the GKSS-NSRM program. 115
- Figure A3.2.** Screenshot of the data input window of the GKSS-NSRM program. 116
- Figure A3.3.** Screenshot of the Self-diffusivity module of the GKSS-NSRM program. 116

List of Symbols

Latin letters

A	Membrane area [m^2]
\dot{A}	Area per mole of molecule $\left[\frac{m^2}{mol}\right]$
A^W	Surface area $\left[\frac{m^2}{mol}\right]$
\hat{a}	Group interaction parameter from the UNIFAC method [K]
a	Activity [–]
\bar{c}	Average molar concentration $\left[\frac{mol}{m^3}\right]$
c	Molar concentration $\left[\frac{mol}{m^3}\right]$
D	Thermodynamic diffusion coefficient (diffusivity) $\left[\frac{m^2}{s}\right]$
D^F	Diffusion coefficient according to the Fick's law $\left[\frac{m^2}{s}\right]$
\hat{D}	Self-Diffusion coefficient $\left[\frac{m^2}{s}\right]$
\check{D}	Tracer diffusion coefficient $\left[\frac{m^2}{s}\right]$
\dot{D}	Constant pre-exponential factor from the Vrentas & Duda diffusion theory $\left[\frac{m^2}{s}\right]$
\ddot{D}	Constant pre-exponential factor from free volume diffusion theory when the activation energy for a jump is considered equal to zero $\left[\frac{m^2}{s}\right]$
d	Molecular diameter [m]
E	Molecular energy necessary to overcome attractive forces which hold it to its neighbors [J]
F	Friction force of between a permeant and the membrane $\left[\frac{N}{mol}\right]$
G	Gibbs free energy of mixing [J]
\check{G}	Gradient strength from PFG-NMR measurements $\left[\frac{G}{cm}\right]$

List of Symbols

H	Enthalpy [J]
H_v	Enthalpy of vaporization [J]
I	Peak intensity from PFG-NMR measurements [a. u.]
I^0	Maximum peak intensity from PFG-NMR measurements [a. u.]
J	Molar flux $\left[\frac{\text{mol/s}}{\text{m}^2}\right]$
K_{i3}	Polymer free volume parameters $\left[\frac{\text{m}^3}{\text{kg}\cdot\text{K}}\right]$ for ternary mixtures, where i represent a solvent. In case of binary mixtures, the subscript change to $i2$.
K_{33}	Polymer free volume parameters [K] for ternary mixtures, In case of binary mixtures, the subscript change to 22.
K_{ii}	Solvent free-volume parameters $\left[\frac{\text{m}^3}{\text{kg}\cdot\text{K}}\right]$, where i represent a single substance and take a value of 1 for binary mixtures and 1-2 for ternary (polymer-solvent-solvent) mixtures.
K_{3i}	Solvent free volume parameters [K], where i represent a solvent. In the case of binary mixtures, the subscript change to $2i$.
K^*	Viscous permeability of the membrane [m^2]
\tilde{K}	Partial viscous permeability of the membrane [m^2]
k	Boltzmann constant $\left[1.3806504 \cdot 10^{-23} \frac{\text{J}}{\text{K}}\right]$
k^D	Darcy's law coefficient [m^2]
\hat{i}	UNIQUAC factor $\left[\frac{\text{m}^3}{\text{mol}}\right]$
\tilde{L}	Proportionality coefficient which represent the mobility of the permeant. Also known as "Beweglichkeit" from its original definition in german. $\left[\frac{\text{m}^3}{\text{m}^2\cdot\text{s}}\right]$
L	Permeability of a solvent in a membrane when a dependence with the transmembrane pressure is found during the filtration process $\left[\frac{\text{m}^3}{\text{m}^2\cdot\text{s}}\right]$
L^0	Permeability of a substance in a membrane under atmospheric pressure $\left[\frac{\text{m}^3}{\text{m}^2\cdot\text{s}}\right]$
\ddot{i}	Bond distance between some atom i and a given atom \bar{i} to be use in the van der Waals volume [m]

l	Membrane thickness [m]
M	Mass [g]
N_A	Avogadro's number [$6.02214179 \cdot 10^{23} \cdot mol$]
n	Number of moles [mol]
P	Pressure [Pa]
Q	Volumetric flow rate [$\frac{ml}{s}$]
\hat{Q}	UNIQUAC surface parameter [$\frac{m^2}{mol}$]
q	Superficial area [$\frac{m^2}{mol}$]
\dot{R}	Retention factor [$-$]
\hat{R}	UNIQUAC volume parameter [$\frac{m^3}{mol}$]
\check{r}	Polymer chain segment number [$-$]
\check{r}	Pore radius [m]
\bar{r}	Radius of an atom \bar{i} [m]
r	Radius of an atom i [m]
R	Universal gas constant [$8.314472 \frac{J}{K \cdot mol}$]
S	Entropy [$\frac{J}{K}$]
SD	Swelling degree [%]
SU	Solvent uptake [g]
T	Temperature [K]
T_g	Glass transition temperature [K]
\hat{U}	Interaction energy between groups from the UNIFAC method [$\frac{J}{mol}$]
u	Interaction energy between molecules [$\frac{J}{mol}$]
\check{u}	Diffusive velocity [$\frac{m}{s}$]

List of Symbols

$v^{(i)}$	UNIQUAC parameter which represent the number of groups of a specific type
\check{v}	Viscous velocity $\left[\frac{m}{s}\right]$
V^E	Empty volume $\left[\frac{m^3}{mol}\right]$
V^F	Free volume (Expansion volume) $\left[\frac{m^3}{mol}\right]$
V^{FF}	Surface weighted free volume $\left[\frac{m^3}{mol}\right]$
V^C	Zero point molar volume (Compress volume) $\left[\frac{m^3}{mol}\right]$
V^Q	Volume swept out by thermal vibration of one molecule $\left[\frac{m^3}{mol}\right]$
V^W	Van der Waals volume $\left[\frac{m^3}{mol}\right]$
V^f	Fluctuation volume $\left[\frac{m^3}{mol}\right]$
V	Molar volume $\left[\frac{m^3}{mol}\right]$
V^*	Specific volume $\left[\frac{m^3}{kg}\right]$
\hat{V}^*	Specific critical hole free-volume required for a jump $\left[\frac{m^3}{kg}\right]$
\tilde{V}	Molar volume of the polymer jumping unit $\left[\frac{m^3}{mol}\right]$
\hat{V}_{FH}	Average hole free-volume per kilogram of mixture $\left[\frac{m^3}{kg}\right]$
\check{w}	Total velocity of a compound inside the membrane $\left[\frac{m}{s}\right]$
X	Group mole fraction from the UNIFAC method $[-]$
\dot{X}	Degree of crosslinking $[-]$
x	Molar fraction $\left[\frac{mol}{mol}\right]$

Greek letters

α	Compaction factor [–]
$\tilde{\alpha}_i$	Selectivity factor to account differences in permeation between components due to the nature of the imperfections of the membrane [–]
$\check{\alpha}$	Membrane gas selectivity [–]
β	Lattice constant of entropic origin [–]
γ	Activity coefficient [–]t
γ^C	Combinatorial part of the activity coefficient from the UNIQUAC method [–]
γ^R	Residual part of the activity coefficient from the UNIQUAC method [–]
Γ^i	Reference residual activity coefficient from the UNIFAC method [–]
Γ	Residual activity coefficient from the UNIFAC method [–]
δ	Hildebrand solubility parameter [MPa ^{1/2}]
Δ	Variation of as property between two states
∂	Duration of the gradient from PFG-NMR measurements [s]
ε	Membrane porosity [–]
ζ	Mutual friction coefficient $\left[\frac{\text{kg}}{\text{s}\cdot\text{mol}}\right]$
$\zeta_{i\#,i}$	Self-friction coefficient $\left[\frac{\text{kg}}{\text{s}\cdot\text{mol}}\right]$
$\zeta_{i\#,i}^0$	Tracer friction coefficient pre-exponential factor $\left[\frac{\text{kg}}{\text{s}\cdot\text{mol}}\right]$
$\zeta_{i\#,eff}$	Tracer friction coefficient $\left[\frac{\text{kg}}{\text{s}\cdot\text{mol}}\right]$
η	Dynamic viscosity [Pa · s]
θ	Area factor from the UNIQUAC method [–]
Λ	Diffusion time between gradients from PFG-NMR measurements [s]
λ	Overlap factor which accounts for shared free volume [–]
μ	Chemical potential $\left[\frac{\text{J}}{\text{mol}}\right]$

List of Symbols

μ^0	Chemical potential at a reference state $\left[\frac{\text{J}}{\text{mol}}\right]$
μ°	Chemical potential at standard conditions $\left[\frac{\text{J}}{\text{mol}}\right]$
ξ	Ratio between the critical molar volumes of jumping units of two compounds in a mixture [-]
π	Osmotic pressure [Pa]
ρ	Mass density $\left[\frac{\text{kg}}{\text{m}^3}\right]$
ρ^{*c}	Zero point specific density $\left[\frac{\text{kg}}{\text{m}^3}\right]$
ϱ	Parameter which represent the effect of crosslinking on the free volume of the polymer [-]
σ	Surface fractions of a single compounds in a mixture [-]
τ	Tortuosity [-]
$\hat{\tau}$	UNIQUAC binary parameter [-]
γ	Gyromagnetic ratio $\left[\frac{\text{Hz}}{\text{G}}\right]$
Φ	Segment fraction from the UNIQUAC method [-]
ϕ	Volume fraction [-]
χ	Flory-Huggins-Stavermann interaction parameter [-]
ψ	Group interaction parameter from the UNIFAC method [-]
ω	Mass fraction [-]

Subscripts

1	Solvent
2	For binary solvent-polymer mixtures represents the polymer. For ternary solvent-solvent-polymer mixtures represents solvent 2
3	Polymer
$3j$	Polymer jumping unit

<i>C</i>	Property at the critical point
<i>dry</i>	Property of the membrane without swelling
<i>F</i>	Feed side outside the membrane
<i>FS</i>	Binary solvent
<i>i/j</i>	Relationship between two compounds
<i>ij</i>	Solvent jumping unit
<i>M</i>	Property consider as: a) average inside the membrane b) mixture of polymer and solvent(s)
<i>MF</i>	Feed side inside the membrane
<i>MP</i>	Permeate side inside the membrane
<i>P</i>	Permeate side outside the membrane
<i>i, j, k</i>	Component
<i>m</i>	Mixing or mixture
<i>Pol</i>	Membrane polymer
<i>SDM</i>	Solution-diffusion model
<i>VT</i>	Viscous transport
<i>wet</i>	Property of the membrane in the swelled state

Chapter 1. Introduction

Membrane processes have gained an important place in chemical technology and are used in a broad range of applications. The use of an increasing amount of solvents in a variety of industrial processes and the deficiencies associated to classical separation techniques stimulate the development of efficient new separation techniques which reduce the associated cost of materials and benefit the environment with lower energy consumption and higher recovery of residual substances.

One of the most promising new technologies for separating organic substances (no water based systems) are membrane separation processes based on nanofiltration. For the establishment of organic solvent separation processes in the industry, it is necessary to develop nanofiltration membranes with an ideal condition of high permeability (measure of how much passes through) and high selectivity (measure of how good the separation of the substances is). Additionally, optimizations of the processes before, during and after the separation itself are necessary to facilitate the introduction of organic solvent nanofiltration for industrial applications. Various applications are interesting for diverse areas. For example, chemical, food, petrochemical and pharmaceutical industries present the need of improvement in processes such as catalyst recovery, comestible oil purification, fractionation of petroleum products or separation of peptides and antibiotics, respectively.

For the above mentioned development of nanofiltration membranes, as well as for the improvement of the associated processes, a mathematic description and comprehension of the variables which affect the transport mechanism in nanofiltration processes is necessary. In order to describe transport through nanofiltration membranes, approaches like solution-diffusion model, Spiegler-Kedem model, Machado's resistances model, pore flow model, and solution-diffusion with imperfections model have been extensively used, with different levels of success.^[1] For traditional membrane based separation processes where one substance is permeated through the membrane and the other is rejected by the membrane, the affinity between the permeant and the polymer plays a key role during the separation process. This affinity affects the swelling of the polymer and the movement capacity of the permeant inside the membrane, and both variables affect the final behavior of the

¹ Bhanushali, D. and D. Bhattacharyya, *Advances in Solvent-Resistant Nanofiltration Membranes. Experimental Observations and Applications*. Advanced membrane technology, 2003. **984**(1): p. 159-177.

membrane. This is especially true for organic solvent nanofiltration where permeation of both feed substances will occur. Here, the objective of the membrane selection/development is to increase the permeation of one substance, while the permeation of the other one is diminished.

The experience of the GKSS Research Centre Geesthacht GmbH in the understanding of transport mechanisms of nanofiltration membranes is evidenced by the successful modeling of solvent mixtures permeation when the affinity between both permeants and the membrane is similar. Here, nanofiltration experiments of hydrocarbon mixtures with PDMS composite membrane crosslinked by radiation have been carried out and modeled with the solution-diffusion with imperfections model as well as the Maxwell-Stefan transport equation.^[2]

A more complicated situation arises when the affinity between the permeants and the polymer membrane can no longer be considered as identical. In such a case, the permeants behave as a non-ideal mixture, and the interaction between each component in the system needs to be considered in the modeling of the transport mechanism, i.e., interaction between the permeants and the interaction of each permeant with the membrane. By considering the permeants as non-ideal mixtures, the applications of the modeling loose restrictions and come closer to diverse industrial applications.

This doctoral thesis is focused on understanding the transport mechanism of nanofiltration processes when a non-ideal mixture permeates through the membrane, with the ultimate vision of moving forward to a general modeling for the nanofiltration industrial processes. Here, a comprehension of the properties which affect the permeation behavior in membrane separation processes is investigated. Therefore, a study of the theories related with membrane separation processes has been done, as well as of the methods employed to describe the properties involved in the process, as shown in figure 1.1.

² Dijkstra, M.F.J., S. Bach, and K. Ebert, *A transport model for organophilic nanofiltration*. Journal of Membrane Science, 2006. **286**(1-2): p. 60-68.

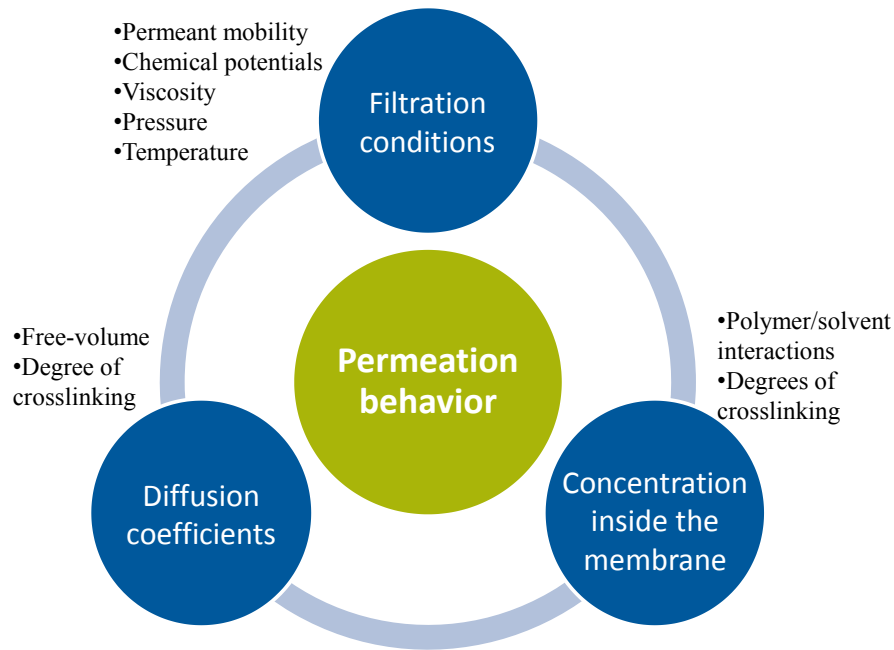


Figure 1.1. Scheme of this doctoral thesis.

The theoretical background of polymer solutions as well as free-volume parameters of substances is extensively described in chapter 2. Afterwards, the chapter immerses the reader in the description of free-volume theories applied to the calculation of diffusion coefficients in polymers. The theoretical background is concluded after the explanation of membrane based processes and the necessary models to describe those engineering processes. The experimental methods employed during the research are presented in chapter 3.

The obtained results are discussed in the fourth chapter, which is divided in three sections: physical properties, diffusion coefficients and nanofiltration. In the first one, section 4.1, the experimental and simulated physical properties of the substances and mixtures are presented. The section 4.2 deals with the determination of the different diffusion coefficients relevant for the simulation. The nanofiltration section (section 4.3) presents the modeling of the transport mechanism.

The concentration of permeants inside the membrane is extensively reviewed in the theoretical part, and the Flory-Huggins-Staverman theory adapted for the nanofiltration conditions is accordingly used in the first section of chapter 4. Here, the effect on polymer-solvent interaction parameters due to the presence of a second permeant is widely analyzed. In the results presented in section 4.2, two different models to describe

experimental diffusion coefficients are used. The advantages and disadvantages, as well as the prediction capabilities of both models, are analyzed. The chapter four finishes with the presentation of the modeling of organic solvent nanofiltration experiments. In this last section, the results obtained from previous sections of the chapter are used. Here, the importance of a good estimation of permeant concentration inside the membrane and thermodynamic diffusion coefficients is discussed in terms of the quality of the nanofiltration modeling.

Later, the conclusions of this work are presented in chapter 5. The programs created during this Ph.D. work are found in the appendixes. In the first appendix, a simulation software to estimate activities as a function of temperature and pressure for multicomponent mixtures is presented. The second appendix shows a software which consists of a graphic user interface that is possible to be applied to any kind of simulation library. The third appendix shows the software code used for the different calculation steps (i.e., concentration inside the membrane, permeant diffusivities and nanofiltration modeling).

Chapter 2. Theoretical Background

2.1 Physical properties

2.1.1 Volumetric properties

The volumetric properties are of tremendous importance for nearly every phenomenon of process. For the next sections it is necessary to define and to clarify the calculation methods of a set of volumetric properties.

The van der Waals volume (V_i^W) of a molecule i is defined as a space which is impenetrable to other molecules with normal thermal energies (i.e., corresponding to regular temperatures).^[1] For its definition, the atoms are considered to be hard spheres, therefore, the volume is assumed to be constant for the involved elements and the distance between the centers of the spheres is the bond distance considered as a constant. The contribution of a given atom \bar{i} with radius \bar{r} to the van der Waals volume is expressed by the following equation:

$$V_i^W = N_A \cdot \left(\frac{4}{3} \cdot \pi \cdot \bar{r}^3 - \sum \pi \cdot h_i^2 \cdot \left(\bar{r} - \frac{h_i}{3} \right) \right) \quad \text{Eq. 2.1}$$
$$h_i = \bar{r} - \frac{\bar{l}_i}{2} - \frac{\bar{r}^2}{2 \cdot \bar{l}_i} + \frac{r_i^2}{2 \cdot \bar{l}_i}$$

where N_A is the Avogadro number, r_i is the radius of atom i covalently bonded to \bar{i} , and \bar{l}_i is the bond distance between the atoms i and \bar{i} . With the previous definition, the contribution of the van der Waals volume depends on the nature of the surrounding atoms and cannot be considered as constant. In order to calculate the van der Waals volume as a sum of structural groups contributions, Bondi calculates the volume contribution of many structural group with the subsequent information of the influence of the surrounding.^[2] Afterwards, the group contribution calculation has been extended by many different authors.^[3, 4] The group contribution values for the calculation of the van der Waals volume are presented in table 2.1.^[1]

The zero point molar density refers to the density of a substance at 0 K. This can be done with extrapolation of crystalline and liquid densities to the absolute zero temperature. For the sake of simplicity, a group contribution method is used in order to

avoid the necessity of experimental data for the calculation of the zero point molar volume (V_i^C).^[1, 5] According to Bondi, the zero point molar volume can be correlated to the van der Waals volume by equation 2.2. A list of atomic and structural constants for the zero point molar volume is presented in table 2.2.^[5]

Table 2.1. Group contribution of van der Waals volume in cm³/mol.

Group	V_i^W	Group	V_i^W	Group	V_i^W
–CH ₂ –	10.23	–CH = CCl–	25.70	–C(CH ₃) ₃	44.35
–CH(CH ₃)–	20.45	–C ≡ C–	16.10	–C ≡ CH	19.50
–CH(iso – C ₃ H ₇)–	40.90	O	11.70	–C ≡ N	14.70
–CH(ter – C ₄ H ₉)–	51.10	–C–	5.50	–OH	8.00
–CH(C ₆ H ₅)–	52.60	–O–	5.00	–SH	14.80
–CH(C ₆ H ₄ –CH ₃)–	63.80	–NH–	4.00	–F	5.70
–CH(OH)–	14.80	–S–	10.80	Al	11.60
–CH(OCH ₃)–	25.5	–S–S–	22.70	–Cl	12.00
–CH(OCOCH ₃)–	37.00	O		ar	12.00
–CH(COOCH ₃)–	37.00	–S–	20.30	–CF ₃	21.30
–CH(CHCN)–	21.50	O		–CHCl ₂	31.30
–CHF–	12.50	–S–	20.30	–CH ₂ Cl	21.85
–CHCl–	19.00	O		–CCl ₃	38.20
–C(CH ₃) ₂ –	30.70	–COO–	15.20	–NO ₂	16.80
–C(CH ₃)(C ₆ H ₅)–	62.80	–OCOO–	18.90	–SO ₄	35.10
–C(CH ₃)COOCH ₃ –	46.70	–CONH–	13.00	CH–	6.80
–CF ₂ –	14.80	–OCONH–	18.00	HC = C	13.50
–CFCl–	21.00	–NHCONH–	18.00	–N	4.30
–CCl ₂ –	27.80	–Si(CH ₃) ₂ –	42.20	C	3.30
–CH = CH–	16.90	–H	3.44	= C =	6.95
–CH = C(CH ₃)–	27.20	–CH ₃	13.67	–C ≡	8.00
		–CH(CH ₃) ₂	34.10	Si	16.60

$$\frac{V_i^C}{V_i^W} \approx 1.3 \quad \text{Eq. 2.2}$$

Table 2.2. Group contribution for the zero point molar volume cm³/mol.

Atomic constants		Structural constants	
H = 6.7	Br = 22.1	3-membered ring = 4.8	Double bond = 8.0
C = 1.1	I = 28.3	4-membered ring = 3.2	Triple bond = 15.5
N = 3.6	P = 12.7	5-membered ring = 1.8	
O = 5.0	S = 14.3	6-membered ring = 0.6	
F = 10.3	O (in alcohols) = 3.0	Semipolar double bond = 0.0	
Cl = 19.3	N (in amines) = 0.0		

2.1.2 Flory-Huggins-Staverman phase equilibria solution theory

The thermodynamic equation of the Gibbs free energy accounts for the maximum amount of non-expansion work that can be extracted from a close system; this maximum can be attained only in a completely reversible process when a system changes from a well-defined initial state to a well-defined final state.^[6, 7] Therefore, the Gibbs free energy (ΔG_m) equals the work exchanged by the system with its surroundings without taking into account the work of pressure forces.^[8] The change denoted by the symbol Δ represents the value of a variable for a solution or mixture minus the values for the pure components considered separately at standard conditions. Equation 2.3 shows the change of the Gibbs free energy as a function of the variation of the enthalpy (ΔH_m) and entropy (ΔS_m) during a mixing process at a given temperature (T).

$$\Delta G_m = \Delta H_m - T \cdot \Delta S_m \quad \text{Eq. 2.3}$$

The Flory-Huggins-Staverman lattice theory is generally the starting point for most of the theoretical interpretations of polymer solutions and it is based on the general Gibbs free energy equation.^[9] For polymer systems, the main problem is to find an expression for the entropy of mixing because polymer solutions show significant deviations from the values for ideal solutions. With the assumption of a rigid cubic lattice model, Flory, Huggins and Staverman solved the problem for polymer solutions.^[9] The main difference between ideal solutions and polymer solutions consists in the restricted

number of rearrangements that a polymer molecule can achieve in a solution compared to a small molecule in the presence of the same solvent. A schematic representation of the Flory-Huggins-Staverman lattice model for polymer solutions and polymer blends is shown in figure 2.1. It can be seen that, for low molar mass molecules, the number of possible arrangements is greater than the ones for polymer solutions and even more than for polymer blends.

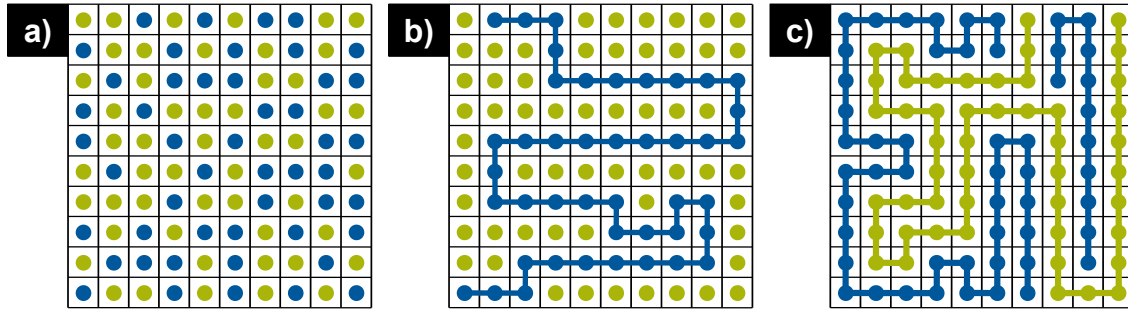


Figure 2.1. Schematic representation of the Flory-Huggins-Staverman cubic lattice model for binary systems: a) low molar mass components; b) polymer solutions; and c) polymer blends.

In the Flory-Huggins-Staverman lattice treatment, the probability of a random lattice site being occupied is calculated with the assumption that every lattice site is occupied by polymer segments or solvent molecules without superposition between each other. The enthalpy change is calculated with the consideration that only binary interactions occur during the mixing. For instance, only solvent-solvent, solvent-monomer and monomer-monomer interactions are considered to affect the mixing process. The Gibbs free energy for a polymer-solvent can be described as follows:

$$\Delta G_m = R \cdot T \cdot [n_1 \cdot \ln \phi_1 + n_2 \cdot \ln \phi_2 + \chi \cdot n_1 \cdot \phi_2] \quad \text{Eq. 2.4}$$

where n represents the number of moles and ϕ the volume fraction of the compounds in the mixture. The subscripts 1 and 2 symbolize the solvent and the polymer, respectively. T is the temperature at which the mixture occurs. χ corresponds to the polymer-solvent interaction parameter, which takes into account the energy of interdispersing polymer and solvent molecules. The Flory-Huggins-Staverman interaction parameter is treated as constant, but it has been shown to change with polymer concentration, temperature and pressure.^[10] In the case of athermal mixtures, the interaction parameter will become

zero, positive for endothermic mixing and negative for exothermic mixing.^[11] The Flory-Huggins-Staverman interaction parameter is described by equation 2.5.^[9, 12]

$$\chi = \frac{\Delta H_m}{k \cdot T \cdot N_1 \cdot \phi_2} \quad \text{Eq. 2.5}$$

where, k is the Boltzmann constant and N_1 is a count of the number of polymer molecules in the solution. With the introduction of Hildebrand solubility parameters δ_1 for the solvent and δ_2 for the polymer, the Flory-Huggins-Staverman interaction parameter can be calculated as follows:

$$\chi = \beta_1 + \frac{V_1}{R \cdot T} (\delta_1 - \delta_2)^2 \quad \text{Eq. 2.6}$$

$$\delta_i = \sqrt{\frac{H_v + R \cdot T}{V_1}} \quad \text{Eq. 2.7}$$

In equation 2.6, β_1 is a lattice constant of entropic origin. The second term represents the enthalpic contribution of the Flory-Huggins-Staverman interaction parameter, where R is the universal gas constant, V_1 is the molar volume of the solvent and ΔH_v is the enthalpy of vaporization.^[12] Bristow and Watson estimated, by a semiempirical equation, that the entropic contribution for the interaction parameter can be approximated to a value of 0.35.^[13]

According to Flory, Huggins and Staverman, the chemical potential μ_1 of the solvent in the solution relative to the one in the pure liquid at standard conditions (μ_1°) is obtained by differentiating the Gibbs free energy of mixing with respect to the number of solvent molecules (n_1).

$$\frac{\Delta\mu_1}{R \cdot T} = \ln \phi_1 + \phi_2 \cdot \left(1 - \frac{1}{\check{r}}\right) + \chi_1 \cdot \phi_2^2 \quad \text{Eq. 2.8}$$

where \check{r} is the chain segment number which is calculated as the ratio of polymer molar volume to solvent molar volume. Therefore, for polymers with long chains, the ratio $1 / \check{r}$ can be neglected.^[14, 15]

For systems of superior order, a slightly concentration dependent χ parameter has been reported elsewhere.^[16, 17] For sake of simplicity, Baik et al. extended the Flory-Huggins-Staverman lattice

theory for a quaternary system with the consideration that only binary interactions occurs and the interaction parameters are constant despite of changes in concentration.^[18]

$$\begin{aligned} \frac{\Delta G_m}{R \cdot T} = & n_1 \cdot \ln \phi_1 + n_2 \cdot \ln \phi_2 + n_3 \cdot \ln \phi_3 + n_4 \cdot \ln \phi_4 + \chi_{12} \\ & \cdot n_1 \cdot \phi_2 + \chi_{13} \cdot n_1 \cdot \phi_3 + \chi_{14} \cdot n_1 \cdot \phi_4 + \chi_{23} \\ & \cdot n_2 \cdot \phi_3 + \chi_{24} \cdot n_2 \cdot \phi_4 + \chi_{34} \cdot n_3 \cdot \phi_4 \end{aligned} \quad \text{Eq. 2.9}$$

$$\chi_{ij} = \chi_{ji} \cdot \frac{V_i}{V_j} \quad \text{Eq. 2.10}$$

$$\begin{aligned} \frac{\Delta \mu_1}{R \cdot T} = & \ln \phi_1 - \phi_2 \cdot \frac{V_1}{V_2} - \phi_3 \cdot \frac{V_1}{V_3} - \phi_4 \cdot \frac{V_1}{V_4} \\ & + (1 + \chi_{12} \cdot \phi_2 + \chi_{13} \cdot \phi_3 + \chi_{14} \cdot \phi_4) \\ & \cdot (1 - \phi_1) - \chi_{23} \cdot \phi_2 \cdot \phi_3 \cdot \frac{V_1}{V_2} - \chi_{34} \cdot \phi_3 \cdot \phi_4 \\ & \cdot \frac{V_1}{V_3} - \chi_{24} \cdot \phi_2 \cdot \phi_4 \cdot \frac{V_1}{V_2} \end{aligned} \quad \text{Eq. 2.11}$$

$$\begin{aligned} \frac{\Delta \mu_2}{R \cdot T} = & \ln \phi_2 - \phi_1 \cdot \frac{V_2}{V_1} - \phi_3 \cdot \frac{V_2}{V_3} - \phi_4 \cdot \frac{V_2}{V_4} \\ & + \left(1 + \chi_{12} \cdot \phi_1 \cdot \frac{V_2}{V_1} + \chi_{23} \cdot \phi_3 + \chi_{24} \cdot \phi_4\right) \\ & \cdot (1 - \phi_2) - \chi_{13} \cdot \phi_1 \cdot \phi_3 \cdot \frac{V_2}{V_1} - \chi_{14} \cdot \phi_1 \cdot \phi_4 \\ & \cdot \frac{V_2}{V_1} - \chi_{34} \cdot \phi_3 \cdot \phi_4 \cdot \frac{V_2}{V_3} \end{aligned} \quad \text{Eq. 2.12}$$

$$\begin{aligned} \frac{\Delta \mu_3}{R \cdot T} = & \ln \phi_3 - \phi_1 \cdot \frac{V_3}{V_1} - \phi_2 \cdot \frac{V_3}{V_2} - \phi_4 \cdot \frac{V_3}{V_4} \\ & + \left(1 + \chi_{13} \cdot \phi_1 \cdot \frac{V_3}{V_1} + \chi_{23} \cdot \phi_2 \cdot \frac{V_3}{V_2} + \chi_{34} \right. \\ & \cdot \phi_4) \cdot (1 - \phi_3) - \chi_{12} \cdot \phi_1 \cdot \phi_2 \cdot \frac{V_3}{V_1} - \chi_{14} \\ & \cdot \phi_1 \cdot \phi_4 \cdot \frac{V_3}{V_1} - \chi_{24} \cdot \phi_2 \cdot \phi_4 \cdot \frac{V_3}{V_2} \end{aligned} \quad \text{Eq. 2.13}$$

$$\begin{aligned}
 \frac{\Delta\mu_4}{R \cdot T} = & \ln \phi_4 - \phi_1 \cdot \frac{V_4}{V_1} - \phi_2 \cdot \frac{V_4}{V_2} - \phi_3 \cdot \frac{V_4}{V_3} \\
 & + \left(1 + \chi_{14} \cdot \phi_1 \cdot \frac{V_4}{V_1} + \chi_{24} \cdot \phi_2 \cdot \frac{V_4}{V_2} + \chi_{34} \cdot \phi_3 \right. \\
 & \cdot \left. \frac{V_4}{V_3} \right) \cdot (1 - \phi_4) - \chi_{12} \cdot \phi_1 \cdot \phi_2 \cdot \frac{V_4}{V_1} - \chi_{13} \\
 & \cdot \phi_1 \cdot \phi_3 \cdot \frac{V_4}{V_1} - \chi_{23} \cdot \phi_2 \cdot \phi_3 \cdot \frac{V_4}{V_2}
 \end{aligned} \tag{Eq. 2.14}$$

2.1.2 Activity coefficients

The activity and the activity coefficient quantify the effective concentration in a mixture and consider interactions between the molecules of the different components. The activity accounts for the tendency of a substance in a solution to escape to another solution with lower concentration. The activity coefficient is a measure of the divergence between a real substance and an ideal one. Therefore, the left term of equations 2.8 and 2.11 to 2.14 is often expressed in terms of the activity coefficient of the different solvents, as follows:^[19, 20]

$$\mu_i = \mu_i^\theta + R \cdot T \cdot \ln(\gamma_i \cdot x_i) \tag{Eq. 2.15}$$

$$a_i = \gamma_i \cdot x_i \tag{Eq. 2.16}$$

$$\ln a_i = \frac{\Delta\mu_i}{R \cdot T} \tag{Eq. 2.17}$$

where a_i is the activity, γ_i is the activity coefficient and x_i is the molar fraction of a compound i in a mixture. For the calculation of the activity coefficients, there are many theoretical and experimental equations with different degrees of success. For systems with low deviations from ideal systems (e.g., non-polar systems), equations based on a Gibbs free energy treatment with two or more binary parameters provide reasonable estimations. For the simplest cases, equations as Van Laar or Margules are effective with the advantage of its simplicity of use. For systems with higher deviations from the ideal behavior, it is possible to use equations as Wilson, NRTL or UNIQUAC. The disadvantage is the high number of fit parameters present in those equations, i.e., more than 2 binary parameters which need to be calculated from experimental data.

In order to correlate different thermodynamic properties (e.g., activity and activity coefficients) without the calculation process of the binary parameter from the above mentioned methods, it is often convenient to consider the use of group contribution methods (i.e., ASOG or UNIFAC).^[20] The basic idea of a group contribution method is that the functional groups that constitute any substance are less than the possible number of substances of interest for chemical technology. Therefore, the properties of any substance are assumed as the addition of the properties of its constituent groups. The ASOG group contribution method was often used for the calculation of the Flory-Huggins-Staverman equation for the first part and the Wilson equation was applied to functional groups for the second part of the method. This arbitrary procedure can be avoided with the use of the UNIQUAC equation.

The UNIQUAC equation gives a good representation of the vapor-liquid and liquid-liquid equilibrium for binary and multicomponent mixtures of non-electrolytic components as hydrocarbons, ketones, esters, water, etc. For a multicomponent mixture, the UNIQUAC equation can be written as shown in equations 2.18 to 2.20. The subscript i represents each component of the mixture and the summations are over all components. The superscripts C and R represent the combinatorial and the residual part of the method. θ is an area factor, Φ is the segment fraction, V_i^W is the van der Waals volume and q_i are the superficial areas. The parameters τ_{ij} and τ_{ji} are the binary parameters of the UNIQUAC method that need to be calculated from experimental phase equilibrium data.

$$\ln \gamma_i = \ln \gamma_i^C + \ln \gamma_i^R \quad \text{Eq. 2.18}$$

$$\ln \gamma_i^C = \ln \frac{\Phi_i}{x_i} + 5 \cdot q_i \cdot \ln \frac{\theta_i}{\Phi_i} + \hat{l}_i - \frac{\Phi_i}{x_i} \cdot \sum_j x_j \cdot \hat{l}_j \quad \text{Eq. 2.19}$$

$$\ln \gamma_i^R = q_i \cdot \left(1 - \ln \sum_j \theta_j \cdot \hat{\tau}_{ji} - \sum_j \frac{\theta_j \cdot \hat{\tau}_{ji}}{\sum_k \theta_k \cdot \hat{\tau}_{kj}} \right) \quad \text{Eq. 2.20}$$

$$\hat{l}_i = 5 \cdot (V_i^W - q_i) - (V_i^W - 1)$$

$$\theta_i = \frac{q_i \cdot x_i}{\sum_j q_j \cdot x_j} \quad ; \quad \Phi_i = \frac{V_i^W \cdot x_i}{\sum_j V_j^W \cdot x_j} \quad ; \quad \hat{\tau}_{ji} = \exp \left(-\frac{u_{ji} - u_{ii}}{R \cdot T} \right)$$

The UNIFAC group contribution method preserves the combinatorial part of the UNIQUAC equation and combines it with the group contribution concept, with the

consequent avoidance of the binary parameters calculation. Only pure component properties are used in this method. The van der Waals volume and the superficial area are calculated as the sum of its correspondent group properties.

$$V_i^W = \sum_k v_k^{(i)} \cdot \hat{R}_k \quad ; \quad q_i = \sum_k v_k^{(i)} \cdot \hat{Q}_k \quad \text{Eq. 2.21}$$

$$\hat{R}_k = \frac{V_k^W}{15.17} \quad ; \quad \hat{Q}_k = \frac{A_k^W}{2.5 \cdot 10^9} \quad \text{Eq. 2.22}$$

The parameter $v_k^{(i)}$ is always an integer and represents the number of groups of type k in the substance molecule i . The parameters \hat{R}_k and \hat{Q}_k are obtained from the van der Waals group volume and surface areas V_k^W and A_k^W given by Bondi.^[2] As a result, the residual part of equation 2.18 is replaced by a group contribution approach.

$$\ln \gamma_i^R = \sum_{\substack{k \\ \text{all groups}}} v_k^{(i)} \cdot (\ln \Gamma_k - \ln \Gamma_k^i) \quad \text{Eq. 2.23}$$

Above, Γ_k is the group residual activity coefficient and Γ_k^i is the residual activity coefficient of group k in a reference solution which contains only molecules of type i . The last term is a normalization term necessary in order to obtain an activity coefficient equal to 1 when the concentration tends to 1. The parameter Γ_k^i can be calculated with the use of the same equation under the proper conditions for the reference solution.

$$\ln \Gamma_k = Q_k \cdot \left[1 - \ln(\theta_m \cdot \Psi_m) - \sum_m \frac{\theta_m \cdot \Psi_{km}}{\sum_n \theta_n \cdot \Psi_{nm}} \right] \quad \text{Eq. 2.24}$$

$$\theta_m = \frac{Q_m \cdot X_n}{\sum_n \theta_n \cdot X_n} \quad \text{Eq. 2.25}$$

$$\Psi_{mn} = \exp\left(-\frac{\hat{U}_{mn} - \hat{U}_{nm}}{R \cdot T}\right) = \exp\left(-\frac{\hat{a}_{mn}}{T}\right)$$

In the previous equation, θ_m is the area fraction of group m and the sums are taken over all different groups. X_n is the mole fraction of group m in the mixture. Ψ_m is a group interaction parameter. \hat{U}_{mn} is a measure of the energy of interaction between groups m and n . The variable \hat{a}_{mn} represents a non symmetric ($mn \neq nm$) group interaction parameter and has been obtained from experimental results. A program (ActDF) written

in Visual Basic for Applications under an Excel interface has been developed for ternary mixtures. The ActDF allows the calculation of the activities and the activity coefficients as a function of the concentration in a mixture and can be found in appendix A. A table with the necessary group interaction, volume and surface area parameters can be found as a part of the software.

2.2 Free volume theory

The free-volume theory has been developed by different people in different times, therefore, there are many different variants of the same theory.^[21] All of them refer to the difference between the observed molar volume at a defined temperature (V) and the volume occupied for the same molecule at defined reference condition.^[22, 23]

The empty volume (V_i^E) uses as a reference state the van der Waals volume, meaning that V_i^E is the total volume outside the van der Waals volume (eq. 2.26). The expansion volume (V_i^F) refers to the difference between the observed volume and the one which should occupy a molecule at 0 K in a close packed crystalline state (eq. 2.27). V_i^f refers to the fluctuation volume, which is proportional to the volume swept out by the center of gravity of 1 molecule as the result of its thermal vibration (V_i^Q) (eq. 2.28). From the above definitions, up to date the expansion volume is the most accepted as the free volume definition. Equations 2.26 to 2.28 show the definition of the different versions of the free volume theory.^[22, 23]

$$V_i^E = V_i - V_i^W \quad \text{Eq. 2.26}$$

$$V_i^F = V_i - V_i^C \quad \text{Eq. 2.27}$$

$$V_i^f = N_{A_i} \cdot V_i^Q$$
$$V_i^f = \frac{4}{3} \cdot \frac{V_i^{E3}}{\dot{A}_i} \cdot N_{A_i} \quad \text{Eq. 2.28}$$

$$V_i^f = \frac{V_i^{E3}}{27 \cdot V_i^{W2}}$$

The initial interest of the development of the free volume theory, was based on the intention to predict viscosity variations of pure liquids.^[24] Later, Fujita adapted this theory in order to describe diffusion in polymer-solvent systems.^[25] Vrentas and Duda

developed a model to describe tracer diffusion coefficients and binary diffusion coefficients for polymer-solvent systems.^[26, 27] Later, Ferguson and von Meerwall extended the Fujita diffusion equation for ternary concentrated solutions.^[28]

2.2.1 Diffusion of small molecules through polymers

Theoretical analysis of diffusion processes is an important step for a great number of applications. Different types of diffusion coefficients have to be considered in order to apply them under the proper conditions.

Tracer diffusion coefficients account for the mobility of a molecule in the absence of a concentration gradient. Techniques such as pulse field gradient NMR spectroscopy allow the measurement of tracer diffusion coefficients.^[29-43] The term tracer diffusion coefficient is often called self-diffusion coefficient, mainly referring to the diffusion of a given molecule in its pure liquid.^[44]

The Fickian diffusion coefficient is the most often used diffusion coefficient in engineering computational calculations. It refers to the diffusion of molecules due to the presence of a concentration gradient. Therefore, without any other driving force, the molecules will move from a high concentrated region to a region with lower concentration.

A third type of diffusion coefficient is the thermodynamic diffusion coefficient. This definition intends to express the rigorous driving force for mass transfer, i.e., it considers the chemical potential gradient instead of the sole concentration gradient. A relationship between the Fickian diffusivity and the thermodynamic diffusion coefficient is expressed in equation 2.29.

$$\frac{D_{12}^F}{D_{12}} = 1 + \frac{d \ln \gamma_1}{d \ln x_1} \quad \text{Eq. 2.29}$$

where D_{12}^F is the mutual diffusion coefficient, between the solvent and the polymer, for diffusion processes with a concentration gradient driving force according to the Fick's law, whereas, D_{12} is the thermodynamic diffusion coefficient. γ_1 and x_1 are the activity coefficient and the mole fraction of the solvent in the mixture, respectively.

For dilute solutions, the differences between all three diffusion coefficient definitions vanish. The oldest equation to describe this is the Einstein-Stokes equation (equation 2.30).^[45, 46] A most sophisticated one is the Wilke-Chang equation.^[47] One of the most used due to its simplicity is the Dullien equation, a simple relationship of critical and specific volumes.^[48]

$$D^{x \rightarrow 1} = \frac{k \cdot T}{6\pi \cdot \eta \cdot r} \quad \text{Eq. 2.30}$$

For the prediction and correlation of multicomponent thermodynamic diffusion coefficients, Vrentas et al. proposed an extension for ternary systems of the Vrentas & Duda diffusion theory.^[49] It is stated that this ternary extension can be reduced to the Fujita equation under sufficient conditions. Both versions of the free-volume theory suffer from not having predictive capabilities.^[44] More recently, based on the Maxwell-Stefan diffusion approach and the statistical model from Cohen & Turnbull, Wesselingh and Bollen developed an extension of the free-volume diffusion theory for multicomponent mixtures. This approach allows the calculation of Maxwell-Stefan diffusivities for simple liquid mixtures.^[21, 24, 50, 51]

2.1.1.1 Dullien equation

Based on a simple molecular model of liquids, the Dullien equation is capable to predict self-diffusion coefficients without the inclusion of any adjustable parameters. A combination of the molecular kinetic model and the elementary kinetic theory model of gases at the critical temperature allows the prediction of self-diffusion coefficients of liquids in terms of the critical volume, as shown in equation 2.31. For the Dullien equation, V_C represents the critical volume, MW is the molecular weight and V^* is the specific volume.

$$\hat{D} = \frac{1.124 \cdot 10^{-17} \cdot \text{mol}^{2/3} \cdot V_C^{2/3} \cdot R \cdot T}{\eta \cdot MW \cdot V^*} \quad \text{Eq. 2.31}$$

2.1.1.2 Vrentas & Duda theory

Although the free volume model for molecular transport is based on a simplified version of molecular processes, there exists a significant amount of evidence that supports the use of the theory in the prediction and correlation of viscosities and tracer diffusion

coefficients of simple liquids and polymeric materials.^[26] According to the Vrentas & Duda free volume diffusion model, the tracer diffusion coefficient for a diffusing solvent in a polymer is given by equation 2.32.^[26, 27]

$$\check{D}_1 = \dot{D}_1 \cdot e^{-\frac{E}{R \cdot T}} \cdot \exp\left(\frac{-\omega_1 \cdot \hat{V}_1^* - \xi_{12} \cdot \omega_2 \cdot \hat{V}_2^*}{\omega_1 \cdot \frac{K_{11}}{\lambda} \cdot (K_{21} - T_{g_1} + T) + \omega_2 \cdot \frac{K_{12}}{\lambda} \cdot (K_{22} - T_{g_2} + T)}\right) \quad \text{Eq. 2.32}$$

Here, \dot{D}_1 is a constant pre-exponential factor for the solvent, E is the energy that a molecule needs to overcome attractive forces which hold it to its neighbors. ω_i are the mass fraction of each component. \hat{V}_1^* and \hat{V}_2^* refer to the specific critical hole free-volume required for a jump of a solvent and a polymer, respectively. These two critical hole free volume values can be estimated as the specific volume of the solvent and the polymer at 0 K, i.e., the conversion in mass units of the zero point molar volume V^C .

ξ is the ratio of the critical molar volumes of a jumping unit of solvent to the one of the polymer jumping unit. λ represents an overlap factor in order to account for the fact that the same free-volume is available for more than one molecule (this parameter should be between 0.5 and 1). K_{11}/λ and K_{21} are the free-volume parameters for the solvent referred to itself and to the polymer, respectively; K_{12}/λ and K_{22} are the parameters for the polymer and are related to the Williams-Landel-Ferry (WLF) constants.^[52, 53] T_{g_1} stands for the glass transition temperature of the solvent and T_{g_2} for the one of the polymer.

For pure polymers, the temperature dependencies of the viscosity can be expressed by the WLF equation. Consequently, the free volume parameters for polymers are related to the WLF constants as shown in equations 2.34 and 2.35. A set of polymer free volume parameters are provided in table 2.3.^[52-54]

$$\log\left(\frac{\eta_2(T)}{\eta_2(T_{g_2})}\right) = \frac{-C_{12}^{WLF} \cdot (T - T_{g_2})}{C_{22}^{WLF} - T_{g_2} + T} \quad \text{Eq. 2.33}$$

$$K_{22} = C_{22}^{WLF} \quad \text{Eq. 2.34}$$

$$\frac{K_{12}}{\lambda} = \frac{\hat{V}_2^*}{2.303 \cdot C_{12}^{WLF} \cdot C_{22}^{WLF}} \quad \text{Eq. 2.35}$$

Table 2.3. Polymer free volume parameters.

Polymer	$K_{12}/\zeta \cdot 10^{-7}$	$K_{22} - T_{g_2}$	T_{g_2}
Poly(α -methylstyrene)	5.74	-395.7	445
Polybutadiene cis:trans:vinyl=43:50:7	6.10	-111.5	172
Polybutadiene cis:trans:vinyl=96:2:2	6.12	-101.4	161
Polycarbonate	5.64	-362.7	418
Poly(dimethylsiloxane)	9.32	-81.0	150
Poly(ethyl methacrylate)	3.40	-269.5	335
Poly(ethylene- <i>co</i> -propylene) 56:44 by mol	8.17	-175.3	216
Poly(ethylstyrene)	4.49	-286.9	355
Poly(isobutylene)	2.51	-100.6	205
Poly(isopropyl acrylate)	5.44	-208.4	262
Poly(methyl acrylate)	3.98	-231.0	276
Poly(methyl methacrylate) <i>atactic</i>	3.05	-301.0	381
Polypropylene	5.02	-205.4	253
Poly(propylene oxide)	9.52	-174.0	198
Poly(<i>p</i> -methylstyrene)	5.18	-330.0	348
Polystyrene	5.82	-327.0	373
Poly(vinyl acetate)	4.33	-258.2	305
Natural rubber	4.64	-146.4	200
Neoprene	3.91	-163.3	228

There are no feasible methods to model both the variation of the jumping activation energy E and the variation of the free volume with composition changes, therefore, E needs to be considered as a constant.^[44] Nevertheless, there are several diffusion studies which assumed a negligible effect of the activation energy over the diffusion behavior under a reasonable temperature range.^[44, 49, 53, 55] Rewriting equation 2.32, the Vrentas & Duda diffusion theory for binary systems is expressed as follows:

$$\begin{aligned} \tilde{D}_1 &= \ddot{D}_1 \\ \exp\left(\frac{-\omega_1 \cdot \hat{V}_1^* - \xi_{12} \cdot \omega_2 \cdot \hat{V}_2^*}{\omega_1 \cdot \frac{K_{11}}{\lambda} \cdot (K_{21} - T_{g_1} + T) + \omega_2 \cdot \frac{K_{12}}{\lambda} \cdot (K_{22} - T_{g_2} + T)}\right) & \text{Eq. 2.37} \end{aligned}$$

\ddot{D}_1 is a constant diffusion pre-exponential factor when the jumping activation energy is considered equal to zero. This equation becomes similar to the one for self-diffusion coefficients when the proper conditions are taken as presented in equation 2.38.^[24, 56]

$$\check{D}_i = \dot{D}_i \cdot \exp\left(-\lambda \cdot \frac{V_i^C}{V_i^F}\right) \quad \text{Eq. 2.38}$$

For the sake of simplicity, equation 2.37 can be rewritten with the introduction of the average hole free-volume per gram of mixture \hat{V}_{FH} . With the assumption of a negligible concentration dependence of the partial specific volumes of all components, equation 2.39 takes the following form for a ternary solvent–solvent–polymer system:^[49]

$$\tilde{D}_1 = \ddot{D}_1 \cdot \exp\left(\frac{-\omega_1 \cdot \hat{V}_1^* - \xi_{12} \cdot \omega_2 \cdot \hat{V}_2^*}{\hat{V}_{FH}/\lambda}\right) \quad \text{Eq. 2.39}$$

$$\begin{aligned} \hat{V}_{FH}/\gamma &= \omega_1 \cdot \frac{K_{11}}{\lambda} \cdot (K_{21} - T_{g_1} + T) + \omega_2 \cdot \frac{K_{12}}{\lambda} \\ &\quad \cdot (K_{22} - T_{g_2} + T) \end{aligned}$$

$$\tilde{D}_1 = \ddot{D}_1 \cdot \exp\left(\frac{-\omega_1 \cdot \hat{V}_1^* - \omega_2 \cdot \hat{V}_2^* \cdot \frac{\xi_{13}}{\xi_{23}} - \xi_{13} \cdot \omega_3 \cdot \hat{V}_3^*}{\hat{V}_{FH}/\lambda}\right) \quad \text{Eq. 2.40}$$

$$\tilde{D}_2 = \ddot{D}_2 \cdot \exp\left(\frac{-\omega_1 \cdot \hat{V}_1^* \cdot \frac{\xi_{23}}{\xi_{13}} - \omega_2 \cdot \hat{V}_2^* - \xi_{23} \cdot \omega_3 \cdot \hat{V}_3^*}{\hat{V}_{FH}/\lambda}\right) \quad \text{Eq. 2.41}$$

$$\begin{aligned} \frac{\hat{V}_{FH}}{\lambda} = & \omega_3 \cdot \frac{K_{13}}{\lambda} \cdot (K_{33} - T_{g_3} + T) \\ & + \sum_{j=1}^2 \omega_j \cdot \frac{K_{jj}}{\lambda} \cdot (K_{Pj} - T_{g_j} + T) \end{aligned} \quad \text{Eq. 2.42}$$

$$\frac{\hat{V}_{FH}}{\lambda} = \sum_{j=1}^3 \omega_j \cdot \frac{f_j}{\lambda} \cdot V_j^*$$

where f_j is the fractional hole free volume of pure component j . With the use of equations 2.40-2.42 it is possible to predict the tracer diffusion coefficients for ternary systems.

The accuracy of the diffusion coefficient calculation is largely governed by the estimation of ξ_{i3} .^[57] If binary data \check{D}_i vs. ω_i for both solvent-polymer systems is available, a nonlinear regression of equation 2.39 to estimate the parameters \check{D}_1 , \check{D}_2 , ξ_{13} , ξ_{23} , f_1/λ and f_2/λ can be done. Consequently, equations 2.40 to 2.42 are used in order to complete the calculation of the ternary tracer diffusion coefficients.

By following the procedure proposed by Zielinski and Duda and further explored by Hong, it is possible to determine all the free-volume parameters on a pseudo-predictive basis with the only use of liquid viscosity data as a function of temperature.^[53, 58] The parameter \check{D} from the Vrentas & Duda diffusion theory can be estimated by merging the Dullien self-diffusivity equation^[48] with the Vrentas & Duda equation simplified for a pure solvent. Later, the free volume parameters for a solvent i can be estimated by nonlinear regression of pure component viscosity and specific volume as a function of temperature.

$$\begin{aligned} \ln \left(\frac{1.124 \cdot 10^{-17} \cdot \text{mol}^{2/3} \cdot V_{Ci}^{2/3} \cdot R \cdot T}{\eta \cdot MW \cdot V_i^*} \right) \\ \frac{\hat{V}_i^*}{K_{i3}/\lambda} \\ = \ln(\check{D}_i) - \frac{\quad}{(K_{3i} - T_{g_i}) + T} \end{aligned} \quad \text{Eq. 2.43}$$

Afterwards, the computation of the ξ_{i3} parameters is needed. A linear correlation of the molar volume of polymer jumping unit with the glass transition temperature can be used

to estimate the overlap factors as shown in equations 2.44 and 2.45. These equations have not been extensively tested and the results can change with polymer properties variations, such as the degree of crosslinking. Nevertheless, the equations offer a prediction capability for the theory.^[53]

$$\xi_{i3} = \frac{V_i^C}{\tilde{V}_{3j}} = \frac{\hat{V}_i^* \cdot MW_{ij}}{\hat{V}_3^* \cdot MW_{3j}} \quad \text{Eq. 2.44}$$

$$\tilde{V}_{3j} = \frac{0.0925 \cdot T_{g3} + 69.47}{100^3} \quad (T_{g3} < 295 \text{ K})$$

$$\tilde{V}_{3j} = \frac{0.6224 \cdot T_{g3} + 86.95}{100^3} \quad (T_{g3} \geq 295 \text{ K}) \quad \text{Eq. 2.45}$$

The accuracy of the diffusion coefficient calculation is largely governed by the estimation of the ratio of critical molar volume of jumping units. Due to the vague definition and the consequently uncertain calculation of ξ_{i3} , the parameters are frequently adjusted from the diffusion data.^[44, 49, 59] However, ξ_{i3} has a broader meaning than simply being a correlative parameter used in free volume theory, since it signifies the extent to which the activation energy of shear viscosity and tracer diffusion are coupled, and whether there exists an apparent activation energy ceiling value for penetrant diffusion into polymers.^[57, 60-62] From a theoretical point of view ξ_{i3} can achieve any positive value, either greater or less than 1.^[63, 64] Nevertheless, experimental calculations suggest that the ξ_{i3} parameter should be less than 1.^[58, 65]

The above mentioned method is valid for uncrosslinked polymers. Nevertheless, it seems reasonable to expect that the theory can be extended to describe the tracer diffusion coefficient of solvent in amorphous crosslinked polymers. Vrentas et al. proposed an extension of the Vrentas & Duda diffusion theory for not too tightly crosslinked polymers. An inspection of equations 2.32, 2.40, 2.41, 2.42 and 2.44 reveals the following considerations:^[66]

- The energy of solvent migration and the jump distance for the solvent molecule are independent of the degree of crosslinking. Consequently, the constant pre-exponential diffusion factor of the solvents (\dot{D}_i) and the molecular energy necessary to overcome attractive forces which hold it to its neighbors (E) are independent of the degree of crosslinking of the polymer.

- The solvent properties are independent of the degree of crosslinking. Namely, the specific critical hole free-volume required for a jump (\hat{V}_i^*), the molecular weight of the solvent jumping unit (MW_{ij}) and the specific critical hole free-volume of the solvent ($\hat{V}_{FH_i} = f_i \cdot V_i^*$) are constant.
- The free volume configuration in the polymer (ζ) and the size of its jumping unit (MW_{3j}) are independent of the degree of crosslinking. As a result, $\xi_{13} \cdot \hat{V}_3^*$ remains unaffected by the degree of crosslinking.
- The thermal expansion coefficient for the total specific volume of the polymer and the thermal expansion coefficient for the sum of the specific occupied volume and the specific interstitial free volume are assumed to be independent of the degree of crosslinking.

From the above considerations, the introduction of crosslinking into the polymer affects the tracer diffusion coefficient only through the specific critical hole free-volume of the polymer \hat{V}_{FH_3} . Furthermore, from the last assumption, the following volumetric relationship is valid:

$$\frac{\hat{V}_{FH_3}(T, \dot{X})}{\hat{V}_{FH_3}(T, 0)} = \frac{V_3^*(0, \dot{X})}{V_3^*(0, 0)} = \frac{V_3^*(T, \dot{X})}{V_3^*(T, 0)} = \frac{V_3^*(T, \dot{X})}{V_3^*} = \varrho \quad \text{Eq. 2.46}$$

Here, $V_3^*(T, \dot{X})$ is the specific volume of the pure polymer at a temperature T and a degree of crosslinking \dot{X} . The effect of crosslinking on the free volume of the polymer is represented by ϱ . Lastly, for polymers without strong crosslinking, equations 2.40, 2.41, 2.42 are expressed as follows:

$$\check{D}_1 = \check{D}_1 \cdot \exp \left(\frac{-\omega_1 \cdot \hat{V}_1^* - \omega_2 \cdot \hat{V}_2^* \cdot \frac{\xi_{13}}{\xi_{23}} - \xi_{13} \cdot \omega_3 \cdot \hat{V}_3^*}{\hat{V}_{FH}/\lambda} \right) \quad \text{Eq. 2.47}$$

$$\check{D}_2 = \check{D}_2 \cdot \exp \left(\frac{-\omega_1 \cdot \hat{V}_1^* \cdot \frac{\xi_{23}}{\xi_{13}} - \omega_2 \cdot \hat{V}_2^* - \xi_{23} \cdot \omega_3 \cdot \hat{V}_3^*}{\hat{V}_{FH}/\lambda} \right) \quad \text{Eq. 2.48}$$

$$\begin{aligned}
 \frac{\hat{V}_{FH}}{\lambda} &= \sum_{\substack{j=1 \\ \text{solvents}}}^2 \omega_j \cdot \hat{V}_{FHj} + \omega_3 \cdot V_3^*(T, \dot{X}) \\
 &= \sum_{\substack{j=1 \\ \text{solvents}}}^2 \omega_j \cdot \frac{f_j}{\lambda} \cdot V_j^* + \omega_3 \cdot \frac{f_3}{\lambda} \cdot V_3^* \cdot \varrho
 \end{aligned}
 \tag{Eq. 2.49}$$

2.1.1.2 Wesselingh & Bollen method

Based on the Maxwell-Stefan diffusion approach^[50, 51] and the statistical model from Cohen and Turnbull^[24], Wesselingh and Bollen^[21] developed an extension of the binary free volume diffusion theory for multicomponent mixtures. This approach allows the calculation of Maxwell-Stefan (thermodynamic) mutual diffusivities for simple liquid mixtures. Wesselingh and Bollen proposed three mixing rules. The first mixing rules are oriented to the calculation of the tracer friction coefficients; the third one is addressed to the calculation of the mutual diffusion coefficient (section 2.1.1.3). Therefore, with the use of effective tracer friction coefficients ($\zeta_{i\#, \text{eff}}$), the tracer diffusion coefficients can be calculated.

The first mixing rule assumes a linear mixing of the free volume of pure components as shown in equation 2.50.^[67] The second mixing rule considers spherical molecules, and the free volume is considered as a function of the surface fraction (equation 2.51). For the calculation of the tracer friction factor, the third mixing rule considers the density of the mixture instead of the density of the single compounds. The density of the mixture is assumed as a linear mixing of the compounds as shown in equation 2.52. To achieve the calculation of the tracer friction factors, it is assumed that a compressed substance is arranged on a cubic lattice, with a lattice distance close to the molecular diameter (d).

$$V_M^F = \sum_{i=1}^{\text{all comp.}} x_i \cdot V_i^F
 \tag{Eq. 2.50}$$

$$\sigma_i = \frac{(V_i)^{\frac{2}{3}}}{\sum_{j=1}^n x_j \cdot (V_j)^{\frac{2}{3}}} \qquad V_i^{FF} = \frac{\sigma_i}{x_i} \cdot V_M^F
 \tag{Eq. 2.51}$$

$$\zeta_{i\#, i}^0 = 2 \cdot N_A \cdot \sqrt{3 \cdot k \cdot T \cdot \rho^{*C} \cdot d_i}
 \tag{Eq. 2.52}$$

$$\rho^{*C} = \sum_{i=1}^{all\ comp.} \frac{x_i \cdot MW_i}{V_i^C} \quad d_i = 2 \sqrt{\frac{V_i^C}{4/3 \cdot \pi \cdot N_A}}$$

Here, V_M^F is the total free volume of the mixture of polymer-solvent(s) and V_i^F are the single compound free volumes. σ_i represents the surface fractions of single compounds in the mixture. V_i represents the molar volume of the solvents and the molar volume of the polymer chain unit. V_i^{FF} are the surface weighted free volume which represents the free volume of a pseudo-pure solution. $\zeta_{i\#,i}^0$ is the tracer friction coefficient pre-exponential factor. V_i^C is the compressed molar volume, and ρ^{*C} is the compressed specific volume of the mixture.

According to the free volume theory, the tracer friction factor of a molecule which is assumed to be diffusing through an otherwise stagnant mixture of all components can be estimated as shown in equations 2.53 and 2.54. The method shown below allows the calculation of the tracer diffusivities of substances in a mixture. Note that, for a single substance, the tracer diffusion coefficient for a mixture reduces to the self-diffusion coefficient presented in equation 2.38.^[21, 26, 68, 69]

$$\zeta_{i\#,eff} = \zeta_{i\#,i}^0 \cdot \exp\left(\lambda \cdot \frac{V_i^C}{V_i^{FF}}\right) \quad \text{Eq. 2.53}$$

$$\check{D}_1 = \frac{R \cdot T}{\zeta_{i\#,i}^0} \quad \text{Eq. 2.54}$$

$$\check{D}_i = \check{D}_1 \cdot \exp\left(-\lambda \cdot \frac{V_i^C}{V_i^{FF}}\right)$$

2.1.1.3 Mutual diffusion coefficient

The mutual diffusion coefficients are vital for the analysis of many polymer processing operations.^[26] The term tends to be confusing for mixtures of superior order, therefore, it is often call as thermodynamic or Maxwell-Stefan diffusion coefficient.

In order to obtain an expression for the mutual diffusion coefficients, an expression which relates the self-friction coefficient is needed. Unfortunately, there appears to be no appropriate theory which can be readily evaluated to produce an expression which relates the self-friction factors between each other for polymer-solvent systems.^[21, 26] A

common assumption is to consider that the mutual coefficients are the geometrical average of the two corresponding self-coefficients, as shown in equation 2.55.

$$\zeta_{i,j} \forall i \neq j = \sqrt{\zeta_{i\#,i} \cdot \zeta_{j\#,j}} \quad \text{Eq. 2.55}$$

Hence, the mutual diffusion coefficient for a binary polymer–solvent system can be determined as follows:^[68, 70, 71]

$$D = \check{D}_1 \cdot (1 - \phi_1)^2 \cdot (1 - 2 \cdot \chi \cdot \phi_1) \quad \text{Eq. 2.56}$$

For the most engineering and membrane processes where diffusion plays a key role, equation 2.56 can be applied. However, for middle-high permeant concentration as well as multicomponent mixtures, additional parameters – which need to be fitted from experimental diffusion data – have to be included in order to describe the mutual diffusivities of the system.

The above mentioned equations to estimate the binary diffusion coefficients cannot be easily extended for ternary systems without the introduction of unknown parameters which need to be adjusted from the experimental data. To achieve the extension for ternary systems, Wesselingh and Bollen consider that the effective tracer friction coefficients are linearly related with the self-diffusion friction coefficients, as shown in equation 2.57. Therefore, it is considered that the tracer friction coefficients have a low concentration dependence, so they do not influence each other.^[21]

$$\zeta_{i\#,eff} = x_i \cdot \zeta_{i\#,i} + \sum_{\forall j \neq i} x_j \cdot \zeta_{i\#,j} \quad \text{Eq. 2.57}$$

By introducing equation 2.55 into equation 2.57, and after proper reorganization, the mutual friction coefficients for ternary solvent–solvent–polymer systems can be calculated with equation 2.58.

$$\zeta_{ij} = \frac{\zeta_{i\#,eff} \cdot \zeta_{j\#,eff}}{\sum_k x_k \cdot \zeta_{k\#,eff}} \quad \forall i \neq j \quad \text{Eq. 2.58}$$

where ζ_{ij} represents the mutual diffusion coefficient and the summation is done over the whole number of components. The mutual diffusion coefficient is estimated with equation 2.59.

$$D_{ij} = \frac{R \cdot T}{\zeta_{ij}} \quad \forall i \neq j \quad \text{Eq. 2.59}$$

2.3 Membrane separation process

2.3.1 Polymer membranes

A membrane is a layer which serves as a selective barrier between two or more substances and has the ability to transport one element faster than the other ones.^[72, 73] Some components are allowed in different grades to pass through the membrane into the permeate stream, whereas the nonpermeated substances are kept in the retentate side. A schematic representation of a membrane separation process is shown in figure 2.2.

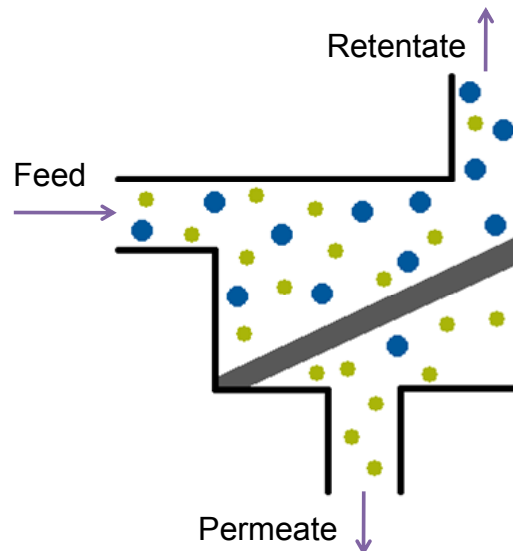


Figure 2.2. Schematic representation of a membrane separation module.

There are different types of membranes and they can be classified by the material, porosity and structure. The following sections are focused on polymeric membranes, whereas the explanations are not necessary exclusive and can be applied to metal and ceramic membranes as well.

A microporous membrane, which is similar to a conventional filter, is a structure with interconnected pores on the order of 10 nm to 10 μm in diameter.^[73] Due to the membrane conformation, variations in the pore diameter over the membrane are found in mostly all polymeric pore membranes. Therefore, the separation process consists in

size exclusion where the particles bigger than the biggest pore are totally rejected, whereas the particles smaller than the smallest pore pass totally through the membrane. Particles with a size in between the biggest pore diameter and the smallest one are partially rejected according to the pore size distribution. Generally, only molecules with a notably difference in size can be separated effectively by a microporous membrane. For that reason, a common area for the use of microporous membrane are microfiltration and ultrafiltration, e.g., water filtration.

Nonporous membranes, also known as dense membranes, are dense films where the permeants are transported by diffusion through the layer under the influence of driving forces such as pressure, concentration, or electrical potential gradient.^[73] In nonporous membranes, the glass transition temperature of the polymer plays a key role on the characteristics of the membrane. The separation process is related to the relative transport of the substances through the membrane, i.e., diffusivity and solubility of the substances in the mixture with the membrane material. Nonporous membranes have the capability to separate substances with similar size if their diffusivity and/or solubility are different enough. Most gas separation, pervaporation, reverse osmosis and nanofiltration processes use dense membrane for the separation process. The above mentioned classification is used for the sake of simplicity, but there is no distinct transition between porous and nonporous membranes. Many of the membranes (e.g., membranes for reverse osmosis applications) can be considered as an intermediate between porous and nonporous membranes.^[72]

The membranes can be also classified by their structure. Anisotropic membranes, also known as asymmetric membranes, are formed by a thin porous or dense layer supported by a thicker porous structure. Isotropic membranes, also known as symmetric membranes, have a homogeneous pore structure over the cross section.^[72] Anisotropic membranes can be further classified in integral and composite membranes. Integral anisotropic membranes are formed by a single material with a structure variation over the cross section, whilst composite ones are formed by two or more distinctive layers, usually made from different polymers.^[73] Anisotropic membranes allow high transport rates due to the small thickness of the thin layer which exclusively determines the separation properties of the whole membrane. A schematic representation of different types of membranes by structure and porosity is presented in figure 2.3.

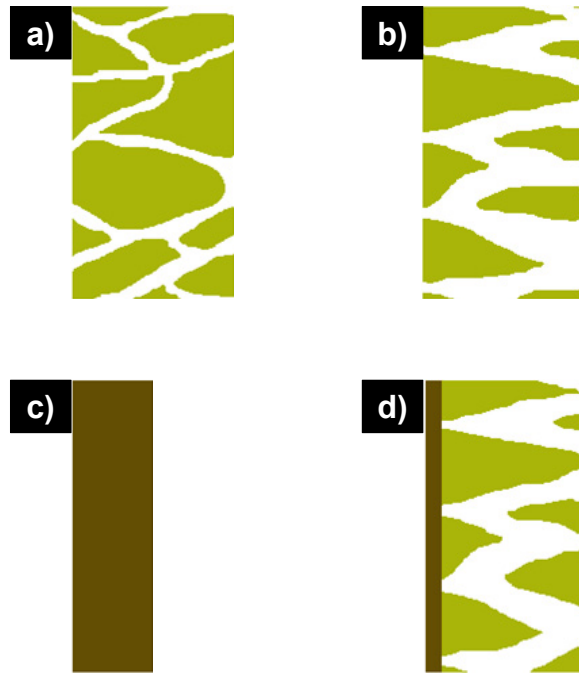


Figure 2.3. Schematic representation of four basic types of membranes. a) Isotropic porous membrane b) Integral anisotropic porous membrane c) Isotropic dense membrane d) Composite anisotropic membrane

2.3.1.1 Chain mobility as a function of temperature

Great differences in membrane performances can be found when the polymer behavior in the glassy and rubbery state are compared, i.e., below and above the glass transition temperature. The glassy state can be considered as a *frozen* state with highly restricted mobility of chain segments and low thermal energy to allow rotation around the main chain.^[72] In contrast, in the rubbery state the mobility of chain segments is increased and a *frozen* state is no longer present, facilitating the increment of the free volume with the temperature as shown in figure 2.4. Therefore, the micro-voids formed by the free volume facilitate the passing of the molecules through the polymer with the consequent increment of the permeation rates.

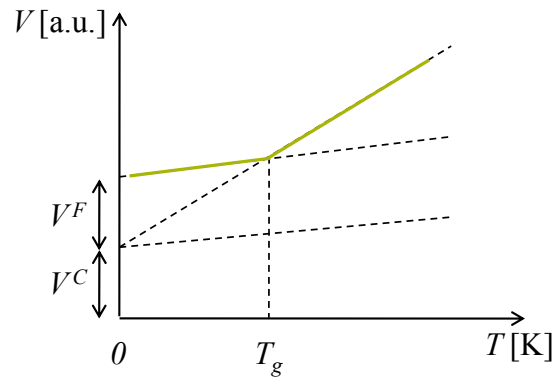


Figure 2.4. Volume of an amorphous polymer as a function of temperature.

A large number of polymers are semi-crystalline, i.e., they present a combination of amorphous and crystalline fractions. The degree of crystallinity influences the transport through nonporous membranes for both gas and liquid permeants. The presence of crystals impedes the diffusion of permeants through the membrane. Therefore, the crystalline fraction is considered to be impermeable whereas the diffusion is considered to take place only through the amorphous fraction.^[72]

2.3.1.2 Membrane separation processes

There are many developed membrane separation processes involving the liquid and gas states. In gas separation, gas mixtures at high pressure pass across a membrane that is selectively permeable to one component of the feed mixture. To separate mixtures with similar boiling point or azeotropes which are difficult to separate by distillation, a pervaporation process can be used. This process consists in a separation of a mixture of liquids by partial vaporization through the membrane. Therefore, the driving force for the process is the low vapor pressure on the permeate side of the membrane generated by cooling and condensing the permeate vapor.

Microfiltration and ultrafiltration separation processes are based on molecular sieving through increasingly big pores, with the difference between both processes being only in the type of molecules to be separated as depicted in figure 2.5. As microfiltration and ultrafiltration, nanofiltration and reverse osmosis are pressure driven separation processes. Both, nanofiltration and reverse osmosis, are used to separate low molecular weight solutes or small organic molecules from a solution, with the use of membranes which are between open porous and dense ones.^[72] The main differences between

nanofiltration and reverse osmosis are the application where they are used. For instance, nanofiltration membranes are basically the same as the ones for reverse osmosis, differing only in the more open network structure for the nanofiltration ones. Hence, lower pressures have to be applied in nanofiltration (up to 60 bar) than in reverse osmosis (up to 200 bar).

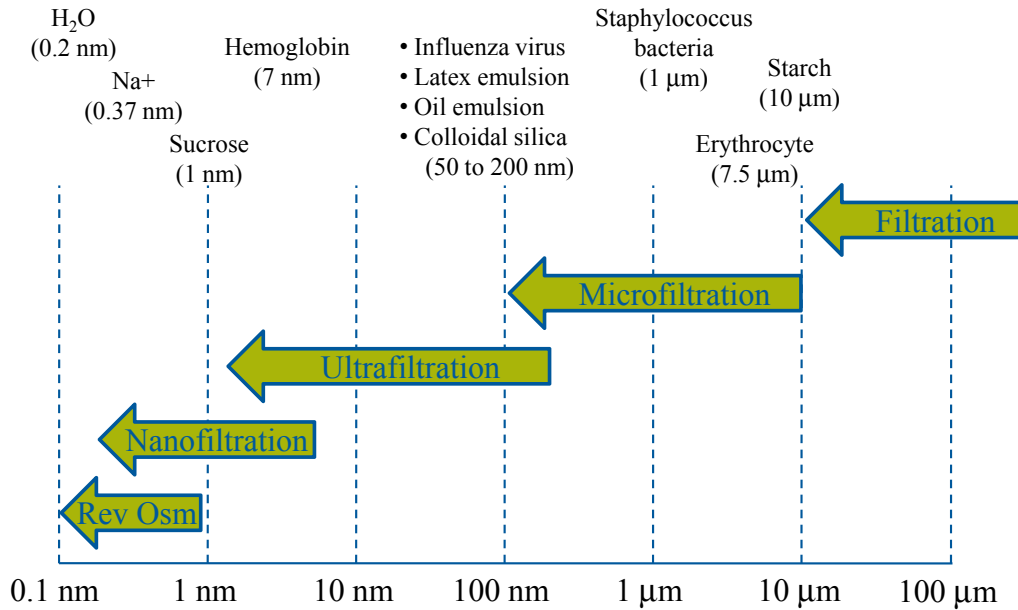


Figure 2.5. Application range of different liquid filtration processes

For pressure driven processes, the quality of a given membrane is generally represented through the retention factor \dot{R} and the permeability of a component i is represented by L_i . The retention factor represents the quality of the separation process, while the permeability indicates how fast the separation in the membrane occurs. Equations 2.60 and 2.61 show the way of calculation for the retention factor and the permeability of the membrane for binary mixtures. In these equations, c represents the concentration of the component which is desired to separate form the mixture, the subscripts F and P represent the feed and the permeate side, J is the molar flux and ΔP is the transmembrane pressure.

$$\dot{R} = 1 - \frac{c_F}{c_P} \quad \text{Eq. 2.60}$$

$$L_i = \frac{J_i}{\Delta P} \quad \text{Eq. 2.61}$$

For some composite membranes under the effect of high pressure, a falling rate behavior of the permeation flux has been found somewhere else.^[74] This behavior can be explained by the fact that the majority of composite membranes can compact themselves during the filtration process. The consequence of this compaction resides in a decrease of the membrane thickness with the consequent reduction of the free volume inside the membrane and the further reduction of the permeation flux. Consequently, the flux decreases when the pressure increases, as if the effective thickness of the selective layer would increase without any change on the free volume.

Machado et al. described the falling behavior with the following relations (equations 2.62 and 2.63). There, L_i^0 and l_i^0 are the permeability and the membrane thickness under atmospheric pressure, respectively.^[75]

$$J_i = L_i^0 \cdot e^{-\alpha \cdot \Delta P} \cdot \Delta P$$

$$L_i^0 \sim \frac{1}{l^0} \quad \text{Eq. 2.62}$$

$$J_i = L_i(P) \cdot \Delta P$$

$$L_i = \frac{1}{l} \quad \text{Eq. 2.63}$$

$$l = l^0 \cdot e^{\alpha \cdot \Delta P}$$

The compaction factor α is extensively related to the swelling degree of the membrane. Therefore, for a mixture of solvents, a mixing rule which describes the compaction for a broad concentration range needs to be considered.^[76]

$$\alpha = \sum_{\substack{i \\ \text{all comp.}}} a_i \cdot \alpha_i \quad \text{Eq. 2.64}$$

Here, α is the compaction factor of the membrane and α_i is the compaction factor which appears in the presence of a pure solvent i . The selection of a mixing rule which is a function of the solvent activities instead of the molar fractions was done in order to consider the whole contribution of the chemical potential instead of only the one from the molar fractions.

2.3.2 Pore–flow model

The transport mechanism through porous membranes is based on the pore–flow model. The principle of the separation process is based on size exclusion, which is the filtration process that resembles the most to a conventional filtration. The starting point for the mathematical description of permeation in all membranes is that the driving forces of pressure, temperature, concentration and electromotive force are interrelated and that the overall driving force producing movement of a permeant is the gradient in its chemical potential.^[77] Equation 2.65 represents the volumetric flux of a substance i (J_i) as a function of the molar concentration, the mobility or flexibility of the substance i when it goes through the membrane and the driving force.^[78]

$$J_i = -\bar{c}_i \cdot \tilde{L}_i \frac{d\mu_i}{dz} \quad \text{Eq. 2.65}$$

where $d\mu_i/dz$ is the chemical potential gradient which appears over the membrane thickness. \tilde{L}_i is a proportionality coefficient which represents the mobility of the permeant and is not necessarily constant, and \bar{c}_i is the average molar concentration of the component i . With the consideration of driving forces that are only generated by concentration and pressure gradients, the chemical potential can be described as presented in equation 2.66. c_i is the molar concentration of component i , γ_i is the activity coefficient, P is the pressure and V_i is the molar volume.

$$d\mu_i = R \cdot T \cdot d \ln(\gamma_i \cdot x_i) + V_i \cdot dP \quad \text{Eq. 2.66}$$

The first assumption that has to be made in order to define any model of permeation is that the fluids on either side of membrane are in equilibrium with the membrane at the interface. Consequently, there is a continuous gradient of the chemical potential across the membrane. Additionally, the pore–flow model assumes that the concentrations of solvent and solute within a membrane are uniform and that the chemical potential gradient across the membrane can be expressed only as a pressure gradient (as represented in figure 2.6). In the pore–flow model, the pressure difference produces a smooth gradient in pressure through the membrane, but the solvent activity ($\gamma_i c_i$) remains constant within the membrane.^[77]

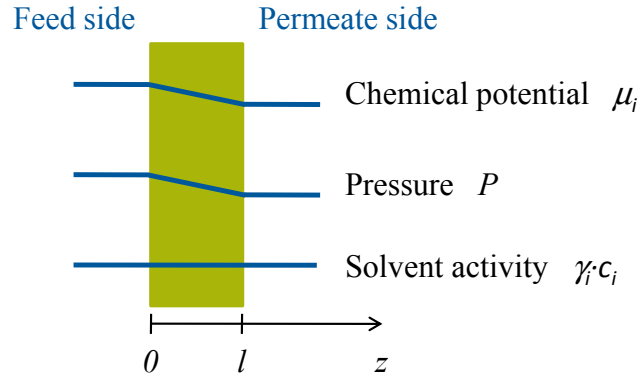


Figure 2.6. Pressure-driven permeation process through a membrane, according to the pore-flow transport model.

When considering a constant solvent activity within the cross section of the membrane, equations 2.65 and 2.66 can be combined and integrated over the membrane thickness in order to obtain an expression for the flux of a component i through the pores of the membrane.

$$J_i = -c_{i,F} \cdot \tilde{L}_i \cdot V_i \cdot \frac{dP}{dx} \quad \text{Eq. 2.67}$$

$$J_i = \frac{c_{i,F} \cdot k_i^D}{l \cdot \eta_i} \cdot \Delta P \quad \text{Eq. 2.68}$$

where $c_{i,F}$ is the molar concentration upstream from the membrane, k_i^D is the Darcy's law coefficient, and l is the thickness of the membrane. The negative sign is missing in order to show that the flux direction goes from the high pressure side to the low pressure one. The Darcy's law coefficient can be related to the pore properties of the membrane. The most widely used parameters are the porosity (ϵ), the tortuosity (τ) and the pore radius (\check{r}). A schematic is shown in figure 2.7. The membrane porosity is the fraction of the total membrane volume that corresponds to the volume of the pores. The tortuosity expresses a measure of the average pore length compared to the thickness of the membrane. The pore diameter determines the ability of the membrane to separate a determined substance from the mixture according to the size exclusion principle. With the introduction of the above mentioned parameters, for laminar convective flow through a porous system, the Hagen-Poiseuille equation can be applied as presented in equation 2.69.

$$j_i = c_{i,F} \cdot \frac{\varepsilon \cdot \check{\gamma}^2}{8 \cdot \eta_i \cdot \tau} \cdot \frac{\Delta P}{l} \quad \text{Eq. 2.69}$$

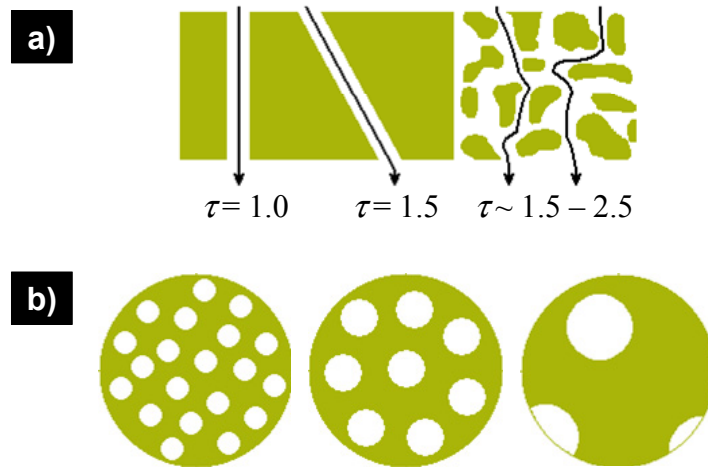


Figure 2.7. Schema of the different parameters which affect the behavior of microporous membranes. a) Cross section of porous membranes with different tortuosity. b) Surface view of porous membranes with same porosity and different pore diameters.

2.3.3 Solution–diffusion model

The transport through non–porous membranes (dense membranes) is described with the solution-diffusion model. Reverse osmosis, nanofiltration, pervaporation and gas permeation polymeric membranes have a dense layer with no visible pores, which is the layer where the separation occurs. These kinds of membranes make possible the separation of molecules smaller than the ones separated with microfiltration or ultrafiltration porous membranes due to their higher hydrodynamic resistance.^[72] For those processes, the transport mechanism implies three steps: absorption on the feed side, diffusion through the membrane and desorption on the permeate side. To be coherent with the general assumption of a continuous gradient of the chemical potential, it is implicit that the rate of absorption and desorption at the membrane interface are much higher than the rate of diffusion through the membrane. The absorption and desorption processes do not influence the overall transport rate of the molecules through the membrane, therefore, the limiting process for the permeation rate is only the diffusion of the substances through the membrane. The last considerations are no longer

valid in transport involving chemical reactions or in diffusion of gases through metals, where the absorption/desorption rates are slow.^[73]

Contrary to the pore–flow model, the solution-diffusion model assumes that the pressure within the membrane is constant. Therefore, the chemical potential gradient across the membrane is produced only as a concentration gradient between the feed and the permeate side, as shown in figure 2.8. This assumption implies that the membrane transmits the pressure in the same way as liquids.^[77]

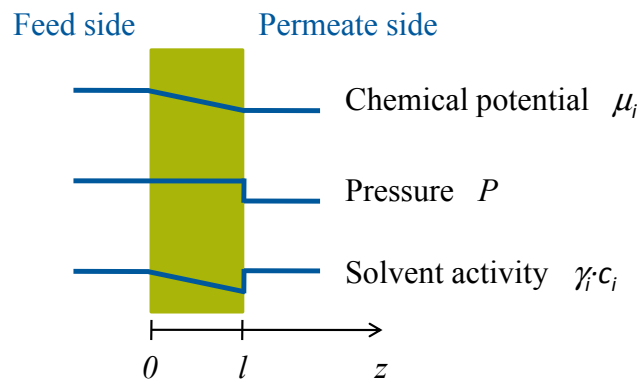


Figure 2.8. Pressure-driven permeation process through a membrane according to the solution-diffusion model.

The solution-diffusion model has the same starting point as the pore–flow model, as shown in equation 2.65, where the flux is related to the concentration, the mobility or flexibility of the permeating molecule and the driving force expressed by the chemical potential gradient. The Nernst-Einstein equation offers a relationship between the thermodynamic diffusion coefficient (D_i) and the mobility of the permeating molecule. With the combination of equations 2.65, 2.66 and 2.70, the general transport equation can be written as a function of a constant diffusion coefficient as presented in equation 2.71.

$$D_i = \tilde{L}_i \cdot R \cdot T \quad \text{Eq. 2.70}$$

$$J_i = -\bar{c}_{i,M} \cdot D_i \cdot \left(\frac{d \ln(a_i)}{dz} + \frac{V_i}{R \cdot T} \cdot \frac{dP}{dz} \right) \quad \text{Eq. 2.71}$$

Equation 2.71 can be reduced to the well known Fick’s first law of diffusion, when the concentration gradient is considered as the only driving force. Therefore, under the

proper conditions, the thermodynamic diffusion coefficient becomes equal to the Fick's diffusion coefficient.

$$J_i = -D_i^F \cdot \left(\frac{dc_i}{dz} \right) \quad \text{Eq. 2.72}$$

With the consideration of a constant pressure over the whole cross section of the membrane, the term dP/dz from equation 2.66 is equal to zero after the integration inside the membrane over the membrane thickness. Consequently, the flux of a component i can be expressed as follows:

$$J_i = -\frac{\bar{c}_{i,M} \cdot D_i}{l} \cdot \ln \left(\frac{a_{i,MP}}{a_{i,MF}} \right) \quad \text{Eq. 2.73}$$

$$J_i = \frac{\bar{c}_{i,M} \cdot D_i}{l} \cdot (\ln a_{i,MF} - \ln a_{i,MP})$$

With the consideration that the feed and permeate mixtures are in equilibrium with the membrane interfaces, the chemical potential of each component outside the membrane are equal to the ones inside the membrane. Therefore, this consideration allows the estimation of the activities inside the membrane by calculating the activities at the feed and permeate side outside the membrane.

$$\begin{aligned} \mu_{i,F} &= \mu_{i,MF} \\ \mu_{i,F} - \mu_i^0 &= \mu_{i,MF} - \mu_i^0 \\ R \cdot T \cdot \ln a_{i,F} + V_i \cdot (P_F - P_0) &= R \cdot T \cdot \ln a_{i,MF} + V_i \cdot (P_{MF} - P_0) \end{aligned} \quad \text{Eq. 2.74}$$

$$\xrightarrow{P_F = P_{MF}} a_{i,F} = a_{i,MF}$$

$$\begin{aligned} \mu_{i,P} &= \mu_{i,MP} \\ \mu_{i,P} - \mu_i^0 &= \mu_{i,MP} - \mu_i^0 \\ R \cdot T \cdot \ln a_{i,P} + V_i \cdot (P_P - P_0) &= R \cdot T \cdot \ln a_{i,MP} + V_i \cdot (P_{MP} - P_0) \end{aligned} \quad \text{Eq. 2.75}$$

$$\xrightarrow{P_{MP} = P_P} R \cdot T \cdot \ln a_{i,P} = R \cdot T \cdot \ln a_{i,MP} + V_i \cdot (P_F - P_P)$$

$$\ln a_{i,P} - \frac{V_i}{R \cdot T} \cdot \Delta P = \ln a_{i,MP}$$

$$J_i = \frac{\bar{c}_{i,M} \cdot D_i}{l} \cdot \left[\ln a_{i,F} - \left(\ln a_{i,P} - \frac{V_i}{R \cdot T} \cdot \Delta P \right) \right] \quad \text{Eq. 2.76}$$

$$J_i = \frac{\bar{c}_{i,M} \cdot D_i}{l} \cdot \frac{V_i}{R \cdot T} \cdot \left[\Delta P + \frac{R \cdot T}{V_i} \cdot \ln \left(\frac{a_{i,F}}{a_{i,P}} \right) \right] \quad \text{Eq. 2.77}$$

Equation 2.71 can be integrated in the outer membrane surfaces obtaining an identical result as shown in equation 2.76. To achieve this result, it is not necessary to consider a constant pressure over the cross section of the membrane. The pressure inside the membrane can be considered as a linear gradient; therefore, the most controversial assumption of the solution-diffusion model (i.e., constant pressure inside the membrane) vanishes, as shown in figure 2.9.

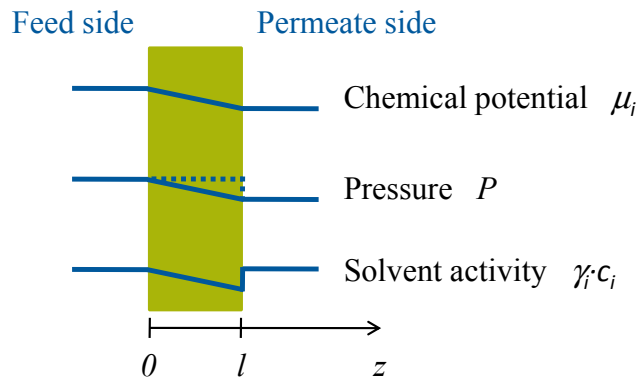


Figure 2.9. Pressure-driven permeation process through a membrane according to the solution-diffusion model without constant pressure consideration.

$$\begin{aligned} \int_0^l J_i \cdot dz &= -\bar{c}_{i,M} \cdot D_i \cdot \left(\int_{a_{i,F}}^{a_{i,P}} d \ln(a_i) + \frac{V_i}{R \cdot T} \cdot \int_{P_F}^{P_P} dP \right) \\ J_i \cdot l &= -\bar{c}_{i,M} \cdot D_i \cdot \left[\frac{V_i}{R \cdot T} \cdot \Delta P + \ln \left(\frac{a_{i,P}}{a_{i,F}} \right) \right] \\ J_i \cdot l &= -\bar{c}_{i,M} \cdot D_i \cdot \frac{V_i}{R \cdot T} \cdot \left[(P_P - P_F) + \frac{R \cdot T}{V_i} \cdot \ln \left(\frac{a_{i,P}}{a_{i,F}} \right) \right] \\ J_i &= \frac{\bar{c}_{i,M} \cdot D_i}{l} \cdot \frac{V_i}{R \cdot T} \cdot \left[\Delta P + \frac{R \cdot T}{V_i} \cdot \ln \left(\frac{a_{i,F}}{a_{i,P}} \right) \right] \end{aligned} \quad \text{Eq. 2.78}$$

2.3.3.1 Concentration inside the membrane

The concentration inside the membrane can be estimated with the Flory-Huggins-Staverman theory for ternary systems after the consideration presented in equation 2.74, as follows:

$$\begin{aligned} \ln a_{1,F} = \ln \phi_{1,M} + (1 - \phi_{1,M}) - \frac{V_1}{V_2} \cdot \phi_{2,M} - \frac{V_1}{V_3} \cdot \phi_{3,M} \\ + (\chi_{12} \cdot \phi_{2,M} + \chi_{13} \cdot \phi_{3,M}) \cdot (\phi_{2,M} + \phi_{3,M}) \\ - \chi_{23} \cdot \frac{V_1}{V_2} \cdot \phi_{2,M} \cdot \phi_{3,M} \end{aligned} \quad \text{Eq. 2.79}$$

$$\begin{aligned} \ln a_{2,F} = \ln \phi_{2,M} + (1 - \phi_{2,M}) - \frac{V_2}{V_1} \cdot \phi_{1,M} - \frac{V_2}{V_3} \cdot \phi_{3,M} \\ + \left(\chi_{12} \cdot \phi_{1,M} \cdot \frac{V_2}{V_1} + \chi_{23} \cdot \phi_{3,M} \right) \\ \cdot (\phi_{1,M} + \phi_{3,M}) - \chi_{13} \cdot \frac{V_2}{V_1} \cdot \phi_{1,M} \cdot \phi_{3,M} \end{aligned} \quad \text{Eq. 2.80}$$

$$\phi_{1,M} + \phi_{2,M} + \phi_{3,M} = 1 \quad \text{Eq. 2.81}$$

2.3.4 Solution–diffusion with imperfections model

The solution-diffusion with imperfections model was an early modification of the solution-diffusion model. Sherwood et al. postulated that the transport mechanism can be expressed as a combination of diffusion through the dense layer of the membrane and pore transport through small imperfections or defects in the membrane.^[79] Therefore, the model adds a second term to the solution-diffusion model, corresponding to the possible viscous transport across the membrane, as shown in equation 2.82.^[79-81]

$$\begin{aligned} J_i &= J_{i,SDM} + J_{i,VT} \\ J_i &= J_{i,SDM} + c_{i,F} \cdot \frac{K^*}{l \cdot \eta_m} \cdot \Delta P \end{aligned} \quad \text{Eq. 2.82}$$

Here, $J_{i,SDM}$ represents the flux calculated with the solution diffusion model and $J_{i,VT}$ the flux from the viscous contribution. The term K^* is a coupling coefficient describing the pore flow similar to the Darcy's law coefficient. η_m corresponds to the viscosity of the mixture of permeants.

Equation 2.82 considers that the solute concentration at the exit of an imperfection is the same as at the entrance, which is only justified with the assumption that the imperfections are nonselective. However, the imperfections are surrounded by a matrix where the solute exit concentration is decreased. That gives rise to diffusion along the membrane which causes a concentration decrease at the exit of the imperfection.

Therefore, modifications to the solution-diffusion with imperfections model have been proposed in order to consider lateral diffusion to level the solute concentration at the end of the imperfections.^[82]

For mixtures of organic compounds with different sizes, a selectivity factor needs to be included in equation 2.82 in order to account for any separation discrimination between small and large molecules within the imperfections.^[47] Moreover, for a general case where the imperfections are inhomogeneous, equation 2.82 becomes as follows:

$$J_i = J_{i,SDM} + c_{i,F} \cdot \frac{K^* \cdot \tilde{\alpha}_i}{l \cdot \eta_m} \cdot \Delta P$$

$$J_i = J_{i,SDM} + c_{i,F} \cdot \frac{\tilde{K}_i}{l \cdot \eta_m} \cdot \Delta P$$

Eq. 2.83

Here, $\tilde{\alpha}_i$ represents a selectivity factor due to the nature of the imperfections and \tilde{K}_i corresponds to the partial mechanical permeability of the imperfections. The solution-diffusion with imperfection model has shown in the past years an excellent improvement over the solution-diffusion model when permeation data for reverse-osmosis and nanofiltration membrane processes are analyzed. Nevertheless, the solution-diffusion with imperfections model has two major disadvantages. The first inconvenience is related to the partial mechanical permeability (\tilde{K}_i) due to the nature of the imperfections (pores), which value is not possible to determine from the pore-flow model parameters (i.e., pore diameter, tortuosity and porosity). Therefore, for real membranes the parameter has to be found experimentally. The second disadvantage resides in the nature of the parameters which describe the diffusive flux. These parameters normally can be affected by both the concentration and the applied pressure (e.g., diffusion coefficients) with the consequent deviation between the experimental data and the calculated one.^[80]

2.3.5 Stefan–Maxwell multicomponent diffusion transport equation

The Maxwell–Stefan transport equation represents a force balance between the driving forces of one component expressed as an energy gradient and its friction forces with all other components.^[83]

$$\frac{-d(R \cdot T \cdot \ln a_i)}{dz} - V_i \cdot \frac{dP}{dz} = \sum_{\substack{j=1 \\ \forall j \neq i}}^n x_j \cdot \zeta_{ij} \cdot (\check{u}_i - \check{u}_j) \quad \text{Eq. 2.84}$$

Here, \check{u} represents the diffusive velocity. According to Straatsma et al., the friction force of an i component with the membrane (F_M) can be taken into account by adding the following term:^[84]

$$F_M = \zeta_{iM} \cdot \check{u}_i \quad \text{Eq. 2.85}$$

As mentioned in the previous section, the viscous transport occurs next to the diffusive transport in dense membranes. Therefore, the total velocity (\check{w}_i) is expressed as the sum of the diffusive velocity and the viscous one.

$$\check{v}_i = -\frac{K^*}{\eta} \cdot \frac{dP}{dz} \quad \text{Eq. 2.86}$$

$$\check{w}_i = \check{u}_i + \check{v}_i \quad \text{Eq. 2.87}$$

Finally, equation 2.84 can be rewritten as follows:

$$\begin{aligned} \frac{-d(R \cdot T \cdot \ln a_i)}{dz} - V_i \cdot \frac{dP}{dz} - \zeta_{iM} \cdot \frac{K^*}{\eta} \cdot \frac{dP}{dz} \\ = \sum_{\substack{j=1 \\ \forall j \neq i}}^n x_j \cdot \zeta_{ij} \cdot (w_i - w_j) + \zeta_{iM} \cdot w_i \end{aligned} \quad \text{Eq. 2.88}$$

The solution-diffusion with imperfections model, as the majority of filtration type specific transport models, has not started from general transport equations (i.e., statistical–mechanical transport equation or Stefan–Maxwell equation for multicomponent diffusion), but instead is based on experimental observations of the particularities of each specific separation process.^[47] Mason and Lonsdale^[47] showed how the general transport equations yield to the solution-diffusion with imperfections model when the inherent conditions of the nanofiltration process are taken.

2.4 References

1. Van Krevelen, D.W., *Properties of Polymers*. 3rd ed. 1990, Amsterdam: Elsevier.

2. Bondi, A., *Physical Properties of Molecular Crystals, Liquids and Glasses*. 1968, New York: John Wiley and Sons Inc. 502.
3. Slonimskii, G.L., A.A. Askadskii, and A.I. Kitaigorodskii, *Visokomolekuliarnie Soedinenia*, 1970. **12**: p. 494.
4. Askadskii, A.A., *Chemical Yearbook IV*, ed. R.A. Pethrick and G.E. Zaikov. 1987, London: Harwood Acad. Publ.
5. Sugden, S., *Molecular Volumes at Absolute Zero. Part II. Zero Volumes and Chemical Composition*. *Journal of the Chemical Society (Resumed)*, 1927. **1927**: p. 1786-1798.
6. Gibbs, J.W., *A method of geometrical representation of the thermodynamic properties of substances by means of surfaces*. 1873, New Haven.
7. Gibbs, J.W., *Josiah W. Gibbs papers*. 1873.
8. Perrot, P., *A to Z of thermodynamics*. 1998, Oxford; New York: Oxford University Press.
9. Flory, P.J., *Principles of polymer chemistry*. 15. printing ed. The George Fisher Baker non-resident lectureship in chemistry at Cornell University. 1953, Ithaca: Cornell University Press.
10. Allcock, H.R., F.W. Lampe, and J.E. Mark, *Contemporary polymer chemistry*. 2003, Upper Saddle River, N.J.: Pearson Education/Prentice Hall.
11. Hiemenz, P.C. and T.P. Lodge, *Polymer chemistry*. 2007, Boca Raton, Fla. [u.a.]: CRC Press.
12. Sperling, L.H., *Introduction to physical polymer science*. 2006, Hoboken, N.J.: Wiley.
13. Bristow, G.M. and W.F. Watson, *Cohesive Energy Densities of Polymers: Part I.- Cohesive Energy Densities of Rubbers by Swelling measurements*. *Transactions of the Faraday Society*, 1958. **54**(1): p. 1731-1741.
14. Prausnitz, J.M., R.N. Lichtenthaler, and E.G.d. Azevedo, *Molecular thermodynamics of fluid-phase equilibria*. Prentice-Hall international series in the physical and chemical engineering sciences. 1999, Upper Saddle River, N.J.: Prentice Hall PTR.
15. Fried, J.R., *Polymer science and technology*. 2003, Upper Saddle River, NJ: Prentice Hall PTR.
16. Zeman, L. and G. Tkacik, *Thermodynamic analysis of a membrane-forming system water/N-methyl-2-pyrrolidone/polyethersulfone*. *Journal of Membrane Science*, 1988. **36**: p. 119-140.

17. Boom, R.M., et al., *Equilibrium Thermodynamics of a Quaternary Membrane-Forming System with Two Polymers. 2. Experiments*. *Macromolecules*, 1994. **27**(8): p. 2041-2044.
18. Baik, K.-J., et al., *Liquid-liquid phase separation in polysulfone/polyethersulfone/ N-methyl-2-pyrrolidone/water quaternary system*. *Journal of Applied Polymer Science*, 1999. **74**(9): p. 2113-2123.
19. Mills, I., et al., *Quantities, units and symbols in physical chemistry*. 2nd Edition ed, ed. IUPAC. 2007, Oxford: Blackwell Science Ltd.
20. Poling, B.E., J.M. Prausnitz, and J.P. O'Connell, *The properties of gases and liquids*. 2001, New York: McGraw-Hill.
21. Wesselingh, J.A. and A.M. Bollen, *Multicomponent Diffusivities from the Free Volume Theory*. *Chemical Engineering Research and Design*, 1997. **75**(6): p. 590-602.
22. Bondi, A., *Free Volumes and Free Rotation in Simple Liquids and Liquid Saturated Hydrocarbons*. *The Journal of Physical Chemistry*, 1954. **58**(11): p. 929-939.
23. Haward, R.N., *Occupied Volume of Liquids and Polymers*. *Polymer Reviews*, 1970. **4**(2): p. 191 - 242.
24. Cohen, M.H. and D. Turnbull, *Molecular Transport in Liquids and Glasses*. *The Journal of Chemical Physics*, 1959. **31**(5): p. 1164-1169.
25. Fujita, H., *Diffusion in polymer-diluent systems*. *Algebra Universalis*, 1961. **3**(1): p. 1-47.
26. Vrentas, J.S. and J.L. Duda, *Diffusion in polymer-solvent systems. I. Reexamination of the free-volume theory*. *Journal of Polymer Science B: Polymer Physics*, 1977. **15**(3): p. 403-416.
27. Vrentas, J.S. and J.L. Duda, *Diffusion in polymer-solvent systems. II. A predictive theory for the dependence of diffusion coefficients on temperature, concentration, and molecular weight*. *Journal of Polymer Science B: Polymer Physics*, 1977. **15**(3): p. 417-439.
28. Ferguson, R.D. and E.D. von Meerwall, *Free-volume interpretations of self-diffusion in ternary solutions: n-Paraffin-hexafluorobenzene-cis-4-polybutadiene*. *Journal of Polymer Science B: Polymer Physics*, 1980. **18**(6): p. 1285-1301.
29. Volkov, V.I., et al., *Self-diffusion of water-ethanol mixtures in polyacrylic acid-polysulfone composite membranes obtained by pulsed-field gradient nuclear magnetic resonance spectroscopy*. *Journal of Membrane Science*, 1995. **100**(3): p. 273-286.

30. Heink, W., et al., *Application of pulsed field gradient NMR to characterize the transport properties of microporous membranes*, in *Membrane Science and Technology*. 2000, Elsevier. p. 97-108.
31. Yan, X.W., et al., *Self-diffusion coefficients of organic solvents in linear and branched high density polyethylene particles measured by PFG NMR*. Chinese Chemical Letters, 2008. **19**(1): p. 110-114.
32. Harding, S.G. and L.F. Gladden, *Diffusion of liquids into semicrystalline polyethylene*. Magnetic Resonance Imaging, 1998. **16**(5-6): p. 647-649.
33. Hoerner, P., et al., *Emulsification of poly(ethylene glycol) in thermoplastic elastomers by using polybutadiene-block-poly(ethylene oxide) diblock copolymers as stabilisers. Determination of the liquid phase mobility by pulsed field gradient NMR*. Macromolecular Chemistry and Physics, 1998. **199**(3): p. 343-352.
34. Nyden, M., O. Soderman, and G. Karlstrom, *A PFG NMR Self-Diffusion Investigation of Probe Diffusion in an Ethyl(hydroxyethyl)cellulose Matrix*. 1999. p. 127-135.
35. Hietala, S., et al., *Water sorption and diffusion coefficients of protons and water in PVDF-g-PSSA polymer electrolyte membranes*. 1999. p. 2893-2900.
36. Roberts, C., et al., *Diffusion of Poly(dimethylsiloxane) Mixtures with Silicate Nanoparticles*. 2001. p. 538-543.
37. Lin, G., et al., *A Lattice Model for the Simulation of Diffusion in Heterogeneous Polymer Systems. Simulation of Apparent Diffusion Constants as Determined by Pulse-Field-Gradient Nuclear Magnetic Resonance*. 2003. p. 6179-6186.
38. Sagidullin, A., J. Meier-Haack, and U. Scheler, *Molecular mobility and transport in polymer membranes and polyelectrolyte multilayers*. Magnetic Resonance Imaging, 2007. **25**(4): p. 541-543.
39. Demco, D.E., et al., *Self-Diffusion Anisotropy of Small Penetrant Molecules in Deformed Elastomers*. Macromolecules, 2005. **38**(13): p. 5647-5653.
40. vonMeerwall, E.D., H. Lin, and W.L. Mattice, *Trace Diffusion of Alkanes in Polyethylene: Spin-Echo Experiment and Monte Carlo Simulation*. Macromolecules, 2007. **40**(6): p. 2002-2007.
41. Fleischer, G., *A pulsed field gradient NMR study of diffusion in semicrystalline polymers: self-diffusion of alkanes in polyethylenes*. Colloid & Polymer Science, 1984. **262**(12): p. 919 - 928.
42. Fleischer, G., *Self diffusion of alkanes in low density polyethylene as measured by pulsed field gradient NMR*. Polymer Bulletin, 1982. **7**(8): p. 1436 - 2449.
43. Hedenqvist, M., et al., *Diffusion of small-molecule penetrants in polyethylene: free volume and morphology*. Polymer, 1996. **37**(14): p. 2887-2902.

44. Mauviel, G. and E. Favre, *Free-Volume Theory Applied to Diffusion in Liquids: A Critical Analysis*. Industrial and Engineering Chemistry Research, 2004. **43**(21): p. 6847-6854.
45. Einstein, A., *Über die von der molekularkinetischen Theorie der Wärme geforderte Bewegung von in ruhenden Flüssigkeiten suspendierten Teilchen*. Annalen der Physik, 1905. **322**(8): p. 549-560.
46. Sutherland, W., *A dynamical theory of diffusion for non-electrolytes and the molecular mass of albumin*. Philosophical Magazine, 1905. **9**(6): p. 1798 - 1977.
47. Mason, E.A. and H.K. Lonsdale, *Statistical-mechanical theory of membrane transport*. Journal of Membrane Science, 1990. **51**(1-2): p. 1-81.
48. Dullien, F.A.L., *Predictive equations for self-diffusion in liquids: A different approach*. AIChE Journal, 1972. **18**(1): p. 62-70.
49. Vrentas, J.S., J.L. Duda, and H.C. Ling, *Self-diffusion in polymer-solvent-solvent systems*. Journal of Polymer Science: Polymer Physics Edition, 1984. **22**(3): p. 459-469.
50. Taylor, R. and R. Krishna, *Multicomponent Mass Transfer*. 1993, New York: John Wiley & Sons.
51. Wesselingh, J.A. and R. Krishna, *Mass Transfer*. 1990, Chichester: Ellis Horwood.
52. Williams, M.L., R.F. Landel, and J.D. Ferry, *The Temperature Dependence of Relaxation Mechanisms in Amorphous Polymers and Other Glass-forming Liquids*. Journal of the American Chemical Society, 1955. **77**(14): p. 3701-3707.
53. Hong, S.-U., *Prediction of Polymer/Solvent Diffusion Behavior Using Free-Volume Theory*. Industrial and Engineering Chemistry Research, 1995. **34**(7): p. 2536-2544.
54. Vrentas, J.S., J.L. Duda, and M.K. Lau, *Solvent diffusion in molten polyethylene*. Journal of Applied Polymer Science, 1982. **27**(10): p. 3987-3997.
55. Jiang, W.H., et al., *Infinite dilution diffusion coefficients of n-hexane, n-heptane and n-octane in polyisobutylene by inverse gas chromatographic measurements*. European Polymer Journal, 2001. **37**(8): p. 1705-1712.
56. Doolittle, A.K., *Studies in Newtonian Flow. II. The Dependence of the Viscosity of Liquids on Free-Space*. Journal of Applied Physics, 1951. **22**(12): p. 1471-1475.
57. Zielinski, J.M., *An Alternate Interpretation of Polymer/Solvent Jump Size Units for Free-Volume Diffusion Models*. Macromolecules, 1996. **29**(18): p. 6044-6047.
58. Zielinski, J.M. and J.L. Duda, *Predicting polymer/solvent diffusion coefficients using free-volume theory*. AIChE Journal, 1992. **38**(3): p. 405-415.

59. Hong, S.-U., *Predicting ability of free-volume theory for solvent self-diffusion coefficients in rubbers*. Journal of Applied Polymer Science, 1996. **61**(5): p. 833-841.
60. Kokes, R.J. and F.A. Long, *Diffusion of Organic Vapors into Polyvinyl Acetate*. Journal of the American Chemical Society, 1953. **75**(24): p. 6142-6146.
61. Fujita, H., *Diffusion in polymers* edited by J. Crank and G. S. Park, Academic Press, London and New York, 1968; 452 pg. Journal of Applied Polymer Science, 1970. **14**(6): p. 1657.
62. Meares, P., *Polymers: structure and bulk properties*. 1965, London; New York: Van Nostrand.
63. Vrentas, J.S., H.T. Liu, and J.L. Duda, *Estimation of diffusion coefficients for trace amounts of solvents in glassy and molten polymers*. Journal of Applied Polymer Science, 1980. **25**(7): p. 1297-1310.
64. Vrentas, J.S., H.T. Liu, and J.L. Duda, *Effect of solvent size on diffusion in polymer-solvent systems*. Journal of Applied Polymer Science, 1980. **25**(8): p. 1793-1797.
65. Ehlich, D. and H. Sillescu, *Tracer diffusion at the glass transition*. Macromolecules, 1990. **23**(6): p. 1600-1610.
66. Vrentas, J.S. and C.M. Vrentas, *Solvent self-diffusion in crosslinked polymers*. Journal of Applied Polymer Science, 1991. **42**(7): p. 1931-1937.
67. Fujita, H. and A. Kishimoto, *Interpretation of Viscosity Data for Concentrated Polymer Solutions*. The Journal of Chemical Physics, 1961. **34**(2): p. 393-398.
68. Bearman, R.J., *On Molecular Basis of Some Current Theories of Diffusion*. Journal of Physical Chemistry, 1961. **65**(11): p. 1961-&.
69. Price Jr, P.E. and I.H. Romdhane, *Multicomponent diffusion theory and its applications to polymer-solvent systems*. AIChE Journal, 2003. **49**(2): p. 309-322.
70. Duda, J.L., et al., *Prediction of diffusion coefficients for polymer-solvent systems*. 1982. p. 279-285.
71. Loflin, T. and E. McLaughlin, *Diffusion in binary liquid mixtures*. The Journal of Physical Chemistry, 1969. **73**(1): p. 186-190.
72. Mulder, M., *Basic principles of membrane technology*. 1997, Dordrecht; Boston: Kluwer Academic.
73. Baker, R.W. and I. NetLibrary, *Membrane technology and applications*. 2004, Chichester; New York: J. Wiley.
74. Sourirajan, S., *Reverse osmosis*. 1970, New York: Academic Press.

75. Machado, D.R., D. Hasson, and R. Semiat, *Effect of solvent properties on permeate flow through nanofiltration membranes. Part I: investigation of parameters affecting solvent flux*. Journal of Membrane Science, 1999. **163**(1): p. 93-102.
76. Dijkstra, M.F.J., S. Bach, and K. Ebert, *A transport model for organophilic nanofiltration*. Journal of Membrane Science, 2006. **286**(1-2): p. 60-68.
77. Wijmans, J.G. and R.W. Baker, *The solution-diffusion model: a review*. Journal of Membrane Science, 1995. **107**(1-2): p. 1-21.
78. Rautenbach, R., *Membranverfahren. Grundlagen der modul- und Anlagenauslegung*. 1997, Berlin: Springer-Verlag.
79. Sherwood, T.K., P.L.T. Brian, and R.E. Fisher, *Desalination by Reverse Osmosis*. Industrial & Engineering Chemistry Fundamentals, 1967. **6**(1): p. 2-12.
80. Soltanieh, M. and W.N. Gill, *Review of Reverse Osmosis Membranes and Transport models*. Chemical Engineering Communications, 1981. **12**(4): p. 279 - 363.
81. Bhattacharyya, D. and M. Williams, *Introduction and Definitions - Reverse Osmosis*. Membrane handbook, ed. W.S.W. Ho and K.K. Sirkar. 1992, New York: Van Nostrand Reinhold.
82. Yaroshchuk, A.E., *Solution-diffusion-imperfection model revised*. Journal of Membrane Science, 1995. **101**(1-2): p. 83-87.
83. Wesselingh, J.A. and R. Krishna, *Mass transfer in multicomponent mixtures*. 2000, Delft, Netherland: Delft University Press.
84. Straatsma, J., et al., *Can nanofiltration be fully predicted by a model?* Journal of Membrane Science, 2002. **198**(2): p. 273-284.

Chapter 3. Experimental Part

3.1 Materials

The membrane used in this study is a composite membrane developed at GKSS-Forschungszentrum Geesthacht GmbH. The membrane is formed by a solvent resistant support layer made of polyacrylonitrile (PAN) and a selective top layer of a high molecular weight polydimethylsiloxane (PDMS).

The PAN support was prepared by phase-inversion over a non-woven layer of poly(ethylene terephthalate) with a density of 100 g/m^2 and an approximated thickness of $140 \text{ }\mu\text{m}$.

The PDMS layer was coated over the PAN support with an industrial coating machine from a solution of high molecular weight PDMS, curing agent, solvent (hydrocarbon) and platinum catalyst which allows the polymer to thermally crosslink. Additionally, the membrane was crosslinked with a low energy electron beam of 150 kGy by IOM/Leipzig in order to obtain the desired chemically resistant membrane with a PDMS layer thickness of $5 \text{ }\mu\text{m}$, as shown in figure 3.1.

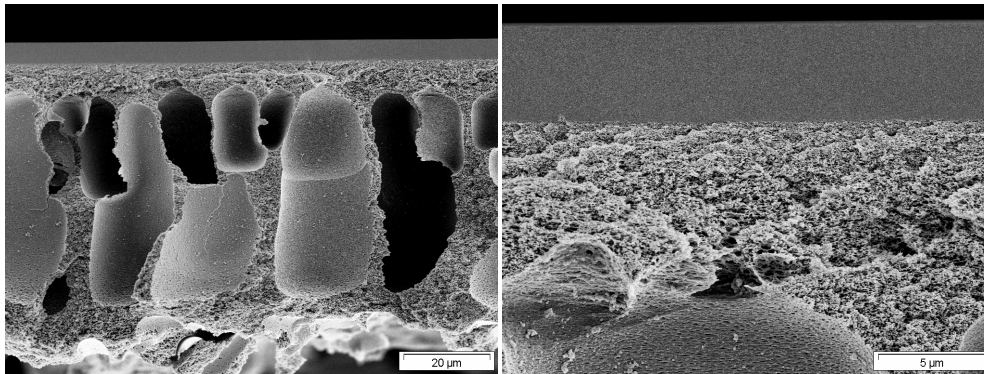


Figure 3.1. Scanning electron micrograph of a PDMS composite membrane.

The critical hole free volume of PDMS is considered to be $9.05 \cdot 10^{-4} \text{ m}^3/\text{kg}$.^[1] According to Roth, the Hildebrand solubility parameters for PDMS can be estimated as shown in equation 3.1.^[2, 3]

$$\delta_{PDMS} [MPa^{1/2}] = 15.7 - 0.026 \cdot T [^{\circ}C] \quad \text{Eq. 3.1}$$

Solvents with synthesis grade for diffusion and nanofiltration measurements were used as received. For the experiments with mixtures of solvents, a ketone was selected as a good permeant and a glycol as a bad one (solute). The selected ketones were ethyl methyl ketone (MEK) and diethyl ketone (DEK). The used glycols were tetraethylene glycol (TEG), tetraethylene glycol dimethyl ether (TEGDME) and polyethylene glycol dimethyl ether 250 (PEGDME). The PEGDME was obtained from Fluka[®] and the rest of the solvents from MERCK[®].

A list of the properties of the used substances is shown in table 3.1. For the case of PDMS, the molecular weight of the polymer chain repeating unit is shown instead of the molecular weight of the whole polymer.

Table 3.1. Chemical structure and physical properties of the used substances.

Substance	CAS MERCK	MW (g/mol)	V_c (m ³ /mol)
PDMS	–	74.11 ^(a)	–
MEK	78-93-3 822253	72.11	$2.67 \cdot 10^{-4}$ ^(c)
DEK	96-22-0 803605	86.13	$3.36 \cdot 10^{-4}$ ^(c)
TEG	112-60-7 808619	194.23	$5.63 \cdot 10^{-4}$ ^(d)
TEGDME	143-24-8 820959	222.28	$6.91 \cdot 10^{-4}$ ^(b)
PEGDME	24991-55-7 814173	298.21 ^(b)	$9.15 \cdot 10^{-4}$ ^(b)

a) Molecular weight of the polymer chain repeating unit, b) Conesa et al.^[4], c) Korea thermophysical properties data bank^[5], d) CHEM group data sheets^[6]

According to Conesa et al., the PEGDME 250 from Fluka® is a mixture of ethylene glycol dimethyl ethers with different chain lengths – between 3 and 9 – but is often considered as a pseudo pure compound. Therefore, a pseudo chain unit value of 5.723 was found, which corresponds to a molecular weight of 298.21 g/mol.^[4] Additionally, density and viscosity data for a range of temperature between 10 °C and 80 °C are found in tables 3.2 and 3.3, whereas the density of the PDMS is considered a constant value of 0.970 for the whole range.^[3]

Table 3.2. Solvent densities as a function of the temperature.

Temperature (K)	Density $\left(\frac{\text{kg}}{\text{m}^3}\right)$				
	MEK ^{a)}	DEK ^{a)}	TEG ^{a)}	TEGDME ^{b)}	PEGDME ^{b)}
283.15	$8.157 \cdot 10^2$	$8.242 \cdot 10^2$	$1.134 \cdot 10^3$	$1.020 \cdot 10^3$	$1.044 \cdot 10^3$
288.15	$8.103 \cdot 10^2$	$8.193 \cdot 10^2$	$1.131 \cdot 10^3$	$1.016 \cdot 10^3$	$1.040 \cdot 10^3$
293.15	$8.049 \cdot 10^2$	$8.144 \cdot 10^2$	$1.127 \cdot 10^3$	$1.012 \cdot 10^3$	$1.036 \cdot 10^3$
298.15	$7.995 \cdot 10^2$	$8.095 \cdot 10^2$	$1.124 \cdot 10^3$	$1.007 \cdot 10^3$	$1.031 \cdot 10^3$
303.15	$7.940 \cdot 10^2$	$8.045 \cdot 10^2$	$1.120 \cdot 10^3$	$1.003 \cdot 10^3$	$1.026 \cdot 10^3$
308.15	$7.884 \cdot 10^2$	$7.995 \cdot 10^2$	$1.116 \cdot 10^3$	$9.984 \cdot 10^2$	$1.022 \cdot 10^3$
313.15	$7.828 \cdot 10^2$	$7.944 \cdot 10^2$	$1.113 \cdot 10^3$	$9.938 \cdot 10^2$	$1.017 \cdot 10^3$
318.15	$7.772 \cdot 10^2$	$7.893 \cdot 10^2$	$1.109 \cdot 10^3$	$9.892 \cdot 10^2$	$1.013 \cdot 10^3$
323.15	$7.715 \cdot 10^2$	$7.842 \cdot 10^2$	$1.105 \cdot 10^3$	$9.846 \cdot 10^2$	$1.008 \cdot 10^3$
328.15	$7.658 \cdot 10^2$	$7.790 \cdot 10^2$	$1.102 \cdot 10^3$	$9.799 \cdot 10^2$	$1.004 \cdot 10^3$
333.15	$7.600 \cdot 10^2$	$7.738 \cdot 10^2$	$1.098 \cdot 10^3$	$9.752 \cdot 10^2$	$9.995 \cdot 10^2$
338.15	$7.541 \cdot 10^2$	$7.685 \cdot 10^2$	$1.094 \cdot 10^3$	$9.705 \cdot 10^2$	$9.951 \cdot 10^2$
343.15	$7.482 \cdot 10^2$	$7.632 \cdot 10^2$	$1.090 \cdot 10^3$	$9.658 \cdot 10^2$	$9.906 \cdot 10^2$
348.15	$7.422 \cdot 10^2$	$7.578 \cdot 10^2$	$1.086 \cdot 10^3$	$9.611 \cdot 10^2$	$9.862 \cdot 10^2$
353.15	$7.362 \cdot 10^2$	$7.523 \cdot 10^2$	$1.083 \cdot 10^3$	$9.564 \cdot 10^2$	$9.817 \cdot 10^2$

^{a)} Estimated by ASPEN® Properties, ^{b)} Interpolated from Conesa et al. data^[4]

Table 3.3. Solvent viscosities as a function of temperature.

Temperature (K)	Viscosity (Pa · s)				
	MEK ^{a)}	DEK ^{a)}	TEG ^{a)}	TEGDME ^{b)}	PEGDME ^{b)}
283.15	$4.676 \cdot 10^{-4}$	$5.247 \cdot 10^{-4}$	$1.004 \cdot 10^{-1}$	$4.979 \cdot 10^{-3}$	$1.023 \cdot 10^{-2}$
288.15	$4.412 \cdot 10^{-4}$	$4.953 \cdot 10^{-4}$	$7.705 \cdot 10^{-2}$	$4.361 \cdot 10^{-3}$	$8.843 \cdot 10^{-3}$
293.15	$4.170 \cdot 10^{-4}$	$4.683 \cdot 10^{-4}$	$5.965 \cdot 10^{-2}$	$3.749 \cdot 10^{-3}$	$7.471 \cdot 10^{-3}$
298.15	$3.946 \cdot 10^{-4}$	$4.435 \cdot 10^{-4}$	$4.657 \cdot 10^{-2}$	$3.348 \cdot 10^{-3}$	$6.532 \cdot 10^{-3}$
303.15	$3.740 \cdot 10^{-4}$	$4.206 \cdot 10^{-4}$	$3.666 \cdot 10^{-2}$	$2.951 \cdot 10^{-3}$	$5.601 \cdot 10^{-3}$
308.15	$3.549 \cdot 10^{-4}$	$3.995 \cdot 10^{-4}$	$2.908 \cdot 10^{-2}$	$2.673 \cdot 10^{-3}$	$4.980 \cdot 10^{-3}$
313.15	$3.373 \cdot 10^{-4}$	$3.799 \cdot 10^{-4}$	$2.324 \cdot 10^{-2}$	$2.398 \cdot 10^{-3}$	$4.365 \cdot 10^{-3}$
318.15	$3.209 \cdot 10^{-4}$	$3.617 \cdot 10^{-4}$	$1.870 \cdot 10^{-2}$	$2.201 \cdot 10^{-3}$	$3.927 \cdot 10^{-3}$
323.15	$3.056 \cdot 10^{-4}$	$3.449 \cdot 10^{-4}$	$1.515 \cdot 10^{-2}$	$2.007 \cdot 10^{-3}$	$3.493 \cdot 10^{-3}$
328.15	$2.914 \cdot 10^{-4}$	$3.292 \cdot 10^{-4}$	$1.236 \cdot 10^{-2}$	$1.848 \cdot 10^{-3}$	$3.180 \cdot 10^{-3}$
333.15	$2.782 \cdot 10^{-4}$	$3.145 \cdot 10^{-4}$	$1.014 \cdot 10^{-2}$	$1.691 \cdot 10^{-3}$	$2.869 \cdot 10^{-3}$
338.15	$2.659 \cdot 10^{-4}$	$3.009 \cdot 10^{-4}$	$8.368 \cdot 10^{-3}$	$1.569 \cdot 10^{-3}$	$2.618 \cdot 10^{-3}$
343.15	$2.543 \cdot 10^{-4}$	$2.881 \cdot 10^{-4}$	$6.944 \cdot 10^{-3}$	$1.449 \cdot 10^{-3}$	$2.369 \cdot 10^{-3}$
348.15	$2.435 \cdot 10^{-4}$	$2.762 \cdot 10^{-4}$	$5.794 \cdot 10^{-3}$	$1.352 \cdot 10^{-3}$	$2.212 \cdot 10^{-3}$
353.15	$2.334 \cdot 10^{-4}$	$2.650 \cdot 10^{-4}$	$4.859 \cdot 10^{-3}$	$1.257 \cdot 10^{-3}$	$2.058 \cdot 10^{-3}$

a) Estimated by ASPEN® Properties, b) Interpolated from Conesa et al. data^[4]

3.2 Measurements

3.2.1 Scanning electron microscopy (SEM)

Scanning electron microscopy is a microscopy technique which scans the surface of a sample with a high-energy electron beam in a raster scan pattern. This technique is one of the most often used for morphological membrane characterization.^[7] The cross-section of a PDMS composite membrane was studied with a Zeiss LEO Gemini 1550VP (1kV) SEM. The samples were taken as delivered after the electron beam crosslinking without any further treatment. Afterward, the membranes were fractured under liquid nitrogen and sputtered with a fine Au/Pd layer.

3.2.2 Differential scanning calorimetry (DSC)

Differential scanning calorimetry is a thermoanalytical procedure where, for a sample and a reference, the energy required for increasing the temperature, as well as the energy released when the temperature decreases, are measured. This technique allows, among others, the quantification of the glass transition temperature of a polymer. The equipment employed for the DSC measurements was a Netzsch DSC Phoenix, under N₂ atmosphere with a liquid nitrogen cooling device. For all measurements, a two-point calibration with cyclohexane and indium was carried out. Standard aluminum pans were used to encapsulate polymer samples. Heating and cooling scans were performed by initially heating the sample up to 30 °C and holding it at that temperature for 5 min in order to erase effects resulting from any previous thermal history. Then, the sample was cooled down to -195 °C and kept at that temperature for 5 min for the sake of equipment stabilization. Finally, a second heating scan up to 30 °C was applied. All the standard scan experiments were carried out at a scanning rate of 10 °C/min. As a general rule, the shown cooling traces correspond to the first cooling, while the shown heating traces correspond to the following (second) heating scan. In this way, the analyzed traces correspond to the applied thermal history and are independent of the previous treatments, i.e., conditions of precipitation from solution, storage, etc.

3.2.3 Tracer-diffusion measurements

Diffusion-ordered spectroscopy (DOSY) experiments provide accurate and noninvasive molecular diffusion measurements on biofluids, complex chemical mixtures and multicomponent solutions.^[8] A standard pulse field gradient based on spin-echo sequences (PFG-NMR) allows measurements of tracer diffusion coefficient when a series of NMR spectra are taken when the overall gradient strength (\check{G}) is progressively incremented.^[8, 9] A schematic representation of the PFG-NMR measurement is shown in figure 3.2. Later, the attenuation of the acquired signal follows equation 3.1.

$$I_i = I_i^0 \cdot \exp\left(-\check{D}_i \cdot (2\pi \cdot \gamma \cdot \check{G}_i \cdot \partial)^2 \cdot \left(\Lambda \cdot \frac{\partial}{3}\right) \cdot 10^4\right) \quad \text{Eq. 3.1}$$

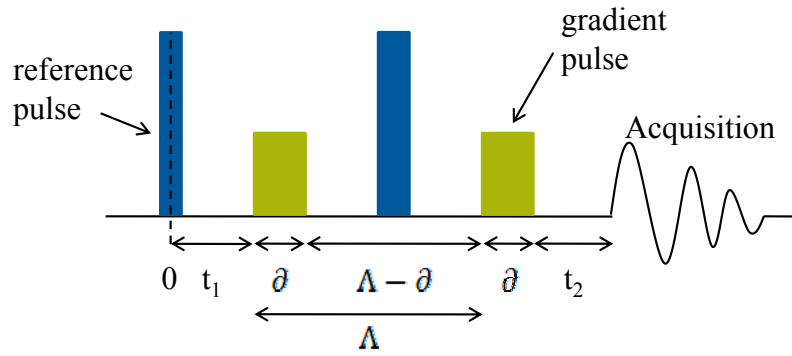


Figure 3.2. Schematic representation of spin-echo sequence in PFG-NMR measurements.

Here, I_i is the measured peak intensity and I_i^0 is the maximum peak intensity. \check{D}_i is the tracer diffusion coefficient, also known as translational diffusion coefficient. γ represents the gyromagnetic ratio ($4258 \cdot \text{Hz/G}$). δ corresponds to the duration of the gradient and Λ is the diffusion time which corresponds to the time between gradients. \check{G}_i is the gradient strength. The calculation of the tracer diffusion coefficient can be done with the slope of the curve obtained when the data is plotted accordingly to the following equation.

$$-\ln\left(\frac{I_i}{I_i^0}\right) = \check{G}_i^2 \cdot \gamma^2 \cdot \delta^2 \cdot \left(\Lambda \cdot \frac{\delta}{3}\right) \cdot 10^4 \quad \text{Eq. 3.2}$$

The measurements have been done in a Bruker DCX-300 Spectrometer with a separate diffusion cell. To perform tracer diffusion coefficient measurements for binary and ternary polymer-solvent systems, cubic pieces of polymer with a lateral size of 1.5 mm are required and the temperature was controlled with a cooling agent like ethylene glycol or methanol.^[10] The polymer blocks need to be leaved before the measurement for at least 30 min inside the magnetic field in order to achieve a constant temperature of 25 °C. For the measurements of both ethylene glycol dimethyl ethers (EGDMEs) the diffusion time (Λ) was 200 ms, for all the rest the diffusion time was 20 ms. The gradient pulse (δ) was considered for 1 ms in all the measurements. The gradient strength can be increased in a continuous way in 20 steps from 20 to 240 G/cm depending on the substance, for both EGDMEs the maximum value corresponds to 200 G/cm, for TEG up to 240 G/cm and for all the rest up to 160 G/cm. For every step, the data was acquired 16 times with an average temperature increment of 0.1 °C. Additionally, every measurement was done 7 times and the signal intensity was

averaged between different sample points. The invariability of the calibration during the measurements was done by measuring the self-diffusivities of water and deuterated water before and after the measurements.

Before the tracer diffusivities of the desired substances can be measured, the gradient needs to be calibrated with self-diffusion values of known substances. For a constant temperature of 25 °C, the self-diffusion coefficient of pure water is $2.30 \cdot 10^{-9} \text{ m}^2/\text{s}$ and for deuterated water $1.89 \cdot 10^{-9} \text{ m}^2/\text{s}$. Later, the quality of the measurement is observed by comparison between experimental and literature tracer-diffusivities values for different substances.

From the results obtained by PFG-NMR measurements, it is expected an inaccuracy up to 10 % in the diffusivities values due to convection in the samples, Wirbelstrom effect and non-linearity from the sender. Specially, a bigger difference for substances with high proton density due to radiation damping is expected.

3.2.4 Swelling experiments

In order to investigate concentration of the permeants inside the polymer, polymer pieces were immersed in different solvents for 8 hours and their dry and wet weights were compared. Hence, a polydimethylsiloxane film was prepared according to the recipe used in the preparation of the composite membranes (recipe is not shown). Afterward, cubic pieces of 5 mm length were cut and weighted (M_{dry}). The preweighted dry PDMS pieces were immersed in pure solvents or mixture of solvents. After a minimum of 8 hours, the pieces were removed from the solution and the excess of liquid was wiped out. To avoid possible evaporation, the wet pieces were weighted (M_{wet}) as fast as possible. The solvent uptake (SU) and the swelling degree (SD) of the polymer are calculated with equations 3.3 and 3.4.

$$SU = (M_{wet} - M_{dry}) \quad \text{Eq. 3.3}$$

$$SD = \frac{M_{wet} - M_{dry}}{M_{dry}} \cdot 100 \quad \text{Eq. 3.4}$$

With the information of the solvent uptake and assuming that the concentration inside the polymer sample is equal to the one in the surroundings, the weight fraction of a

solvent inside the polymer can be calculated with equation 3.5. The weight fraction of the polymer in the ternary solvent-solvent-system is calculated by equation 3.6.

$$\omega_{i,Pol} = \frac{\omega_{i,FS} \cdot (SU)}{M_{wet}} \quad \text{Eq. 3.5}$$

$$\omega_{Pol} = \frac{M_{dry}}{M_{wet}} \quad \text{Eq. 3.6}$$

where $\omega_{i,Pol}$ is the weight fraction of a solvent i in the ternary system (solvent–solvent–polymer), $\omega_{i,FS}$ represents the weight fraction of a solvent i in the binary solvent–solvent free solution. The previous assumption is based on the consideration that after 8 hours the system reaches equilibrium. Therefore, at both polymer interfaces the solvent activities are equal to the ones in the free solution.

3.2.5 Solution concentration

To estimate the flux amount of each permeant, it is necessary to know the exact concentration of the permeated solution. In the same way, to know the final retention of the membrane during the filtration process, it is necessary to know the concentration of the feed solution. Therefore, two different methods to calculate the concentration in a solution are proposed, i.e., density and size exclusion chromatography measurements.

3.2.5.1 Density

For solutions formed by two different substances with nonsimilar densities, the average molar density can be used as shown in equation 3.7.

$$\rho_M = \sum_i^2 x_i \cdot \rho_i \quad \text{Eq. 3.7}$$
$$\rho_M = \rho_1 + (\rho_2 - \rho_1) \cdot x_2$$

To avoid any nonlinearity in the measurement, i.e., non-linearity in the mixture density or nonlinearity in the detector, a calibration curve for a set of different concentrations was done. For the preparation of the calibration curve, solutions of 20 ml with different concentrations were prepared, i.e., from 0 wt % to 20 wt % in steps of 1 wt %. The solutions were deposited in closed glass bottles and stirred over 8 hours without heating.

The curve obtained after plotting the concentration as a function of the density can be directly related with the density results from feed and permeate solutions.

The measurements have been done in a densimeter DMA 46 from Anton Paar KG. The equipment includes an integrated thermostat which keeps the temperature at the desired value. The equipment allows density estimation of organic substances when the display results are properly calibrated with water solution patterns. Due to the nature of the measurement, the calibration curve allows the calculation of solution concentrations without any equipment calibration. However, a proper calibration of the equipment is still needed if the exact density of the mixture is required.

3.2.5.2 Size Exclusion Chromatography (SEC)

When the densities of the substances in the solution are similar, SEC measurements can be used to determine the concentration in the solution. Similar to the above presented method, a calibration curve is needed in order to correlate the intensity/area of the peaks in volts with the concentration of the solution. To avoid any difficulty setting the base line for the calculation of peaks area, specifically when the peaks superposed each other, the use of the maximum peak intensity is preferred (figure 3.3).

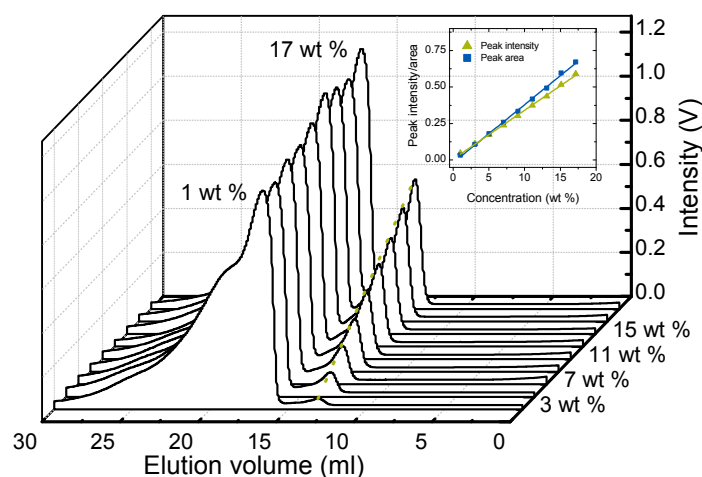


Figure 3.3. GPC calibration to estimate the mixtures concentration.

The measurements were done on a Waters[®] instrument with a PSS[®] column (0.8 × 300 mm, 10μm, Suprema Linear M), IR detector Knauer[®], autosampler Waters717+ and a flow rate of 1 ml/min.

3.2.6 Gas permeation

The quality of the coating of a composite membrane is assessed by performing single gas permeation measurements of O₂ and N₂.^[11] A set-up form by a gas cylinder, a membrane cell and a flowmeter is shown in figure 3.4.

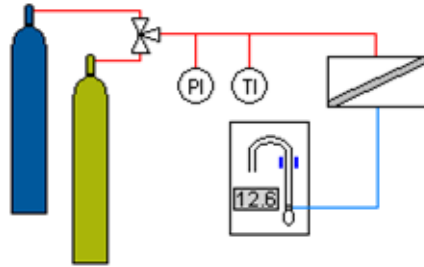


Figure 3.4. Schematic representation of the gas permeation set-up.

The gas permeation was measured with a Bioblock-Scientific[®] soap-bubble flowmeter. The experiments were carried out with the use of a transmembrane pressure of 2.5 bar. The selectivity of the polymer/membrane is defined as the fluxes ratio between two different permeating gases as shown in equation 3.8.

$$\check{\alpha}_{i/j} = \frac{Q_i}{Q_j} \quad \text{Eq. 3.8}$$

where $\check{\alpha}_{i/j}$ represents the selectivity between the gases i and j . Q represents the volumetric flow rate of the permeating gases. A defect-free PDMS composite membrane should have selectivity close to the intrinsic selectivity of the PDMS in bulk. The PDMS bulk selectivity between O₂ and N₂ varies from 2.10 to 2.15 depending on the polymer molecular weight.^[3, 12-14] Therefore, the membranes were considered free of defects when the selectivity between O₂ and N₂ was at least 2.10.

3.2.7 Nanofiltration

A nanofiltration setup (figure 3.5) was used to investigate the effect of pressure and temperature over the filtration performance on dense membranes. The equipment is formed by a supply vessel with a recirculation cooling bath where the feed solution is kept to control its temperature. The equipment has the capability to pump the solution into the membrane cell with a relative pressure from 1 bar to 45 bar. The dead-end type membrane cell can fit a membrane with a diameter of 7.4 cm with an effective area of

37.94 cm² after including an o-ring which prevents any leak in the test cell. Samples from the feed, permeate and retentate solutions can be taken for the estimation of the solution concentration at those points. Hence, it is possible to take samples in the points denoted as “a”, “b” and “c” in figure 3.5.

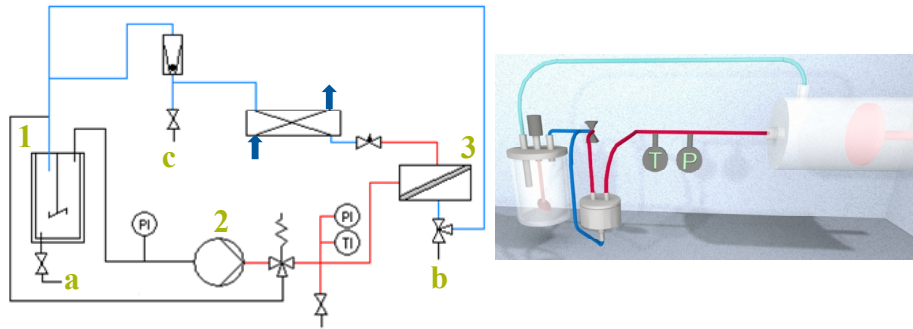


Figure 3.5. Schematic representation of the nanofiltration equipment. Left-hand side: 1) supply vessel, 2) pump, 3) membrane cell, a) feed solution sample, b) permeate solution sample, c) retentate solution sample. Right-hand side: 3D representation of the equipment.

The pressure of the system can be regulated with an expansion valve located after the membrane cell. The temperature was changed between 20 °C and 30 °C in order to study the temperature effects over the permeation properties. For this, a thermostat was attached to the supply vessel and a cross-flow exchanger after the membrane cell was used. The temperature of the feed solution was controlled with the use of a digital thermometer attached at the entrance of the test cell.

The system needs to be under steady-state conditions to carry out the measurement. Therefore, the system was left running under the experimental conditions, i.e., stable temperature and pressure, for at least 30 min before any sample is collected from the system. In order to achieve faster the steady-state of the experiment, the membranes were left overnight inside a flask with the permeation solvent with a consequent pre-swelling of the membrane stamps. Nevertheless, the final swelling and compaction of the membrane is only achieved under the experimental conditions of temperature and pressure.

The permeation rate is calculated by collecting a sample of a determined volume at the point “b” of the equipment (see figure 3.5 above) and measuring the corresponding

permeation time. To eliminate any non-uniformity effect between the different stamps, permeation fluxes for each stamp were normalized by the corresponding nitrogen flux. This procedure accounts for changes in thickness, porosity and pore size distribution between the stamps. Consequently, the nitrogen flux was measured according to procedure 3.2.6. The normalized flux for the permeation mixture was calculated with the following equation:

$$J_{Norm_k} = \frac{Q_{N_2k}}{\bar{Q}_{N_2}} \cdot J_k \quad \text{Eq. 3.9}$$

where J_{Norm_i} is the normalized flux and J_i the non-normalized one for the used stamp k . Q_{N_2k} and \bar{Q}_{N_2} represent the nitrogen volumetric flow rate for the stamp k and the average one from the whole set of stamps used in this work, respectively.

3.3 References

1. Hong, S.-U., *Prediction of Polymer/Solvent Diffusion Behavior Using Free-Volume Theory*. Industrial and Engineering Chemistry Research, 1995. **34**(7): p. 2536-2544.
2. Roth, M., *Solubility parameter of poly(dimethyl siloxane) as a function of temperature and chain length*. Journal of Polymer Science B: Polymer Physics, 1990. **28**(13): p. 2715-2719.
3. Mark, J.E., *Polymer data handbook*. 1999, New York: Oxford University Press.
4. Conesa, A., S. Shen, and A. Coronas, *Liquid Densities, Kinematic Viscosities, and Heat Capacities of Some Ethylene Glycol Dimethyl Ethers at Temperatures from 283.15 to 423.15 K*. International Journal of Thermophysics, 1998. **19**(5): p. 1343-1358.
5. Department of Chemical Engineering, K.U. *Korea thermophysical properties data bank*. [cited 2009 12/04]; Available from: www.cheric.org/kdb/.
6. CHEM-group. *Tetraethylene glycol data sheet*. [cited 2009 14/04]; Available from: www.chem-group.com/services/tteg.tpl.
7. Mulder, M., *Basic principles of membrane technology*. 1997, Dordrecht; Boston: Kluwer Academic.
8. Parella, T. *eNMR*. NMRGuide3.5 2003 [cited 2008 03/28/2008]; Available from: <http://rmn.iqfr.csic.es/guide/eNMR/proteins/diffusion.html>.

9. Stejskal, E.O. and J.E. Tanner, *Spin Diffusion Measurements: Spin Echoes in the Presence of a Time-Dependent Field Gradient*. The Journal of Chemical Physics, 1965. **42**(1): p. 288-292.
10. Ammann, C., P. Meier, and A. Merbach, *A simple multinuclear NMR thermometer*. Journal of Magnetic Resonance (1969), 1982. **46**(2): p. 319-321.
11. Stafie, N., D.F. Stamatialis, and M. Wessling, *Insight into the transport of hexane-solute systems through tailor-made composite membranes*. Journal of Membrane Science, 2004. **228**(1): p. 103-116.
12. Koros, W.J., et al., *Polymeric membrane materials for solution-diffusion based permeation separations*. Progress in Polymer Science, 1988. **13**(4): p. 339-401.
13. Zimmerman, C.M., A. Singh, and W.J. Koros, *Tailoring mixed matrix composite membranes for gas separations*. Journal of Membrane Science, 1997. **137**(1-2): p. 145-154.
14. Kroschwitz, J.I. and H.F. Mark, *Encyclopedia of polymer science and technology*. 2003, Hoboken, N.J.: Wiley-Interscience.

Chapter 4. Results and Discussion

The present chapter is divided into sections that mirror the three steps taken in order to achieve a comprehensive modeling of the transport during the membrane separation process. In the first section, the physical properties of the employed substances and the corresponding mixtures will be addressed. In the second section, different calculations and derivations related with the diffusion coefficients will be discussed. The last section will deal with the permeation experiments and the corresponding simulation.

4.1 Physical properties

4.1.1 Interaction parameters

The volumetric properties of polydimethylsiloxane and the here employed solvents are summarized in table 4.1. Van der Waals and compressed molar volumes were estimated by volume contribution of structural groups as described in section 2.1.1. Nevertheless, it should be noted that the shown PDMS properties correspond to the contribution of the repeating unit.

Table 4.1. Van der Waals volume and zero point molar volume for the polymer and employed solvents.

Substance	V^W (a)	V^C (b)	V^C (c)
PDMS	$4.92 \cdot 10^{-5}$	-	$6.40 \cdot 10^{-5}$
MEK	$4.93 \cdot 10^{-5}$	$6.39 \cdot 10^{-5}$	$6.41 \cdot 10^{-5}$
DEK	$5.95 \cdot 10^{-5}$	$7.84 \cdot 10^{-5}$	$7.74 \cdot 10^{-5}$
TEG	$1.35 \cdot 10^{-4}$	$1.88 \cdot 10^{-4}$	$1.76 \cdot 10^{-5}$
TEGDME	$1.80 \cdot 10^{-4}$	$2.48 \cdot 10^{-4}$	$2.34 \cdot 10^{-5}$
PEGDME	$1.14 \cdot 10^{-4}$	$1.54 \cdot 10^{-4}$	$1.48 \cdot 10^{-5}$

a) Estimated by table 2.1, b) Estimated by table 2.2, c) Calculated by equation 2.2.

The compressed volume values obtained by group contribution are in good agreement when compared to the ones calculated by equation 2.2 as a function of the van der Waals volume. For all the solvents, the discrepancies between both methods are less than 6 %, being the long substances (i.e., TEG, TEGDME, PEGDME) the ones with the

greatest differences. It should be noted that the compressed volume calculated by a proportionality of the van der Waals volume is, for most of the cases, lower than the ones estimated by density extrapolation at 0 K (group contribution).

The discrepancies between both methods of calculation of compressed volume could be explained by the fact that the proportionality one does not consider the possible free volume remaining among the molecules when the temperature tends to the absolute zero. It should be remarked that the group contribution method is based on experimental data extrapolated to the zero point, therefore, possible spaces between molecules are considered.

4.1.2 Interaction parameters as a function of temperature

Hildebrand solubility parameters of the solvents were obtained by enthalpy of vaporization data obtained from ASPEN Properties[®]. A comparison between the estimated values and available experimental data shows for MEK an underestimation of 1.0 % and for DEK an overestimation of 1.8 %. Nevertheless, for further calculations, the experimental data is preferred because small differences in solubility parameters affect greatly the further estimation of interaction parameters, e.g., for DEK/TEGDME the interaction parameter vary from 0.001 to 0.008 (≈ 700 %). The Hildebrand solubility parameters for PDMS at different temperatures were estimated by the correlation proposed by Roth (equation 3.1). A summary of solubility parameters of the polymer and the solvents are summarized in table 4.2. The enthalpic interaction parameters of solvent-solvent and solvent-polymer systems are calculated According to equation 2.6, and summarized in table 4.3.

Table 4.2. Solubility parameters of polymer and solvents as a function of temperature.

Substance	$\delta_{@20\text{ }^{\circ}\text{C}}$ (MPa ^{1/2})	$\delta_{@25\text{ }^{\circ}\text{C}}$ (MPa ^{1/2})	$\delta_{@30\text{ }^{\circ}\text{C}}$ (MPa ^{1/2})
PDMS	15.18 ^(a)	15.05 ^(a)	14.92 ^(a)
MEK	19.14 ^(b)	19.00 ^(b)	18.85 ^(b)
DEK	18.14 ^(b)	18.00 ^(b)	17.86 ^(b)
TEG	23.59 ^(c)	23.51 ^(c)	23.42 ^(c)
TEGDME	17.95 ^(c)	17.88 ^(c)	17.81 ^(c)
PEGDME	16.05 ^(c)	16.13 ^(c)	16.26 ^(c)

a) Correlated data from Roth^[1], b) data from Barton^[2], c) Calculated by equation 2.7 from predicted properties by ASPEN[®] Properties.

Table 4.3. Enthalpic interaction parameter of the mixtures estimated with solubility parameters.

	Temperature (°C)	TEG	TEGDME	PEGDME	PDMS
MEK	20	0.728	0.052	0.351	0.576
	25	0.738	0.046	0.299	0.567
	30	0.751	0.039	0.242	0.556
DEK	20	1.289	0.002	0.190	0.380
	25	1.300	0.001	0.149	0.373
	30	1.311	0.000	0.109	0.367
PDMS	20	5.000	0.690	0.089	
	25	4.983	0.711	0.137	-
	30	4.964	0.732	0.206	

Equation 2.6 allows only positive values and does not consider any concentration dependence of the Flory-Huggins-Staverman interaction parameter. Even so, the calculated MEK/PDMS interaction parameters are close to the ones found in literature. Additionally, as most of the systems exhibiting UCST, the interaction parameter between MEK/PDMS presents a slight decrement when the temperature increases.^[3] The binary interaction parameters between the different ethylene glycol dimethyl ethers (EGDMEs) and the PDMS are the only ones which present an increase when the temperature increases.

In addition, the interaction parameter between EGDMEs and PDMS decreases when the molecular weight of the EGDME increases. This behavior is in accordance to scaling laws and experimental data found elsewhere.^[3, 4]

4.1.3 Swelling experiments

Swelling degrees of free standing polymer pieces were measured according to section 3.2.4, whereas the results are shown in figure 4.1. For both MEK and DEK, the swelling degree decreases when the EGDME concentration increases. In addition, the swelling degree for ternary systems containing DEK is around 2 times higher than the one corresponding to MEK under the same conditions of solute concentration.

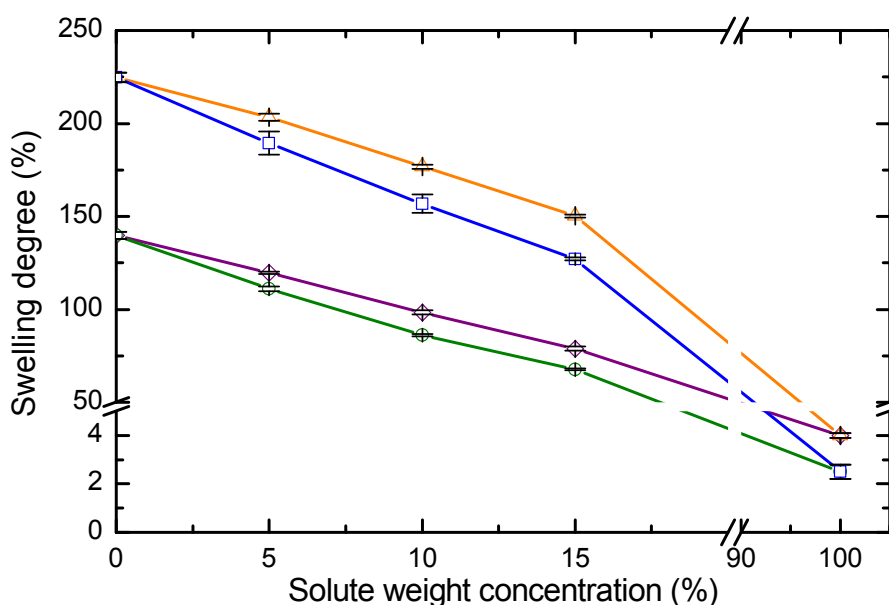


Figure 4.1. Polymer swelling degree as a function of solute (TEGDME or PEGDME) concentration in binary mixtures. ◇ MEK / TEGDME, ○ MEK / PEGDME, △ DEK / TEGDME, □ DEK / PEGDME.

Later, the weight fraction of each compound in a ternary system is calculated according to equations 3.5 and 3.6. A summary of weight concentration for ternary solvent-solvent-polymer systems is presented in table 4.4. The weight concentration obtained for solvent-polymer systems is as follows: MEK 58.3 wt %, DEK 69.2 wt %, TEGDME 3.9 wt % and PEGDME 2.4 wt %.

Table 4.4. Weight fraction (%) from polymer swelling experiments as a function of solute concentration of binary mixtures.

System	Weight fraction (%)		
	5 wt %	10 wt %	15 wt %
MEK / TEGDME	51.6 ± 0.3 / 2.7 ± 0.0	44.6 ± 0.3 / 5.0 ± 0.0	37.5 ± 0.3 / 6.6 ± 0.0
PDMS	45.7 ± 0.3	50.4 ± 0.3	55.9 ± 0.3
MEK / PEGDME	50.0 ± 0.2 / 2.6 ± 0.0	41.7 ± 0.2 / 4.6 ± 0.0	34.3 ± 0.2 / 6.1 ± 0.0
PDMS	47.4 ± 0.3	53.7 ± 0.2	59.6 ± 0.2
DEK / TEGDME	63.7 ± 0.2 / 3.4 ± 0.0	57.5 ± 0.1 / 6.4 ± 0.0	51.0 ± 0.1 / 9.0 ± 0.0
PDMS	33.0 ± 0.2	36.1 ± 0.1	40.0 ± 0.1
DEK / PEGDME	62.2 ± 0.7 / 3.3 ± 0.0	54.9 ± 0.7 / 6.1 ± 0.1	47.6 ± 0.1 / 8.4 ± 0.0
PDMS	34.6 ± 0.8	39.0 ± 0.7	44.0 ± 0.1

Later, with the consideration of additive volumes, the volume fraction of each compound can be easily estimated with equation 4.1.

$$\phi_i = \frac{w_i / \rho_i}{\sum_j w_j / \rho_j} \quad \text{Eq. 4.1}$$

where ϕ_i corresponds to the volume fraction, w_i is the weight fraction and ρ_i is the mass density. A set of volume concentrations (Φ) estimated by equation 4.1 from swelling experiments are summarized in table 4.5.

Table 4.5. Volume fraction (%) from polymer swelling experiments as a function of solute concentration of binary mixtures.

System	Volume fraction (%)		
	5 wt %	10 wt %	15 wt %
MEK / TEGDME	56.6 ± 0.3 / 2.3 ± 0.0	49.6 ± 0.3 / 4.4 ± 0.0	42.3 ± 0.3 / 5.9 ± 0.0
PDMS	41.1 ± 0.3	46.0 ± 0.3	51.8 ± 0.3
MEK / PEGDME	55.0 ± 0.2 / 2.2 ± 0.0	46.7 ± 0.2 / 4.0 ± 0.0	39.0 ± 0.2 / 5.4 ± 0.0
PDMS	42.8 ± 0.2	49.3 ± 0.3	55.6 ± 0.3
DEK / TEGDME	67.9 ± 0.2 / 2.9 ± 0.0	62.1 ± 0.2 / 5.6 ± 0.0	55.8 ± 0.2 / 7.9 ± 0.0
PDMS	29.2 ± 0.2	32.4 ± 0.2	36.3 ± 0.2
DEK / PEGDME	66.5 ± 0.7 / 2.8 ± 0.0	59.6 ± 0.7 / 5.2 ± 0.1	52.4 ± 0.7 / 7.3 ± 0.1
PDMS	30.7 ± 0.7	35.2 ± 0.7	40.3 ± 0.7

4.1.4 Polymer crosslinking parameters

The Flory-Rehner theory assumes linear superposition of the free energy changes associated with the swelling of the network, the free energy of mixing and elastic free energy. Consequently, a similar equation to the one developed in the Flory-Huggins-Staverman theory is developed with the addition of an elastic term due to the effect of the crosslinked network.^[5]

From swelling experiments of binary solvent-polymer systems, the Flory-Rehner theory can be applied in order to determine the crosslink density of the PDMS as follow.^[6, 7]

$$\ln(1 - \phi_2) + \phi_2 + \chi_{12} \cdot \phi_2^2 \frac{MW_1 / \rho_1 \cdot \rho_2}{\overline{Mc}} \cdot \left(\phi_2^{1/3} - \frac{\phi_2}{2} \right) = 0 \quad \text{Eq. 4.2}$$

$$\check{\rho} = \frac{\rho_2}{\overline{Mc}} \quad \text{Eq. 4.3}$$

where the subscripts 1 and 2 represent the solvent and the polymer, respectively, ρ is the mass density, \overline{Mc} is the average molecular weight between two cross-links and $\check{\rho}$ represents the crosslink density. Consequently, from swelling experiments of binary solvent-polymer systems, the crosslink parameters of the PDMS (thermally crosslinked)

are as shown in table 4.6. It is worth noticing that the effect of dangling chains in the crosslinked network is not being here considered.

Table 4.6. PDMS (thermally crosslinked) crosslink parameters for binary systems.

System	\overline{M}_c (kg/mol)	$\check{\rho}$ (mol/m ³)	$\overline{M}_c/MW_{\text{PDMS,CU}}$
MEK / PDMS	3.2	300.4	43.8
DEK / PDMS	2.8	352.0	37.3

The estimated average molecular weight between two crosslink points for the MEK/PDMS system is slightly higher when compared with the one calculated for the DEK/PDMS system. The observed discrepancy between the average molecular weight between two crosslink points for different solvents (MEK or DEK) is explained by the strong dependence of \overline{M}_c from the solvent-polymer interaction parameter, i.e., a variation of less than 3 % in one of the interaction parameters induces an identical \overline{M}_c for both systems. With the above consideration, it can be concluded that, for the used PDMS, the distance between two crosslink points corresponds to approximately 40 repeating units of PDMS.

The effect on the glass transition temperature was studied for PDMS with different degrees of crosslinking. The first sample measured was a thermally crosslinked one, just as the ones used for diffusion measurements. Second, the polyacrylonitrile support of a PDMS composite membrane was dissolved in order to obtain a PDMS sample just as the ones used for nanofiltration experiments. The difference between the PDMS from the diffusion experiments and the one obtained from the membrane resides in a further crosslink treatment via radiation exposure for the polymer in the real membrane. The second thermal heating scans for both samples are shown in figure 4.2.

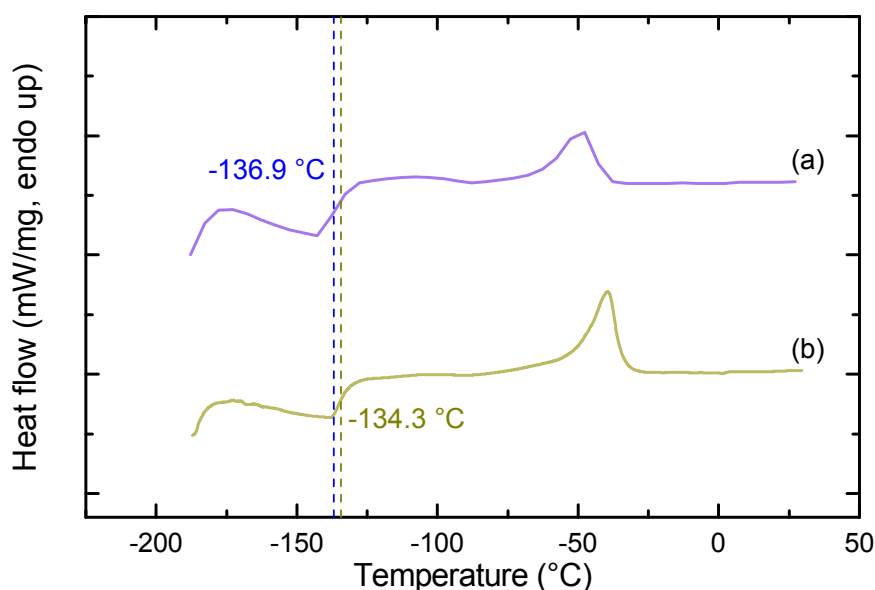


Figure 4.2. DSC second heating scans for the PDMS samples, crosslinked: (a) chemically; (b) chemically and by radiation.

The glass transition temperature of the sample which was further crosslinked is higher than the one of the only thermally crosslinked sample. As expected, the sample with higher degree of crosslinking, i.e., lower molecular weight between crosslink points, needs more energy to overcome the glassy state, which is explained due to the increasing lack of mobility of the chain segments between branching points. Surprisingly, only a small variation between the glass transition temperatures of both samples was found. The above result facilitates the assumption that the diffusion experiments carried out with the sample crosslinked only thermally can be used for further calculations (i.e., nanofiltration modeling) without deviating much from the behavior expected for the further crosslinked sample.

It is worth noticing that the more crosslinked sample shows a melting peak at higher temperature, which indicates more perfect crystals. That is inconsistent with the idea of more crosslink points, which typically hinder the ordered packing of segments. An important difference between the two samples is that, while the only thermally crosslinked sample is a bulk sample, the one further crosslinked by radiation is a thin film. It has been observed that different types of additives and surface interactions result in an enhancement of the crystallization rate as compared to native PDMS melts. This may explain the higher crystallization temperature (results not shown) and a consequently higher melting temperature despite the lower $\overline{M_c}$ (i.e., higher crosslinking

degree). The observed effect has been attributed to entropic interactions in the boundary layer.^[8]

4.1.5 Interaction parameters as a function of concentration

With the use of the Flory-Huggins-Staverman theory for ternary solvent-solvent-polymer systems it is possible to estimate the concentration dependence of the solvent-polymer interaction parameters. It has been observed that, in order to describe the swelling behavior of polymers in organic solutions, the elastic terms presented in the Flory-Rehner theory could be neglected when the polymer corresponds to PDMS.^[6, 9, 10]

Similar considerations to the ones presented in section 2.3.2 can be taken for the swelling experiments. The system reaches thermodynamic equilibrium after 8 hours, meaning that the chemical potential of the solvents at the interface is equal outside and inside the polymer, as shown in figure 4.3.

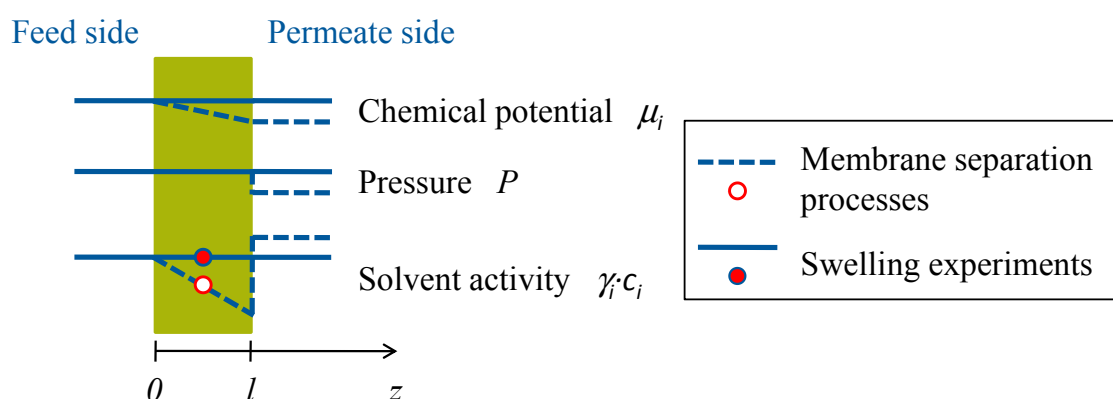


Figure 4.3. Schematic representation of the differences between swelling experiments and membrane separation process. The points represent the place where the solvent/solute average concentration inside the polymer is considered.

Therefore, the activities of the solvent in the free standing binary solvent-solvent solution are needed in order to make them equal to the activities inside the polymer. An estimation of the activity of the solvents as a function of TEG/EGDMEs concentration was done following the UNIFAC group contribution method with the software ActDF, and are summarized in figure 4.4. The non-linearity observed for the activities of the compounds relates with a deviation from ideality in the system, i.e., a closer behavior of

the activities to a linear proportionality with the concentration means that the system behaves more closely to the ideal behavior.

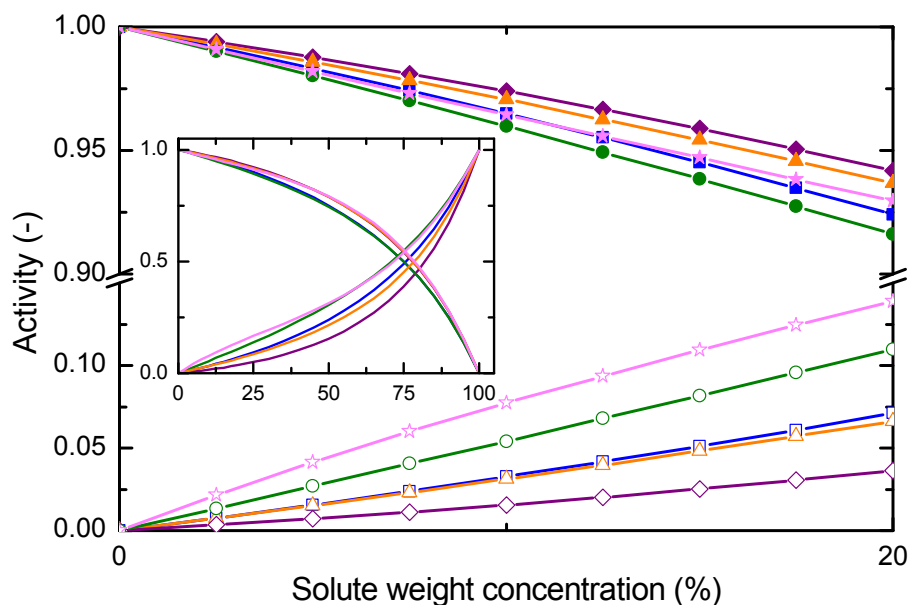


Figure 4.4. Activities of binary solvent mixtures, as a function of solute weight concentration. For each mixture, solvent and solute are represented by filled and open symbols respectively. ◆ MEK / TEGDME, ● MEK / PEGDME, ▲ DEK / TEGDME, ■ DEK / PEGDME, ★ MEK / TEG.

In figure 4.4, the activities of the TEG system are the ones which deviate most from linear behavior, having an inflection point where the curvature of the line changes from concave to convex. For all other systems, a deviation from an ideal behavior is also recognizable, but without the curvature change observed for the TEG system.

By matching the activities outside and inside the polymer, the Flory-Huggins-Staverman theory for ternary systems allows the estimation of the interaction parameters. A set of interaction parameters for different EGDME concentration values and for every ternary system are presented in table 4.7.

Table 4.7. Enthalpic interaction parameter of the mixtures estimated by the Flory-Huggins-Staverman solution theory.

System		Interaction parameter ^{a)}	Interaction parameter ^{b)}		
			5 wt %	10 wt %	15 wt %
MEK/TEGDME PDMS	s ₁ /s ₂	0.046	0.054	0.053	0.052
	s ₁ /pdms	0.567	0.732	0.798	0.864
	s ₂ /pdms	0.711	0.965	0.804	0.739
MEK/PEGDME PDMS	s ₁ /s ₂	0.299	0.089	0.084	0.084
	s ₁ /pdms	0.567	0.736	0.813	0.899
	s ₂ /pdms	0.137	0.133	0.129	0.129
DEK/TEGDME PDMS	s ₁ /s ₂	0.001	0.246	0.243	0.237
	s ₁ /pdms	0.373	0.661	0.710	0.756
	s ₂ /pdms	0.711	1.062	1.061	1.014
DEK/PEGDME PDMS	s ₁ /s ₂	0.149	0.309	0.330	0.339
	s ₁ /pdms	0.373	0.649	0.684	0.729
	s ₂ /pdms	0.137	0.141	0.141	0.140
MEK/TEG PDMS	s ₁ /s ₂	0.738	0.080	0.079	0.079
	s ₁ /pdms	0.567	0.764	0.858	0.942
	s ₂ /pdms	4.983	2.824	2.243	1.938

a) Interaction parameters calculated from solubility parameters; b) Interaction parameters calculated from swelling experiments.

It can be observed from the values presented in table 4.7 that the interaction parameter between ketones and EGDMEs slightly decreases when the EGDME concentration increases (with the exception of the DEK/PEGDME/PDMS system, where the interaction parameter increases). At the same time, the interaction parameter between the ketones and PDMS increases when the EGDME concentration increases. On the other hand, the interaction parameter between the EGDMEs and PDMS slightly decreases when the EGDME concentration increases. The interaction parameter between TEG and PDMS is the greatest one, which means that TEG is the worst solvent for PDMS among the studied solvents.

It should be noted that the Flory-Huggins-Staverman solution theory does not take into account neither the free volume of the polymer nor any difficulty to arrange a long molecule inside the polymer. Nevertheless, the swelling of the EGDME in the polymer seems to govern the estimation of the interaction parameter by the Flory-Huggins-Staverman equation (FHSe). Consequently, the interaction parameter between solvent and polymer needs to increase in order to balance the FHSe with lower amount of solvent inside the polymer. It should be noted that the molar volume of EGDME is at least 5 times higher than the ones corresponding to the solvents, therefore, much of the spaces inside the polymer are filled by the EGDME, with the consequent low volume fraction of solvent inside the polymer. This decrease of the solvent volume fraction induces an increase of the apparent solvent-polymer interaction parameter from the Flory-Huggins-Staverman equation. Therefore, the discrepancies between solvent-EGDME interaction parameters are a consequence of the above mentioned effects. Even so, the tendency of lower PEGDME/PDMS interaction parameter than the TEGDME/PDMS one is observed for both systems. Additionally, the DEK/PDMS interaction parameters are lower than the MEK/PDMS ones for both EGDMEs systems, as expected from the higher achieved swelling.

4.2 Diffusion coefficients

4.2.1 Self-diffusion coefficients

The self-diffusion coefficients of pure substances were investigated with the use of the Dullien equation (equation 2.31). Figure 4.5 shows the self-diffusion coefficient as a function of temperature.

Figure 4.5 shows that, when the self-diffusion of similar substances are compared (i.e., MEK/DEK and TEGDME/PEGDME), the self-diffusivities of smaller substances are higher than the ones corresponding to bigger molecules. As expected, MEK has more mobility than DEK and TEGDME more than PEGDME. On the other hand, even though TEG is a smaller molecule than both EGDMEs, the presence of hydrogen bonds induces molecule coupling which hinders the mobility, and this is evidenced by a higher viscosity of TEG than those of both EGDMEs. The diffusion coefficients of pure substances were measured with PFG-NMR according to the process described in section 3.2.3 at 25 °C, and the results are summarized in table 4.8.

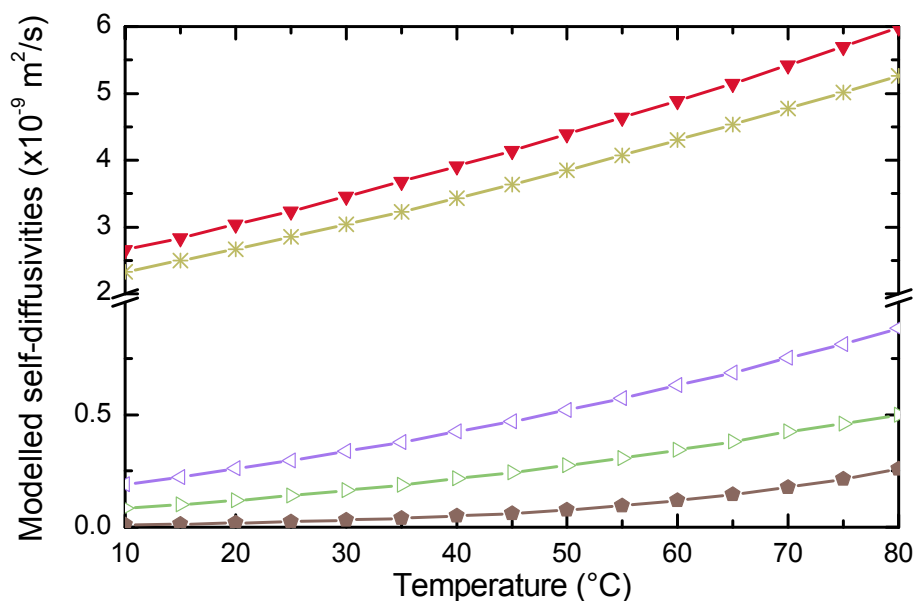


Figure 4.5. Self-diffusion coefficients for ▼ MEK, * DEK, ◁ TEGDME, ▷ PEGDME, ◆ TEG as a function of temperature.

It can be observed from the experimental self-diffusivities presented in table 4.8 that, for the ketones and the EGDMEs, as expected, the self-diffusion coefficients of smaller molecules are higher than the ones of bigger molecules due to the facility of the smaller molecules to move through other molecules of the same substance. The self-diffusivity of TEG is lower than the one of both EGDMEs considered here. This result is analogous to the one observed in the simulation (see figure 4.5) and is caused by the hindered mobility of TEG due to the formation of hydrogen bonds.

Table 4.8. Measured solvents self-diffusion coefficients at 25 °C with PFG-NMR.

Substance	$\hat{D} \left(10^{-9} \text{ m}^2/\text{s} \right)$
MEK	3.49 ± 0.35
DEK	2.91 ± 0.29
TEGDME	0.30 ± 0.03
PEGDME	$0.13 \pm (> 0.01)$
TEG	$0.03 \pm (>> 0.01)$

Due to convection effects, Wirbelstrom and non-linearity of the sender, an inaccuracy of 10 % is expected from the measurements. Therefore, when compared to the values obtained by the Dullien equation, all of the measurements lead to similar values within the expected error.

A merge of the Dullien equation with the pure solvent simplified version of the Vrentas & Duda diffusion equation allows the calculation of the necessary free volume parameters for each solvent, as described in section 2.1.1.2. Figure 4.6 shows the quality of the viscosity regression, whereas table 4.9 presents the regressed values of the Vrentas & Dudas free volume parameters. Two different methods were used to obtain the free volume diffusion parameters: a curve fitting method based on the steepest decent method minimizing the sum of square errors, and a non-linear regression with constrains based on the Levenberg-Marquardt algorithm.

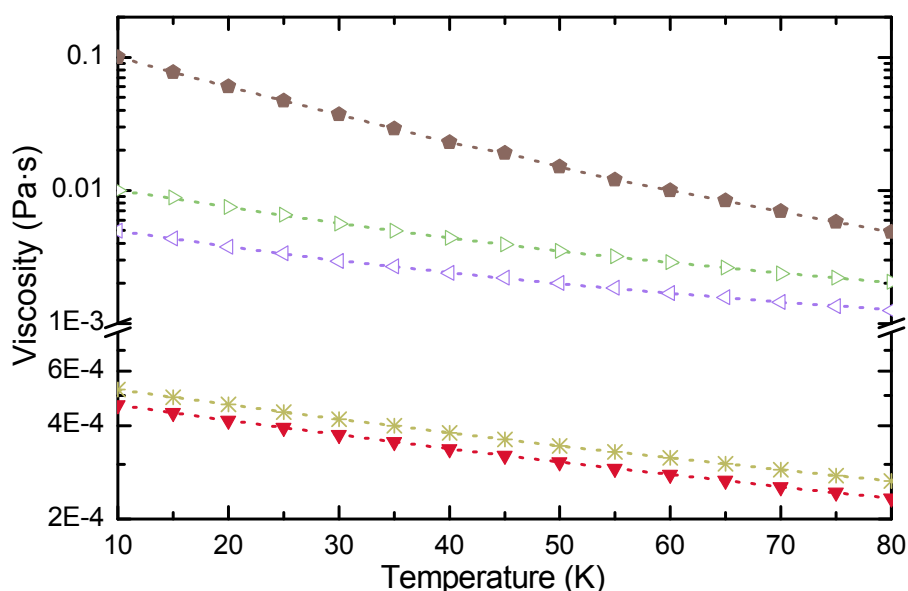


Figure 4.6. Solvent viscosity as a function of temperature. The broken lines correspond to simulated data and the symbols represent experimental data with the following identification: ▼ MEK, * DEK, ◁ TEGDME, ▷ PEGDME, ◆ TEG.

Table 4.9. Diffusion and free-volume parameters calculated from the Vrentas & Duda diffusion theory.

Substance	$\ddot{D} \left(10^{-8} \text{ m}^2/\text{s} \right)$	$K_{3i} - T_{g_i} \text{ (K)}$	$K_{ii}/\lambda \left(10^{-7} \text{ m}^3/\text{kg} \cdot \text{K} \right)$
PDMS ^(a)	–	-81.0	9.32
MEK ^(b)	30.97	56.3	5.49
DEK ^(b)	24.98	49.2	5.86
TEGDME ^(b)	2.01	-139.1	12.66
PEGDME ^(b)	3.20	-120.5	8.62
TEG ^(b,c)	1730.85 ^(b)	9.4 ^(b)	1.64 ^(b)
	165.60 ^(c)	-84.4 ^(c)	3.34 ^(c)
Ethylene glycol ^(a)	88.20	-139.38	7.50

a) From Hong^[11], b) Curve fitting, c) Non-linear regression.

For the ketones and EGDMEs both methods (i.e., curve fitting and non-linear regression) provided similar results, whereas for TEG significant differences were found. As expected, the diffusion pre-exponential factor and $K_{3i} - T_{g_i}$ increases and K_{ii}/λ decreases when the molecular weight decreases if both EGDMEs are compared.^[12] The same tendency is observed for the TEG results obtained by both regression methods. However, the values obtained by curve fitting seem to be too different when compared to ethylene glycol. Nonetheless, both results are able to describe the viscosity of TEG satisfactorily, as shown in figure 4.7.

The best fit of the viscosity is found with the curve fitting method (solid line), whereas only small deviations are found with the non-linear regression method (dashed line). These differences are too small to be observed in figure 4.7, however they can be appreciated when the sum of square error is calculated (shown in appendix 3). Therefore, more reliable viscosity data for TEG is needed in order to define which result represents better the experimental data.

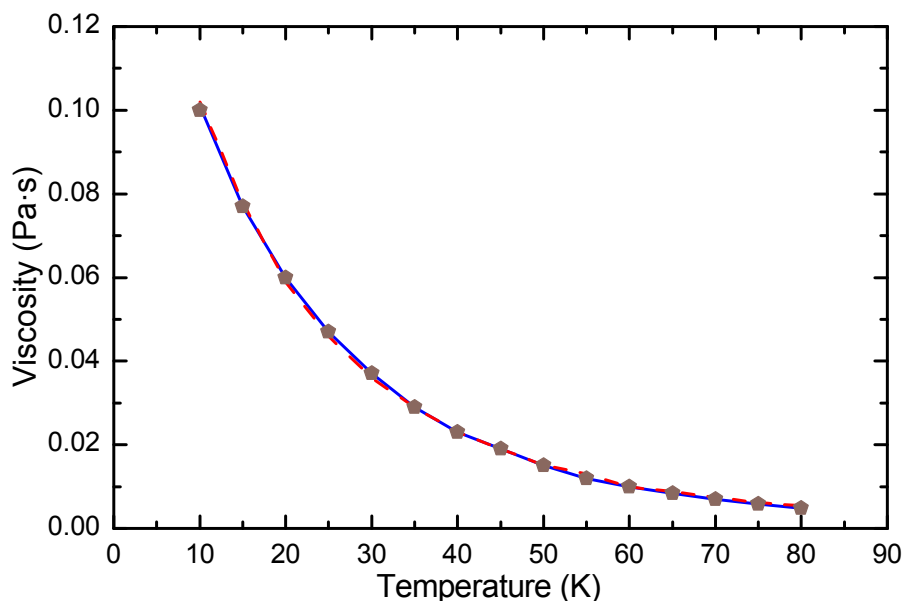


Figure 4.7. TEG viscosity as a function of temperature. The symbol \blacklozenge corresponds to viscosity data estimated by ASPEN Properties, the solid line represents the estimation by curve fitting and the dashed line corresponds to the non-linear regression.

4.2.1 Tracer diffusion coefficients

Tracer diffusion coefficients for ternary solvent-solvent-polymer systems were measured by PFG-NMR spectroscopy as described in section 3.2.3. The results are summarized in table 4.10.

The measured solvent tracer diffusion coefficients for binary solvent-polymer mixtures are lower than the corresponding self-diffusion coefficients. As expected, the mobility of the molecules is diminished inside the polymer network. Additionally, the tracer diffusivities are lower for bigger molecular sizes, that is, the tracer diffusion coefficient of MEK and TEGDME are higher than the DEK or PEGDME tracer diffusivities, respectively. For both comparisons, a lower mobility inside the polymer network is expected for the bigger molecules – with a similar chemical potential – because of the existence of less possible configurations inside the lattice. It should be remarked that the tracer diffusion coefficients of DEK are lower than the ones of MEK, despite the fact that the swelling degrees of the DEK systems are higher than the ones of MEK systems.

Table 4.10. Tracer diffusion coefficients for binary solvent-polymer systems and ternary solvent-solvent-polymer systems as a function of EGDME concentrations.

Binary system		Tracer diffusion coefficients ($10^{-9} \text{ m}^2/\text{s}$)		
MEK/PDMS	MEK	2.2 ± 0.2		
DEK/PDMS	DEK	2.0 ± 0.2		
TEGDME/PDMS	TEGDME	0.27 ± 0.03		
PEGDME/PDMS	PEGDME	0.13 ± 0.01		
Ternary system		Tracer diffusion coefficients ($10^{-9} \text{ m}^2/\text{s}$)		
		5 wt %	10 wt %	15 wt %
MEK/TEGDME/PDMS	MEK	2.1 ± 0.2	2.0 ± 0.2	1.9 ± 0.2
	TEGDME	1.0 ± 0.1	0.8 ± 0.1	0.79 ± 0.09
MEK/PEGDME/PDMS	MEK	2.1 ± 0.2	1.9 ± 0.2	1.6 ± 0.2
	PEGDME	0.70 ± 0.07	0.56 ± 0.06	0.44 ± 0.05
MEK/TEG/PDMS	MEK	1.44 ± 0.1	1.44 ± 0.1	1.17 ± 0.1
	TEG	0.65 ± 0.07	0.62 ± 0.06	0.65 ± 0.07
DEK/TEGDME/PDMS	DEK	1.9 ± 0.2	1.8 ± 0.2	1.6 ± 0.2
	TEGDME	0.9 ± 0.2	0.85 ± 0.09	0.68 ± 0.08
DEK/PEGDME/PDMS	DEK	2.0 ± 0.2	1.8 ± 0.2	1.6 ± 0.2
	PEGDME	0.73 ± 0.07	0.67 ± 0.07	0.54 ± 0.05

For ternary systems, it is expected that the presence of slow diffusive substances (i.e., EGDME) decreases the diffusivity of high diffusive substances (i.e., MEK/DEK) due to dragging effects. Therefore, the tracer diffusivities of both MEK and DEK should be upper bounded by the tracer diffusion found in the ketone/PDMS mixtures. Additionally, the swelling induced in the polymer by the presence of the ketones facilitates the mobility of the low diffusive substances inside the polymer network. Contrary, the tracer diffusion coefficient of EGDME/PDMS systems should be the lower bound of the corresponding ternary ketone/EGDME/PDMS system.

The tracer diffusion coefficients are simulated by the use of the Vrentas & Duda diffusion theory (section 2.1.1.2) or the Wesselingh & Bollen model (2.1.1.2). In addition to the free volume parameters estimated from previous sections, the Vrentas &

Duda model requires the estimation of the ratio between critical molar volume of a jumping unit of a substance to the one of the jumping unit of the polymer (ξ). As described in section 2.1.1.2, this factor is defined by equation 2.44 and the calculation is completed with the experimental correlation 2.45. However, the estimation of the critical molar volume of the polymer jumping unit still remains uncertain and inaccurate. Therefore, this parameter is often estimated by diffusion data regression as stated in the theoretical part of this book. A set of ξ parameters calculated by equations 2.44-2.45 and estimated from diffusion data are summarized in table 4.11.

Table 4.11. Critical molar volume ratio between jumping units in a binary mixture.

Substance	$\xi^{a)}$	$\xi^{b)}$	$\xi^{c)}$
MEK	0.779	1.193	0.806
DEK	0.955	1.209	0.807
TEGDME	2.289	0.770	0.510
PEGDME	3.022	0.950	0.640

a) Estimated by equations 2.44 and 2.45; b) Calculated by diffusion data regression for an non-crosslinked polymer; c) Calculated by diffusion data regression for a crosslinked polymer.

The values shown in the column denoted by the superscript “b” in table 4.11 represent the critical molar volume ratio between jumping units regressed from the Vrentas & Duda diffusion theory without any consideration of crosslinking in the polymer. The results show an overestimation of both MEK and DEK parameters. Besides showing a good correlation of the tracer diffusion data, the parameters for both ketones are higher than 1.0, differing from experimental calculations found elsewhere.^[13, 14] Nevertheless, for correlating purposes, parameters higher than 1.0 are often used because the free volume theory allows it without any boundary.^[15, 16]

Additionally, the values found for TEGDME and PEGDME are lower than the ones estimated by equations 2.44-2.45. From equation 2.44, a decrease of the ratio of critical molar volume of jumping units indicates that the permeant molecule is moving in sections rather than as a whole molecule. The later is especially true for large molecules which have difficulties to arrange themselves inside the lattice. Therefore, ξ parameters

for the EGDMEs are expected to be lower than the ones calculated by equations 2.44-2.45.

In order to take into account any effect of the degree of crosslinking, the ratio between critical molar volume of jumping units and the free volume crosslink parameter were solved together by non-linear regression of the available diffusion data. The results are presented in table 4.11 in the column denoted by the superscript “c”. The estimated ξ parameter for MEK is close to the one estimated by equations 2.44 and 2.45. The results corresponding to DEK indicate a segmental movement of the solvent inside the polymer, with a main unit similar to the one of the MEK (i.e., one ethyl group of DEK is moving separately from the rest of the molecule). The regressed TEGDME and PEGDME values correspond to 22.3 % and 21.2 % of the values estimated by equations 2.44 and 2.45. Therefore, the movement of each EGDME molecule across the polymer can be assumed to take place in approximately 5 sections. For these results, the corresponding crosslink factor from the Vrentas & Duda diffusion theory is 0.643.

An inspection in the Vrentas & Duda theory reveals that if the polymer crosslinking is not considered, the ξ parameter should increase to compensate the term corresponding to the free volume per kilogram of mixture, which is higher for non-crosslinked polymers than for crosslinked ones. Therefore, the observed differences between columns “b” and “c” in table 4.11 are expected. To qualify the goodness of the regression, a graph of measured tracer diffusivities versus simulated ones for a crosslinked polymer is presented in figure 4.8, while the insert corresponds to the correlation for a non-crosslinked polymer.

For both approaches of the Vrentas & Duda diffusion theory (i.e., for crosslinked and non-crosslinked polymers), the simulation of tracer diffusion data describes well the values from the PFG-NMR spectroscopy measurements. Alternatively, tracer diffusion coefficients for ternary mixtures can be estimated by the Wesselingh & Bollen model as described in section 2.1.1.2. As stated in the theoretical part, multicomponent mixtures are treated as pseudo-pure substances in this model, in order to extend the self-diffusion equations to be used in the estimation of tracer diffusivities. It should be remarked that in the model developed by Wesselingh & Bollen, the overlap factor which considers that the same free-volume is available for more than one molecule (λ) was arbitrary set

to be 0.70.^[17] The results obtained by the Wesselingh & Bollen model with a λ parameter equal to 0.70 are shown in figure 4.9.

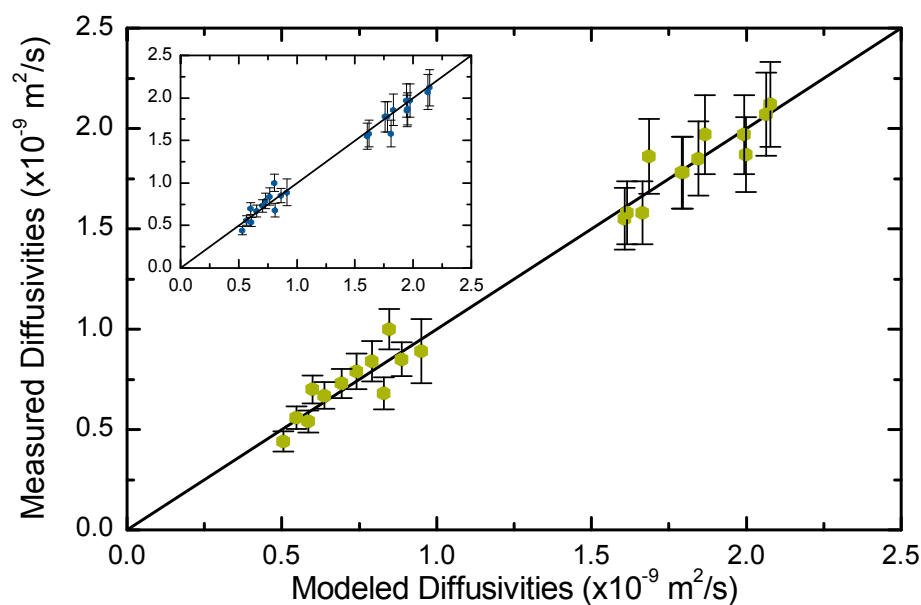


Figure 4.8. Correlation between experimental PFG-NMR diffusion data and simulated data from the Vrentas & Duda diffusion theory for crosslinked polymers (the insert corresponds to non-crosslinked polymers).

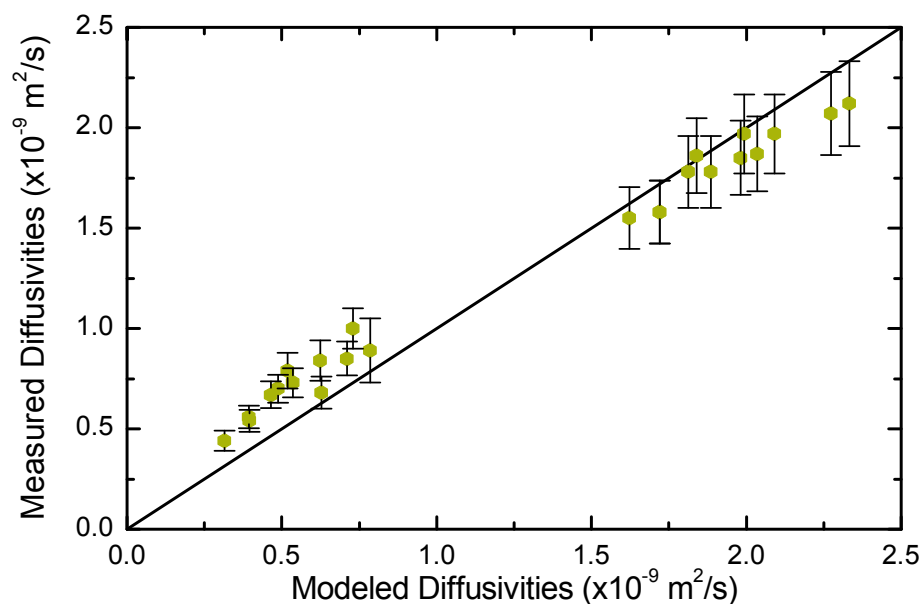


Figure 4.9. Correlation between experimental PFG-NMR diffusion data (measured diffusivities) and simulated data from the Wesselingh & Bollen diffusion model (modeled diffusivities).

For most of the cases, an underestimation of the tracer diffusivities of EGDMEs (up to 30 %) as well as an overestimation tendency of the ones corresponding to the ketones were found. However, if the λ factor remains equal for all the substances, but is moved between 0.50 and 1.00 – which are the theoretical boundaries – the tracer diffusion coefficients move as a block, as shown in figure 4.10. An inspection of different λ parameters reveals the best fit value to be 0.69.

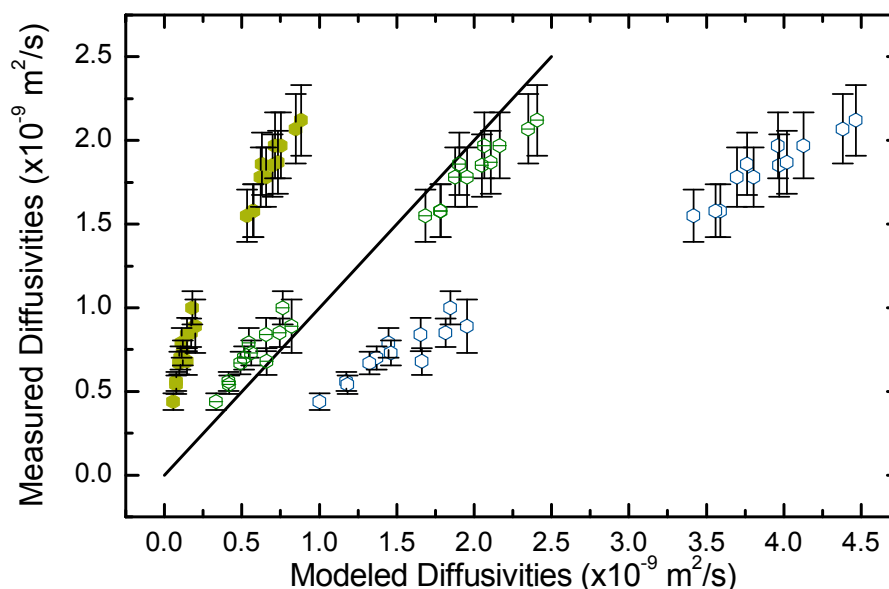


Figure 4.10. Correlation between experimental PFG-NMR diffusion data and simulated data from the Wesselingh & Bollen diffusion model. The filled, struck and open symbols correspond to $\lambda = 1.0$, $\lambda = 0.69$ and $\lambda = 0.5$, respectively.

Nonetheless, the free volume overlap factor for pure substances can be estimated by equation 4.4, which is known as the first application of the free volume theory. Therefore, non-linear regressions of pure viscosity data as well as diffusivity data allow the estimation of the overlap factor of pure substances. The regressed values are shown in table 4.12.

$$\eta_i = \eta_0 \cdot \exp\left(\lambda_i \cdot \frac{V_i^C}{V_i^F}\right) \quad \text{Eq. 4.4}$$

Table 4.12. Critical molar volume ratio between jumping units in a binary mixture.

Substance	λ^a	η_0 (10^{-5} Pa · s)	λ^b
MEK	0.950	3.922	0.750
DEK	0.823	4.427	0.725
TEGDME	0.685	6.692	0.650
PEGDME	0.760	6.767	0.750

a) Estimated by equation 4.4; b) Estimated by non-linear regression of tracer diffusion data.

By comparison, the free-volume overlap factors calculated by regression of diffusion data (column λ^b) in table 4.12) show lower values compared to the ones estimated by viscosity regression (column λ^a) in table 4.12). This difference may be explained by the fact that the presence of an “*i*” permeant inside the polymer diminishes the availability of a molecule of permeant “*j*” to occupy a specific place from the total free-volume. Therefore, the λ parameter calculated by regression of diffusion data tends to account not only for the competition between molecules of the same substance to occupy a specific lattice place but also for competition between molecules of both substances (i.e., “*i*” and “*j*”). This is not the case for the λ parameter estimated by viscosity regression, since the later one is calculated with equation 4.4 which describes only the viscosity of pure substances. A correlation between experimental and simulated tracer diffusivities when the λ parameters are estimated from diffusion data regression is shown in figure 4.11.

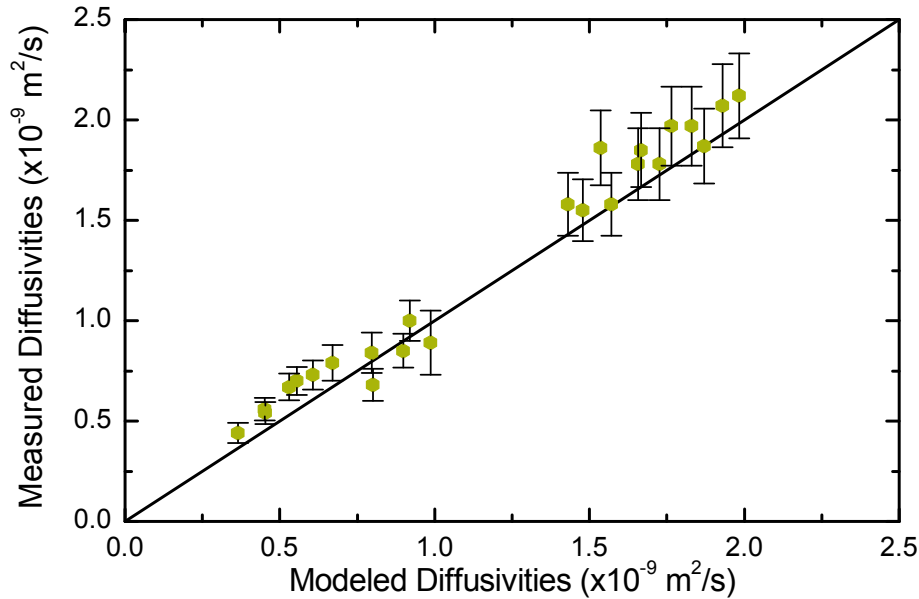


Figure 4.11. Correlation between experimental PFG-NMR diffusion data and simulated data from the Wesselingh & Bollen diffusion model when the free volume overlap factor is regressed from experimental ternary diffusivities.

From the results presented in figure 4.11 it is evident that there is a good agreement between the experimental and the simulated values of the tracer diffusivities. Nevertheless, this introduces an additional fit parameter into the simulation, with the consequent loss of any prediction capability.

4.3 Nanofiltration

4.3.1 Permeation experiments

Nanofiltration measurements were carried out as described in section 3.2.7. The effect of the chain length of the permeants was investigated by comparing the permeation behavior of MEK/TEGDME and MEK/PEGDME systems. In addition, the affinity between the solvent and the polymeric membrane is studied by comparing the MEK/TEGDME and DEK/TEGDME systems. Later, the permeation behavior of a system similar in chain length of the permeant and affinity between solvent and polymeric matrix is studied by the analysis of the permeation properties of a MEK/TEG mixture. A summary of the permeation fluxes for different systems at 25 °C is shown in figures 4.12 to 4.15.

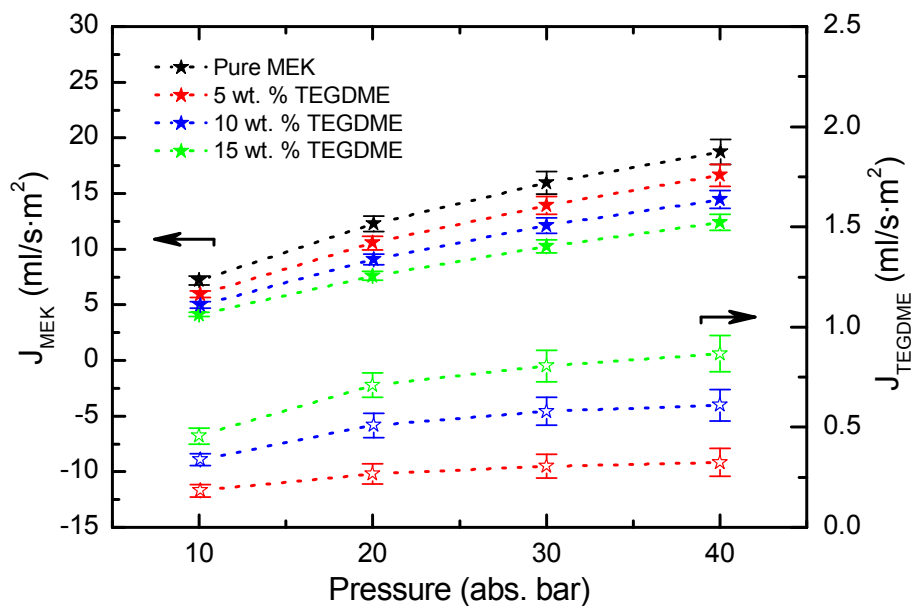


Figure 4.12. Experimental permeation fluxes at 25 °C for a MEK/TEGDME system as a function of the absolute applied pressure for different TEGDME feed concentrations. The filled symbols represent the fluxes of MEK, whereas the open symbols correspond to TEGDME fluxes.

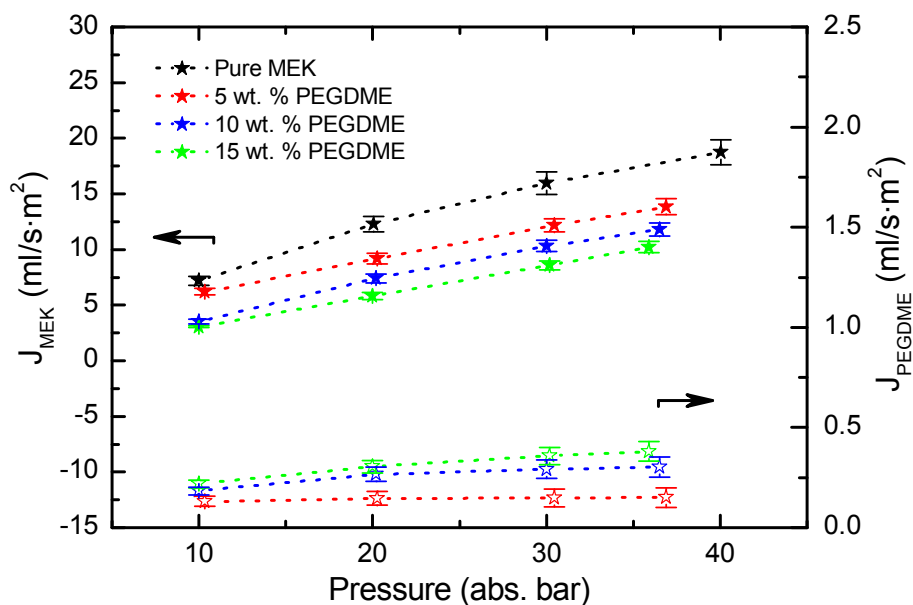


Figure 4.13. Experimental permeation fluxes at 25 °C for a MEK/PEGDME system as a function of absolute applied pressure for different PEGDME feed concentrations. The filled symbols represent the fluxes of MEK, whereas the open symbols correspond to PEGDME fluxes.

As expected, by comparing MEK/TEGDME and MEK/PEGDME permeation behavior shown in figures 4.12 and 4.13, respectively, the system with the longer EGDME chain presents lower permeation fluxes than the one with the shorter chain length. When the MEK/TEGDME system is compared to the MEK/PEGDME system, the higher permeation observed is produced by the higher swelling degree, higher thermodynamic diffusivities and lower viscosity of the MEK/TEGDME mixture than the ones corresponding to the MEK/PEGDME system, according to the results presented in the previous sections in figure 4.1, table 4.10³ and table 3.3, respectively.

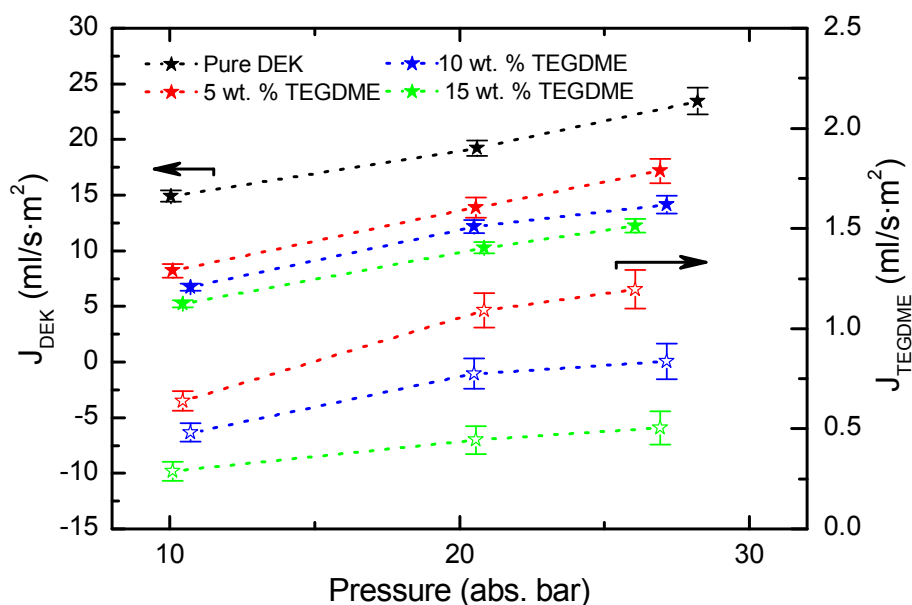


Figure 4.14. Experimental permeation fluxes at 25 °C for a DEK/TEGDME system as a function of absolute applied pressure for different TEGDME feed concentrations. The filled symbols represent the fluxes of DEK, whereas the open symbols correspond to TEGDME fluxes.

Similarly, the permeations found for the system formed by DEK/TEGDME and presented in figure 4.14 are higher than the corresponding ones for MEK/TEGDME (figure 4.12). Even though both mixtures present similar thermodynamic diffusivities (see tracer diffusivities in table 4.10), the higher polymer swelling presented in the system of DEK/TEGDME (shown in figure 4.1) induces a greater permeation through the membrane when compared to the system of MEK/TEGDME.

³ The behavior of the thermodynamic diffusivities corresponds to the one of tracer diffusivities presented in the mentioned table (results not shown).

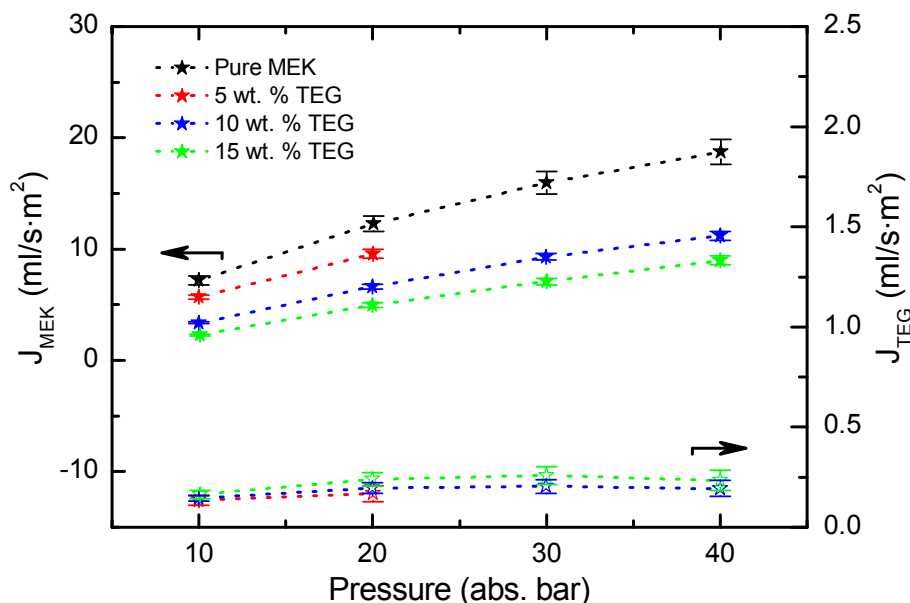


Figure 4.15. Experimental permeation fluxes at 25 °C for a MEK/TEG system as a function of absolute applied pressure for different TEG feed concentrations. The filled symbols represent the fluxes of MEK, whereas the open symbols correspond to TEG fluxes.

Finally, as shown in figure 4.15, the permeation of the system MEK/TEG is lower than the one of MEK/TEGDME (figure 4.12), and even lower than the one of MEK/PEGDME (figure 4.13). Here, the appearance of hydrogen bonds between TEG molecules hinders the permeation through the membrane. The high viscosity of the system and low thermodynamic diffusivities (tracer diffusivities are presented in table 4.10) are consequences of the formation of those hydrogen bonds. The arrangement of a determined molecule inside the polymer lattice is affected by the size of the permeating molecule. Therefore, it could be concluded that the coupling of TEG molecules by attractive interactions diminishes the possible number of arrangements in the polymer lattice, with the subsequent detriment of swelling degree and permeation through the polymer.

The effect of temperature over the permeation behavior was investigated by MEK/TEGDME nanofiltration measurements at different temperatures (i.e., 20 °C, 25 °C and 30 °C). The summary of the measurements at 20 °C and 30 °C is presented in figures 4.16 and 4.17, respectively, whereas the permeation at 25 °C is shown in figure 4.12.

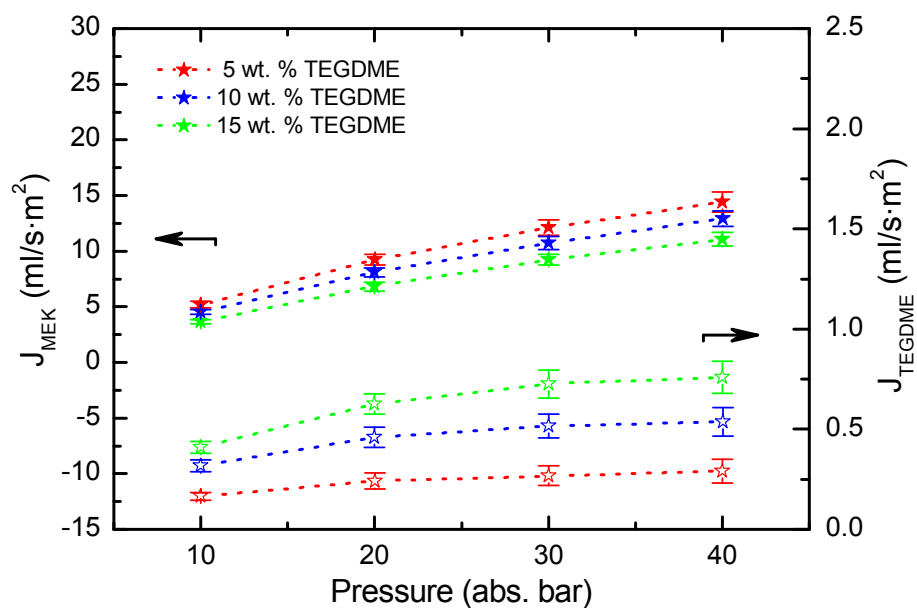


Figure 4.16. Experimental permeation fluxes at 20 °C for a MEK/TEGDME system as a function of absolute applied pressure for different TEGDME feed concentrations. The filled symbols represent the fluxes of MEK, whereas the open symbols correspond to TEGDME fluxes.

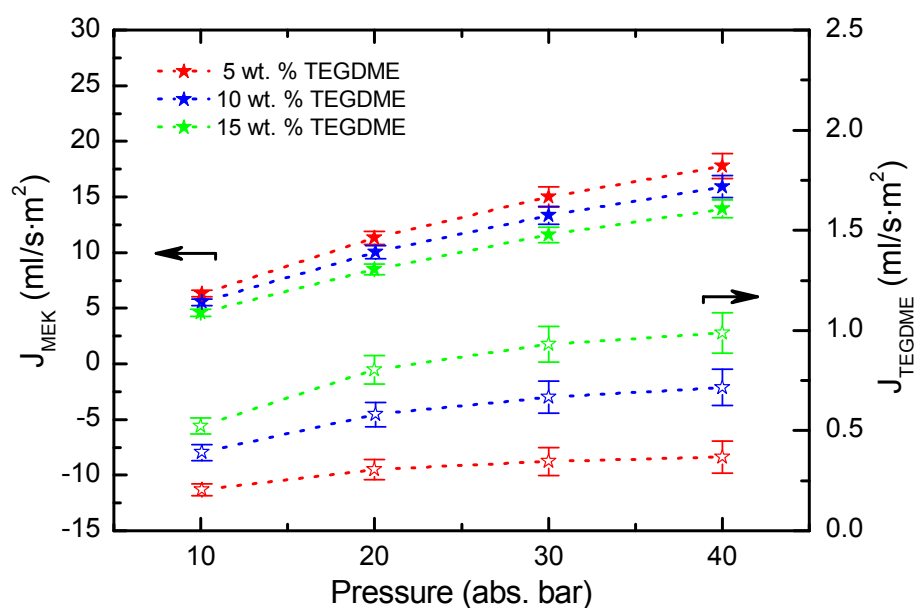


Figure 4.17. Experimental permeation fluxes at 30 °C for a MEK/TEGDME system as a function of absolute applied pressure for different TEGDME feed concentrations. The filled symbols represent the fluxes of MEK, whereas the open symbols correspond to TEGDME fluxes.

As shown in figures 4.12, 4.16 and 4.17, the permeation fluxes for both MEK and TEGDME increase when the temperature increases. This behavior is expected due to two independent contributions. First, the viscosity of any of the mixtures decreases when the temperature increases. Therefore, the viscous contribution of the permeation fluxes increases with the temperature. The second contribution refers to the increase of the polymer free volume when the temperature increases.^[18, 19] This increase in the free volume of the polymer has as a consequence the increase of the diffusion coefficients, and therefore higher permeation fluxes are expected.

4.3.2 Concentration inside the membrane

The average molar concentration inside the membrane represents a key parameter necessary for the further modeling. Therefore, the considerations of the solution-diffusion model together with the Flory-Huggins-Staverman equation for ternary systems are used.

According to section 2.3.3, a chemical potential balance at the membrane interfaces produces the following relations:

$$a_{i,F} = a_{i,MF} \quad \text{Eq. 4.2}$$

$$\ln a_{i,P} - \frac{V_i}{R \cdot T} \cdot \Delta P = \ln a_{i,MP} \quad \text{Eq. 4.3}$$

The concentration of the binary ketone/glycol mixture (e.g., MEK/TEGDME) is known from experimental data, as described in section 3.2.5. Therefore, the activities of the free solutions at the feed and permeate side are estimated by the use of the UNIFAC group contribution method (see figure 4.4). A set of molar concentrations inside the membrane at different experimental conditions for the MEK/TEGDME system are summarized in table 4.13, whereas the values for the complete set of experiments are found in appendix 3.

Table 4.13. Concentration inside the membrane for the MEK/TEGDME system at different experimental conditions.

<i>P</i> (abs. bar)	Weight concentration in the free solution (%)		Weight concentration inside the membrane (%)			Average molar concentration (mol/m ³)		
	Feed	Permeate	S1	S2	PDMS	S1	S2	PDMS
10-40	0.00	0.00	54.2	0.0	45.8	6548.6	0.0	5376.2
10	4.72	3.73	45.1	1.9	53.0	5542.5	76.7	6347.3
20	4.76	3.10	42.1	1.7	56.2	5212.8	67.3	6765.4
30	4.86	2.69	40.2	1.6	58.2	4995.3	63.3	7035.2
40	4.77	2.40	38.8	1.5	59.7	4832.6	61.0	7234.8
10	9.89	7.86	39.2	3.7	57.1	4885.6	147.5	6921.0
20	9.97	6.60	36.9	3.2	59.9	4612.5	131.0	7292.9
30	9.78	5.69	35.3	3.0	61.7	4434.9	122.3	7528.8
40	9.85	5.05	34.1	2.9	63.0	4293.3	117.2	7711.5
10	15.21	12.22	33.7	5.1	61.2	4242.4	208.4	7505.3
20	15.12	10.55	31.8	4.5	63.7	4016.8	184.6	7843.9
30	15.13	9.02	30.5	4.1	65.4	3861.9	169.8	8070.7
40	15.05	8.09	29.4	3.9	66.6	3739.5	162.2	8237.8

“S1” corresponds to MEK and “S2” corresponds to TEGDME

As shown in table 4.13, the concentration of PDMS increases when the TEGDME feed concentration increases, as expected from the swelling experiments previously presented in figure 4.1. Additionally, the concentration of PDMS increases when the applied transmembrane pressure increases. This behavior could be explained by the compaction of the composite membrane caused by the increment of the pressure. Therefore, when high pressures are applied, the PDMS layer is not able to increase its thickness – due to the swelling – as much as under the influence of low pressures.

4.3.3 Mutual diffusion coefficients

As discussed in section 2.1.1.3, the estimation of mutual diffusivities for ternary systems cannot be easily achieved without the introduction of adjustable parameters.^[17] Three different approaches are proposed in order to accomplish the calculation. First,

the Wesselingh & Bollen model allows the estimation of the tracer diffusion coefficients (section 2.1.1.2) as well as it proposes a way to estimate the mutual diffusivities as a function of the tracer diffusivities (equation 2.58). The second approach consists of the use of experimental tracer diffusion data (PFG-NMR measurements) and its combination with the polymer tracer diffusivity obtained by the Wesselingh & Bollen model, and then following the further steps presented in that model. The third approach is similar to the second one. It consists of the use of the Vrentas & Duda diffusion theory to calculate tracer diffusion coefficients of the permeants, and combining these values with the Wesselingh & Bollen model. A scheme of the different calculation methods is presented in figure 4.18, whereas the estimated mutual diffusion coefficients, among other calculations, can be found in appendix 3.

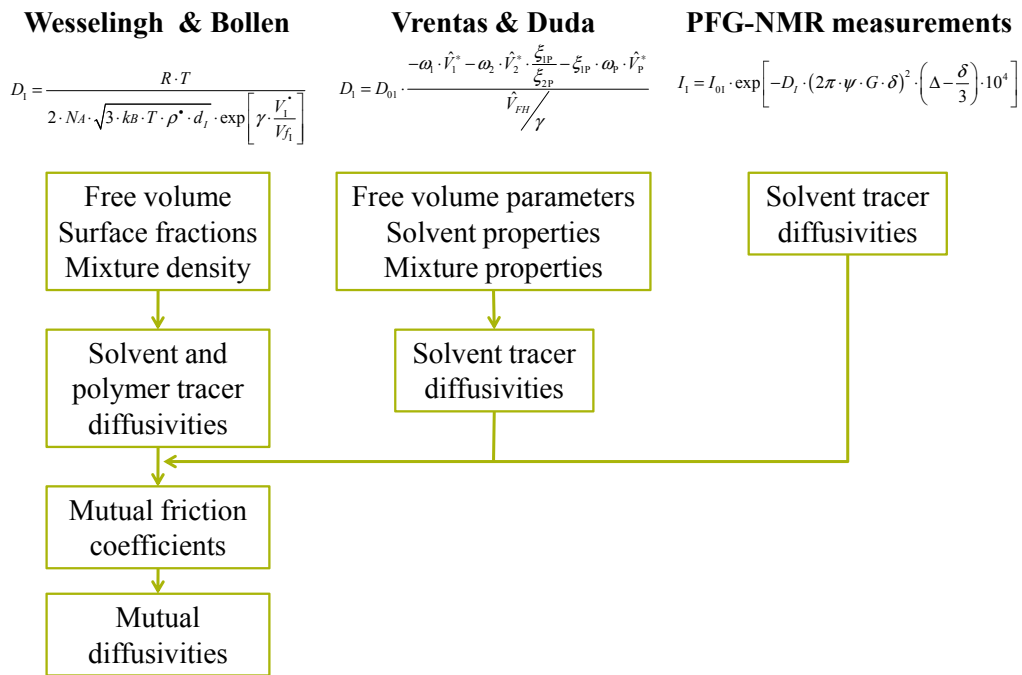


Figure 4.18. Scheme of different calculation methods for the estimation of mutual diffusion coefficients.

The difference between carrying out the calculation only with the use of the Wesselingh & Bollen model or by the combination of methods proposed by the two approaches resides in the reliability of the tracer diffusivities. The Vrentas & Duda diffusion theory seems to be more precise and consistent than the Wesselingh & Bollen model when the results are compared to experimental data. As explained in previous sections, for the Vrentas & Duda theory it is necessary to estimate the ratio between the critical molar

volumes of jumping units of two compounds in a mixture (ξ), which is dependent on the interaction between solvent and polymer. On the contrary, the overlap factor from the Wesselingh & Bollen model (λ) seems to be more dependent on the nature of the mixture than on the interaction with the polymer.

4.3.4 Modeling of organic solvent nanofiltration

The nanofiltration experiments at room temperature were modeled by the solution-diffusion with imperfections model as described in section 2.3.4. The correlations between modeled and experimental data for different ketone/EGDME systems are shown in figures 4.19 to 4.21, whereas the regressed parameters of the model are shown in table 4.14.

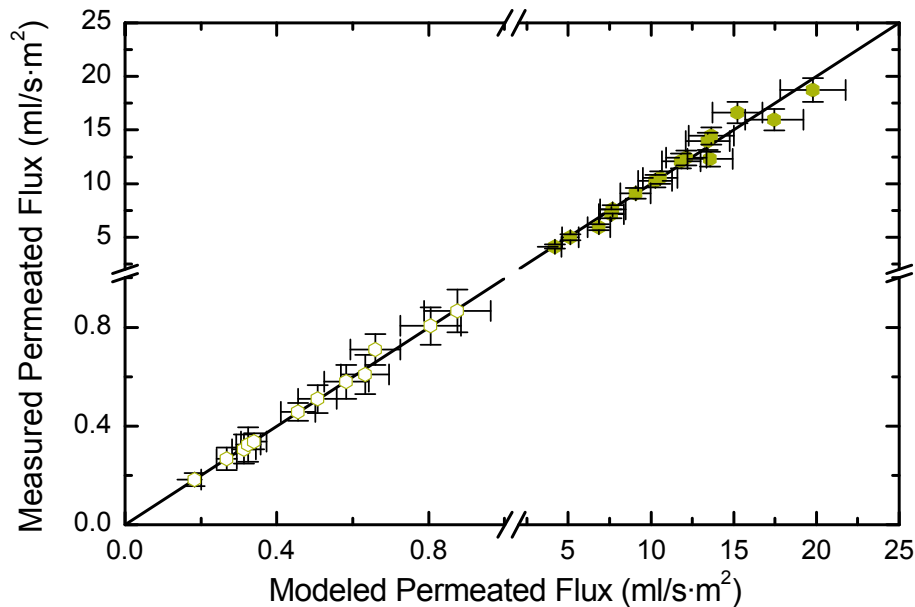


Figure 4.19. Correlation between measured MEK/TEGDME permeation fluxes and simulated data calculated by the solution-diffusion with imperfections model. The filled symbols represent the fluxes of MEK, whereas the open symbols correspond to TEGDME fluxes.

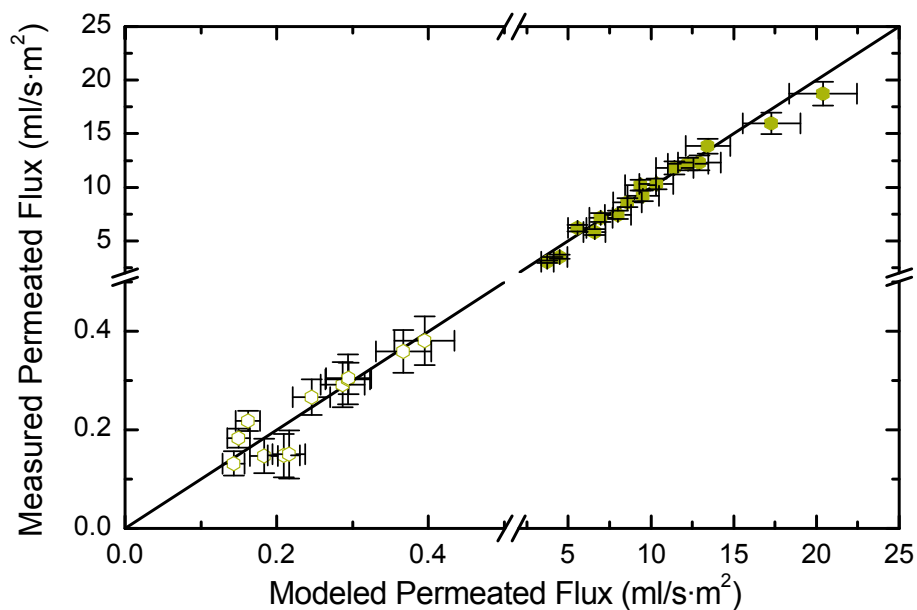


Figure 4.20. Correlation between measured MEK/PEGDME permeation fluxes and simulated data calculated by the solution-diffusion with imperfections model. The filled symbols represent the fluxes of MEK, whereas the open symbols correspond to PEGDME fluxes.

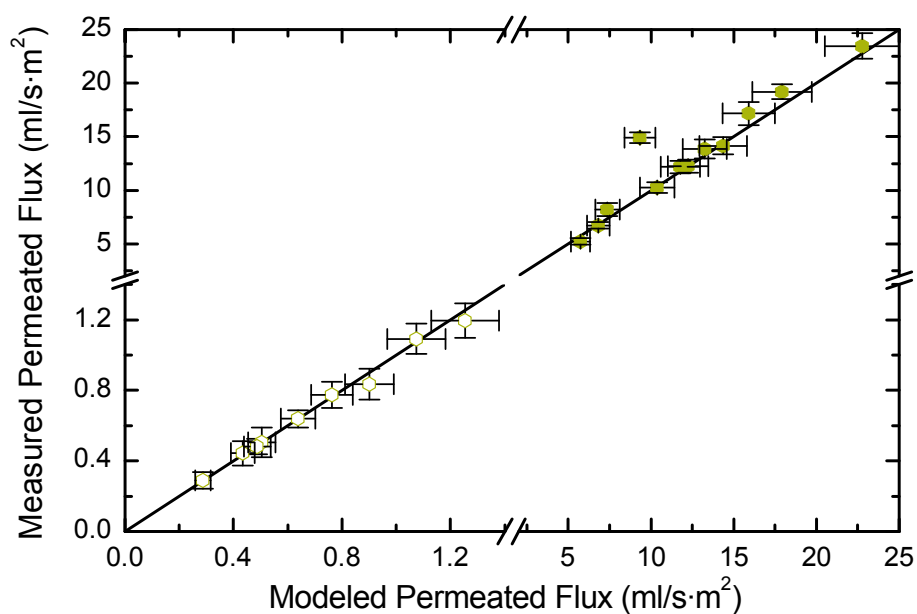


Figure 4.21. Correlation between measured DEK/TEGDME permeation fluxes and simulated data calculated by the solution-diffusion with imperfections model. The filled symbols represent the fluxes of DEK, whereas the open symbols correspond to TEGDME fluxes.

Table 4.14. Regressed parameters from the solution-diffusion with imperfections model: membrane thickness (l), partial viscous permeability of the membrane (\tilde{K}) and compaction factor as a function of different feed concentrations (α).

Substance	$l(\mu\text{m})$	$\tilde{K}_i (10^{-10} \cdot \text{m}^2)$		$\alpha (10^{-7} \cdot \text{Pa}^{-1})$			
		S1	S2	0 wt %	5 wt %	10 wt %	15 wt %
MEK/TEGDME	26.6	1.99	0.36	1.70	1.39	1.22	1.01
MEK/PEGDME	50.0	1.02	0.19	1.70	1.29	1.27	1.25
DEK/TEGDME	44.4	1.44	0.88	1.16	1.12	1.02	0.92
MEK/TEG	19.7	2.19	0.49	1.70	1.00	0.84	0.64

An excellent correlation between experimental and modeled data has been found, within the errors, for all the ketone/EGDME systems, as can be appreciated in the figures 4.19 to 4.21. The estimated thickness shown in table 4.14 corresponds to the one of a swelled PDMS layer, which is affected by both the swelling degree and the compaction factor. For the MEK/TEGDME system, a lower thickness than the one for DEK/TEGDME is found. This tendency is expected from a comparison between the swelling degrees for both systems. Nevertheless, the estimated values of the membrane thickness are affected in both cases by the used concentrations which were obtained by the swelling experiments (i.e., concentrations inside a polymer only thermally crosslinked) instead of actual concentrations in the membrane. It is expected that the concentration of permeants should be lower for a polymer with higher degree of crosslinking (i.e., crosslinked thermally and by radiation) than for polymers with lower degree of crosslinking (i.e., only thermally crosslinked).

Additionally, the estimated thickness for the MEK/PEGDME system is slightly higher than the one estimated for MEK/TEGDME. This difference is not expected, since the thickness depends mainly on the swelling degree of the polymer in a given system, and this is higher in the MEK/TEGDME system than in the MEK/PEGDME system. However, this could be explained by a higher difference in the concentration of the permeants between the thermally crosslinked polymer and the one with a further crosslinking by radiation. This difference will be higher for big molecules than for small ones due to the increased difficulty to accommodate the big molecule inside the polymer lattice when the polymer chains are more rigid.

In order to illustrate the importance of an accurate estimation of the concentration inside the membrane, the simulation results for the MEK/TEGDME system when the concentration inside the membrane is not estimated from the swelling experiments are shown in figure 4.22. Here, the concentration inside the membrane was calculated with the Flory-Huggins-Staverman theory with interaction parameters estimated only by solubility parameters. Therefore, the effects of the presence of a second solvent inside the membrane are not considered (sections 4.1.2 and 4.1.5).

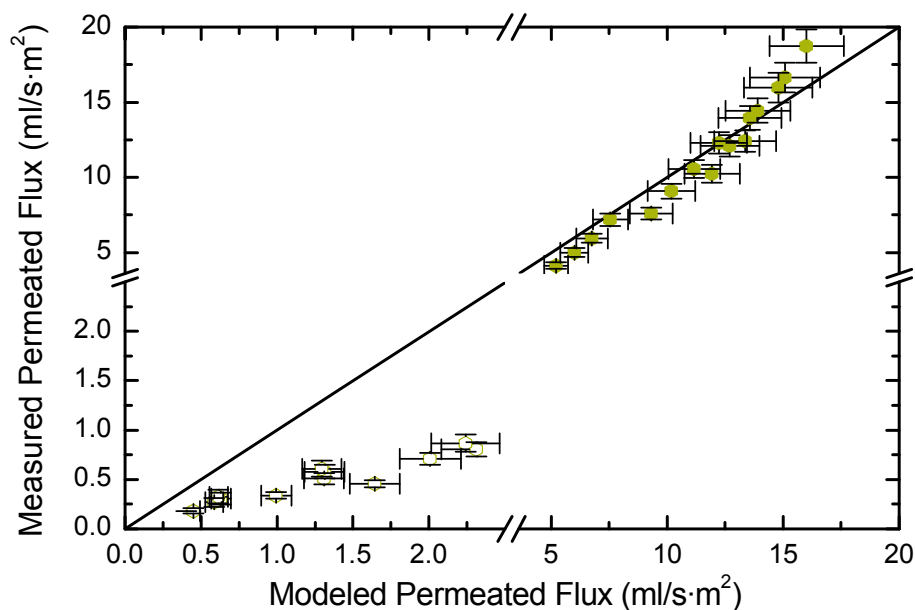


Figure 4.22. Correlation between measured MEK/TEGDME permeation fluxes and simulated data calculated by the solution-diffusion with imperfections model, with permeant concentrations estimated by interaction parameters from binary systems. The filled symbols represent the fluxes of MEK, whereas the open symbols correspond to TEGDME fluxes.

Figure 4.22 shows a bad correlation between the TEGDME experimental fluxes and the experimental ones. Here, the modeled results differ between 50 % and 400 % from the experimental fluxes. The difference is explained by a bad representation of the concentration inside the membrane which affects both the estimation of binary diffusion and the solution-diffusion with imperfections equation. On the other hand, the modeled results of the MEK fluxes show a much better correlation. This good correlation comes from a combination of two effects: the overestimation of the concentration inside the membrane is balanced by the underestimation of the diffusion coefficient value. Such balance does not take place in the TEGDME simulation, in which case both the

concentration and the diffusion coefficient are overestimated. Nevertheless, the regressed parameters for this modeling are as follows: $l = 12.7 \mu\text{m}$, $\tilde{K}_{\text{MEK}} = 1.93 \cdot 10^{-10} \text{ m}^2$ and $\tilde{K}_{\text{TEGDME}} = 7.84 \cdot 10^{-16} \text{ m}^2$.

As the last system, figure 4.23 shows the correlation between experimental and modeled data for the MEK/TEG system. Here, experimental diffusivity values are used and the concentrations of the permeants inside the membrane are estimated by swelling experiments. The regressed parameters of the model for this system were already shown in table 4.14.

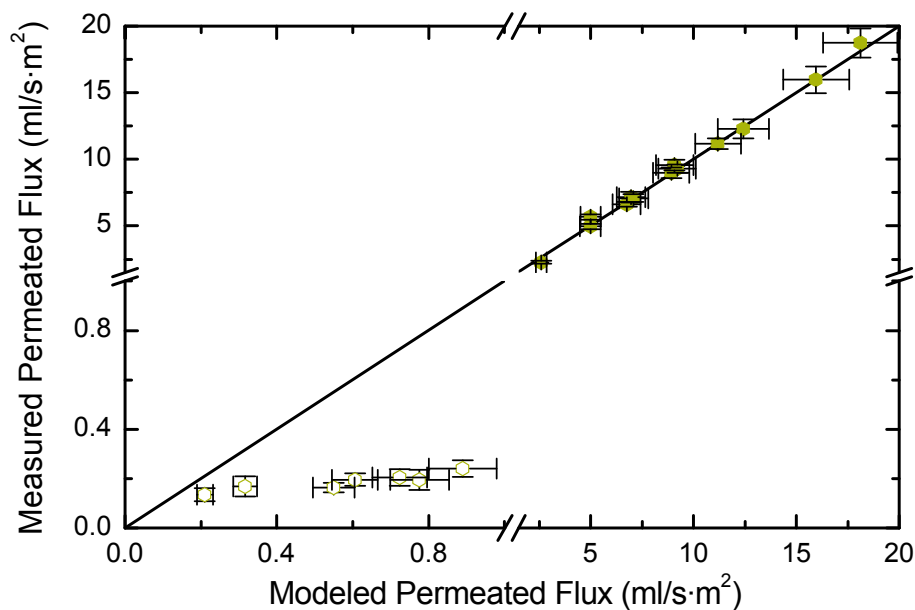


Figure 4.23. Correlation between measured MEK/TEG permeation fluxes and simulated data calculated by the solution-diffusion with imperfections model. The filled symbols represent the fluxes of MEK, whereas the open symbols correspond to TEG fluxes.

It can be seen from the data presented in figure 4.23 that the modeled TEG fluxes are overestimated for all the cases when compared to measured data. Here, the presence of hydrogen bonds hinders the permeation of TEG molecules through the membrane. The huge difference between experimental and modeled data is explained by an effect similar to the one that explains the difference in thickness for both MEK/EGDME systems. The appearance of hydrogen bonds induces a huge deviation between the solvent concentration calculated from the swelling experiments and the ones inside the membrane. This is more evident for the most concentrated system (15 wt %) which has

more probability of TEG molecular coupling, and, as a result, the difference between experimental and modeled data arises up to 400 %. The differences for the less concentrated solutions are up to 50 %. It should be noted that the difference of concentration inside the polymer for the case of MEK/PEGDME affects equally the entire set of concentrations, and subsequently causes an increase in the thickness without reflecting any deviations between modeled and experimental fluxes.

Nevertheless, when both systems with similar molecular size are compared (i.e., MEK/TEG and MEK/TEGDME), a lower thickness is found for the MEK/TEG system (see table 4.14). This is coherent with the fact that the swelling degree of the polymer in MEK/TEGDME is higher than the corresponding one in the MEK/TEG mixture.

The effect of different temperatures over the modeling of nanofiltration experiments affects both the diffusive and the viscous part. As mentioned in section 4.3.1, both the viscosity and the diffusion coefficients are affected by the temperature, showing an increase of the diffusive and viscous flux contribution with a temperature increase. Additionally, an increase of the concentration of the permeants inside the polymer is expected due to a decrease of the polymer-solvent interaction parameters (i.e., increase of the affinity between polymer and solvent) when the temperature increases.^[3]

Consequently, to accomplish the modeling of diffusion coefficients at different temperatures, it is necessary to estimate the energy that a molecule needs to overcome attractive forces which holds it to its neighbors (E) from equation 2.32. Additionally, swelling experiments with temperature dependence for polymer-solvent-solvent system are needed in order to complete both the estimation of diffusion coefficients and to complete the calculation with the solution-diffusion with imperfections model. This should be done as a future work, as well as measurements of concentrations of the permeants inside a real membrane at different temperatures and feed concentrations.

4.4 References

1. Roth, M., *Solubility parameter of poly(dimethyl siloxane) as a function of temperature and chain length*. Journal of Polymer Science B: Polymer Physics, 1990. **28**(13): p. 2715-2719.
2. Barton, A.F.M., *Solubility parameters*. Chemical Reviews, 1975. **75**(6): p. 731-753.

3. Brandrup, J., E.H. Immergut, and E.A. Grulke, *Polymer handbook*. 1999, Hoboken, N.J.: John Wiley & Sons.
4. Ashworth, A.J. and G.J. Price, *Static investigation of the influence of polymer molecular weight and loading in the gas chromatographic determination of poly(dimethylsiloxane) interaction parameters*. *Macromolecules*, 1986. **19**(2): p. 358-361.
5. Flory, P.J., *Principles of polymer chemistry*. 15. printing ed. The George Fisher Baker non-resident lectureship in chemistry at Cornell University. 1953, Ithaca: Cornell University Press.
6. Lee, H.K., et al., *Liquid-liquid phase separation in a ternary system of segmented polyetherurethane/dimethylformamide/water: effect of hard segment content*. *Polymer*, 2001. **42**(8): p. 3893-3900.
7. Nandi, S. and H.H. Winter, *Swelling Behavior of Partially Cross-Linked Polymers: A Ternary System*. *Macromolecules*, 2005. **38**(10): p. 4447-4455.
8. Dollase, T., et al., *Effect of Interfaces on the Crystallization Behavior of PDMS*. *Interface Science*, 2003. **11**(2): p. 199-209.
9. Favre, E., et al., *Sorption of organic solvents into dense silicone membranes. Part I.—Validity and limitations of Flory–Huggins and related theories*. *Journal of the Chemical Society, Faraday Transactions*, 1993. **89**(24): p. 4339-4346.
10. Favre, E., et al., *Multicomponent polymer/solvents equilibria: an evaluation of flory-huggins theory for crosslinked pdms networks swelled by binary mixtures*. *Chemical Engineering Communications*, 1994. **140**(1): p. 193 - 205.
11. Hong, S.-U., *Prediction of Polymer/Solvent Diffusion Behavior Using Free-Volume Theory*. *Industrial and Engineering Chemistry Research*, 1995. **34**(7): p. 2536-2544.
12. Hong, S.-U., *Predicting ability of free-volume theory for solvent self-diffusion coefficients in rubbers*. *Journal of Applied Polymer Science*, 1996. **61**(5): p. 833-841.
13. Zielinski, J.M. and J.L. Duda, *Predicting polymer/solvent diffusion coefficients using free-volume theory*. *AIChE Journal*, 1992. **38**(3): p. 405-415.
14. Ehlich, D. and H. Sillescu, *Tracer diffusion at the glass transition*. *Macromolecules*, 1990. **23**(6): p. 1600-1610.
15. Vrentas, J.S., H.T. Liu, and J.L. Duda, *Effect of solvent size on diffusion in polymer-solvent systems*. *Journal of Applied Polymer Science*, 1980. **25**(8): p. 1793-1797.
16. Vrentas, J.S., H.T. Liu, and J.L. Duda, *Estimation of diffusion coefficients for trace amounts of solvents in glassy and molten polymers*. *Journal of Applied Polymer Science*, 1980. **25**(7): p. 1297-1310.

17. Wesselingh, J.A. and A.M. Bollen, *Multicomponent Diffusivities from the Free Volume Theory*. Chemical Engineering Research and Design, 1997. **75**(6): p. 590-602.
18. Kritiak, J., et al., *Temperature dependence of free volume distributions in polymers studied by positron lifetime spectroscopy*. Le Journal de Physique IV, 1993. **03**(C4): p. C4-265-C4-270.
19. Wang, B., et al., *Effect of Temperature on the Free Volume in Glassy Poly(ethylene terephthalate)*. Macromolecules, 2002. **35**(10): p. 3993-3996.

Chapter 5. Summary and Conclusions

The aim of the present work was the modeling of organic solvent nanofiltration, in order to address the optimization of industrial separation processes by the powerful tool of computer simulation. This goal was successfully achieved by the use of the so-called “solution-diffusion with imperfections model”. In the approach used here the key parameters that affect the permeation behavior of the membrane have been studied. Therefore, the concentration of permeants inside the membrane and the diffusion coefficients of the permeants were intensively investigated in order to properly describe the nanofiltration process as a whole. The strategy employed here, i.e., a combination of models that describe the physical properties of the substances, the polymer swelling and the transport mechanisms through the membrane, allows the consideration of real separation procedures and has been proven in different actual systems.

In order to estimate the concentration inside the membrane, it was necessary to estimate the activities of the systems by the UNIFAC group contribution method. This determination demonstrated the non-ideality of the used systems, observed by the non-linearity between the values of activity and solution concentration. By combining the calculation of the activities with the Flory-Huggins-Staverman (FHS) solution theory applied for free-standing polymer swelling experiments, it was possible to investigate the dependence of the FHS interaction parameter with the change of solution concentration in ternary polymer–solvent–solvent systems.

From the free-standing polymer swelling experiments it was found that, for mixtures of the same EGDME, the swelling degree was always higher for the DEK systems than for the MEK systems. Additionally, for mixtures containing the same ketone, a higher swelling degree was found for TEGDME – the smaller solute molecule – than for PEGDME. As already mentioned, these results were employed in the determination of the FHS interaction parameters, from where it could be concluded that the presence of a second permeant induced variations in the interaction parameters when this is calculated by Hildebrand solubility parameters and by the FHS equation. The possible arrangement of ketone molecules inside the lattice is hindered by the presence of a big molecule (any of the two EGDME), which occupies more than one of the possible lattice places where the ketone molecule could be arranged.

As mentioned in chapter 4, the FHS equation describes the swelling behavior of the crosslinked PDMS. Nevertheless, the Flory-Rehner theory was used to characterize the crosslink density of the employed polymer. The distance between two crosslink points was found to be around 40 repeating chain units. A small discrepancy was found in the crosslink density calculated by the swelling experiments with the two ketone solvents. This difference has been attributed to the strong dependence of the crosslink density with the estimated interaction parameters.

Later, the Flory-Huggins-Staverman solution theory could be particularized with the considerations stated by the solution-diffusion model in order to estimate the concentration of permeants at the feed and permeate interface of the membrane. The results were later used directly in the solution-diffusion with imperfections model equation and in the estimation of the thermodynamic diffusion coefficients, which are also necessary for the permeation model equation.

The thermodynamic diffusion coefficients were estimated by free-standing polymer PFG-NMR measurements at the same solution concentrations used for the feed solutions in the nanofiltration experiments. The PFG-NMR results were later correlated with available diffusion models (i.e., Vrentas & Duda diffusion theory and Wesselingh & Bollen multicomponent diffusion model) in order to estimate the diffusion coefficients corresponding to the average permeant concentration inside the membrane, as needed for the solution-diffusion with imperfections model.

A simulation routine to model the permeation behavior of the nanofiltration experiments based on the solution-diffusion with imperfections model consisting of three different stages was done, where the different values involved were theoretically estimated and compared to experimental measurements. First, the estimation of self-diffusion coefficients of pure substances has been done by the use of the Dullien equation. As expected, higher self-diffusivities were obtained for smaller substances than those values obtained for bigger ones, as long as the substances in question present comparable activities. The low self-diffusivity found for the smallest glycol molecule, i.e., TEG, has been attributed to the formation of hydrogen bonds between TEG molecules, which hinders the mobility and increases the viscosity. For all the substances, a good correlation was found between the experimental and the theoretically estimated values.

As a second stage in the developed simulation routine, tracer diffusivities were experimentally modeled by the use of the Vrentas & Duda diffusion theory and the Wesselingh & Bollen multicomponent diffusion model. At this stage, experimental diffusion data was required in order to estimate missing parameters from both theories. A good correlation was found between the modeled results and the PFG-NMR measurements. For substances with similar activities, lower mobility and lesser possibilities of configuration inside the polymer lattice have been observed for bigger molecules than for smaller ones. A similar effect of low tracer diffusivities was observed when the molecule presents hydrogen bonds which hinder the mobility of the molecule and increase the apparent molecular size.

The last simulation stage consisted of the estimation of thermodynamic diffusion coefficients by the use of Maxwell-Stefan friction factors. The friction factors are related with the tracer diffusivities as stated in the theoretical part (chapter 2). Here, the concentration of the permeants inside the actual membrane has been estimated with the FHS equation under the conditions stated by the solution-diffusion model. The exact concentration in the membrane was used to calculate the corresponding thermodynamic diffusion coefficient under the experimental conditions.

The modeled permeation fluxes were directly compared with the experimental nanofiltration results in order to evaluate the quality of the simulation routine. Good correlations were found for all ketone/EGDME systems when both concentration and diffusion coefficients were estimated as previously described. Particularly, it is worth noticing the importance of a good estimation of the diffusion coefficient values and, even more, a reliable estimation of the actual concentration of the permeants inside the membrane.

The modeling of organic solvent nanofiltration has been successfully achieved for real systems. The model could be still further improved in order to describe the hexane/sunflower oil system, which is one actual industrial application where the membrane separation process is very promising when compared to standard separation techniques. For this purpose, the diffusion behavior of the sunflower oil should be extensively studied, for example by PFG-NMR measurements.

Chapter 6. Acknowledgments

I would like to especially thank to Prof. Dr. Volker Abetz for giving me the opportunity to develop my PhD research in this topic. His amazing interest in scientific discussions gave me the opportunity to benefit from his experience and to become more exigent in the understanding of the work. I deeply appreciate the cooperative and friendly mood, especially during the transition across different departments in GKSS. I would like also to thanks Dr. Marga Dijkstra who initiated the research in this topic and gave me her best support and guidance during her stay in GKSS. I am grateful with Dr. Nico Scharnagl for his interesting discussions which help me to understand the particularities involved in the PFG-NMR measurements, as well as his support in the continuity of the measurements and their analysis even after his departure from the institute. Many thanks to Dr. Adriana Boschetti-de-Fierro for her best support and orientation in all the topics involved in this work, mainly for the fruitful discussions which evolved the concept of the thesis and the understanding of the results here presented.

From my GKSS colleagues, I thank to Karen-Marita Prause, Clarissa Abetz and Sabrina Bolmer for the hard work in the different microscopy techniques during these years. I also thank Dr. Thomas Emmler and Ing. Susanne Nowak for NMR and DSC support. I thank to Ing. Joachim Koll, Ing. Kristian Buhr, Berthold Wendland, Dr. Peter Simon and Maren Brinkmann for they support in different topics. I would also include my PMM colleagues, which enriched this work with their profitable questions and recommendations, and for the day-to-day work.

I truly appreciate the financial support, which was given by the German Federal Ministry of Education and Research under the project “Organophile Nanofiltration für die nachhaltige Produktion in der Industrie” and GKSS Research Centre Geesthacht GmbH.

Last but not least, I thank my family and friends, for their support not only in the good moments during these years.

Appendix 1. Organic solvent nanofiltration of Hexane/Polyisobutylene and Hexane/Sunflower Oil systems

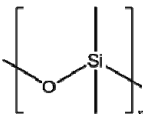

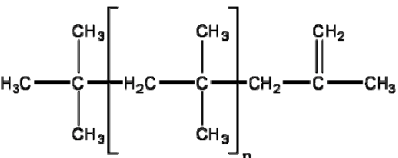
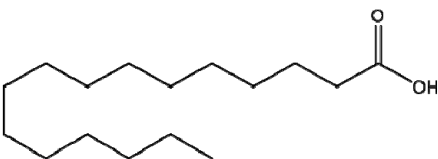
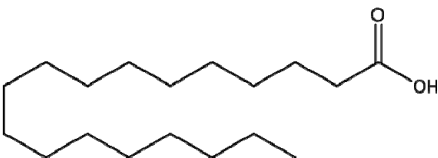
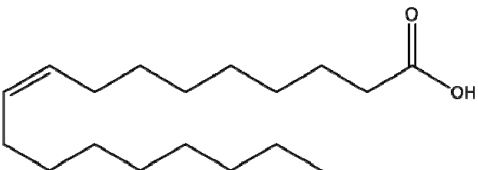
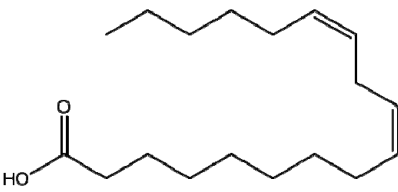
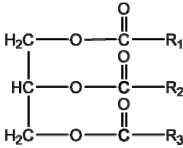
The following appendix deals with the modeling of organic solvent nanofiltration of hexane/polyisobutylene and hexane/sunflower oil mixtures. The corresponding experimental data has been taken from Stafie et al.^[1] The data has been modeled by the solution-diffusion with imperfections model, with the procedures presented in the present thesis. The concentration inside the membrane has been estimated by swelling experiments.

The membrane used in this study is a composite membrane developed at the University of Twente in the Netherlands. The membrane is formed by a solvent resistant support layer made of polyacrylonitrile (PAN) provided by GKSS-Forschungszentrum Geesthacht GmbH, and a selective top layer of a high molecular weight polydimethylsiloxane (PDMS).

The PDMS layer was coated over the PAN support from a solution of high molecular weight PDMS, curing agent, solvent and platinum catalyst which allows the polymer to thermally crosslink. The effective thickness of the membrane is found to be in the range of 1.7 – 2.2 μm , with a transition area where the PDMS penetrate into the pores of the PAN support that allows a better anchoring of the selective top layer to the support.

The solvents for nanofiltration measurements were used as received, without further purification. For both systems, mixtures formed by hexane (MERCK[®]) and a solute were prepared for a fixed solute concentration of 8 wt %. The solutes consist of sunflower oil purchased from Fluka[®] and high reactivity polyisobutylene provided by BASF[®]. The sunflower oil consist of a mixture of triglycerides with a average molecular weight of around 900 g/mol, whereas the polyisobutylene has an average molecular weight of 1300 g/mol. A list of chemical structures and molecular weights of the used substances is shown in table 3.1. For the case of PDMS, the molecular weight of the polymer chain repeating unit is shown instead of the molecular weight of the whole polymer.

Table A1.1. Chemical structure and molecular weight of the used substances.

Substance ^(a)	Chemical Structure	MW (g/mol)
PDMS		74.11 ^(b)
n-Hexane		86.18
Polyisobutylene		1300
Palmitic Acid (6.7 %)		256.43
Stearic Acid (3.3 %)		284.48
Oleic Acid (25.8 %)		282.47
Linoleic Acid (64.2 %)		280.45
Pseudo-triacylglyceride (Pseudo-sunflower oil)	 $R_1+R_2+R_3 = (CH=CH)_5(CH_2)_{38}(CH_3)_3$	881.54

(a) The numbers in brackets indicate the content of each component in a mixture of simple triacylglycerides that represents the sunflower oil.

(b) Molecular weight of the polymer chain repeating unit.

As stated by Espinosa et al.^[2], it is not possible to know the exact distribution of the different saturated/unsaturated fatty acid chains in the sunflower oil. One approach consists on representing the oil as a mixture of simple triacylglycerides according to the fatty acid composition of the natural oil. The second approach consists in the representation of the oil as a single pseudo-triacylglyceride, which has the same molecular weight and degree of unsaturation of the original oil. Both approaches can be used to estimate the activity of the hexane/sunflower oil system. The software ActDF can be used to estimate both the activity of the sunflower oil as a combination of triacylglycerides and the activity of the single pseudo-triacylglyceride molecule, and both approaches lead to a similar result. For the following, the latest approach will be used in order to estimate the permeation behavior of the hexane/sunflower oil system. The modeling of the nanofiltration experiments is presented in figure A1.1.

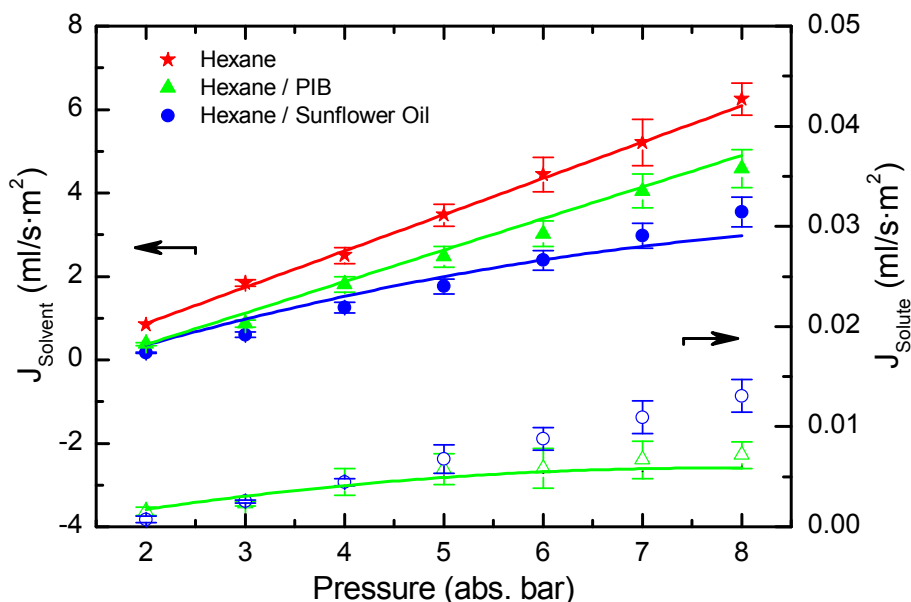


Figure A1.1. Permeation fluxes of hexane/sunflower oil and hexane/PIB 1300 systems (8 wt%) as a function of the applied pressure. The symbols correspond to experimental values and the lines correspond to simulated data. The filled symbols represent the hexane fluxes, whereas the open symbols correspond to solute fluxes. ★ Pure hexane, ▲ hexane/PIB 1300, ● hexane/sunflower oil.

The modeling results presented in figure A1.1 show that the solvent flux, i.e., the hexane flux, is well described by the solution-diffusion with imperfections model for the pure substance as well as for both mixed systems. The solute flux is also well described by the employed model for the PIB 1300 system. On the other hand, the

simulated flux values for the sunflower oil are overestimated in approximately 300% (simulated values are not shown). An inspection of the simulation results reveals that the overestimation in the sunflower oil is originated by the diffusion component of the equation, whereas the viscous part is in the right order of magnitude. A simulation of the hexane/sunflower oil where only the contribution of viscous flow is considered to describe the sunflower oil fluxes is shown in figure A1.2.

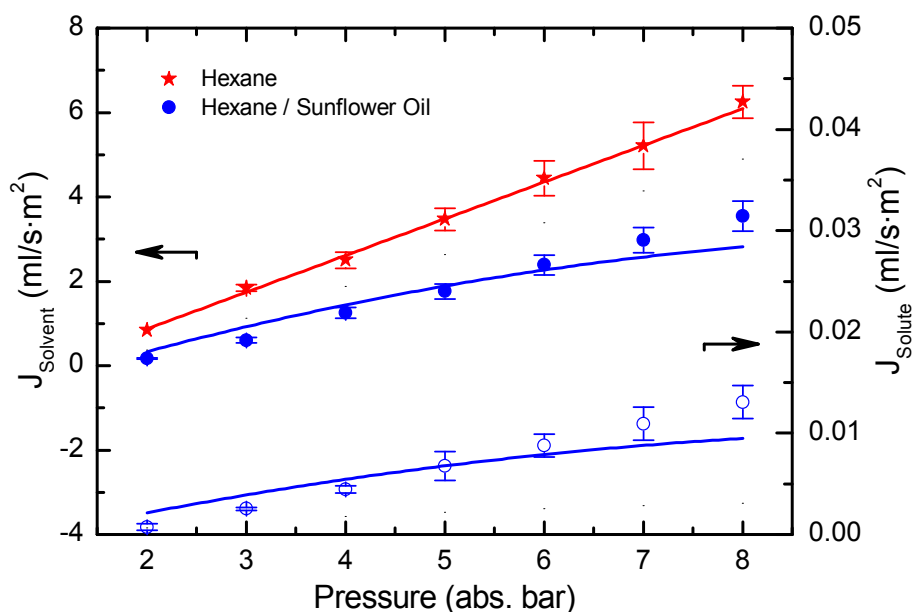


Figure A1.2. Permeation fluxes of hexane/sunflower oil system (8 wt %) as a function of the applied pressure. The symbols correspond to experimental values and the lines correspond to simulated data. The filled symbols represent the hexane fluxes, whereas the open symbols correspond to sunflower oil fluxes.

Figure A1.2 shows a good correlation between simulated and experimental sunflower oil fluxes data. Nevertheless, a difference in slope for both fluxes in the hexane/sunflower oil could be explained by the different assumptions taken during the simulation. Here, the determination of the concentration of permeants inside the membrane was not rigorously determined due to the lack of relievable experimental data, i.e., the exact feed concentration is unknown. Additionally, broad ranges for swelling data extrapolation were used.

The negligible diffusion contribution in the sunflower oil fluxes could be explained by a more restricted mobility of the triacylglyceride molecules compared to long linear molecules, which are able to move in sections (e.g., TEGDME, PEGDME, PIB). The

lack of a broad number of possibilities to arrange the triacylglyceride molecules inside the polymer lattice is not considered in the calculations used in this chapter (i.e., diffusivities estimated by Wesselingh & Bollen model).

References

1. Stafie, N., D.F. Stamatialis, and M. Wessling, *Insight into the transport of hexane-solute systems through tailor-made composite membranes*. Journal of Membrane Science, 2004. **228**(1): p. 103-116.
2. Espinosa, S., et al., *Phase equilibria in mixtures of fatty oils and derivatives with near critical fluids using the GC-EOS model*. The Journal of Supercritical Fluids, 2002. **23**(2): p. 91-102.

Appendix 2. ActDF software

The software ActDF pretends to estimate activities of the components of a mixture of solvents, and it is based on the UNIFAC method described in the chapter 2. The software is distributed under the terms established by GNU Lesser General Public License (GNU LGPL) published by the Free Software Foundation. Two different variants of the software are presented. First, a general software for the estimation of binary and ternary mixtures, called “ActDF (2 and 3 components)” is presented. The second version consists of a modification of the general one in order to estimate activities of a solvent-sunflower oil mixture, called “ActDF (Sunflower oil)”. The later has the particularity to estimate the activities of each individual constituent of commercial sunflower oil when the concentration of solvent-oil changes.

The software is based on a Microsoft[®] Excel[®] interface and the code to estimate the activities is a combination of predefined Excel[®] functions and codes for Visual Basic for Applications (VBA). The final version of both programs can be found annexed to this doctoral thesis in their electronic versions on CD, whereas screenshots of the programs are found in figures A2.1 to A2.3.

Figure A2.1. Screenshot of the main window of the program ActDF.

Concentration					Hexane		Palmitic Acid		Stearic Acid		Oleic Acid		Linoleic Acid	
Hexane	Palmitic Acid	Stearic Acid	Oleic Acid	Linoleic Acid	γ	a	γ	a	γ	a	γ	a	γ	a
0.000	0.070	0.045	0.220	0.652			1.0394	0.0728	1.0446	0.0470	1.0172	0.2238	1.0157	0.6622
0.025	0.068	0.044	0.215	0.636	0.9303	0.0233	1.0400	0.0710	1.0422	0.0457	1.0160	0.2179	1.0156	0.6456
0.050	0.067	0.043	0.209	0.619	0.9258	0.0468	1.0404	0.0693	1.0396	0.0444	1.0146	0.2120	1.0153	0.6289
0.075	0.065	0.042	0.204	0.603	0.9413	0.0706	1.0406	0.0674	1.0367	0.0432	1.0130	0.2061	1.0149	0.6121
0.100	0.063	0.041	0.198	0.587	0.9467	0.0947	1.0407	0.0656	1.0336	0.0419	1.0112	0.2002	1.0143	0.5952
0.125	0.061	0.039	0.193	0.571	0.9521	0.1190	1.0407	0.0637	1.0303	0.0406	1.0091	0.1943	1.0135	0.5782
0.150	0.060	0.038	0.187	0.554	0.9574	0.1436	1.0404	0.0619	1.0267	0.0393	1.0069	0.1883	1.0126	0.5612
0.175	0.058	0.037	0.182	0.538	0.9627	0.1686	1.0400	0.0601	1.0228	0.0380	1.0044	0.1823	1.0115	0.5441
0.200	0.056	0.036	0.176	0.522	0.9679	0.1936	1.0394	0.0582	1.0186	0.0367	1.0017	0.1763	1.0102	0.5269
0.225	0.054	0.035	0.171	0.505	0.9731	0.2189	1.0386	0.0563	1.0141	0.0354	0.9988	0.1703	1.0087	0.5097
0.250	0.053	0.034	0.165	0.489	0.9782	0.2445	1.0377	0.0545	1.0094	0.0341	0.9957	0.1643	1.0070	0.4924
0.275	0.051	0.033	0.160	0.473	0.9831	0.2704	1.0365	0.0526	1.0044	0.0328	0.9923	0.1583	1.0052	0.4752
0.300	0.049	0.032	0.154	0.456	0.9880	0.2964	1.0352	0.0507	0.9990	0.0315	0.9886	0.1523	1.0032	0.4579
0.325	0.047	0.030	0.149	0.440	0.9927	0.3226	1.0336	0.0488	0.9934	0.0302	0.9848	0.1462	1.0010	0.4405
0.350	0.046	0.029	0.143	0.424	0.9973	0.3491	1.0319	0.0470	0.9875	0.0289	0.9807	0.1402	0.9986	0.4232
0.375	0.044	0.028	0.138	0.408	1.0017	0.3757	1.0301	0.0451	0.9812	0.0276	0.9763	0.1342	0.9961	0.4059
0.400	0.042	0.027	0.132	0.391	1.0060	0.4024	1.0280	0.0432	0.9747	0.0263	0.9718	0.1283	0.9934	0.3886
0.425	0.040	0.026	0.127	0.375	1.0101	0.4293	1.0258	0.0413	0.9679	0.0250	0.9670	0.1223	0.9907	0.3714
0.450	0.039	0.025	0.121	0.359	1.0139	0.4563	1.0235	0.0394	0.9608	0.0238	0.9621	0.1164	0.9878	0.3542
0.475	0.037	0.024	0.116	0.342	1.0175	0.4833	1.0210	0.0375	0.9535	0.0225	0.9569	0.1105	0.9848	0.3371
0.500	0.035	0.023	0.110	0.326	1.0208	0.5104	1.0185	0.0356	0.9459	0.0213	0.9517	0.1047	0.9818	0.3201
0.525	0.033	0.021	0.105	0.310	1.0239	0.5375	1.0159	0.0338	0.9381	0.0201	0.9463	0.0989	0.9788	0.3031
0.550	0.032	0.020	0.099	0.293	1.0266	0.5646	1.0133	0.0319	0.9302	0.0188	0.9409	0.0931	0.9758	0.2863
0.575	0.030	0.019	0.094	0.277	1.0290	0.5917	1.0108	0.0301	0.9221	0.0176	0.9354	0.0875	0.9730	0.2696
0.600	0.028	0.018	0.088	0.261	1.0310	0.6186	1.0084	0.0282	0.9140	0.0165	0.9301	0.0818	0.9705	0.2531
0.625	0.026	0.017	0.083	0.245	1.0325	0.6453	1.0063	0.0264	0.9059	0.0153	0.9249	0.0763	0.9683	0.2368
0.650	0.025	0.016	0.077	0.228	1.0337	0.6719	1.0046	0.0246	0.8979	0.0141	0.9200	0.0708	0.9666	0.2206
0.675	0.023	0.015	0.072	0.212	1.0343	0.6982	1.0035	0.0228	0.8902	0.0130	0.9156	0.0655	0.9657	0.2046
0.700	0.021	0.014	0.066	0.196	1.0344	0.7241	1.0031	0.0211	0.8830	0.0119	0.9119	0.0602	0.9657	0.1889
0.725	0.019	0.012	0.061	0.179	1.0340	0.7496	1.0038	0.0193	0.8764	0.0108	0.9091	0.0550	0.9670	0.1734
0.750	0.018	0.011	0.055	0.163	1.0330	0.7747	1.0059	0.0176	0.8707	0.0098	0.9076	0.0499	0.9701	0.1581
0.775	0.016	0.010	0.050	0.147	1.0313	0.7993	1.0100	0.0159	0.8664	0.0088	0.9079	0.0449	0.9754	0.1431
0.800	0.014	0.009	0.044	0.130	1.0291	0.8233	1.0167	0.0142	0.8640	0.0078	0.9105	0.0401	0.9839	0.1283
0.825	0.012	0.008	0.039	0.114	1.0262	0.8466	1.0269	0.0126	0.8640	0.0069	0.9164	0.0353	0.9965	0.1137
0.850	0.011	0.007	0.033	0.098	1.0228	0.8694	1.0419	0.0109	0.8676	0.0059	0.9266	0.0306	1.0147	0.0992
0.875	0.009	0.006	0.028	0.082	1.0188	0.8914	1.0635	0.0093	0.8761	0.0049	0.9430	0.0259	1.0408	0.0848
0.900	0.007	0.005	0.022	0.065	1.0144	0.9129	1.0945	0.0077	0.8914	0.0040	0.9681	0.0213	1.0779	0.0703
0.925	0.005	0.003	0.017	0.049	1.0098	0.9341	1.1389	0.0060	0.9168	0.0031	1.0057	0.0166	1.1312	0.0553
0.950	0.004	0.002	0.011	0.033	1.0054	0.9551	1.2035	0.0042	0.9571	0.0022	1.0622	0.0117	1.2088	0.0394
0.975	0.002	0.001	0.006	0.016	1.0018	0.9767	1.2994	0.0023	1.0207	0.0011	1.1486	0.0063	1.3252	0.0216
1.000	0.000	0.000	0.000	0.000	1.0000	1.0000								

Figure A2.2. Screenshot of the result window of the program ActDF.

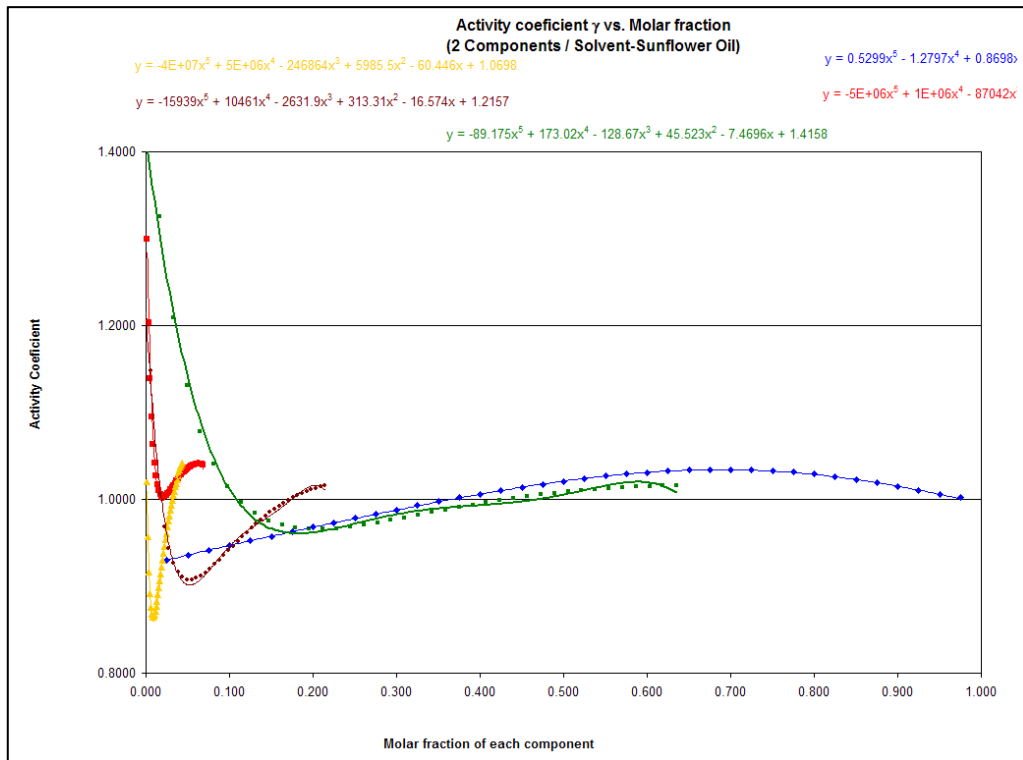


Figure A2.3. Screenshot of the graphic window of the program ActDF.

Appendix 3. GKSS-NSRM program

The software “GKSS-Nanofiltration with solvent resistant membranes” (GKSS-NSRM) is a multipurpose graphic user interface developed in Java[®]. The software is intended to be a launcher of different solver modules necessary for the modeling of organic solvent nanofiltration. Additionally, few modifications allow the software to work as a launcher of any mathematical module. The user interface is distributed under the terms established by GNU Lesser General Public License (GNU LGPL) published by the Free Software Foundation, while the mathematical modules are copyright from GKSS-Forschungszentrum Geesthacht GmbH and their use, copy, distribution or changing should be authorized by the copyright holder. Screenshots of selected windows of the program are shown in figures A3.1 to A3.3, whereas the source code is shown as electronic version in the enclosed CD.



Figure A3.1. Screenshot of the main windows of the GKSS-NSRM program.

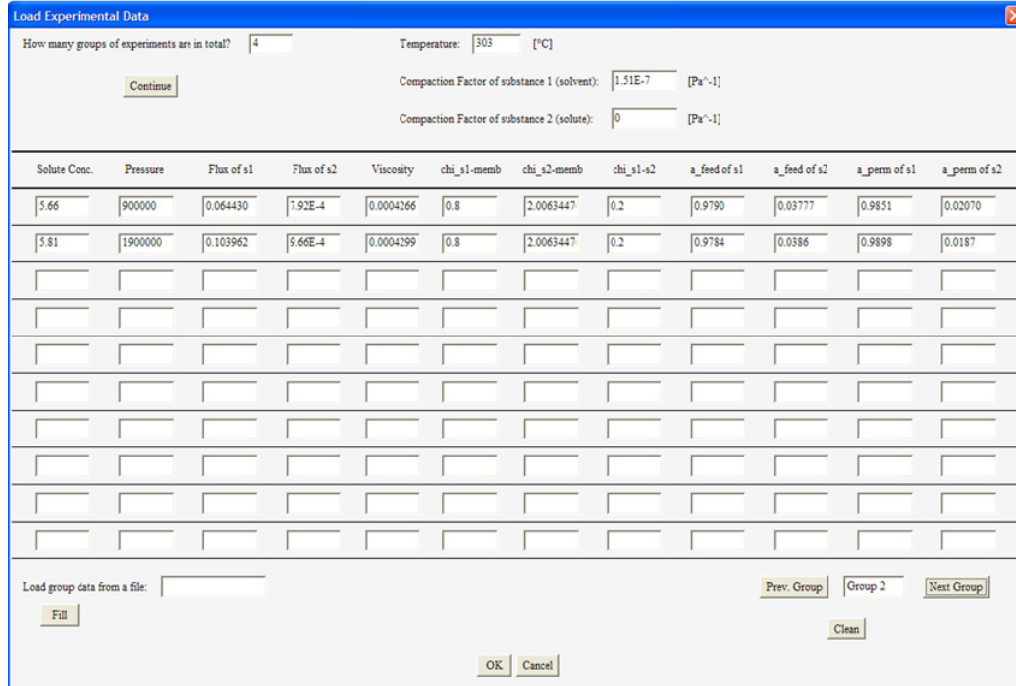


Figure A3.2. Screenshot of the data input window of the GKSS-NSRM program.

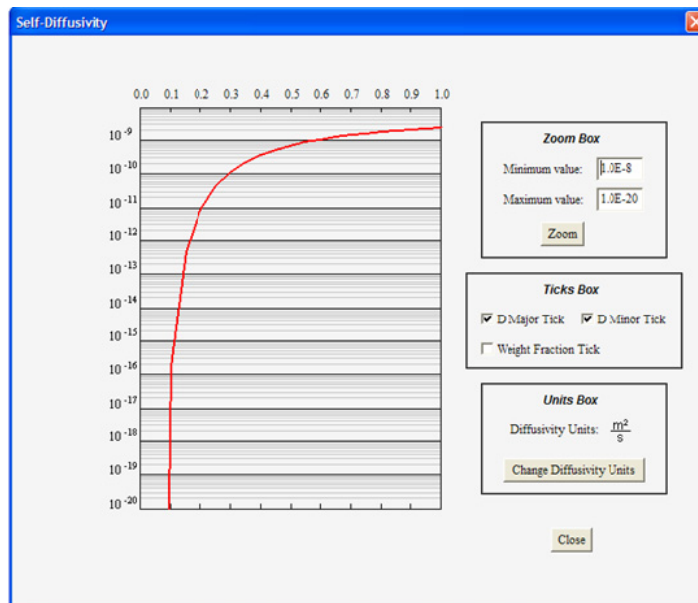


Figure A3.3. Screenshot of the Self-diffusivity module of the GKSS-NSRM program.

Appendix 4. Modeling example

In the following, an example of the calculation methods will be presented. Specifically the necessary steps to model nanofiltration experiments for the MEK/TEGDME system will be shown. The complete nanofiltration modeling is divided in three Mathcad[®] programs. The first program consists in the estimation of tracer diffusion coefficients from PFG-NMR experimental data, the second program estimates the concentration inside the membrane under experimental nanofiltration conditions and the third program calculates thermodynamic diffusion coefficients.

A4.1 Estimation of tracer diffusion coefficients

Tracer-Diffusion in Polymer-Solvent-Solvent System

0) Units definition

$$R := 8.314 \cdot \frac{\text{kg m}^2}{\text{s}^2 \text{K mol}}$$

$$\text{mPa} := \frac{\text{Pa}}{1000}$$

$$\text{Avog} := 6.022 \cdot 10^{23} \cdot \frac{1}{\text{mol}}$$

$$k_B := 1.38 \cdot 10^{-23} \cdot \frac{\text{J}}{\text{K}}$$

$$\text{bar} := 100000 \cdot \text{Pa}$$

$$\text{kmol} := 1000 \cdot \text{mol}$$

$$\text{Avog} := 6.02214179 \cdot 10^{23} \cdot \text{mol}^{-1}$$

$$\text{ml} := 1 \cdot \text{cm}^3$$

1) Component list

Component Index

PDMS	:=	1
MEK		2
DEK		3
TEGDME		4
PEGDME		5
TEG		6

Ncompounds := 1..6

j := Ncompounds

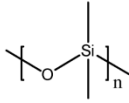
k := 2..6 **All except the polymer**

283.15	:=	K	T - 273.15K =	K	Npoints := 1..15	
288.15		1				10
293.15		2				15
298.15		3				20
303.15		4				25
308.15		5				30
313.15		6				35
318.15		7				40
323.15		8				45
328.15		9				50
333.15		10				55
338.15		11				60
343.15		12				65
348.15		13				70
353.15		14				75
	15	80				

i := Npoints

2) Pure properties

2.1 PDMS



$$V_{PDMS} := 1.027 \cdot 10^{-3} \cdot \frac{\text{m}^3}{\text{kg}}$$

$$MW_{PDMS} := 74.1 \cdot \frac{\text{gm}}{\text{mol}}$$

$$V_{vdw,PDMS} := (16.6 + 5.25 + 2 \cdot 13.67) \cdot \frac{\text{cm}^3}{\text{mol}}$$

$$V_{vdw,PDMS} = 4.919 \times 10^{-5} \frac{\text{m}^3}{\text{mol}}$$

$\rho_{1,PDMS}$	
$\rho_{2,PDMS}$	(0.974)
$\rho_{3,PDMS}$	0.974
$\rho_{4,PDMS}$	0.974
$\rho_{5,PDMS}$	0.974
$\rho_{6,PDMS}$	0.974
$\rho_{7,PDMS}$	0.974
$\rho_{8,PDMS}$	$:= 0.974 \cdot \frac{\text{gm}}{\text{cm}^3}$
$\rho_{9,PDMS}$	0.974
$\rho_{10,PDMS}$	0.974
$\rho_{11,PDMS}$	0.974
$\rho_{12,PDMS}$	0.974
$\rho_{13,PDMS}$	0.974
$\rho_{14,PDMS}$	(0.974)
$\rho_{15,PDMS}$	

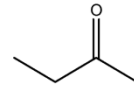
$$V_{ch,PDMS} := 0.905 \cdot \frac{\text{cm}^3}{\text{gm}}$$

$$V_{mol,PDMS} := \frac{MW_{PDMS}}{\rho_{4,PDMS}}$$

2.2 MEK

$$MW_{MEK} := 72.10692 \cdot \frac{\text{gm}}{\text{mol}}$$

$$V_{at0K,MEK} := 63.9 \cdot \frac{\text{cm}^3}{\text{mol}}$$



$$V_{c,MEK} := 267 \cdot \frac{\text{cm}^3}{\text{mol}}$$

<http://www.thermo.com/kdb/kdb/hcprop/showprop.php?cmpid=1192>

$$V_{vdw,MEK} := (2 \cdot 13.67 + 10.23 + 11.7) \cdot \frac{\text{cm}^3}{\text{mol}}$$

$$V_{vdw,MEK} = 4.927 \times 10^{-5} \frac{\text{m}^3}{\text{mol}}$$

$\rho_{1,MEK}$	
$\rho_{2,MEK}$	(0.816)
$\rho_{3,MEK}$	0.810
$\rho_{4,MEK}$	0.805
$\rho_{5,MEK}$	0.799
$\rho_{6,MEK}$	0.794
$\rho_{7,MEK}$	0.788
$\rho_{8,MEK}$	$:= 0.777 \cdot \frac{\text{gm}}{\text{cm}^3}$
$\rho_{9,MEK}$	0.772
$\rho_{10,MEK}$	0.766
$\rho_{11,MEK}$	0.760
$\rho_{12,MEK}$	0.754
$\rho_{13,MEK}$	0.748
$\rho_{14,MEK}$	0.742
$\rho_{15,MEK}$	(0.736)

$\eta_{1,MEK}$	(4.6762×10^{-4})
$\eta_{2,MEK}$	4.4122×10^{-4}
$\eta_{3,MEK}$	4.1696×10^{-4}
$\eta_{4,MEK}$	3.9461×10^{-4}
$\eta_{5,MEK}$	3.7399×10^{-4}
$\eta_{6,MEK}$	3.5491×10^{-4}
$\eta_{7,MEK}$	3.3725×10^{-4}
$\eta_{8,MEK}$	$:= 3.2085 \times 10^{-4} \cdot \text{Pa} \cdot \text{s}$
$\eta_{9,MEK}$	3.0562×10^{-4}
$\eta_{10,MEK}$	2.9143×10^{-4}
$\eta_{11,MEK}$	2.7821×10^{-4}
$\eta_{12,MEK}$	2.6586×10^{-4}
$\eta_{13,MEK}$	2.5432×10^{-4}
$\eta_{14,MEK}$	2.4351×10^{-4}
$\eta_{15,MEK}$	(2.3337×10^{-4})

	1
1	283.15
2	288.15
3	293.15
4	298.15
5	303.15
6	308.15
7	313.15
8	318.15
9	323.15
10	328.15
11	333.15
12	338.15
13	343.15
14	348.15
15	353.15

$$V_{mol,MEK} := \frac{MW_{MEK}}{\rho_{4,MEK}}$$

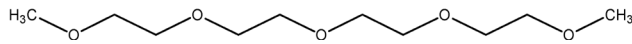
Appendix 4

2.3 DEK

$$\begin{aligned}
 MW_{\text{DEK}} &:= 86.1338 \frac{\text{gm}}{\text{mol}} & \text{Vat0K}_{\text{DEK}} &:= 78.4 \frac{\text{cm}^3}{\text{mol}} & c_{\text{Sh10o}} & & 5 \cdot 1.1 + 10 \cdot 6.7 + 5.9 = 78.4 \\
 V_{\text{cDEK}} &:= 336 \cdot \frac{\text{cm}^3}{\text{mol}} & & & & & 5 \cdot 0.77 + 10 \cdot 6.45 + 5.9 = 74.25 \\
 & & & & & & \text{http://www.therc.org/kdb/kdb/hcprop/showprop.php?cmpid=1196} & & 4 \cdot 0.77 + 8 \cdot 6.45 + 5.9 = 60.58 \\
 V_{\text{vdwDEK}} &:= (2 \cdot 13.67 + 2 \cdot 10.23 + 11.7) \cdot \frac{\text{cm}^3}{\text{mol}}
 \end{aligned}$$

$ \begin{pmatrix} \rho_{1,\text{DEK}} \\ \rho_{2,\text{DEK}} \\ \rho_{3,\text{DEK}} \\ \rho_{4,\text{DEK}} \\ \rho_{5,\text{DEK}} \\ \rho_{6,\text{DEK}} \\ \rho_{7,\text{DEK}} \\ \rho_{8,\text{DEK}} \\ \rho_{9,\text{DEK}} \\ \rho_{10,\text{DEK}} \\ \rho_{11,\text{DEK}} \\ \rho_{12,\text{DEK}} \\ \rho_{13,\text{DEK}} \\ \rho_{14,\text{DEK}} \\ \rho_{15,\text{DEK}} \end{pmatrix} $	$ \begin{pmatrix} 0.8241606 \\ 0.8192934 \\ 0.8143909 \\ 0.809452 \\ 0.8044755 \\ 0.7994602 \\ 0.7944049 \\ 0.7893084 \\ 0.7841691 \\ 0.7789856 \\ 0.7737564 \\ 0.7684799 \\ 0.7631542 \\ 0.7577776 \\ 0.7523481 \end{pmatrix} $	$ \cdot \frac{\text{gm}}{\text{cm}^3} $	$ \begin{pmatrix} \eta_{1,\text{DEK}} \\ \eta_{2,\text{DEK}} \\ \eta_{3,\text{DEK}} \\ \eta_{4,\text{DEK}} \\ \eta_{5,\text{DEK}} \\ \eta_{6,\text{DEK}} \\ \eta_{7,\text{DEK}} \\ \eta_{8,\text{DEK}} \\ \eta_{9,\text{DEK}} \\ \eta_{10,\text{DEK}} \\ \eta_{11,\text{DEK}} \\ \eta_{12,\text{DEK}} \\ \eta_{13,\text{DEK}} \\ \eta_{14,\text{DEK}} \\ \eta_{15,\text{DEK}} \end{pmatrix} $	$ \begin{pmatrix} 5.247 \times 10^{-4} \\ 4.953 \times 10^{-4} \\ 4.683 \times 10^{-4} \\ 4.435 \times 10^{-4} \\ 4.206 \times 10^{-4} \\ 3.995 \times 10^{-4} \\ 3.799 \times 10^{-4} \\ 3.617 \times 10^{-4} \\ 3.449 \times 10^{-4} \\ 3.292 \times 10^{-4} \\ 3.145 \times 10^{-4} \\ 3.009 \times 10^{-4} \\ 2.881 \times 10^{-4} \\ 2.762 \times 10^{-4} \\ 2.650 \times 10^{-4} \end{pmatrix} $	$:= \cdot \text{Pa} \cdot \text{s} $	$ V_{\text{molDEK}} := \frac{MW_{\text{DEK}}}{\rho_{4,\text{DEK}}} $
---	--	---	---	--	---	--

2.5 TEGDME



$$\begin{aligned}
 MW_{\text{TEGDME}} &:= 222.28168 \frac{\text{gm}}{\text{mol}} & \text{Vat0K}_{\text{TEGDME}} &:= 187.9 \frac{\text{cm}^3}{\text{mol}} & & & (2 \cdot 1.1 + 6 \cdot 6.7 + 5.9) + 4 \cdot (5.9 + 2 \cdot 1.1 + 4 \cdot 6.7) = 187.9 \\
 V_{\text{cTEGDME}} &:= 0.691 \frac{\text{m}^3}{\text{kmol}} & V_{\text{vdwTEGDME}} &:= [2 \cdot 13.67 + 5.25 + 4 \cdot (5.25 + 2 \cdot 10.23)] \cdot \frac{\text{cm}^3}{\text{mol}}
 \end{aligned}$$

$ \begin{pmatrix} \rho_{1,\text{TEGDME}} \\ \rho_{2,\text{TEGDME}} \\ \rho_{3,\text{TEGDME}} \\ \rho_{4,\text{TEGDME}} \\ \rho_{5,\text{TEGDME}} \\ \rho_{6,\text{TEGDME}} \\ \rho_{7,\text{TEGDME}} \\ \rho_{8,\text{TEGDME}} \\ \rho_{9,\text{TEGDME}} \\ \rho_{10,\text{TEGDME}} \\ \rho_{11,\text{TEGDME}} \\ \rho_{12,\text{TEGDME}} \\ \rho_{13,\text{TEGDME}} \\ \rho_{14,\text{TEGDME}} \\ \rho_{15,\text{TEGDME}} \end{pmatrix} $	$ \begin{pmatrix} 1020 \\ 1016 \\ 1012 \\ 1007 \\ 1003 \\ 998.4 \\ 993.8 \\ 989.2 \\ 984.6 \\ 979.9 \\ 975.2 \\ 970.5 \\ 965.8 \\ 961.1 \\ 956.4 \end{pmatrix} $	$ \cdot \frac{\text{kg}}{\text{m}^3} $	$ \begin{pmatrix} \eta_{1,\text{TEGDME}} \\ \eta_{2,\text{TEGDME}} \\ \eta_{3,\text{TEGDME}} \\ \eta_{4,\text{TEGDME}} \\ \eta_{5,\text{TEGDME}} \\ \eta_{6,\text{TEGDME}} \\ \eta_{7,\text{TEGDME}} \\ \eta_{8,\text{TEGDME}} \\ \eta_{9,\text{TEGDME}} \\ \eta_{10,\text{TEGDME}} \\ \eta_{11,\text{TEGDME}} \\ \eta_{12,\text{TEGDME}} \\ \eta_{13,\text{TEGDME}} \\ \eta_{14,\text{TEGDME}} \\ \eta_{15,\text{TEGDME}} \end{pmatrix} $	$ \begin{pmatrix} 4.979 \times 10^{-3} \\ 4.361 \times 10^{-3} \\ 3.749 \times 10^{-3} \\ 3.348 \times 10^{-3} \\ 2.951 \times 10^{-3} \\ 2.673 \times 10^{-3} \\ 2.398 \times 10^{-3} \\ 2.201 \times 10^{-3} \\ 2.007 \times 10^{-3} \\ 1.848 \times 10^{-3} \\ 1.691 \times 10^{-3} \\ 1.569 \times 10^{-3} \\ 1.449 \times 10^{-3} \\ 1.352 \times 10^{-3} \\ 1.257 \times 10^{-3} \end{pmatrix} $	$:= \cdot \text{Pa} \cdot \text{s} $	$ V_{\text{molTEGDME}} := \frac{MW_{\text{TEGDME}}}{\rho_{4,\text{TEGDME}}} $
--	--	--	--	--	---	---

2.6 PEGDME 250

$$MW_{\text{PEGDME}} := 298.21 \cdot \frac{\text{gm}}{\text{mol}}$$

$$(2 \cdot 1.1 + 6 \cdot 6.7 + 5.9) + 5.723 \cdot (5.9 + 2 \cdot 1.1 + 4 \cdot 6.7) = 248.033$$

$$V_{\text{cPEGDME}} := \left(0.915 \cdot \frac{\text{m}^3}{\text{kmol}} \right)$$

$$V_{\text{at0KPEGDME}} := 248.03 \cdot \frac{\text{cm}^3}{\text{mol}} \quad n = 5.723$$

$$V_{\text{vdwPEGDME}} := [2 \cdot 13.67 + 5.25 + 5.723 \cdot (5.25 + 2 \cdot 10.23)] \cdot \frac{\text{cm}^3}{\text{mol}}$$

$\rho_{1, \text{PEGDME}}$	
$\rho_{2, \text{PEGDME}}$	1044
$\rho_{3, \text{PEGDME}}$	1040
$\rho_{4, \text{PEGDME}}$	1036
$\rho_{5, \text{PEGDME}}$	1031
$\rho_{6, \text{PEGDME}}$	1026
$\rho_{7, \text{PEGDME}}$	1022
$\rho_{8, \text{PEGDME}}$	1017
$\rho_{9, \text{PEGDME}}$	1013
$\rho_{10, \text{PEGDME}}$	1008
$\rho_{11, \text{PEGDME}}$	1004
$\rho_{12, \text{PEGDME}}$	999.5
$\rho_{13, \text{PEGDME}}$	995.1
$\rho_{14, \text{PEGDME}}$	990.6
$\rho_{15, \text{PEGDME}}$	986.2
	981.7

$$:= \frac{\text{kg}}{\text{m}^3}$$

$\eta_{1, \text{PEGDME}}$	10.23×10^{-3}
$\eta_{2, \text{PEGDME}}$	8.843×10^{-3}
$\eta_{3, \text{PEGDME}}$	7.471×10^{-3}
$\eta_{4, \text{PEGDME}}$	6.532×10^{-3}
$\eta_{5, \text{PEGDME}}$	5.601×10^{-3}
$\eta_{6, \text{PEGDME}}$	4.980×10^{-3}
$\eta_{7, \text{PEGDME}}$	4.365×10^{-3}
$\eta_{8, \text{PEGDME}}$	3.927×10^{-3}
$\eta_{9, \text{PEGDME}}$	3.493×10^{-3}
$\eta_{10, \text{PEGDME}}$	3.180×10^{-3}
$\eta_{11, \text{PEGDME}}$	2.869×10^{-3}
$\eta_{12, \text{PEGDME}}$	2.618×10^{-3}
$\eta_{13, \text{PEGDME}}$	2.369×10^{-3}
$\eta_{14, \text{PEGDME}}$	2.212×10^{-3}
$\eta_{15, \text{PEGDME}}$	2.058×10^{-3}

$$:= (\text{Pa} \cdot \text{s})$$

$$V_{\text{vdwPEGDME}} = 1.797 \times 10^{-4} \frac{\text{m}^3}{\text{mol}}$$

$$V_{\text{molPEGDME}} := \frac{MW_{\text{PEGDME}}}{\rho_{4, \text{PEGDME}}}$$

2.7 TEG

$$MW_{\text{TEG}} := 194.23 \cdot \frac{\text{gm}}{\text{mol}}$$

$$1 \cdot \text{O} + 2 \cdot \text{H} + 4 \cdot (2 \cdot \text{C} + 2 \cdot \text{H} + 1 \cdot \text{O}) \quad 1 \cdot 5 + 2 \cdot 6.7 + 4 \cdot (2 \cdot 1.1 + 4 \cdot 6.7 + 1 \cdot 5) = 154.4 \quad \text{c8h18o5}$$

$$V_{\text{cTEG}} := \left(5.633 \cdot 10^{-4} \cdot \frac{\text{m}^3}{\text{mol}} \right)$$

$$V_{\text{at0KTEG}} := 154.4 \cdot \frac{\text{cm}^3}{\text{mol}} \quad V_{\text{vdwTEG}} := 113.59 \cdot \frac{\text{cm}^3}{\text{mol}}$$

$$2 \cdot \text{OH} + 8 \cdot \text{CH}_2 + 3 \cdot \text{O}$$

$$2 \cdot 8 + 8 \cdot 10.23 + 3 \cdot 5.25 = 113.59$$

$\rho_{1, \text{TEG}}$	
$\rho_{2, \text{TEG}}$	1134
$\rho_{3, \text{TEG}}$	1131
$\rho_{4, \text{TEG}}$	1127
$\rho_{5, \text{TEG}}$	1124
$\rho_{6, \text{TEG}}$	1120
$\rho_{7, \text{TEG}}$	1116
$\rho_{8, \text{TEG}}$	1113
$\rho_{9, \text{TEG}}$	1109
$\rho_{10, \text{TEG}}$	1105
$\rho_{11, \text{TEG}}$	1102
$\rho_{12, \text{TEG}}$	1098
$\rho_{13, \text{TEG}}$	1094
$\rho_{14, \text{TEG}}$	1090
$\rho_{15, \text{TEG}}$	1086
	1083

$$:= \frac{\text{kg}}{\text{m}^3}$$

$\eta_{1, \text{TEG}}$	0.1004
$\eta_{2, \text{TEG}}$	0.0775
$\eta_{3, \text{TEG}}$	0.05965
$\eta_{4, \text{TEG}}$	0.04657
$\eta_{5, \text{TEG}}$	0.03666
$\eta_{6, \text{TEG}}$	0.02908
$\eta_{7, \text{TEG}}$	0.02324
$\eta_{8, \text{TEG}}$	0.01870
$\eta_{9, \text{TEG}}$	0.01515
$\eta_{10, \text{TEG}}$	0.01236
$\eta_{11, \text{TEG}}$	0.01014
$\eta_{12, \text{TEG}}$	0.008368
$\eta_{13, \text{TEG}}$	0.006944
$\eta_{14, \text{TEG}}$	0.005794
$\eta_{15, \text{TEG}}$	0.004859

$$:= (\text{Pa} \cdot \text{s})$$

$$V_{\text{molTEG}} := \frac{MW_{\text{TEG}}}{\rho_{4, \text{TEG}}}$$

$$V_{\text{vdw}} = \begin{pmatrix} 4.919 \times 10^{-5} \\ 4.927 \times 10^{-5} \\ 5.95 \times 10^{-5} \\ 1.354 \times 10^{-4} \\ 1.797 \times 10^{-4} \\ 1.136 \times 10^{-4} \end{pmatrix} \frac{\text{m}^3}{\text{mol}}$$

$$V_{\text{at0K}} = \begin{pmatrix} 0 \\ 6.39 \times 10^{-5} \\ 7.84 \times 10^{-5} \\ 1.879 \times 10^{-4} \\ 2.48 \times 10^{-4} \\ 1.544 \times 10^{-4} \end{pmatrix} \frac{\text{m}^3}{\text{mol}}$$

1) Concentration inside the membrane (polymer pieces)

1.1) Swelling experiments

$$\omega_{mt} := \begin{pmatrix} 0.516 & 0.027 & 0.457 \\ 0.446 & 0.050 & 0.504 \\ 0.375 & 0.066 & 0.559 \end{pmatrix} \quad \omega_{mp} := \begin{pmatrix} 0.500 & 0.026 & 0.474 \\ 0.417 & 0.046 & 0.537 \\ 0.343 & 0.061 & 0.596 \end{pmatrix}$$

$$\omega_{dt} := \begin{pmatrix} 0.637 & 0.034 & 0.330 \\ 0.575 & 0.064 & 0.361 \\ 0.510 & 0.090 & 0.400 \end{pmatrix} \quad \omega_{dp} := \begin{pmatrix} 0.622 & 0.033 & 0.346 \\ 0.549 & 0.061 & 0.390 \\ 0.476 & 0.084 & 0.440 \end{pmatrix}$$

Flory-Rehner

MEK

$$\phi_1 := 0.629795 \quad \chi := 0.567 \quad V_1 := 90.25 \cdot \frac{\text{ml}}{\text{mol}} \quad \text{chi Macromolecules 2005 38 (10) 4447-4455 Souvik Nandi, H. Henning Winter}$$

$$\phi_3 := 1 - \phi_1$$

$$MC := \frac{-V_1 \cdot \rho_{4,PDMS} \cdot \left(\frac{1}{\phi_3^3} - \frac{\phi_3}{2} \right)}{\ln(1 - \phi_3) + \phi_3 + \chi \cdot \phi_3^2}$$

$$v := \frac{\rho_{4,PDMS}}{MC} \quad MC = 3.243 \frac{\text{kg}}{\text{mol}}$$

$$v = 300.381 \frac{\text{mol}}{\text{m}^3} \quad \frac{MC}{MW_{PDMS}} = 43.759$$

DEK

$$\phi_1 := 0.72 \quad \phi_3 := 1 - \phi_1 \quad \chi := 0.373 \quad V_1 := 106.4 \cdot \frac{\text{ml}}{\text{mol}}$$

$$MC := \frac{-V_1 \cdot \rho_{4,PDMS} \cdot \left(\frac{1}{\phi_3^3} - \frac{\phi_3}{2} \right)}{\ln(1 - \phi_3) + \phi_3 + \chi \cdot \phi_3^2}$$

$$v := \frac{\rho_{4,PDMS}}{MC} \quad MC = 2.767 \frac{\text{kg}}{\text{mol}}$$

$$v = 352.039 \frac{\text{mol}}{\text{m}^3}$$

$$\frac{MC}{MW_{PDMS}} = 37.338$$

1.1) MEK/TEGDME

$$MT := 1 \quad MPol := 2 \quad TPol := 3 \quad V_{mol1} := \frac{1}{\rho_{4,MEK}} \cdot MW_{MEK} \quad V_{mol2} := \frac{1}{\rho_{4,TEGDME}} \cdot MW_{TEGDME} \quad V_{mol3} := \frac{1}{\rho_{4,PDMS}} \cdot MW_{PDMS} \quad RU3 := 100000$$

$$MW_{Flory} := \begin{pmatrix} MW_{MEK} \\ MW_{TEGDME} \\ MW_{PDMS} \end{pmatrix}$$

$$\chi_{25} := \begin{pmatrix} 0.396 \\ 0.917 \\ 1.061 \end{pmatrix} \quad \chi_{25} := \chi_{25} - 0.35 \quad \chi_{25} = \begin{pmatrix} 0.046 \\ 0.567 \\ 0.711 \end{pmatrix}$$

$$a1_{25} := \begin{pmatrix} 0.983 \\ 0.965 \\ 0.945 \end{pmatrix} \quad a2_{25} := \begin{pmatrix} 0.016 \\ 0.033 \\ 0.051 \end{pmatrix}$$

T=25°C, 5wt%

$$a1 := a1_25 \quad a2 := a2_25 \quad \chi := \begin{pmatrix} 0.05 \\ 0.567 \\ 0.711 \end{pmatrix}$$

$$\phi1 := 0.566 \quad \phi3 := 0.411 \quad \phi2 := 1 - \phi1 - \phi3$$

conc := 1

$$\text{Given } \ln(\phi1) + (1-\phi1) \left(\frac{Vmol1}{Vmol2} \right) \phi2 - \left(\frac{Vmol1}{Vmol3-RU3} \right) \phi3 + (\chi_1 \phi2 + \chi_2 \phi3) (\phi2 + \phi3) - \chi_3 \left(\frac{Vmol1}{Vmol2} \right) \phi2 \phi3$$

$$a1_{conc} = e$$

$$\ln(\phi2) + (1-\phi2) \left(\frac{Vmol2}{Vmol1} \right) \phi1 - \left(\frac{Vmol2}{Vmol3-RU3} \right) \phi3 + \left(\chi_1 \phi1 \frac{Vmol2}{Vmol1} + \chi_3 \phi3 \right) (\phi1 + \phi3) - \chi_2 \left(\frac{Vmol2}{Vmol1} \right) \phi1 \phi3$$

$$a2_{conc} = e$$

$$\begin{pmatrix} \chi_1 \\ \chi_2 \\ \chi_3 \end{pmatrix} := \text{Minerr}(\chi_1, \chi_2, \chi_3)$$

$$\begin{pmatrix} \chi_1 \\ \chi_2 \\ \chi_3 \end{pmatrix} = \begin{pmatrix} 0.054 \\ 0.732 \\ 0.965 \end{pmatrix}$$

$$e^{\ln(\phi1) + (1-\phi1) \left(\frac{Vmol1}{Vmol2} \right) \phi2 - \left(\frac{Vmol1}{Vmol3-RU3} \right) \phi3 + (\chi_1 \phi2 + \chi_2 \phi3) (\phi2 + \phi3) - \chi_3 \left(\frac{Vmol1}{Vmol2} \right) \phi2 \phi3} = 0.983$$

$$e^{\ln(\phi2) + (1-\phi2) \left(\frac{Vmol2}{Vmol1} \right) \phi1 - \left(\frac{Vmol2}{Vmol3-RU3} \right) \phi3 + \left(\chi_1 \phi1 \frac{Vmol2}{Vmol1} + \chi_3 \phi3 \right) (\phi1 + \phi3) - \chi_2 \left(\frac{Vmol2}{Vmol1} \right) \phi1 \phi3} = 0.016$$

T=25°C, 10wt%

$$a1 := a1_25 \quad a2 := a2_25$$

$$\phi1 := 0.496 \quad \phi3 := 0.46 \quad \phi2 := 1 - \phi1 - \phi3$$

conc := 2

$$\text{Given } \ln(\phi1) + (1-\phi1) \left(\frac{Vmol1}{Vmol2} \right) \phi2 - \left(\frac{Vmol1}{Vmol3-RU3} \right) \phi3 + (\chi_1 \phi2 + \chi_2 \phi3) (\phi2 + \phi3) - \chi_3 \left(\frac{Vmol1}{Vmol2} \right) \phi2 \phi3$$

$$a1_{conc} = e$$

$$\ln(\phi2) + (1-\phi2) \left(\frac{Vmol2}{Vmol1} \right) \phi1 - \left(\frac{Vmol2}{Vmol3-RU3} \right) \phi3 + \left(\chi_1 \phi1 \frac{Vmol2}{Vmol1} + \chi_3 \phi3 \right) (\phi1 + \phi3) - \chi_2 \left(\frac{Vmol2}{Vmol1} \right) \phi1 \phi3$$

$$a2_{conc} = e$$

$$\begin{pmatrix} \chi_1 \\ \chi_2 \\ \chi_3 \end{pmatrix} := \text{Minerr}(\chi_1, \chi_2, \chi_3)$$

$$\begin{pmatrix} \chi_1 \\ \chi_2 \\ \chi_3 \end{pmatrix} = \begin{pmatrix} 0.053 \\ 0.798 \\ 0.804 \end{pmatrix}$$

$$e^{\ln(\phi1) + (1-\phi1) \left(\frac{Vmol1}{Vmol2} \right) \phi2 - \left(\frac{Vmol1}{Vmol3-RU3} \right) \phi3 + (\chi_1 \phi2 + \chi_2 \phi3) (\phi2 + \phi3) - \chi_3 \left(\frac{Vmol1}{Vmol2} \right) \phi2 \phi3} = 0.965$$

$$e^{\ln(\phi2) + (1-\phi2) \left(\frac{Vmol2}{Vmol1} \right) \phi1 - \left(\frac{Vmol2}{Vmol3-RU3} \right) \phi3 + \left(\chi_1 \phi1 \frac{Vmol2}{Vmol1} + \chi_3 \phi3 \right) (\phi1 + \phi3) - \chi_2 \left(\frac{Vmol2}{Vmol1} \right) \phi1 \phi3} = 0.033$$

T=25°C, 15wt%

$$\text{conc} := 3 \quad a1 := a1_25 \quad a2 := a2_25$$

$$\phi1 := 0.423 \quad \phi3 := 0.518 \quad \phi2 := 1 - \phi1 - \phi3$$

Given

$$\ln(\phi2) + (1-\phi2) \left(\frac{Vmol2}{Vmol1} \right) \phi1 - \left(\frac{Vmol2}{Vmol3-RU3} \right) \phi3 + \left(\chi_1 \phi1 \frac{Vmol2}{Vmol1} + \chi_3 \phi3 \right) (\phi1 + \phi3) - \chi_2 \left(\frac{Vmol2}{Vmol1} \right) \phi1 \phi3$$

$$a2_{conc} = e$$

$$\ln(\phi1) + (1-\phi1) \left(\frac{Vmol1}{Vmol2} \right) \phi2 - \left(\frac{Vmol1}{Vmol3-RU3} \right) \phi3 + (\chi_1 \phi2 + \chi_2 \phi3) (\phi2 + \phi3) - \chi_3 \left(\frac{Vmol1}{Vmol2} \right) \phi2 \phi3$$

$$a1_{conc} = e$$

$$\phi3 = 1 - \phi1 - \phi2$$

$$\begin{pmatrix} \chi_1 \\ \chi_2 \\ \chi_3 \end{pmatrix} := \text{Minerr}(\chi_1, \chi_2, \chi_3)$$

$$\begin{pmatrix} \chi_1 \\ \chi_2 \\ \chi_3 \end{pmatrix} = \begin{pmatrix} 0.052 \\ 0.864 \\ 0.739 \end{pmatrix}$$

$$e^{\ln(\phi1) + (1-\phi1) \left(\frac{Vmol1}{Vmol2} \right) \phi2 - \left(\frac{Vmol1}{Vmol3-RU3} \right) \phi3 + (\chi_1 \phi2 + \chi_2 \phi3) (\phi2 + \phi3) - \chi_3 \left(\frac{Vmol1}{Vmol2} \right) \phi2 \phi3} = 0.945$$

$$e^{\ln(\phi2) + (1-\phi2) \left(\frac{Vmol2}{Vmol1} \right) \phi1 - \left(\frac{Vmol2}{Vmol3-RU3} \right) \phi3 + \left(\chi_1 \phi1 \frac{Vmol2}{Vmol1} + \chi_3 \phi3 \right) (\phi1 + \phi3) - \chi_2 \left(\frac{Vmol2}{Vmol1} \right) \phi1 \phi3} = 0.051$$

1.2) MEK/PEGDME

$$V_{mol1} := \frac{1}{\rho_{4,MEK}} \cdot MW_{MEK} \quad V_{mol2} := \frac{1}{\rho_{4,PEGDME}} \cdot MW_{PEGDME} \quad V_{mol3} := \frac{1}{\rho_{4,PDMS}} \cdot MW_{PDMS} \quad RU3 := 100000$$

$$MW_{Flory} := \begin{pmatrix} MW_{MEK} \\ MW_{PEGDME} \\ MW_{PDMS} \end{pmatrix}$$

$$\chi_{25} := \begin{pmatrix} 0.649 \\ 0.917 \\ 0.487 \end{pmatrix} \quad \begin{matrix} M_{PEGDME} := 1 \\ M_{Pol} := 2 \\ PEGDME_Pol := 3 \end{matrix} \quad \chi_{25} := \chi_{25} - 0.35$$

$$a_{1_25} := \begin{pmatrix} 0.9877 \\ 0.9741 \\ 0.9588 \end{pmatrix} \quad a_{2_25} := \begin{pmatrix} 0.0071 \\ 0.0154 \\ 0.0252 \end{pmatrix} \quad \chi_{25} = \begin{pmatrix} 0.299 \\ 0.567 \\ 0.137 \end{pmatrix}$$

$$T = 25^\circ\text{C}, 5\text{wt}\% \quad \chi := \begin{pmatrix} 1 \\ \chi_{25_2} \\ 0.137 \end{pmatrix}$$

$$\text{conc} := 1 \quad a_1 := a_{1_25} \quad a_2 := a_{2_25} \quad \phi_1 := 0.55 \quad \phi_3 := 0.428 \quad \phi_2 := 1 - \phi_1 - \phi_3$$

Given

$$a_{1_conc} = e^{\ln(\phi_1) + (1-\phi_1) \left(\frac{V_{mol1}}{V_{mol2}} \right) \phi_2 - \left(\frac{V_{mol1}}{V_{mol3} \cdot RU3} \right) \phi_3 + (\chi_1 \phi_2 + \chi_2 \phi_3) (\phi_2 + \phi_3) - \chi_3 \left(\frac{V_{mol1}}{V_{mol2}} \right) \phi_2 \phi_3}$$

$$a_{2_conc} = e^{\ln(\phi_2) + (1-\phi_2) \left(\frac{V_{mol2}}{V_{mol1}} \right) \phi_1 - \left(\frac{V_{mol2}}{V_{mol3} \cdot RU3} \right) \phi_3 + (\chi_1 \phi_1 \frac{V_{mol2}}{V_{mol1}} + \chi_3 \phi_3) (\phi_1 + \phi_3) - \chi_2 \left(\frac{V_{mol2}}{V_{mol1}} \right) \phi_1 \phi_3}$$

$$\phi_3 = 1 - \phi_1 - \phi_2$$

$$\begin{pmatrix} \chi_1 \\ \chi_2 \\ \chi_3 \end{pmatrix} := \text{Minerr}(\chi_1, \chi_2, \chi_3) \quad \begin{pmatrix} \chi_1 \\ \chi_2 \\ \chi_3 \end{pmatrix} = \begin{pmatrix} 0.089 \\ 0.736 \\ 0.133 \end{pmatrix}$$

$$e^{\ln(\phi_1) + (1-\phi_1) \left(\frac{V_{mol1}}{V_{mol2}} \right) \phi_2 - \left(\frac{V_{mol1}}{V_{mol3} \cdot RU3} \right) \phi_3 + (\chi_1 \phi_2 + \chi_2 \phi_3) (\phi_2 + \phi_3) - \chi_3 \left(\frac{V_{mol1}}{V_{mol2}} \right) \phi_2 \phi_3} = 0.988$$

$$e^{\ln(\phi_2) + (1-\phi_2) \left(\frac{V_{mol2}}{V_{mol1}} \right) \phi_1 - \left(\frac{V_{mol2}}{V_{mol3} \cdot RU3} \right) \phi_3 + (\chi_1 \phi_1 \frac{V_{mol2}}{V_{mol1}} + \chi_3 \phi_3) (\phi_1 + \phi_3) - \chi_2 \left(\frac{V_{mol2}}{V_{mol1}} \right) \phi_1 \phi_3} = 7.1 \times 10^{-3}$$

T=25°C, 10wt%

$$\text{conc} := 2 \quad a_1 := a_{1_25} \quad a_2 := a_{2_25} \quad \phi_1 := 0.467 \quad \phi_3 := 0.493 \quad \phi_2 := 1 - \phi_1 - \phi_3$$

Given

$$a_{2_conc} = e^{\ln(\phi_2) + (1-\phi_2) \left(\frac{V_{mol2}}{V_{mol1}} \right) \phi_1 - \left(\frac{V_{mol2}}{V_{mol3} \cdot RU3} \right) \phi_3 + (\chi_1 \phi_1 \frac{V_{mol2}}{V_{mol1}} + \chi_3 \phi_3) (\phi_1 + \phi_3) - \chi_2 \left(\frac{V_{mol2}}{V_{mol1}} \right) \phi_1 \phi_3}$$

$$a_{1_conc} = e^{\ln(\phi_1) + (1-\phi_1) \left(\frac{V_{mol1}}{V_{mol2}} \right) \phi_2 - \left(\frac{V_{mol1}}{V_{mol3} \cdot RU3} \right) \phi_3 + (\chi_1 \phi_2 + \chi_2 \phi_3) (\phi_2 + \phi_3) - \chi_3 \left(\frac{V_{mol1}}{V_{mol2}} \right) \phi_2 \phi_3}$$

$$\phi_3 = 1 - \phi_1 - \phi_2$$

$$\begin{pmatrix} \chi_1 \\ \chi_2 \\ \chi_3 \end{pmatrix} := \text{Minerr}(\chi_1, \chi_2, \chi_3) \quad \begin{pmatrix} \chi_1 \\ \chi_2 \\ \chi_3 \end{pmatrix} = \begin{pmatrix} 0.084 \\ 0.813 \\ 0.129 \end{pmatrix}$$

$$e^{\ln(\phi_1) + (1-\phi_1) \left(\frac{V_{mol1}}{V_{mol2}} \right) \phi_2 - \left(\frac{V_{mol1}}{V_{mol3} \cdot RU3} \right) \phi_3 + (\chi_1 \phi_2 + \chi_2 \phi_3) (\phi_2 + \phi_3) - \chi_3 \left(\frac{V_{mol1}}{V_{mol2}} \right) \phi_2 \phi_3} = 0.974$$

$$e^{\ln(\phi_2) + (1-\phi_2) \left(\frac{V_{mol2}}{V_{mol1}} \right) \phi_1 - \left(\frac{V_{mol2}}{V_{mol3} \cdot RU3} \right) \phi_3 + (\chi_1 \phi_1 \frac{V_{mol2}}{V_{mol1}} + \chi_3 \phi_3) (\phi_1 + \phi_3) - \chi_2 \left(\frac{V_{mol2}}{V_{mol1}} \right) \phi_1 \phi_3} = 0.015$$

T=25°C, 15wt%

$$\text{conc} := 3 \quad a1 := a1_25 \quad a2 := a2_25$$

$$\phi1 := 0.39 \quad \phi3 := 0.556 \quad \phi2 := 1 - \phi1 - \phi3$$

Given

$$a2_{\text{conc}} = e^{\ln(\phi2) + (1-\phi2) \left(\frac{V_{\text{mol}2}}{V_{\text{mol}1}} \right) \phi1 - \left(\frac{V_{\text{mol}2}}{V_{\text{mol}3} \text{RU}3} \right) \phi3 + \left(\chi_1 \phi1 \frac{V_{\text{mol}2}}{V_{\text{mol}1}} + \chi_3 \phi3 \right) (\phi1 + \phi3) - \chi_2 \left(\frac{V_{\text{mol}2}}{V_{\text{mol}1}} \right) \phi1 \phi3}$$

$$a1_{\text{conc}} = e^{\ln(\phi1) + (1-\phi1) \left(\frac{V_{\text{mol}1}}{V_{\text{mol}2}} \right) \phi2 - \left(\frac{V_{\text{mol}1}}{V_{\text{mol}3} \text{RU}3} \right) \phi3 + \left(\chi_1 \phi2 + \chi_2 \phi3 \right) (\phi2 + \phi3) - \chi_3 \left(\frac{V_{\text{mol}1}}{V_{\text{mol}2}} \right) \phi2 \phi3}$$

$$\phi3 = 1 - \phi1 - \phi2$$

$$\begin{pmatrix} \chi_1 \\ \chi_2 \\ \chi_3 \end{pmatrix} := \text{Minerr}(\chi_1, \chi_2, \chi_3) \quad \begin{pmatrix} \chi_1 \\ \chi_2 \\ \chi_3 \end{pmatrix} = \begin{pmatrix} 0.084 \\ 0.899 \\ 0.129 \end{pmatrix}$$

$$e^{\ln(\phi1) + (1-\phi1) \left(\frac{V_{\text{mol}1}}{V_{\text{mol}2}} \right) \phi2 - \left(\frac{V_{\text{mol}1}}{V_{\text{mol}3} \text{RU}3} \right) \phi3 + \left(\chi_1 \phi2 + \chi_2 \phi3 \right) (\phi2 + \phi3) - \chi_3 \left(\frac{V_{\text{mol}1}}{V_{\text{mol}2}} \right) \phi2 \phi3} = 0.959$$

$$e^{\ln(\phi2) + (1-\phi2) \left(\frac{V_{\text{mol}2}}{V_{\text{mol}1}} \right) \phi1 - \left(\frac{V_{\text{mol}2}}{V_{\text{mol}3} \text{RU}3} \right) \phi3 + \left(\chi_1 \phi1 \frac{V_{\text{mol}2}}{V_{\text{mol}1}} + \chi_3 \phi3 \right) (\phi1 + \phi3) - \chi_2 \left(\frac{V_{\text{mol}2}}{V_{\text{mol}1}} \right) \phi1 \phi3} = 0.025$$

1.2) DEK/TEGDME

$$V_{\text{mol}1} := \frac{1}{\rho_{4, \text{DEK}}} \cdot MW_{\text{DEK}}$$

$$V_{\text{mol}2} := \frac{1}{\rho_{4, \text{TEGDME}}} \cdot MW_{\text{TEGDME}}$$

$$V_{\text{mol}3} := \frac{1}{\rho_{4, \text{PDMS}}} \cdot MW_{\text{PDMS}}$$

$$\text{RU}3 := 100000$$

$$MW_{\text{Flory}} := \begin{pmatrix} MW_{\text{DEK}} \\ MW_{\text{TEGDME}} \\ MW_{\text{PDMS}} \end{pmatrix}$$

$$\chi_{25} := \begin{pmatrix} 0.351 \\ 0.723 \\ 1.061 \end{pmatrix} \quad \begin{array}{l} \text{DTEGDME} := 1 \\ \text{DPol} := 2 \\ \text{TEGDME_Pol} := 3 \end{array}$$

$$a1_25 := \begin{pmatrix} 0.980 \\ 0.960 \\ 0.938 \end{pmatrix}$$

$$\chi_{25} := \chi_{25} - 0.35$$

$$a2_25 := \begin{pmatrix} 0.027 \\ 0.054 \\ 0.082 \end{pmatrix}$$

$$\chi_{25} = \begin{pmatrix} 1 \times 10^{-3} \\ 0.373 \\ 0.711 \end{pmatrix}$$

T=25°C, 5wt%

$$\text{conc} := 1 \quad a1 := a1_25 \quad a2 := a2_25$$

$$\chi := \begin{pmatrix} 0.2 \\ 0.7 \\ 0.886 \end{pmatrix}$$

$$\phi1 := 0.679 \quad \phi3 := 0.292 \quad \phi2 := 1 - \phi1 - \phi3$$

Given

$$a1_{\text{conc}} = e^{\ln(\phi1) + (1-\phi1) \left(\frac{V_{\text{mol}1}}{V_{\text{mol}2}} \right) \phi2 - \left(\frac{V_{\text{mol}1}}{V_{\text{mol}3} \text{RU}3} \right) \phi3 + \left(\chi_1 \phi2 + \chi_2 \phi3 \right) (\phi2 + \phi3) - \chi_3 \left(\frac{V_{\text{mol}1}}{V_{\text{mol}2}} \right) \phi2 \phi3}$$

$$a2_{\text{conc}} = e^{\ln(\phi2) + (1-\phi2) \left(\frac{V_{\text{mol}2}}{V_{\text{mol}1}} \right) \phi1 - \left(\frac{V_{\text{mol}2}}{V_{\text{mol}3} \text{RU}3} \right) \phi3 + \left(\chi_1 \phi1 \frac{V_{\text{mol}2}}{V_{\text{mol}1}} + \chi_3 \phi3 \right) (\phi1 + \phi3) - \chi_2 \left(\frac{V_{\text{mol}2}}{V_{\text{mol}1}} \right) \phi1 \phi3}$$

$$\begin{pmatrix} \chi_1 \\ \chi_2 \\ \chi_3 \end{pmatrix} := \text{Minerr}(\chi_1, \chi_2, \chi_3) \quad \begin{pmatrix} \chi_1 \\ \chi_2 \\ \chi_3 \end{pmatrix} = \begin{pmatrix} 0.246 \\ 0.661 \\ 1.062 \end{pmatrix}$$

$$e^{\ln(\phi1) + (1-\phi1) \left(\frac{V_{\text{mol}1}}{V_{\text{mol}2}} \right) \phi2 - \left(\frac{V_{\text{mol}1}}{V_{\text{mol}3} \text{RU}3} \right) \phi3 + \left(\chi_1 \phi2 + \chi_2 \phi3 \right) (\phi2 + \phi3) - \chi_3 \left(\frac{V_{\text{mol}1}}{V_{\text{mol}2}} \right) \phi2 \phi3} = 0.98$$

$$e^{\ln(\phi2) + (1-\phi2) \left(\frac{V_{\text{mol}2}}{V_{\text{mol}1}} \right) \phi1 - \left(\frac{V_{\text{mol}2}}{V_{\text{mol}3} \text{RU}3} \right) \phi3 + \left(\chi_1 \phi1 \frac{V_{\text{mol}2}}{V_{\text{mol}1}} + \chi_3 \phi3 \right) (\phi1 + \phi3) - \chi_2 \left(\frac{V_{\text{mol}2}}{V_{\text{mol}1}} \right) \phi1 \phi3} = 0.027$$

Appendix 4

T=25°C, 10wt%

$$\text{conc} := 2 \quad a1 := a1_25 \quad a2 := a2_25$$

$$\phi1 := 0.621 \quad \phi3 := 0.324 \quad \phi2 := 1 - \phi1 - \phi3$$

Given

$$a2_{\text{conc}} = e^{\ln(\phi2) + (1-\phi2) \left(\frac{V_{\text{mol}2}}{V_{\text{mol}1}} \right) \phi1 - \left(\frac{V_{\text{mol}2}}{V_{\text{mol}3} \cdot \text{RU}3} \right) \phi3 + \left(\chi_1 \phi1 \frac{V_{\text{mol}2}}{V_{\text{mol}1} + \chi_3 \phi3} \right) (\phi1 + \phi3) - \chi_2 \left(\frac{V_{\text{mol}2}}{V_{\text{mol}1}} \right) \phi1 \phi3}$$

$$a1_{\text{conc}} = e^{\ln(\phi1) + (1-\phi1) \left(\frac{V_{\text{mol}1}}{V_{\text{mol}2}} \right) \phi2 - \left(\frac{V_{\text{mol}1}}{V_{\text{mol}3} \cdot \text{RU}3} \right) \phi3 + \left(\chi_1 \phi2 + \chi_2 \phi3 \right) (\phi2 + \phi3) - \chi_3 \left(\frac{V_{\text{mol}1}}{V_{\text{mol}2}} \right) \phi2 \phi3}$$

$$\phi3 = 1 - \phi1 - \phi2$$

$$\begin{pmatrix} \chi_1 \\ \chi_2 \\ \chi_3 \end{pmatrix} := \text{Minerr}(\chi_1, \chi_2, \chi_3) \quad \begin{pmatrix} \chi_1 \\ \chi_2 \\ \chi_3 \end{pmatrix} = \begin{pmatrix} 0.243 \\ 0.71 \\ 1.061 \end{pmatrix}$$

T=25°C, 15wt%

$$\text{conc} := 3 \quad a1 := a1_25 \quad a2 := a2_25$$

$$\phi1 := 0.558 \quad \phi3 := 0.363 \quad \phi2 := 1 - \phi1 - \phi3$$

Given

$$a2_{\text{conc}} = e^{\ln(\phi2) + (1-\phi2) \left(\frac{V_{\text{mol}2}}{V_{\text{mol}1}} \right) \phi1 - \left(\frac{V_{\text{mol}2}}{V_{\text{mol}3} \cdot \text{RU}3} \right) \phi3 + \left(\chi_1 \phi1 \frac{V_{\text{mol}2}}{V_{\text{mol}1} + \chi_3 \phi3} \right) (\phi1 + \phi3) - \chi_2 \left(\frac{V_{\text{mol}2}}{V_{\text{mol}1}} \right) \phi1 \phi3}$$

$$a1_{\text{conc}} = e^{\ln(\phi1) + (1-\phi1) \left(\frac{V_{\text{mol}1}}{V_{\text{mol}2}} \right) \phi2 - \left(\frac{V_{\text{mol}1}}{V_{\text{mol}3} \cdot \text{RU}3} \right) \phi3 + \left(\chi_1 \phi2 + \chi_2 \phi3 \right) (\phi2 + \phi3) - \chi_3 \left(\frac{V_{\text{mol}1}}{V_{\text{mol}2}} \right) \phi2 \phi3}$$

$$\phi3 = 1 - \phi1 - \phi2$$

$$\begin{pmatrix} \chi_1 \\ \chi_2 \\ \chi_3 \end{pmatrix} := \text{Minerr}(\chi_1, \chi_2, \chi_3) \quad \begin{pmatrix} \chi_1 \\ \chi_2 \\ \chi_3 \end{pmatrix} = \begin{pmatrix} 0.237 \\ 0.756 \\ 1.014 \end{pmatrix}$$

1.4) DEK/PEGDME

$$V_{\text{mol}1} := \frac{1}{\rho_{4,\text{DEK}}} \cdot \text{MW}_{\text{DEK}} \quad V_{\text{mol}2} := \frac{1}{\rho_{4,\text{PEGDME}}} \cdot \text{MW}_{\text{PEGDME}} \quad V_{\text{mol}3} := \frac{1}{\rho_{4,\text{PDMS}}} \cdot \text{MW}_{\text{PDMS}} \quad \text{RU}3 := 100000$$

$$\text{MW_Flory} := \begin{pmatrix} \text{MW}_{\text{DEK}} \\ \text{MW}_{\text{PEGDME}} \\ \text{MW}_{\text{PDMS}} \end{pmatrix}$$

$$\chi_{25} := \begin{pmatrix} 0.449 \\ 0.723 \\ 0.487 \end{pmatrix} \quad \begin{matrix} \text{DPEGDME} := 1 \\ \text{DPol} := 2 \\ \text{PEGDME_Pol} := 3 \end{matrix} \quad \chi_{25} := \chi_{25} - 0.35$$

$$a1_25 := \begin{pmatrix} 0.986 \\ 0.971 \\ 0.954 \end{pmatrix}$$

$$a2_25 := \begin{pmatrix} 0.0152 \\ 0.0313 \\ 0.0482 \end{pmatrix} \quad \chi_{25} = \begin{pmatrix} 0.099 \\ 0.373 \\ 0.137 \end{pmatrix}$$

T=25°C, 5wt%

$$\text{conc} := 1 \quad a1 := a1_25 \quad a2 := a2_25$$

$$\chi := \begin{pmatrix} 0.2 \\ 0.661 \\ 0.133 \end{pmatrix}$$

$$\phi1 := 0.665 \quad \phi3 := 0.307 \quad \phi2 := 1 - \phi1 - \phi3$$

Given

$$a1_{\text{conc}} = e^{\ln(\phi1) + (1-\phi1) \left(\frac{V_{\text{mol}1}}{V_{\text{mol}2}} \right) \phi2 - \left(\frac{V_{\text{mol}1}}{V_{\text{mol}3} \cdot \text{RU}3} \right) \phi3 + \left(\chi_1 \phi2 + \chi_2 \phi3 \right) (\phi2 + \phi3) - \chi_3 \left(\frac{V_{\text{mol}1}}{V_{\text{mol}2}} \right) \phi2 \phi3}$$

$$a2_{\text{conc}} = e^{\ln(\phi2) + (1-\phi2) \left(\frac{V_{\text{mol}2}}{V_{\text{mol}1}} \right) \phi1 - \left(\frac{V_{\text{mol}2}}{V_{\text{mol}3} \cdot \text{RU}3} \right) \phi3 + \left(\chi_1 \phi1 \frac{V_{\text{mol}2}}{V_{\text{mol}1} + \chi_3 \phi3} \right) (\phi1 + \phi3) - \chi_2 \left(\frac{V_{\text{mol}2}}{V_{\text{mol}1}} \right) \phi1 \phi3}$$

$$\phi3 = 1 - \phi1 - \phi2$$

$$\begin{pmatrix} X_1 \\ X_2 \\ X_3 \end{pmatrix} := \text{Minert}(X_1, X_2, X_3) \qquad \begin{pmatrix} X_1 \\ X_2 \\ X_3 \end{pmatrix} = \begin{pmatrix} 0.309 \\ 0.649 \\ 0.141 \end{pmatrix}$$

T=25°C, 10wt%

a1 := a1_25 a2 := a2_25 $\phi_1 := 0.596$ $\phi_3 := 0.352$ $\phi_2 := 1 - \phi_1 - \phi_3$
 conc := 2

Given
 $a_{2\text{conc}} = e^{\ln(\phi_2) + (1-\phi_2) \left(\frac{V_{\text{mol}2}}{V_{\text{mol}1}} \right) \phi_1 - \left(\frac{V_{\text{mol}2}}{V_{\text{mol}3} \cdot \text{RU}3} \right) \phi_3 + \left(X_1 \phi_1 \frac{V_{\text{mol}2}}{V_{\text{mol}1}} + X_3 \phi_3 \right) (\phi_1 + \phi_3) - X_2 \left(\frac{V_{\text{mol}2}}{V_{\text{mol}1}} \right) \phi_1 \phi_3}$

$$a_{1\text{conc}} = e^{\ln(\phi_1) + (1-\phi_1) \left(\frac{V_{\text{mol}1}}{V_{\text{mol}2}} \right) \phi_2 - \left(\frac{V_{\text{mol}1}}{V_{\text{mol}3} \cdot \text{RU}3} \right) \phi_3 + \left(X_1 \phi_1 \phi_2 + X_2 \phi_3 \right) (\phi_2 + \phi_3) - X_3 \left(\frac{V_{\text{mol}1}}{V_{\text{mol}2}} \right) \phi_2 \phi_3}$$

$\phi_3 = 1 - \phi_1 - \phi_2$

$$\begin{pmatrix} X_1 \\ X_2 \\ X_3 \end{pmatrix} := \text{Minert}(X_1, X_2, X_3) \qquad \begin{pmatrix} X_1 \\ X_2 \\ X_3 \end{pmatrix} = \begin{pmatrix} 0.33 \\ 0.684 \\ 0.141 \end{pmatrix}$$

T=25°C, 15wt%

conc := 3 a1 := a1_25 a2 := a2_25 $\phi_1 := 0.524$ $\phi_3 := 0.403$ $\phi_2 := 1 - \phi_1 - \phi_3$

Given
 $a_{2\text{conc}} = e^{\ln(\phi_2) + (1-\phi_2) \left(\frac{V_{\text{mol}2}}{V_{\text{mol}1}} \right) \phi_1 - \left(\frac{V_{\text{mol}2}}{V_{\text{mol}3} \cdot \text{RU}3} \right) \phi_3 + \left(X_1 \phi_1 \frac{V_{\text{mol}2}}{V_{\text{mol}1}} + X_3 \phi_3 \right) (\phi_1 + \phi_3) - X_2 \left(\frac{V_{\text{mol}2}}{V_{\text{mol}1}} \right) \phi_1 \phi_3}$

$$a_{1\text{conc}} = e^{\ln(\phi_1) + (1-\phi_1) \left(\frac{V_{\text{mol}1}}{V_{\text{mol}2}} \right) \phi_2 - \left(\frac{V_{\text{mol}1}}{V_{\text{mol}3} \cdot \text{RU}3} \right) \phi_3 + \left(X_1 \phi_1 \phi_2 + X_2 \phi_3 \right) (\phi_2 + \phi_3) - X_3 \left(\frac{V_{\text{mol}1}}{V_{\text{mol}2}} \right) \phi_2 \phi_3}$$

$\phi_3 = 1 - \phi_1 - \phi_2$

$$\begin{pmatrix} X_1 \\ X_2 \\ X_3 \end{pmatrix} := \text{Minert}(X_1, X_2, X_3) \qquad \begin{pmatrix} X_1 \\ X_2 \\ X_3 \end{pmatrix} = \begin{pmatrix} 0.339 \\ 0.729 \\ 0.14 \end{pmatrix}$$

2.X Specific Volumes and Critical hole free volume required for jump

$$V_{P_{i,j}} := \frac{1}{\rho_{i,j}}$$

$$V_{\text{ch}k} := \frac{V_{\text{at}0Kk}}{\text{MW}_k}$$

3) Calculation of the Self-Diffusion coefficient for each component with the use of Dullien's equation

$$D_{\text{pure}i,j} := \frac{1.124 \cdot 10^{-17} \cdot \text{mol}^2 \cdot (V_{Cj})^2 \cdot R \cdot T_i}{\eta_{i,j} \cdot \text{MW}_j \cdot V_{P_{i,j}}}$$

	1	2	3	4	5	6
1	0	2.655·10 ⁻⁹	2.332·10 ⁻⁹	1.906·10 ⁻¹⁰	8.534·10 ⁻¹¹	1.049·10 ⁻¹¹
2	0	2.843·10 ⁻⁹	2.499·10 ⁻⁹	2.206·10 ⁻¹⁰	1.001·10 ⁻¹⁰	1.38·10 ⁻¹¹
3	0	3.041·10 ⁻⁹	2.673·10 ⁻⁹	2.6·10 ⁻¹⁰	1.201·10 ⁻¹⁰	1.818·10 ⁻¹¹
4	0	3.244·10 ⁻⁹	2.853·10 ⁻⁹	2.947·10 ⁻¹⁰	1.39·10 ⁻¹⁰	2.361·10 ⁻¹¹
5	0	3.459·10 ⁻⁹	3.04·10 ⁻⁹	3.386·10 ⁻¹⁰	1.64·10 ⁻¹⁰	3.039·10 ⁻¹¹
6	0	3.677·10 ⁻⁹	3.233·10 ⁻⁹	3.782·10 ⁻¹⁰	1.868·10 ⁻¹⁰	3.881·10 ⁻¹¹
7	0	3.907·10 ⁻⁹	3.434·10 ⁻⁹	4.264·10 ⁻¹⁰	2.155·10 ⁻¹⁰	4.922·10 ⁻¹¹
8	0	4.14·10 ⁻⁹	3.64·10 ⁻⁹	4.698·10 ⁻¹⁰	2.424·10 ⁻¹⁰	6.192·10 ⁻¹¹
9	0	4.386·10 ⁻⁹	3.853·10 ⁻⁹	5.209·10 ⁻¹⁰	2.754·10 ⁻¹⁰	7.735·10 ⁻¹¹
10	0	4.635·10 ⁻⁹	4.072·10 ⁻⁹	5.718·10 ⁻¹⁰	3.06·10 ⁻¹⁰	9.601·10 ⁻¹¹
11	0	4.891·10 ⁻⁹	4.298·10 ⁻⁹	6.313·10 ⁻¹⁰	3.428·10 ⁻¹⁰	1.184·10 ⁻¹⁰
12	0	5.153·10 ⁻⁹	4.528·10 ⁻⁹	6.873·10 ⁻¹⁰	3.796·10 ⁻¹⁰	1.451·10 ⁻¹⁰
13	0	5.423·10 ⁻⁹	4.766·10 ⁻⁹	7.516·10 ⁻¹⁰	4.238·10 ⁻¹⁰	1.768·10 ⁻¹⁰
14	0	5.701·10 ⁻⁹	5.009·10 ⁻⁹	8.132·10 ⁻¹⁰	4.584·10 ⁻¹⁰	2.141·10 ⁻¹⁰
15	0	5.985·10 ⁻⁹	5.257·10 ⁻⁹	8.829·10 ⁻¹⁰	4.975·10 ⁻¹⁰	2.583·10 ⁻¹⁰

D_{pure} =

$\frac{\text{m}^2}{\text{s}}$

$$V_{\text{ch}} = \begin{pmatrix} 9.05 \times 10^{-4} \\ 8.862 \times 10^{-4} \\ 9.102 \times 10^{-4} \\ 8.453 \times 10^{-4} \\ 8.317 \times 10^{-4} \\ 7.949 \times 10^{-4} \end{pmatrix} \frac{\text{m}^3}{\text{kg}}$$

$$V_{\text{at}0K} = \begin{pmatrix} 0 \\ 6.39 \times 10^{-5} \\ 7.84 \times 10^{-5} \\ 1.879 \times 10^{-4} \\ 2.48 \times 10^{-4} \\ 1.544 \times 10^{-4} \end{pmatrix} \frac{\text{m}^3}{\text{mol}}$$

$$V_{\text{chPDMS}} \cdot \text{MW}_{\text{PDMS}} = 6.706 \times 10^{-5} \frac{\text{m}^3}{\text{mol}}$$

Appendix 4

TempIndex := 4

$$D_{\text{pureTempIndex, MEK}} = 3.244 \times 10^{-9} \frac{\text{m}^2}{\text{s}}$$

$$D_{\text{pureTempIndex, DEK}} = 2.853 \times 10^{-9} \frac{\text{m}^2}{\text{s}}$$

$$D_{\text{pureTempIndex, TEGDME}} = 2.947 \times 10^{-10} \frac{\text{m}^2}{\text{s}}$$

$$D_{\text{pureTempIndex, PEGDME}} = 1.39 \times 10^{-10} \frac{\text{m}^2}{\text{s}}$$

4) Calculation of Diffusion preexponential factor D_0 and E



Deleting the units because the solver can not manage units.
Every input is in S.I. system and every output should be in S.I

$$T := \frac{T}{\text{K}}$$

$$R := \frac{R}{\frac{\text{kg m}^2}{\text{s}^2 \text{K mol}}}$$

$$MW := \frac{MW}{\frac{\text{kg}}{\text{mol}}}$$

$$\eta := \frac{\eta}{\frac{\text{kg}}{\text{m s}}}$$

$$\rho := \frac{\rho}{\frac{\text{kg}}{\text{m}^3}}$$

$$V_c := \frac{V_c}{\frac{\text{m}^3}{\text{mol}}}$$



$$\text{Const} := 1.124 \cdot 10^{-17}$$

$$F(z, t) := \begin{bmatrix} \left(t_1 \cdot e^{-\frac{t_2}{t_3+z}} \right)^{-1} \cdot \left[\frac{\text{Const} \cdot (V_{c\text{MEK}})^{\frac{2}{3}} \cdot R \cdot z}{MW_{\text{MEK}}} \right] \\ \frac{-1}{(t_1)^2} \cdot \exp\left(\frac{t_2}{t_3+z}\right) \cdot \text{Const} \cdot (V_{c\text{MEK}})^{\frac{2}{3}} \cdot R \cdot \frac{z}{MW_{\text{MEK}}} \\ \frac{1}{t_1} \cdot \exp\left(\frac{t_2}{t_3+z}\right) \cdot \text{Const} \cdot (V_{c\text{MEK}})^{\frac{2}{3}} \cdot R \cdot \frac{z}{MW_{\text{MEK}} \cdot (t_3+z)} \\ \frac{-1}{t_1} \cdot \exp\left(\frac{t_2}{t_3+z}\right) \cdot \text{Const} \cdot (V_{c\text{MEK}})^{\frac{2}{3}} \cdot R \cdot \frac{z}{MW_{\text{MEK}}} \cdot \frac{t_2}{(t_3+z)^2} \end{bmatrix}$$

$$v_{y_i} := \left(\eta^{(\text{MEK})} \right)_i \cdot \frac{1}{\left(\rho^{(\text{MEK})} \right)_i}$$

$$v_g := \begin{pmatrix} 16 \cdot 10^{-7} \\ 1000 \\ -200 \end{pmatrix}$$

Solution := genfit(T, vy, vg, F)

$$\begin{pmatrix} D_{0\text{MEK}} \\ \gamma_{\text{VKMEK}} \\ K_{\text{TMEK}} \end{pmatrix} := \begin{pmatrix} \text{Solution}_1 \\ \text{Solution}_2 \\ \text{Solution}_3 \end{pmatrix}$$

$$D_{0\text{MEK}} = 3.097 \times 10^{-7}$$

$$\gamma_{\text{VKMEK}} = 1.616 \times 10^3$$

$$K_{\text{TMEK}} = 56.325$$

5.2 DEK

$$G(z, t) := \begin{bmatrix} \left(\frac{1}{t_1} \cdot e^{-\frac{t_2}{t_3+z}} \right)^{-1} \cdot \left[\frac{\text{Const} \cdot (V_{c\text{DEK}})^{\frac{2}{3}} \cdot R \cdot z}{\text{MW}_{\text{DEK}}} \right] \\ \frac{-1}{(t_1)^2} \cdot \exp\left(\frac{t_2}{t_3+z}\right) \cdot \text{Const} \cdot (V_{c\text{DEK}})^{\frac{2}{3}} \cdot R \cdot \frac{z}{\text{MW}_{\text{DEK}}} \\ \frac{1}{t_1} \cdot \exp\left(\frac{t_2}{t_3+z}\right) \cdot \text{Const} \cdot (V_{c\text{DEK}})^{\frac{2}{3}} \cdot R \cdot \frac{z}{\text{MW}_{\text{DEK}} \cdot (t_3+z)} \\ \frac{-1}{t_1} \cdot \exp\left(\frac{t_2}{t_3+z}\right) \cdot \text{Const} \cdot (V_{c\text{DEK}})^{\frac{2}{3}} \cdot R \cdot \frac{z}{\text{MW}_{\text{DEK}}} \cdot \frac{t_2}{(t_3+z)^2} \end{bmatrix}$$

$$vy_i := \left(\eta^{(\text{DEK})} \right)_i \cdot \frac{1}{(\rho^{(\text{DEK})})_i} \quad vg := \begin{pmatrix} 16 \cdot 10^{-7} \\ 1000 \\ -200 \end{pmatrix} \quad \text{Solution} := \text{genfit}(T, vy, vg, G)$$

$$\begin{pmatrix} D^0_{\text{DEK}} \\ \gamma V K_{\text{DEK}} \\ K T_{\text{DEK}} \end{pmatrix} := \begin{pmatrix} \text{Solution}_1 \\ \text{Solution}_2 \\ \text{Solution}_3 \end{pmatrix} \quad \boxed{D^0_{\text{DEK}} = 2.498 \times 10^{-7}} \quad \boxed{\gamma V K_{\text{DEK}} = 1.554 \times 10^3} \quad \boxed{K T_{\text{DEK}} = 49.247}$$

5.4 TEGDME

$$H(z, t) := \begin{bmatrix} \left(\frac{1}{t_1} \cdot e^{-\frac{t_2}{t_3+z}} \right)^{-1} \cdot \left[\frac{\text{Const} \cdot (V_{c\text{TEGDME}})^{\frac{2}{3}} \cdot R \cdot z}{\text{MW}_{\text{TEGDME}}} \right] \\ \frac{-1}{(t_1)^2} \cdot \exp\left(\frac{t_2}{t_3+z}\right) \cdot \text{Const} \cdot (V_{c\text{TEGDME}})^{\frac{2}{3}} \cdot R \cdot \frac{z}{\text{MW}_{\text{TEGDME}}} \\ \frac{1}{t_1} \cdot \exp\left(\frac{t_2}{t_3+z}\right) \cdot \text{Const} \cdot (V_{c\text{TEGDME}})^{\frac{2}{3}} \cdot R \cdot \frac{z}{\text{MW}_{\text{TEGDME}} \cdot (t_3+z)} \\ \frac{-1}{t_1} \cdot \exp\left(\frac{t_2}{t_3+z}\right) \cdot \text{Const} \cdot (V_{c\text{TEGDME}})^{\frac{2}{3}} \cdot R \cdot \frac{z}{\text{MW}_{\text{TEGDME}}} \cdot \frac{t_2}{(t_3+z)^2} \end{bmatrix}$$

$$vy_i := \left(\eta^{(\text{TEGDME})} \right)_i \cdot \frac{1}{(\rho^{(\text{TEGDME})})_i} \quad vg := \begin{pmatrix} 0.01 \cdot 10^{-7} \\ 1000 \\ 20 \end{pmatrix} \quad \text{Solution} := \text{genfit}(T, vy, vg, H)$$

$$\begin{pmatrix} D^0_{\text{TEGDME}} \\ \gamma V K_{\text{TEGDME}} \\ K T_{\text{TEGDME}} \end{pmatrix} := \begin{pmatrix} \text{Solution}_1 \\ \text{Solution}_2 \\ \text{Solution}_3 \end{pmatrix} \quad \boxed{D^0_{\text{TEGDME}} = 2.009 \times 10^{-8}} \quad \boxed{\gamma V K_{\text{TEGDME}} = 671.324} \quad \boxed{K T_{\text{TEGDME}} = -139.069}$$

5.5 PEGDME

$$I(z, t) := \begin{bmatrix} \left(t_1 \cdot e^{-\frac{t_2}{t_3+z}} \right)^{-1} \cdot \left[\frac{\text{Const} \cdot (V_{c\text{PEGDME}})^{\frac{2}{3}} \cdot R \cdot z}{\text{MW}_{\text{PEGDME}}} \right] \\ \frac{-1}{(t_1)^2} \cdot \exp\left(\frac{t_2}{t_3+z}\right) \cdot \text{Const} \cdot (V_{c\text{PEGDME}})^{\frac{2}{3}} \cdot R \cdot \frac{z}{\text{MW}_{\text{PEGDME}}} \\ \frac{1}{t_1} \cdot \exp\left(\frac{t_2}{t_3+z}\right) \cdot \text{Const} \cdot (V_{c\text{PEGDME}})^{\frac{2}{3}} \cdot R \cdot \frac{z}{\text{MW}_{\text{PEGDME}} \cdot (t_3+z)} \\ \frac{-1}{t_1} \cdot \exp\left(\frac{t_2}{t_3+z}\right) \cdot \text{Const} \cdot (V_{c\text{PEGDME}})^{\frac{2}{3}} \cdot R \cdot \frac{z}{\text{MW}_{\text{PEGDME}}} \cdot \frac{t_2}{(t_3+z)^2} \end{bmatrix}$$

$$vy_i := \left(\eta^{(\text{PEGDME})} \right)_i \cdot \frac{1}{\left(\rho^{(\text{PEGDME})} \right)_i} \quad vg := \begin{pmatrix} 0.1 \cdot 10^{-7} \\ 100 \\ -10 \end{pmatrix} \quad \text{Solution} := \text{genfit}(T, vy, vg, I)$$

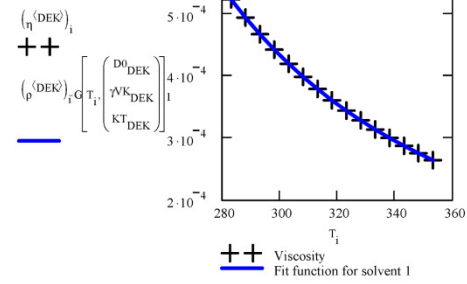
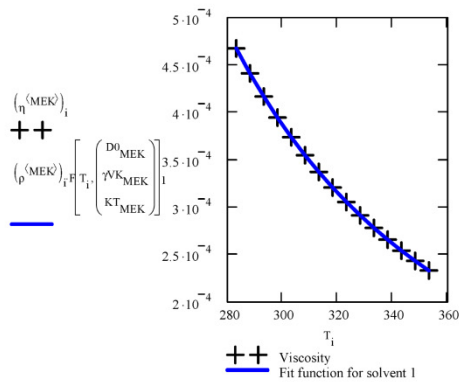
$$\begin{pmatrix} D0_{\text{PEGDME}} \\ \gamma VK_{\text{PEGDME}} \\ KT_{\text{PEGDME}} \end{pmatrix} := \begin{pmatrix} \text{Solution}_1 \\ \text{Solution}_2 \\ \text{Solution}_3 \end{pmatrix} \quad \boxed{D0_{\text{PEGDME}} = 3.199 \times 10^{-8}} \quad \boxed{\gamma VK_{\text{PEGDME}} = 964.607} \quad \boxed{KT_{\text{PEGDME}} = -120.545}$$

5.6 TEG

$$J(z, t) := \begin{bmatrix} \left(t_1 \cdot e^{-\frac{t_2}{t_3+z}} \right)^{-1} \cdot \left[\frac{\text{Const} \cdot (V_{c\text{TEG}})^{\frac{2}{3}} \cdot R \cdot z}{\text{MW}_{\text{TEG}}} \right] \\ \frac{-1}{(t_1)^2} \cdot \exp\left(\frac{t_2}{t_3+z}\right) \cdot \text{Const} \cdot (V_{c\text{TEG}})^{\frac{2}{3}} \cdot R \cdot \frac{z}{\text{MW}_{\text{TEG}}} \\ \frac{1}{t_1} \cdot \exp\left(\frac{t_2}{t_3+z}\right) \cdot \text{Const} \cdot (V_{c\text{TEG}})^{\frac{2}{3}} \cdot R \cdot \frac{z}{\text{MW}_{\text{TEG}} \cdot (t_3+z)} \\ \frac{-1}{t_1} \cdot \exp\left(\frac{t_2}{t_3+z}\right) \cdot \text{Const} \cdot (V_{c\text{TEG}})^{\frac{2}{3}} \cdot R \cdot \frac{z}{\text{MW}_{\text{TEG}}} \cdot \frac{t_2}{(t_3+z)^2} \end{bmatrix}$$

$$vy_i := \left(\eta^{(\text{TEG})} \right)_i \cdot \frac{1}{\left(\rho^{(\text{TEG})} \right)_i} \quad vg := \begin{pmatrix} 0.1 \cdot 10^{-8} \\ 2000 \\ 1000 \end{pmatrix} \quad \text{Solution} := \text{genfit}(T, vy, vg, J)$$

$$\begin{pmatrix} D0_{\text{TEG}} \\ \gamma VK_{\text{TEG}} \\ KT_{\text{TEG}} \end{pmatrix} := \begin{pmatrix} \text{Solution}_1 \\ \text{Solution}_2 \\ \text{Solution}_3 \end{pmatrix} \quad \boxed{D0_{\text{TEG}} = 1.73085 \times 10^{-4}} \quad \boxed{\gamma VK_{\text{TEG}} = 4.862 \times 10^3} \quad \boxed{KT_{\text{TEG}} = 9.402}$$



$Aa := 5 \cdot 10^{-6}$
 $Bb := 2400$
 $Cc := -100$

$8.82 \cdot 10^{-4} \cdot \frac{cm^2}{s} = 8.82 \times 10^{-8} \frac{m^2}{s}$

Given

$\left(\eta^{(TEG)}\right)_2 = \left(\rho^{(TEG)}\right)_2 \cdot \left[\left(Aa \cdot e^{-\frac{Bb}{Cc+T_2}} \right)^{-1} \cdot \frac{Const \cdot (V_{cTEG})^{\frac{2}{3}} \cdot R \cdot T_2}{MW_{TEG}} \right]$

$\left(\eta^{(TEG)}\right)_8 = \left(\rho^{(TEG)}\right)_8 \cdot \left[\left(Aa \cdot e^{-\frac{Bb}{Cc+T_8}} \right)^{-1} \cdot \frac{Const \cdot (V_{cTEG})^{\frac{2}{3}} \cdot R \cdot T_8}{MW_{TEG}} \right]$

$\left(\begin{array}{c} Aa \\ Bb \\ Cc \end{array} \right) := \text{Minerr}(Aa, Bb, Cc)$

$Aa = 1.656 \times 10^{-6}$

$Bb = 2.382 \times 10^3$

$Cc = -84.43$

$\frac{V_{chTEG}}{Bb} = 3.337 \times 10^{-7} \frac{m^3}{kg}$

$Aa1 := 9 \cdot 10^{-8}$
 $Bb1 := 964.607$
 $Cc1 := -200$

$D_0^{PEGDME} = 3.199 \times 10^{-8}$

$KT_{PEGDME} = -120.545$

$\gamma^{VK_{PEGDME}} = 964.607$

Given

$\left(\eta^{(PEGDME)}\right)_2 = \left(\rho^{(PEGDME)}\right)_2 \cdot \left[\left(Aa1 \cdot e^{-\frac{Bb1}{Cc1+T_2}} \right)^{-1} \cdot \frac{Const \cdot (V_{cPEGDME})^{\frac{2}{3}} \cdot R \cdot T_2}{MW_{PEGDME}} \right]$

$\left(\eta^{(PEGDME)}\right)_8 = \left(\rho^{(PEGDME)}\right)_8 \cdot \left[\left(Aa1 \cdot e^{-\frac{Bb1}{Cc1+T_8}} \right)^{-1} \cdot \frac{Const \cdot (V_{cPEGDME})^{\frac{2}{3}} \cdot R \cdot T_8}{MW_{PEGDME}} \right]$

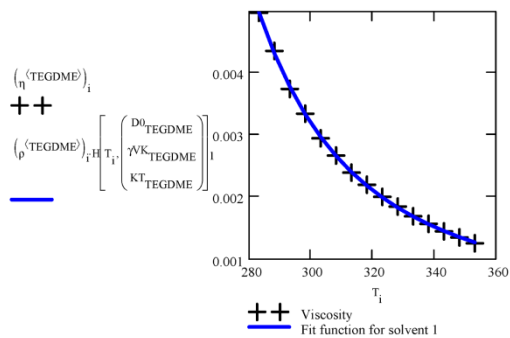
$\left(\begin{array}{c} Aa1 \\ Bb1 \\ Cc1 \end{array} \right) := \text{Minerr}(Aa1, Bb1, Cc1)$

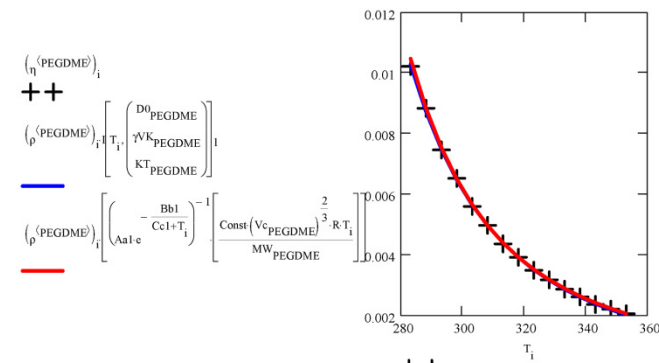
$Aa1 = 1.84 \times 10^{-8}$

$Bb1 = 765.655$

$Cc1 = -141.303$

$\frac{V_{chPEGDME}}{Bb1} = 1.086 \times 10^{-6} \frac{m^3}{kg}$



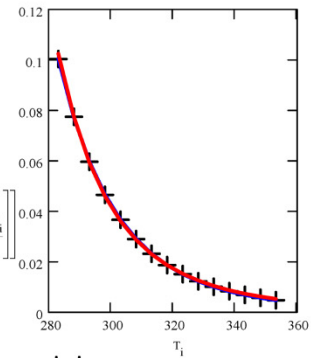


$$\left(\rho^{(TEG)} \right)_i \cdot \left[\frac{D0_{TEG}}{\gamma^{VK}_{TEG} \cdot KT_{TEG}} \right] \cdot \left[\frac{Const \cdot (Vc_{TEG})^{\frac{2}{3}} \cdot R \cdot T_i}{MW_{TEG}} \right]^{-1} \cdot \left[\frac{Bb}{Aa \cdot e^{-Cc/T_i}} \right]^{-1} =$$

0.102
0.078
0.059
0.046
0.036
0.029
0.023
0.019
0.015
0.013
0.01
8.779 · 10 ⁻³
7.403 · 10 ⁻³
6.284 · 10 ⁻³
5.373 · 10 ⁻³

++ Viscosity
 — Fit function for solvent 1
 — Fit function

$$\left(\eta^{(TEG)} \right)_i = \left[\frac{D0_{TEG}}{\gamma^{VK}_{TEG} \cdot KT_{TEG}} \right] \cdot \left[\frac{Const \cdot (Vc_{TEG})^{\frac{2}{3}} \cdot R \cdot T_i}{MW_{TEG}} \right]^{-1} \cdot \left[\frac{Bb}{Aa \cdot e^{-Cc/T_i}} \right]^{-1}$$



++ Viscosity
 — Fit function for solvent 1
 — Fit function

	1
1	4.676 · 10 ⁻⁴
2	4.412 · 10 ⁻⁴
3	4.17 · 10 ⁻⁴
4	3.946 · 10 ⁻⁴
5	3.74 · 10 ⁻⁴
6	3.549 · 10 ⁻⁴
7	3.373 · 10 ⁻⁴
8	3.209 · 10 ⁻⁴
9	3.056 · 10 ⁻⁴
10	2.914 · 10 ⁻⁴
11	2.782 · 10 ⁻⁴
12	2.659 · 10 ⁻⁴
13	2.543 · 10 ⁻⁴
14	2.435 · 10 ⁻⁴
15	2.334 · 10 ⁻⁴

$$\left(\rho^{(MEK)} \right)_i \cdot F \left[\frac{D0_{MEK}}{\gamma^{VK}_{MEK} \cdot KT_{MEK}} \right] =$$

4.678 · 10 ⁻⁴
4.411 · 10 ⁻⁴
4.17 · 10 ⁻⁴
3.944 · 10 ⁻⁴
3.74 · 10 ⁻⁴
3.547 · 10 ⁻⁴
3.373 · 10 ⁻⁴
3.208 · 10 ⁻⁴
3.059 · 10 ⁻⁴
2.916 · 10 ⁻⁴
2.783 · 10 ⁻⁴
2.659 · 10 ⁻⁴
2.543 · 10 ⁻⁴
2.434 · 10 ⁻⁴
2.333 · 10 ⁻⁴

	1
1	5.247 · 10 ⁻⁴
2	4.953 · 10 ⁻⁴
3	4.683 · 10 ⁻⁴
4	4.435 · 10 ⁻⁴
5	4.206 · 10 ⁻⁴
6	3.995 · 10 ⁻⁴
7	3.799 · 10 ⁻⁴
8	3.617 · 10 ⁻⁴
9	3.449 · 10 ⁻⁴
10	3.292 · 10 ⁻⁴
11	3.145 · 10 ⁻⁴
12	3.009 · 10 ⁻⁴
13	2.881 · 10 ⁻⁴
14	2.762 · 10 ⁻⁴
15	2.65 · 10 ⁻⁴

$$\left(\rho^{(DEK)} \right)_i \cdot G \left[\frac{D0_{DEK}}{\gamma^{VK}_{DEK} \cdot KT_{DEK}} \right] =$$

5.247 · 10 ⁻⁴
4.953 · 10 ⁻⁴
4.683 · 10 ⁻⁴
4.435 · 10 ⁻⁴
4.206 · 10 ⁻⁴
3.994 · 10 ⁻⁴
3.799 · 10 ⁻⁴
3.617 · 10 ⁻⁴
3.449 · 10 ⁻⁴
3.292 · 10 ⁻⁴
3.146 · 10 ⁻⁴
3.009 · 10 ⁻⁴
2.881 · 10 ⁻⁴
2.762 · 10 ⁻⁴
2.649 · 10 ⁻⁴

	1
1	4.979 · 10 ⁻³
2	4.361 · 10 ⁻³
3	3.749 · 10 ⁻³
4	3.348 · 10 ⁻³
5	2.951 · 10 ⁻³
6	2.673 · 10 ⁻³
7	2.398 · 10 ⁻³
8	2.201 · 10 ⁻³
9	2.007 · 10 ⁻³
10	1.848 · 10 ⁻³
11	1.691 · 10 ⁻³
12	1.569 · 10 ⁻³
13	1.449 · 10 ⁻³
14	1.352 · 10 ⁻³
15	1.257 · 10 ⁻³

$$\left(\rho^{(TEGDME)} \right)_i \cdot H \left[\frac{D0_{TEGDME}}{\gamma^{VK}_{TEGDME} \cdot KT_{TEGDME}} \right] =$$

4.986 · 10 ⁻³
4.323 · 10 ⁻³
3.785 · 10 ⁻³
3.341 · 10 ⁻³
2.975 · 10 ⁻³
2.667 · 10 ⁻³
2.407 · 10 ⁻³
2.186 · 10 ⁻³
1.996 · 10 ⁻³
1.832 · 10 ⁻³
1.689 · 10 ⁻³
1.564 · 10 ⁻³
1.454 · 10 ⁻³
1.357 · 10 ⁻³
1.271 · 10 ⁻³

	1
1	0.01
2	8.843 · 10 ⁻³
3	7.471 · 10 ⁻³
4	6.532 · 10 ⁻³
5	5.601 · 10 ⁻³
6	4.98 · 10 ⁻³
7	4.365 · 10 ⁻³
8	3.927 · 10 ⁻³
9	3.493 · 10 ⁻³
10	3.18 · 10 ⁻³
11	2.869 · 10 ⁻³
12	2.618 · 10 ⁻³
13	2.369 · 10 ⁻³
14	2.212 · 10 ⁻³
15	2.058 · 10 ⁻³

$$\left(\rho^{(PEGDME)} \right)_i \cdot I \left[\frac{D0_{PEGDME}}{\gamma^{VK}_{PEGDME} \cdot KT_{PEGDME}} \right] =$$

0.01
8.74 · 10 ⁻³
7.497 · 10 ⁻³
6.483 · 10 ⁻³
5.654 · 10 ⁻³
4.973 · 10 ⁻³
4.4 · 10 ⁻³
3.923 · 10 ⁻³
3.515 · 10 ⁻³
3.17 · 10 ⁻³
2.872 · 10 ⁻³
2.615 · 10 ⁻³
2.392 · 10 ⁻³
2.196 · 10 ⁻³
2.025 · 10 ⁻³

	1			
$\eta^{(TEG)} =$	1	0.1	$\left(\rho^{(PEGDME)}\right)_i \cdot \left[\left(\frac{Bb1}{Aa1 \cdot e^{-Cc1+T_i}} \right)^{-1} \cdot \left[\frac{\text{Const} \cdot \left(Vc_{PEGDME} \right)^2}{MW_{PEGDME}} \cdot R \cdot T_i \right] \right] =$	$\left(\rho^{(TEG)}\right)_i \cdot \left[\left(\frac{D0_{TEG}}{\gamma VK_{TEG}} \right) \cdot T_i \right] =$
	2	0.078		
	3	0.06		
	4	0.047		
	5	0.037		
	6	0.029		
	7	0.023		
	8	0.019		
	9	0.015		
	10	0.012		
	11	0.01		
	12	$8.368 \cdot 10^{-3}$		
	13	$6.944 \cdot 10^{-3}$		
	14	$5.794 \cdot 10^{-3}$		
	15	$4.859 \cdot 10^{-3}$		



Giving back the units

$$cP := 0.001 \cdot \text{Pa} \cdot \text{s}$$

$$T := T \cdot (\text{K}) \quad R := R \cdot \left(\frac{\text{kg m}^2}{\text{s}^2 \text{K mol}} \right) \quad \eta_{\text{psinunid}} := \eta \cdot 1000 \quad \eta_{\text{cp}} := \eta_{\text{psinunid}} \cdot cP \quad MW := MW \cdot \left(\frac{\text{kg}}{\text{mol}} \right) \quad \eta := \eta \cdot \left(\frac{\text{kg}}{\text{m s}} \right) \quad \rho := \rho \cdot \left(\frac{\text{kg}}{\text{m}^3} \right)$$

$$\gamma VK := \gamma VK \cdot (\text{K}) \quad KT := KT \cdot (\text{K}) \quad Vc := Vc \cdot \left(\frac{\text{m}^3}{\text{mol}} \right) \quad D0 := D0 \cdot \frac{\text{m}^2}{\text{s}}$$



$$D0 = \begin{pmatrix} 0 \\ 3.097 \times 10^{-7} \\ 2.498 \times 10^{-7} \\ 2.009 \times 10^{-8} \\ 3.199 \times 10^{-8} \\ 1.731 \times 10^{-4} \end{pmatrix} \frac{\text{m}^2}{\text{s}}$$

$$\gamma VK = \begin{pmatrix} 0 \\ 1.616 \times 10^3 \\ 1.554 \times 10^3 \\ 671.324 \\ 964.607 \\ 4.862 \times 10^3 \end{pmatrix} \text{K}$$

$$KT = \begin{pmatrix} 0 \\ 56.325 \\ 49.247 \\ -139.069 \\ -120.545 \\ 9.402 \end{pmatrix} \text{K}$$

6) Calculation of the ratio of the critical molar volume of a jumping unit of component i to the critical molar volume of the jumping unit of the polymer

$$T_{g3} := 136.25 \cdot \text{K}$$

$$273.15 - 136.9 = 136.25$$

$$V_{pju} := \left(0.0925 \cdot \frac{T_{g3}}{\text{K}} + 69.47 \right) \cdot \frac{\text{cm}^3}{\text{mol}}$$

$$V_{pju} = 8.207 \times 10^{-5} \frac{\text{m}^3}{\text{mol}}$$

$$\xi_k := \frac{V_{at0K_k}}{V_{pju}}$$

$$\xi_k =$$

0.779
0.955
2.289
3.022
1.881

$$\frac{66.94 \cdot \frac{\text{cm}^3}{\text{mol}}}{V_{pju}} = 0.816$$

$$\frac{81.08 \cdot \frac{\text{cm}^3}{\text{mol}}}{V_{pju}} = 0.988$$

Appendix 4

7) Calculation of f/γ

7.1 For the polymer

$$KT_1 := -81 \cdot K \quad \implies \quad K_{11} - T_{g1}$$

$$\gamma K_1 := 9.32 \cdot 10^{-4} \cdot \frac{\text{cm}^3}{\text{gm} \cdot \text{K}} \quad \implies \quad \frac{K13}{\gamma}$$

$$f_{i,PDMS} := \frac{\gamma K_{PDMS} \cdot (KT_{PDMS} + T_i)}{V_{P_i,PDMS}}$$

$$\gamma K_{1k} := \frac{V_{ch_k}}{\gamma V K_k}$$

	1	2	3	4	5	6
1	0	0.468	0.525	4.979	10.23	100.4
2	0	0.441	0.495	4.361	8.843	77.5
3	0	0.417	0.468	3.749	7.471	59.65
4	0	0.395	0.444	3.348	6.532	46.57
5	0	0.374	0.421	2.951	5.601	36.66
6	0	0.355	0.4	2.673	4.98	29.08
7	0	0.337	0.38	2.398	4.365	23.24
8	0	0.321	0.362	2.201	3.927	18.7
9	0	0.306	0.345	2.007	3.493	15.15
10	0	0.291	0.329	1.848	3.18	12.36
11	0	0.278	0.315	1.691	2.869	10.14
12	0	0.266	0.301	1.569	2.618	8.368
13	0	0.254	0.288	1.449	2.369	6.944
14	0	0.244	0.276	1.352	2.212	5.794
15	0	0.233	0.265	1.257	2.058	4.859

$\eta_{\text{psinund}} =$

$$DO = \begin{pmatrix} 0 \\ 3.097 \times 10^{-7} \\ 2.498 \times 10^{-7} \\ 2.009 \times 10^{-8} \\ 3.199 \times 10^{-8} \\ 1.731 \times 10^{-4} \end{pmatrix} \frac{\text{m}^2}{\text{s}}$$

$$KT = \begin{pmatrix} -81 \\ 56.325 \\ 49.247 \\ -139.069 \\ -120.545 \\ 9.402 \end{pmatrix} K$$

$$\gamma K_1 = 9.32 \times 10^{-7} \frac{\text{m}^3}{\text{kg} \cdot \text{K}}$$

$$\frac{\text{cal}}{\text{mol}} = 4.187 \frac{\text{kg} \cdot \text{m}^2}{\text{s}^2 \cdot \text{mol}}$$

$$\gamma K_{1k} = \begin{matrix} 5.485 \cdot 10^{-7} \\ 5.859 \cdot 10^{-7} \\ 1.259 \cdot 10^{-6} \\ 8.622 \cdot 10^{-7} \\ 1.635 \cdot 10^{-7} \end{matrix} \frac{\text{m}^3}{\text{kg} \cdot \text{K}}$$

7.1 For the solvents

$$f_{i,k} := \frac{\frac{V_{ch_k}}{\gamma V K_k} \cdot (KT_k + T_i)}{V_{P_i,k}}$$

$$f_{\gamma} =$$

	1	2	3	4	5	6
1	0.184	0.152	0.16	0.185	0.146	0.054
2	0.188	0.153	0.162	0.191	0.15	0.055
3	0.193	0.154	0.163	0.196	0.154	0.056
4	0.197	0.155	0.165	0.202	0.158	0.057
5	0.202	0.157	0.166	0.207	0.162	0.057
6	0.206	0.158	0.167	0.213	0.165	0.058
7	0.211	0.159	0.169	0.218	0.169	0.059
8	0.215	0.16	0.17	0.223	0.173	0.059
9	0.22	0.161	0.171	0.228	0.176	0.06
10	0.224	0.162	0.172	0.233	0.18	0.061
11	0.229	0.162	0.173	0.238	0.183	0.061
12	0.233	0.163	0.174	0.243	0.187	0.062
13	0.238	0.164	0.175	0.248	0.19	0.063
14	0.243	0.165	0.176	0.253	0.194	0.063
15	0.247	0.165	0.177	0.258	0.197	0.064

8) Recalculation of pure Self-Diffusion coefficients

- From Dullien's equation

$$D_{\text{pureDullien},i,j} := \frac{1.124 \cdot 10^{-17} \cdot \text{mol}^{\frac{2}{3}} \cdot (V_{c_j})^{\frac{2}{3}} \cdot R \cdot T_i}{\eta_{i,j} \cdot MW_j \cdot V_{P_i,j}}$$

	1	2	3	4	5	6
1	0	2.655·10 ⁻⁹	2.332·10 ⁻⁹	1.906·10 ⁻¹⁰	8.534·10 ⁻¹¹	1.049·10 ⁻¹¹
2	0	2.843·10 ⁻⁹	2.499·10 ⁻⁹	2.206·10 ⁻¹⁰	1.001·10 ⁻¹⁰	1.38·10 ⁻¹¹
3	0	3.041·10 ⁻⁹	2.673·10 ⁻⁹	2.6·10 ⁻¹⁰	1.201·10 ⁻¹⁰	1.818·10 ⁻¹¹
4	0	3.244·10 ⁻⁹	2.853·10 ⁻⁹	2.947·10 ⁻¹⁰	1.39·10 ⁻¹⁰	2.361·10 ⁻¹¹
5	0	3.459·10 ⁻⁹	3.04·10 ⁻⁹	3.386·10 ⁻¹⁰	1.64·10 ⁻¹⁰	3.039·10 ⁻¹¹
6	0	3.677·10 ⁻⁹	3.233·10 ⁻⁹	3.782·10 ⁻¹⁰	1.868·10 ⁻¹⁰	3.881·10 ⁻¹¹
7	0	3.907·10 ⁻⁹	3.434·10 ⁻⁹	4.264·10 ⁻¹⁰	2.155·10 ⁻¹⁰	4.922·10 ⁻¹¹
8	0	4.14·10 ⁻⁹	3.64·10 ⁻⁹	4.698·10 ⁻¹⁰	2.424·10 ⁻¹⁰	6.192·10 ⁻¹¹
9	0	4.386·10 ⁻⁹	3.853·10 ⁻⁹	5.209·10 ⁻¹⁰	2.754·10 ⁻¹⁰	7.735·10 ⁻¹¹
10	0	4.635·10 ⁻⁹	4.072·10 ⁻⁹	5.718·10 ⁻¹⁰	3.06·10 ⁻¹⁰	9.601·10 ⁻¹¹
11	0	4.891·10 ⁻⁹	4.298·10 ⁻⁹	6.313·10 ⁻¹⁰	3.428·10 ⁻¹⁰	1.184·10 ⁻¹⁰
12	0	5.153·10 ⁻⁹	4.528·10 ⁻⁹	6.873·10 ⁻¹⁰	3.796·10 ⁻¹⁰	1.451·10 ⁻¹⁰
13	0	5.423·10 ⁻⁹	4.766·10 ⁻⁹	7.516·10 ⁻¹⁰	4.238·10 ⁻¹⁰	1.768·10 ⁻¹⁰
14	0	5.701·10 ⁻⁹	5.009·10 ⁻⁹	8.132·10 ⁻¹⁰	4.584·10 ⁻¹⁰	2.141·10 ⁻¹⁰
15	0	5.985·10 ⁻⁹	5.257·10 ⁻⁹	8.829·10 ⁻¹⁰	4.975·10 ⁻¹⁰	2.583·10 ⁻¹⁰

DpureDullien = $\frac{\text{m}^2}{\text{s}}$

TempIndex := 4

$$D_{\text{pureDullien,TempIndex,MEK}} = 3.244 \times 10^{-9} \frac{\text{m}^2}{\text{s}}$$

$$D_{\text{pureDullien,TempIndex,DEK}} = 2.853 \times 10^{-9} \frac{\text{m}^2}{\text{s}}$$

$$D_{\text{pureDullien,TempIndex,TEGDME}} = 2.947 \times 10^{-10} \frac{\text{m}^2}{\text{s}}$$

$$D_{\text{pureDullien,TempIndex,PEGDME}} = 1.39 \times 10^{-10} \frac{\text{m}^2}{\text{s}}$$

- From the Vrentas and Duda's Free Volume Theory

$$D_{\text{pureVD}_k} := D0_k \cdot e^{\frac{-V_{\text{ch}_k}}{f_{\text{TempIndex,k}} \cdot V_{\text{TempIndex,k}}^{\text{VP}}}}$$

$$D_{\text{pureVD}} = \begin{pmatrix} 0 \\ 3.246 \times 10^{-9} \\ 2.854 \times 10^{-9} \\ 2.953 \times 10^{-10} \\ 1.4 \times 10^{-10} \\ 2.357 \times 10^{-11} \end{pmatrix} \frac{\text{m}^2}{\text{s}}$$

9) Weight and molar fractions of the mixtures

$$\omega_{\text{mt}} := \begin{pmatrix} 0.516 & 0.027 & 0.457 \\ 0.446 & 0.050 & 0.504 \\ 0.375 & 0.066 & 0.559 \end{pmatrix}$$

$$\omega_{\text{mp}} := \begin{pmatrix} 0.500 & 0.026 & 0.474 \\ 0.417 & 0.046 & 0.537 \\ 0.343 & 0.061 & 0.596 \end{pmatrix}$$

$$\omega_{m_1} := 0.583 \quad \omega_{m_2} := 1 - \omega_{m_1}$$

$$\omega_{d_1} := 0.692 \quad \omega_{d_2} := 1 - \omega_{d_1}$$

$$\omega_{\text{dt}} := \begin{pmatrix} 0.637 & 0.034 & 0.330 \\ 0.575 & 0.064 & 0.361 \\ 0.510 & 0.090 & 0.400 \end{pmatrix}$$

$$\omega_{\text{dp}} := \begin{pmatrix} 0.622 & 0.033 & 0.346 \\ 0.549 & 0.061 & 0.390 \\ 0.476 & 0.084 & 0.440 \end{pmatrix}$$

$$x_{m_1} := \frac{\frac{\omega_{m_1}}{MW_{\text{MEK}}}}{\frac{\omega_{m_1}}{MW_{\text{MEK}}} + \frac{\omega_{m_2}}{MW_{\text{PDMS}}}} \quad x_{d_1} := \frac{\frac{\omega_{d_1}}{MW_{\text{DEK}}}}{\frac{\omega_{d_1}}{MW_{\text{DEK}}} + \frac{\omega_{d_2}}{MW_{\text{PDMS}}}} \quad x_{m_2} := 1 - x_{m_1} \quad x_{d_2} := 1 - x_{d_1}$$

composition := 1..3

$$x_{\text{mt, composition, 1}} := \frac{\frac{\omega_{\text{mt, composition, 1}}}{MW_{\text{MEK}}}}{\frac{\omega_{\text{mt, composition, 1}}}{MW_{\text{MEK}}} + \frac{\omega_{\text{mt, composition, 2}}}{MW_{\text{TEGDME}}} + \frac{\omega_{\text{mt, composition, 3}}}{MW_{\text{PDMS}}}}$$

$$x_{\text{mt, composition, 2}} := \frac{\frac{\omega_{\text{mt, composition, 2}}}{MW_{\text{TEGDME}}}}{\frac{\omega_{\text{mt, composition, 1}}}{MW_{\text{MEK}}} + \frac{\omega_{\text{mt, composition, 2}}}{MW_{\text{TEGDME}}} + \frac{\omega_{\text{mt, composition, 3}}}{MW_{\text{PDMS}}}}$$

$$x_{\text{mt, composition, 3}} := 1 - (x_{\text{mt, composition, 1}} + x_{\text{mt, composition, 2}})$$

$$x_{\text{mp, composition, 1}} := \frac{\frac{\omega_{\text{mp, composition, 1}}}{MW_{\text{MEK}}}}{\frac{\omega_{\text{mp, composition, 1}}}{MW_{\text{MEK}}} + \frac{\omega_{\text{mp, composition, 2}}}{MW_{\text{PEGDME}}} + \frac{\omega_{\text{mp, composition, 3}}}{MW_{\text{PDMS}}}}$$

$$x_{\text{mp, composition, 2}} := \frac{\frac{\omega_{\text{mp, composition, 2}}}{MW_{\text{PEGDME}}}}{\frac{\omega_{\text{mp, composition, 1}}}{MW_{\text{MEK}}} + \frac{\omega_{\text{mp, composition, 2}}}{MW_{\text{PEGDME}}} + \frac{\omega_{\text{mp, composition, 3}}}{MW_{\text{PDMS}}}}$$

$$x_{\text{mp, composition, 3}} := 1 - (x_{\text{mp, composition, 1}} + x_{\text{mp, composition, 2}})$$

$$x_{\text{dt, composition, 1}} := \frac{\frac{\omega_{\text{dt, composition, 1}}}{MW_{\text{DEK}}}}{\frac{\omega_{\text{dt, composition, 1}}}{MW_{\text{DEK}}} + \frac{\omega_{\text{dt, composition, 2}}}{MW_{\text{TEGDME}}} + \frac{\omega_{\text{dt, composition, 3}}}{MW_{\text{PDMS}}}}$$

$$x_{\text{dt, composition, 2}} := \frac{\frac{\omega_{\text{dt, composition, 2}}}{MW_{\text{TEGDME}}}}{\frac{\omega_{\text{dt, composition, 1}}}{MW_{\text{DEK}}} + \frac{\omega_{\text{dt, composition, 2}}}{MW_{\text{TEGDME}}} + \frac{\omega_{\text{dt, composition, 3}}}{MW_{\text{PDMS}}}}$$

$$x_{\text{dt, composition, 3}} := 1 - (x_{\text{dt, composition, 1}} + x_{\text{dt, composition, 2}})$$

$$x_{\text{dp, composition, 1}} := \frac{\frac{\omega_{\text{dp, composition, 1}}}{MW_{\text{DEK}}}}{\frac{\omega_{\text{dp, composition, 1}}}{MW_{\text{DEK}}} + \frac{\omega_{\text{dp, composition, 2}}}{MW_{\text{PEGDME}}} + \frac{\omega_{\text{dp, composition, 3}}}{MW_{\text{PDMS}}}}$$

$$x_{\text{dp, composition, 2}} := \frac{\frac{\omega_{\text{dp, composition, 2}}}{MW_{\text{PEGDME}}}}{\frac{\omega_{\text{dp, composition, 1}}}{MW_{\text{DEK}}} + \frac{\omega_{\text{dp, composition, 2}}}{MW_{\text{PEGDME}}} + \frac{\omega_{\text{dp, composition, 3}}}{MW_{\text{PDMS}}}}$$

$$x_{\text{dp, composition, 3}} := 1 - (x_{\text{dp, composition, 1}} + x_{\text{dp, composition, 2}})$$

$$x_{\text{mt}} = \begin{pmatrix} 0.532 & 9.035 \times 10^{-3} & 0.459 \\ 0.468 & 0.017 & 0.515 \\ 0.399 & 0.023 & 0.578 \end{pmatrix} \quad x_{\text{mp}} = \begin{pmatrix} 0.517 & 6.498 \times 10^{-3} & 0.477 \\ 0.439 & 0.012 & 0.55 \\ 0.366 & 0.016 & 0.618 \end{pmatrix}$$

$$x_{\text{dt}} = \begin{pmatrix} 0.616 & 0.013 & 0.371 \\ 0.564 & 0.024 & 0.412 \\ 0.505 & 0.035 & 0.46 \end{pmatrix} \quad x_{\text{dp}} = \begin{pmatrix} 0.602 & 9.221 \times 10^{-3} & 0.389 \\ 0.538 & 0.017 & 0.444 \\ 0.47 & 0.024 & 0.506 \end{pmatrix}$$

$$\phi_{\text{mt, composition, 1}} := \frac{\frac{\omega_{\text{mt, composition, 1}}}{\rho_{4, \text{MEK}}}}{\frac{\omega_{\text{mt, composition, 1}}}{\rho_{4, \text{MEK}}} + \frac{\omega_{\text{mt, composition, 2}}}{\rho_{4, \text{TEGDME}}} + \frac{\omega_{\text{mt, composition, 3}}}{\rho_{4, \text{PDMS}}}}$$

$$\phi_{\text{mt, composition, 2}} := \frac{\frac{\omega_{\text{mt, composition, 2}}}{\rho_{4, \text{TEGDME}}}}{\frac{\omega_{\text{mt, composition, 1}}}{\rho_{4, \text{MEK}}} + \frac{\omega_{\text{mt, composition, 2}}}{\rho_{4, \text{TEGDME}}} + \frac{\omega_{\text{mt, composition, 3}}}{\rho_{4, \text{PDMS}}}}$$

$$\phi_{\text{mt, composition, 3}} := 1 - \phi_{\text{mt, composition, 1}} - \phi_{\text{mt, composition, 2}}$$

$$\phi_{\text{mp, composition, 1}} := \frac{\frac{\omega_{\text{mp, composition, 1}}}{\rho_{4, \text{MEK}}}}{\frac{\omega_{\text{mp, composition, 1}}}{\rho_{4, \text{MEK}}} + \frac{\omega_{\text{mp, composition, 2}}}{\rho_{4, \text{PEGDME}}} + \frac{\omega_{\text{mp, composition, 3}}}{\rho_{4, \text{PDMS}}}}$$

$$\phi_{\text{mp, composition, 2}} := \frac{\frac{\omega_{\text{mp, composition, 2}}}{\rho_{4, \text{PEGDME}}}}{\frac{\omega_{\text{mp, composition, 1}}}{\rho_{4, \text{MEK}}} + \frac{\omega_{\text{mp, composition, 2}}}{\rho_{4, \text{PEGDME}}} + \frac{\omega_{\text{mp, composition, 3}}}{\rho_{4, \text{PDMS}}}}$$

$$\phi_{mp, composition, 3} := 1 - \phi_{mp, composition, 1} - \phi_{mp, composition, 2}$$

$$\phi_{dt, composition, 1} := \frac{\frac{\omega_{dt, composition, 1}}{\rho_{4, DEK}}}{\frac{\omega_{dt, composition, 1}}{\rho_{4, DEK}} + \frac{\omega_{dt, composition, 2}}{\rho_{4, TEGDME}} + \frac{\omega_{dt, composition, 3}}{\rho_{4, PDMS}}}$$

$$\phi_{dt, composition, 2} := \frac{\frac{\omega_{dt, composition, 2}}{\rho_{4, TEGDME}}}{\frac{\omega_{dt, composition, 1}}{\rho_{4, DEK}} + \frac{\omega_{dt, composition, 2}}{\rho_{4, TEGDME}} + \frac{\omega_{dt, composition, 3}}{\rho_{4, PDMS}}}$$

$$\phi_{dt, composition, 3} := 1 - \phi_{dt, composition, 1} - \phi_{dt, composition, 2}$$

$$\phi_{dp, composition, 1} := \frac{\frac{\omega_{dp, composition, 1}}{\rho_{4, DEK}}}{\frac{\omega_{dp, composition, 1}}{\rho_{4, DEK}} + \frac{\omega_{dp, composition, 2}}{\rho_{4, PEGDME}} + \frac{\omega_{dp, composition, 3}}{\rho_{4, PDMS}}}$$

$$\phi_{dp, composition, 2} := \frac{\frac{\omega_{dp, composition, 2}}{\rho_{4, PEGDME}}}{\frac{\omega_{dp, composition, 1}}{\rho_{4, DEK}} + \frac{\omega_{dp, composition, 2}}{\rho_{4, PEGDME}} + \frac{\omega_{dp, composition, 3}}{\rho_{4, PDMS}}}$$

$$\phi_{dp, composition, 3} := 1 - \phi_{dp, composition, 1} - \phi_{dp, composition, 2}$$

$$\phi_{mt} = \begin{pmatrix} 0.566 & 0.023 & 0.411 \\ 0.496 & 0.044 & 0.46 \\ 0.423 & 0.059 & 0.518 \end{pmatrix}$$

$$\phi_{mp} = \begin{pmatrix} 0.55 & 0.022 & 0.428 \\ 0.467 & 0.04 & 0.493 \\ 0.39 & 0.054 & 0.556 \end{pmatrix}$$

$$d\omega_{mt} := \frac{\begin{pmatrix} 0.3 & 0.0 & 0.3 \\ 0.3 & 0 & 0.3 \\ 0.3 & 0 & 0.3 \end{pmatrix}}{100} \quad d\omega_{mp} := \frac{\begin{pmatrix} 0.2 & 0 & 0.3 \\ 0.2 & 0.0 & 0.2 \\ 0.2 & 0 & 0.2 \end{pmatrix}}{100}$$

$$\phi_{dt} = \begin{pmatrix} 0.679 & 0.029 & 0.292 \\ 0.621 & 0.056 & 0.324 \\ 0.558 & 0.079 & 0.363 \end{pmatrix}$$

$$\phi_{dp} = \begin{pmatrix} 0.665 & 0.028 & 0.307 \\ 0.596 & 0.052 & 0.352 \\ 0.524 & 0.073 & 0.403 \end{pmatrix}$$

$$d\omega_{dt} := \frac{\begin{pmatrix} 0.2 & 0 & 0.2 \\ 0.2 & 0 & 0.1 \\ 0.1 & 0 & 0.1 \end{pmatrix}}{100} \quad d\omega_{dp} := \frac{\begin{pmatrix} 0.7 & 0 & 0.8 \\ 0.7 & 0.1 & 0.7 \\ 0.1 & 0 & 0.1 \end{pmatrix}}{100}$$

$$d \frac{\frac{A}{\rho A}}{\frac{A}{\rho A} + \frac{B}{\rho B} + \frac{C}{\rho C}}$$

$$dfA(A, B, C, \rho A, \rho B, \rho C) := \frac{1}{\rho A \cdot \left(\frac{A}{\rho A} + \frac{B}{\rho B} + \frac{C}{\rho C}\right)} - \frac{A}{\rho A^2 \cdot \left(\frac{A}{\rho A} + \frac{B}{\rho B} + \frac{C}{\rho C}\right)^2}$$

$$d \frac{\frac{A}{\rho A}}{\frac{A}{\rho A} + \frac{B}{\rho B} + \frac{C}{\rho C}}$$

$$dfB(A, B, C, \rho A, \rho B, \rho C) := \frac{-A}{\rho A \cdot \left(\frac{A}{\rho A} + \frac{B}{\rho B} + \frac{C}{\rho C}\right)^2} \cdot \rho B$$

$$d \frac{\frac{A}{\rho A}}{\frac{A}{\rho A} + \frac{B}{\rho B} + \frac{C}{\rho C}}$$

a := 1..3

$$d\phi_{2, mt, a, 1} := \left(dfA(\omega_{mt, a, 1}, \omega_{mt, a, 2}, \omega_{mt, a, 3}, \rho_{4, MEK}, \rho_{4, TEGDME}, \rho_{4, PDMS})^2 \right)^{0.5} \cdot d\omega_{mt, 1, 1} + \left(dfB(\omega_{mt, a, 1}, \omega_{mt, a, 2}, \omega_{mt, a, 3}, \rho_{4, MEK}, \rho_{4, TEGDME}, \rho_{4, PDMS})^2 \right)^{0.5} \cdot (d\omega_{mt, 1, 2} + d\omega_{mt, 1, 3})$$

$$d\phi_{2, mt, a, 2} := \left(dfA(\omega_{mt, a, 2}, \omega_{mt, a, 1}, \omega_{mt, a, 3}, \rho_{4, TEGDME}, \rho_{4, MEK}, \rho_{4, PDMS})^2 \right)^{0.5} \cdot d\omega_{mt, 1, 2} + \left(dfB(\omega_{mt, a, 2}, \omega_{mt, a, 1}, \omega_{mt, a, 3}, \rho_{4, TEGDME}, \rho_{4, MEK}, \rho_{4, PDMS})^2 \right)^{0.5} \cdot (d\omega_{mt, 1, 1} + d\omega_{mt, 1, 3})$$

$$d\phi_{2, mt, a, 3} := \left(dfA(\omega_{mt, a, 3}, \omega_{mt, a, 1}, \omega_{mt, a, 2}, \rho_{4, PDMS}, \rho_{4, MEK}, \rho_{4, TEGDME})^2 \right)^{0.5} \cdot d\omega_{mt, 1, 3} + \left(dfB(\omega_{mt, a, 3}, \omega_{mt, a, 1}, \omega_{mt, a, 2}, \rho_{4, PDMS}, \rho_{4, MEK}, \rho_{4, TEGDME})^2 \right)^{0.5} \cdot (d\omega_{mt, 1, 1} + d\omega_{mt, 1, 2})$$

$d\phi_{2, mt, a, 1} =$	$d\phi_{2, mt, a, 2} =$	$d\phi_{2, mt, a, 3} =$
$2.904 \cdot 10^{-3}$	$1.544 \cdot 10^{-4}$	$2.94 \cdot 10^{-3}$
$2.995 \cdot 10^{-3}$	$2.944 \cdot 10^{-4}$	$3.013 \cdot 10^{-3}$
$3.09 \cdot 10^{-3}$	$4.003 \cdot 10^{-4}$	$3.093 \cdot 10^{-3}$

$$d\phi_{2, mp, a, 1} := \left(dfA(\omega_{mp, a, 1}, \omega_{mp, a, 2}, \omega_{mp, a, 3}, \rho_{4, MEK}, \rho_{4, PEGDME}, \rho_{4, PDMS})^2 \right)^{0.5} \cdot d\omega_{mp, 1, 1} + \left(dfB(\omega_{mp, a, 1}, \omega_{mp, a, 2}, \omega_{mp, a, 3}, \rho_{4, MEK}, \rho_{4, PEGDME}, \rho_{4, PDMS})^2 \right)^{0.5} \cdot (d\omega_{mp, 1, 2} + d\omega_{mp, 1, 3})$$

$$d\phi_{2, mp, a, 2} := \left(dfA(\omega_{mp, a, 2}, \omega_{mp, a, 1}, \omega_{mp, a, 3}, \rho_{4, PEGDME}, \rho_{4, MEK}, \rho_{4, PDMS})^2 \right)^{0.5} \cdot d\omega_{mp, 1, 2} + \left(dfB(\omega_{mp, a, 2}, \omega_{mp, a, 1}, \omega_{mp, a, 3}, \rho_{4, PEGDME}, \rho_{4, MEK}, \rho_{4, PDMS})^2 \right)^{0.5} \cdot (d\omega_{mp, 1, 1} + d\omega_{mp, 1, 3})$$

$$d\phi_{2, mp, a, 3} := \left(dfA(\omega_{mp, a, 3}, \omega_{mp, a, 1}, \omega_{mp, a, 2}, \rho_{4, PDMS}, \rho_{4, MEK}, \rho_{4, PEGDME})^2 \right)^{0.5} \cdot d\omega_{mp, 1, 3} + \left(dfB(\omega_{mp, a, 3}, \omega_{mp, a, 1}, \omega_{mp, a, 2}, \rho_{4, PDMS}, \rho_{4, MEK}, \rho_{4, PEGDME})^2 \right)^{0.5} \cdot (d\omega_{mp, 1, 1} + d\omega_{mp, 1, 2})$$

$$\begin{array}{l} d\phi_{2_mp_a,1} = \\ \begin{array}{|c|} \hline 2.397 \cdot 10^{-3} \\ \hline 2.409 \cdot 10^{-3} \\ \hline 2.419 \cdot 10^{-3} \\ \hline \end{array} \end{array} \quad \begin{array}{l} d\phi_{2_mp_a,2} = \\ \begin{array}{|c|} \hline 1.219 \cdot 10^{-4} \\ \hline 2.234 \cdot 10^{-4} \\ \hline 3.058 \cdot 10^{-4} \\ \hline \end{array} \end{array} \quad \begin{array}{l} d\phi_{2_mp_a,3} = \\ \begin{array}{|c|} \hline 2.49 \cdot 10^{-3} \\ \hline 2.501 \cdot 10^{-3} \\ \hline 2.508 \cdot 10^{-3} \\ \hline \end{array} \end{array}$$

$$\begin{aligned} d\phi_{2_dt_a,1} &:= \left(dfA(\omega_{dt_a,1}, \omega_{dt_a,2}, \omega_{dt_a,3}, \rho_{4,DEK}, \rho_{4,TEGDME}, \rho_{4,PDMS})^2 \right)^{0.5} \cdot d\omega_{dt,1,1} + \left(dfB(\omega_{dt_a,1}, \omega_{dt_a,2}, \omega_{dt_a,3}, \rho_{4,DEK}, \rho_{4,TEGDME}, \rho_{4,PDMS})^2 \right)^{0.5} \cdot (d\omega_{dt,1,2} + d\omega_{dt,1,3}) \\ d\phi_{2_dt_a,2} &:= \left(dfA(\omega_{dt_a,2}, \omega_{dt_a,1}, \omega_{dt_a,3}, \rho_{4,TEGDME}, \rho_{4,DEK}, \rho_{4,PDMS})^2 \right)^{0.5} \cdot d\omega_{dt,1,2} + \left(dfB(\omega_{dt_a,2}, \omega_{dt_a,1}, \omega_{dt_a,3}, \rho_{4,TEGDME}, \rho_{4,DEK}, \rho_{4,PDMS})^2 \right)^{0.5} \cdot (d\omega_{dt,1,1} + d\omega_{dt,1,3}) \\ d\phi_{2_dt_a,3} &:= \left(dfA(\omega_{dt_a,3}, \omega_{dt_a,1}, \omega_{dt_a,2}, \rho_{4,PDMS}, \rho_{4,DEK}, \rho_{4,TEGDME})^2 \right)^{0.5} \cdot d\omega_{dt,1,3} + \left(dfB(\omega_{dt_a,3}, \omega_{dt_a,1}, \omega_{dt_a,2}, \rho_{4,PDMS}, \rho_{4,DEK}, \rho_{4,TEGDME})^2 \right)^{0.5} \cdot (d\omega_{dt,1,1} + d\omega_{dt,1,2}) \end{aligned}$$

$$\begin{array}{l} d\phi_{2_dt_a,1} = \\ \begin{array}{|c|} \hline 1.847 \cdot 10^{-3} \\ \hline 1.896 \cdot 10^{-3} \\ \hline 1.947 \cdot 10^{-3} \\ \hline \end{array} \end{array} \quad \begin{array}{l} d\phi_{2_dt_a,2} = \\ \begin{array}{|c|} \hline 1.241 \cdot 10^{-4} \\ \hline 2.397 \cdot 10^{-4} \\ \hline 3.458 \cdot 10^{-4} \\ \hline \end{array} \end{array} \quad \begin{array}{l} d\phi_{2_dt_a,3} = \\ \begin{array}{|c|} \hline 1.876 \cdot 10^{-3} \\ \hline 1.912 \cdot 10^{-3} \\ \hline 1.951 \cdot 10^{-3} \\ \hline \end{array} \end{array}$$

$$\begin{aligned} d\phi_{2_dp_a,1} &:= \left(dfA(\omega_{dp_a,1}, \omega_{dp_a,2}, \omega_{dp_a,3}, \rho_{4,DEK}, \rho_{4,PEGDME}, \rho_{4,PDMS})^2 \right)^{0.5} \cdot d\omega_{dp,1,1} + \left(dfB(\omega_{dp_a,1}, \omega_{dp_a,2}, \omega_{dp_a,3}, \rho_{4,DEK}, \rho_{4,PEGDME}, \rho_{4,PDMS})^2 \right)^{0.5} \cdot (d\omega_{dp,1,2} + d\omega_{dp,1,3}) \\ d\phi_{2_dp_a,2} &:= \left(dfA(\omega_{dp_a,2}, \omega_{dp_a,1}, \omega_{dp_a,3}, \rho_{4,PEGDME}, \rho_{4,DEK}, \rho_{4,PDMS})^2 \right)^{0.5} \cdot d\omega_{dp,1,2} + \left(dfB(\omega_{dp_a,2}, \omega_{dp_a,1}, \omega_{dp_a,3}, \rho_{4,PEGDME}, \rho_{4,DEK}, \rho_{4,PDMS})^2 \right)^{0.5} \cdot (d\omega_{dp,1,1} + d\omega_{dp,1,3}) \\ d\phi_{2_dp_a,3} &:= \left(dfA(\omega_{dp_a,3}, \omega_{dp_a,1}, \omega_{dp_a,2}, \rho_{4,PDMS}, \rho_{4,DEK}, \rho_{4,PEGDME})^2 \right)^{0.5} \cdot d\omega_{dp,1,3} + \left(dfB(\omega_{dp_a,3}, \omega_{dp_a,1}, \omega_{dp_a,2}, \rho_{4,PDMS}, \rho_{4,DEK}, \rho_{4,PEGDME})^2 \right)^{0.5} \cdot (d\omega_{dp,1,1} + d\omega_{dp,1,2}) \end{aligned}$$

$$\begin{array}{l} d\phi_{2_dp_a,1} = \\ \begin{array}{|c|} \hline 6.972 \cdot 10^{-3} \\ \hline 7.135 \cdot 10^{-3} \\ \hline 7.297 \cdot 10^{-3} \\ \hline \end{array} \end{array} \quad \begin{array}{l} d\phi_{2_dp_a,2} = \\ \begin{array}{|c|} \hline 4.441 \cdot 10^{-4} \\ \hline 8.469 \cdot 10^{-4} \\ \hline 1.201 \cdot 10^{-3} \\ \hline \end{array} \end{array} \quad \begin{array}{l} d\phi_{2_dp_a,3} = \\ \begin{array}{|c|} \hline 7.223 \cdot 10^{-3} \\ \hline 7.353 \cdot 10^{-3} \\ \hline 7.481 \cdot 10^{-3} \\ \hline \end{array} \end{array}$$

$$\phi_{_mt} \cdot 100 = \begin{pmatrix} 56.6 & 2.3 & 41.1 \\ 49.6 & 4.4 & 46 \\ 42.3 & 5.9 & 51.8 \end{pmatrix} \quad d\phi_{2_mt} \cdot 100 = \begin{pmatrix} 0.3 & 0 & 0.3 \\ 0.3 & 0 & 0.3 \\ 0.3 & 0 & 0.3 \end{pmatrix}$$

$$\phi_{_mp} \cdot 100 = \begin{pmatrix} 55 & 2.2 & 42.8 \\ 46.7 & 4 & 49.3 \\ 39 & 5.4 & 55.6 \end{pmatrix} \quad d\phi_{2_mp} \cdot 100 = \begin{pmatrix} 0.2 & 0 & 0.2 \\ 0.2 & 0 & 0.3 \\ 0.2 & 0 & 0.3 \end{pmatrix}$$

$$\phi_{_dt} \cdot 100 = \begin{pmatrix} 67.9 & 2.9 & 29.2 \\ 62.1 & 5.6 & 32.4 \\ 55.8 & 7.9 & 36.3 \end{pmatrix} \quad d\phi_{2_dt} \cdot 100 = \begin{pmatrix} 0.2 & 0 & 0.2 \\ 0.2 & 0 & 0.2 \\ 0.2 & 0 & 0.2 \end{pmatrix}$$

$$\phi_{_dp} \cdot 100 = \begin{pmatrix} 66.5 & 2.8 & 30.7 \\ 59.6 & 5.2 & 35.2 \\ 52.4 & 7.3 & 40.3 \end{pmatrix} \quad d\phi_{2_dp} \cdot 100 = \begin{pmatrix} 0.7 & 0 & 0.7 \\ 0.7 & 0.1 & 0.7 \\ 0.7 & 0.1 & 0.7 \end{pmatrix}$$

10) Free volumes for each component

$$\begin{aligned} V_{compress} &:= V_{atOK} \\ V_{compress_{PDMS}} &:= 1.3 \cdot V_{vdw_{PDMS}} \\ V_{free_ij} &:= V_{p_{a,j}} \cdot MW_j - V_{compress_j} \end{aligned}$$

$$V_{compress} = \begin{pmatrix} 6.395 \times 10^{-5} \\ 6.39 \times 10^{-5} \\ 7.84 \times 10^{-5} \\ 1.879 \times 10^{-4} \\ 2.48 \times 10^{-4} \\ 1.544 \times 10^{-4} \end{pmatrix} \frac{m^3}{mol} \quad V_{free_i} = \begin{pmatrix} 1.213 \times 10^{-5} \\ 2.635 \times 10^{-5} \\ 2.801 \times 10^{-5} \\ 3.284 \times 10^{-5} \\ 4.121 \times 10^{-5} \\ 1.84 \times 10^{-5} \end{pmatrix} \frac{m^3}{mol}$$

$$\eta_0^k := \frac{3}{\pi} \cdot \frac{\sqrt{\frac{MW_k}{V_{compressk}} \cdot \frac{k_B \cdot T_{TempIndex}}{3 \cdot \left(2 \sqrt{\frac{3 V_{compressk}}{4}} \right) \cdot \pi \cdot Avog}}{\gamma}}}{\eta_0 = \begin{pmatrix} 0 \\ 4.902 \times 10^{-5} \\ 4.675 \times 10^{-5} \\ 4.193 \times 10^{-5} \\ 4.036 \times 10^{-5} \\ 4.468 \times 10^{-5} \end{pmatrix} \frac{\text{kg}}{\text{m s}}}$$

$\gamma := 0.7$

Given

$$\eta_{TempIndex, MEK} = \eta_{MEK}^0 \cdot e^{\frac{\gamma \cdot V_{compress, MEK}}{V_{free, i, MEK}}}$$

Find(γ) = 0.86

Given

$$\eta_{TempIndex, DEK} = \eta_{DEK}^0 \cdot e^{\frac{\gamma \cdot V_{compress, DEK}}{V_{free, i, DEK}}}$$

Find(γ) = 0.804

Given

$$\eta_{TempIndex, TEGDME} = \eta_{TEGDME}^0 \cdot e^{\frac{\gamma \cdot V_{compress, TEGDME}}{V_{free, i, TEGDME}}}$$

Find(γ) = 0.765

Given

$$\eta_{TempIndex, PEGDME} = \eta_{PEGDME}^0 \cdot e^{\frac{\gamma \cdot V_{compress, PEGDME}}{V_{free, i, PEGDME}}}$$

Find(γ) = 0.845

$$V_{free, i} = \begin{pmatrix} 1.213 \times 10^{-5} \\ 2.635 \times 10^{-5} \\ 2.801 \times 10^{-5} \\ 3.284 \times 10^{-5} \\ 4.121 \times 10^{-5} \\ 1.84 \times 10^{-5} \end{pmatrix} \frac{\text{m}^3}{\text{mol}}$$

$$AAA1 := 1 \cdot \text{Pa} \cdot \text{s}$$

$$BBB1 := 0.00001$$

Given

$$\left(\eta^{(PEGDME)} \right)_2 = AAA1 \cdot e^{\frac{BBB1 \cdot V_{compress, PEGDME}}{V_{p2, PEGDME} \cdot MW_{PEGDME} - V_{compress, PEGDME}}}$$

$$\left(\eta^{(PEGDME)} \right)_8 = AAA1 \cdot e^{\frac{BBB1 \cdot V_{compress, PEGDME}}{V_{p8, PEGDME} \cdot MW_{PEGDME} - V_{compress, PEGDME}}}$$

$$\left(\eta^{(PEGDME)} \right)_4 = AAA1 \cdot e^{\frac{BBB1 \cdot V_{compress, PEGDME}}{V_{p4, PEGDME} \cdot MW_{PEGDME} - V_{compress, PEGDME}}}$$

$$\begin{pmatrix} AAA1 \\ BBB1 \end{pmatrix} := \text{Minerr}(AAA1, BBB1)$$

$$AAA1 = 6.363 \times 10^{-5} \frac{\text{kg}}{\text{m s}}$$

$$BBB1 = 0.77$$

Appendix 4

$$AAA2 := 1 \cdot 10^{-5} \cdot \text{Pa} \cdot \text{s}$$

$$BBB2 := 0.00001$$

Given

$$\left(\eta^{(\text{TEGDME})} \right)_2 = AAA2 \cdot e^{\frac{BBB2 \cdot V_{\text{compress_TEGDME}}}{V_{p2, \text{TEGDME}} \cdot MW_{\text{TEGDME}} - V_{\text{compress_TEGDME}}}}$$

$$\left(\eta^{(\text{TEGDME})} \right)_7 = AAA2 \cdot e^{\frac{BBB2 \cdot V_{\text{compress_TEGDME}}}{V_{p8, \text{TEGDME}} \cdot MW_{\text{TEGDME}} - V_{\text{compress_TEGDME}}}}$$

$$\left(\eta^{(\text{TEGDME})} \right)_4 = AAA2 \cdot e^{\frac{BBB2 \cdot V_{\text{compress_TEGDME}}}{V_{p4, \text{TEGDME}} \cdot MW_{\text{TEGDME}} - V_{\text{compress_TEGDME}}}}$$

$$\left(\frac{AAA2}{BBB2} \right) := \text{Minerr}(AAA2, BBB2) \quad AAA2 = 9.835 \times 10^{-5} \frac{\text{kg}}{\text{m s}} \quad BBB2 = 0.621$$

$$AAA2 := 1 \cdot 10^{-10} \cdot \text{Pa} \cdot \text{s}$$

$$BBB2 := 0.01$$

Given

$$\left(\eta^{(\text{MEK})} \right)_2 = AAA2 \cdot e^{\frac{BBB2 \cdot V_{\text{compress_MEK}}}{V_{p2, \text{MEK}} \cdot MW_{\text{MEK}} - V_{\text{compress_MEK}}}}$$

$$\left(\eta^{(\text{MEK})} \right)_8 = AAA2 \cdot e^{\frac{BBB2 \cdot V_{\text{compress_MEK}}}{V_{p8, \text{MEK}} \cdot MW_{\text{MEK}} - V_{\text{compress_MEK}}}}$$

$$\left(\eta^{(\text{MEK})} \right)_4 = AAA2 \cdot e^{\frac{BBB2 \cdot V_{\text{compress_MEK}}}{V_{p4, \text{MEK}} \cdot MW_{\text{MEK}} - V_{\text{compress_MEK}}}}$$

$$\left(\frac{AAA2}{BBB2} \right) := \text{Minerr}(AAA2, BBB2) \quad AAA2 = 3.867 \times 10^{-5} \frac{\text{kg}}{\text{m s}} \quad BBB2 = 0.957$$

$$AAA2 := 1 \cdot 10^{-5} \cdot \text{Pa} \cdot \text{s}$$

$$BBB2 := 0.7$$

Given

$$\left(\eta^{(\text{DEK})} \right)_2 = AAA2 \cdot e^{\frac{BBB2 \cdot V_{\text{compress_DEK}}}{V_{p2, \text{DEK}} \cdot MW_{\text{DEK}} - V_{\text{compress_DEK}}}}$$

$$\left(\eta^{(\text{DEK})} \right)_8 = AAA2 \cdot e^{\frac{BBB2 \cdot V_{\text{compress_DEK}}}{V_{p8, \text{DEK}} \cdot MW_{\text{DEK}} - V_{\text{compress_DEK}}}}$$

$$\left(\eta^{(\text{DEK})} \right)_4 = AAA2 \cdot e^{\frac{BBB2 \cdot V_{\text{compress_DEK}}}{V_{p4, \text{DEK}} \cdot MW_{\text{DEK}} - V_{\text{compress_DEK}}}}$$

$$\left(\frac{AAA2}{BBB2} \right) := \text{Minerr}(AAA2, BBB2) \quad AAA2 = 4.404 \times 10^{-5} \frac{\text{kg}}{\text{m s}} \quad BBB2 = 0.825$$



Deleting the units because the solver can not manage units.
Every input is in S.I. system and every output should be in S.I

$$T := \frac{\text{K}}{\text{K}} \quad R := \frac{\frac{\text{kg m}^2}{\text{s}^2 \text{K mol}}}{\frac{\text{kg m}^2}{\text{s}^2 \text{K mol}}} \quad MW := \frac{\text{kg}}{\text{mol}} \quad \eta := \frac{\frac{\text{kg}}{\text{m s}}}{\frac{\text{kg}}{\text{m s}}} \quad KT := \frac{\text{K}}{\text{K}} \quad \rho := \frac{\frac{\text{kg}}{\text{m}^3}}{\frac{\text{kg}}{\text{m}^3}} \quad Vc := \frac{\frac{\text{m}^3}{\text{mol}}}{\frac{\text{m}^3}{\text{mol}}} \quad Vp := \frac{\frac{\text{m}^3}{\text{kg}}}{\frac{\text{m}^3}{\text{kg}}} \quad V_{\text{compress}} := \frac{\frac{\text{m}^3}{\text{mol}}}{\frac{\text{m}^3}{\text{mol}}}$$



$$F(z, t) := \begin{pmatrix} t_1 \cdot e^{-t_2 \frac{z \cdot MW_{PEGDME} - V_{compressPEGDME}}{z \cdot MW_{PEGDME} - V_{compressPEGDME}}} \\ \exp\left(-t_2 \frac{V_{compressPEGDME}}{z \cdot MW_{PEGDME} - V_{compressPEGDME}}\right) \\ -t_1 \frac{V_{compressPEGDME}}{z \cdot MW_{PEGDME} - V_{compressPEGDME}} \cdot \exp\left(-t_2 \frac{V_{compressPEGDME}}{z \cdot MW_{PEGDME} - V_{compressPEGDME}}\right) \end{pmatrix}$$

$$Y_i := VP_{i, PEGDME}$$

$$vy_i := \left(\eta^{(PEGDME)} \right)_i \quad vg := \begin{pmatrix} 1 \cdot 10^{-4} \\ 0.02 \end{pmatrix} \quad \text{Solution} := \text{genfit}(Y, vy, vg, F)$$

$$\begin{pmatrix} \eta^0_{PEGDME} \\ \gamma_{PEGDME} \end{pmatrix} := \begin{pmatrix} \text{Solution}_1 \\ \text{Solution}_2 \cdot -1 \end{pmatrix} \quad \boxed{\gamma_{PEGDME} = 0.76} \quad \boxed{\eta^0_{PEGDME} = 6.767 \times 10^{-5}}$$

$$F(z, t) := \begin{pmatrix} t_1 \cdot e^{-t_2 \frac{z \cdot MW_{TEGDME} - V_{compressTEGDME}}{z \cdot MW_{TEGDME} - V_{compressTEGDME}}} \\ \exp\left(-t_2 \frac{V_{compressTEGDME}}{z \cdot MW_{TEGDME} - V_{compressTEGDME}}\right) \\ -t_1 \frac{V_{compressTEGDME}}{z \cdot MW_{TEGDME} - V_{compressTEGDME}} \cdot \exp\left(-t_2 \frac{V_{compressTEGDME}}{z \cdot MW_{TEGDME} - V_{compressTEGDME}}\right) \end{pmatrix}$$

$$Y_i := VP_{i, TEGDME}$$

$$vy_i := \left(\eta^{(TEGDME)} \right)_i \quad vg := \begin{pmatrix} 4 \cdot 10^{-4} \\ -0.7 \end{pmatrix} \quad \text{Solution} := \text{genfit}(Y, vy, vg, F)$$

$$\begin{pmatrix} \eta^0_{TEGDME} \\ \gamma_{TEGDME} \end{pmatrix} := \begin{pmatrix} \text{Solution}_1 \\ \text{Solution}_2 \cdot -1 \end{pmatrix} \quad \boxed{\gamma_{TEGDME} = 0.685} \quad \boxed{\eta^0_{TEGDME} = 6.692 \times 10^{-5}}$$

$$F(z, t) := \begin{pmatrix} t_1 \cdot e^{-t_2 \frac{z \cdot MW_{MEK} - V_{compressMEK}}{z \cdot MW_{MEK} - V_{compressMEK}}} \\ \exp\left(-t_2 \frac{V_{compressMEK}}{z \cdot MW_{MEK} - V_{compressMEK}}\right) \\ -t_1 \frac{V_{compressMEK}}{z \cdot MW_{MEK} - V_{compressMEK}} \cdot \exp\left(-t_2 \frac{V_{compressMEK}}{z \cdot MW_{MEK} - V_{compressMEK}}\right) \end{pmatrix}$$

$$Y_i := VP_{i, MEK}$$

$$vy_i := \left(\eta^{(MEK)} \right)_i \quad vg := \begin{pmatrix} 10 \cdot 10^{-4} \\ -0.5 \end{pmatrix} \quad \text{Solution} := \text{genfit}(Y, vy, vg, F)$$

$$\begin{pmatrix} \eta^0_{MEK} \\ \gamma_{MEK} \end{pmatrix} := \begin{pmatrix} \text{Solution}_1 \\ \text{Solution}_2 \cdot -1 \end{pmatrix} \quad \boxed{\gamma_{MEK} = 0.95} \quad \boxed{\eta^0_{MEK} = 3.922 \times 10^{-5}}$$

$$F(z, t) := \begin{pmatrix} t_1 \cdot e^{-t_2 \frac{z \cdot MW_{DEK} - V_{compressDEK}}{z \cdot MW_{DEK} - V_{compressDEK}}} \\ \exp\left(-t_2 \frac{V_{compressDEK}}{z \cdot MW_{DEK} - V_{compressDEK}}\right) \\ -t_1 \frac{V_{compressDEK}}{z \cdot MW_{DEK} - V_{compressDEK}} \cdot \exp\left(-t_2 \frac{V_{compressDEK}}{z \cdot MW_{DEK} - V_{compressDEK}}\right) \end{pmatrix}$$

Appendix 4

$$Y_i := V p_{i, \text{DEK}}$$

$$v y_i := \left(\eta^{(\text{DEK})} \right)_i \quad v g := \begin{pmatrix} 100 \\ -0.5 \end{pmatrix}$$

Solution := genfit(Y, vy, vg, F)

$$\begin{pmatrix} \eta^{0\text{DEK}} \\ \gamma^{\text{DEK}} \end{pmatrix} := \begin{pmatrix} \text{Solution}_1 \\ \text{Solution}_2 \cdot -1 \end{pmatrix} \quad \boxed{\gamma^{\text{DEK}} = 0.823} \quad \boxed{\eta^{0\text{DEK}} = 4.427 \times 10^{-5}}$$



Giving back the units

$$T := T \cdot (\text{K}) \quad R := R \cdot \left(\frac{\text{kg m}^2}{\text{s}^2 \text{K mol}} \right)$$

$$MW := MW \cdot \left(\frac{\text{kg}}{\text{mol}} \right) \quad \eta := \eta \cdot \left(\frac{\text{kg}}{\text{m s}} \right) \quad \rho := \rho \cdot \left(\frac{\text{kg}}{\text{m}^3} \right)$$

$$\gamma_{VK} := \gamma_{VK} \cdot (\text{K}) \quad KT := KT \cdot (\text{K}) \quad Vc := Vc \cdot \left(\frac{\text{m}^3}{\text{mol}} \right)$$

$$V_{\text{compress}} := V_{\text{compress}} \cdot \frac{\text{m}^3}{\text{mol}}$$

$$V_p := V_p \cdot \frac{\text{m}^3}{\text{kg}}$$



11) Diffusion coefficient according to Wesseling

count := 1 .. 2

Pure MEK

$$x := x_m$$

$$\begin{pmatrix} \gamma^{\text{PDMS}} \\ \gamma^{\text{MEK}} \\ \gamma^{\text{DEK}} \\ \gamma^{\text{TEGDME}} \\ \gamma^{\text{PEGDME}} \end{pmatrix} := \begin{pmatrix} 0.7 \\ 0.7 \\ 0.7 \\ 0.7 \\ 0.7 \end{pmatrix}$$

comp1 := MEK

comp2 := PDMS

$$V_{\text{comp}} := \begin{pmatrix} V_{\text{compressMEK}} \\ V_{\text{compressPDMS}} \end{pmatrix}$$

$$mw := \begin{pmatrix} MW_{\text{MEK}} \\ MW_{\text{PDMS}} \end{pmatrix}$$

$$d_{\text{count}} := 2 \sqrt{\frac{3}{4} \frac{V_{\text{compcount}}}{\pi \cdot Avog}}$$

$$\rho_{\text{compcount}} := \frac{mw_{\text{count}}}{V_{\text{compcount}}}$$

$$\sigma_{\text{count}} := \frac{x_{\text{count}} \cdot (V_{\text{compcount}})^{\frac{2}{3}}}{\sum_{\text{count}} x_{\text{count}} \cdot (V_{\text{compcount}})^{\frac{2}{3}}}$$

$$V_{\text{free}} := x_1 \cdot V_{\text{free_i_comp1}} + x_2 \cdot V_{\text{free_i_comp2}}$$

$$V_{\text{ff_count}} := \frac{\sigma_{\text{count}}}{x_{\text{count}}} \cdot V_{\text{free}}$$

$$\rho_{\text{mix}} := \sum_{\text{count}} x_{\text{count}} \cdot \rho_{\text{compcount}}$$

$$\zeta_{0_count} := 2 \cdot \text{Avog} \cdot \sqrt{3 \cdot k_B \cdot T_{\text{TempIndex}} \cdot \rho_{\text{mix}} \cdot d_{\text{count}}}$$

$$\zeta_{\text{eff}_1} := \zeta_{0_1} \cdot e^{\frac{\gamma_{\text{comp1}} \cdot V_{\text{comp1}}}{V_{\text{ff}_1}}} \quad \zeta_{\text{eff}_2} := \zeta_{0_2} \cdot e^{\frac{\gamma_{\text{comp2}} \cdot V_{\text{comp2}}}{V_{\text{ff}_2}}}$$

$$D_{\text{m_count}} := \frac{R \cdot T_{\text{TempIndex}}}{\zeta_{\text{eff_count}}} \quad D_{\text{m}} = \begin{pmatrix} 2.555 \times 10^{-9} \\ 2.554 \times 10^{-9} \end{pmatrix} \frac{\text{m}^2}{\text{s}}$$

$$x := x_{\text{d}} \quad \begin{pmatrix} \gamma_{\text{PDMS}} \\ \gamma_{\text{MEK}} \\ \gamma_{\text{DEK}} \\ \gamma_{\text{TEGDME}} \\ \gamma_{\text{PEGDME}} \end{pmatrix} := \begin{pmatrix} 0.7 \\ 0.7 \\ 0.7 \\ 0.7 \\ 0.7 \end{pmatrix}$$

$$\text{comp1} := \text{DEK} \quad \text{comp2} := \text{PDMS} \quad V_{\text{comp}} := \begin{pmatrix} V_{\text{compressDEK}} \\ V_{\text{compressPDMS}} \end{pmatrix} \quad \text{mw} := \begin{pmatrix} \text{MW}_{\text{DEK}} \\ \text{MW}_{\text{PDMS}} \end{pmatrix}$$

$$d_{\text{count}} := 2 \sqrt{\frac{3}{4} \cdot \frac{V_{\text{compcount}}}{\pi \cdot \text{Avog}}} \quad \rho_{\text{compcount}} := \frac{\text{mw}_{\text{count}}}{V_{\text{compcount}}} \quad \sigma_{\text{count}} := \frac{x_{\text{count}} \cdot (V_{\text{compcount}})^{\frac{2}{3}}}{\sum_{\text{count}} x_{\text{count}} \cdot (V_{\text{compcount}})^{\frac{2}{3}}} \quad V_{\text{free}} := x_1 \cdot V_{\text{free_comp1}} + x_2 \cdot V_{\text{free_comp2}}$$

$$V_{\text{ff_count}} := \frac{\sigma_{\text{count}}}{x_{\text{count}}} \cdot V_{\text{free}} \quad \rho_{\text{mix}} := \sum_{\text{count}} x_{\text{count}} \cdot \rho_{\text{compcount}}$$

$$\zeta_{0_count} := 2 \cdot \text{Avog} \cdot \sqrt{3 \cdot k_B \cdot T_{\text{TempIndex}} \cdot \rho_{\text{mix}} \cdot d_{\text{count}}}$$

$$\zeta_{\text{eff}_1} := \zeta_{0_1} \cdot e^{\frac{\gamma_{\text{comp1}} \cdot V_{\text{comp1}}}{V_{\text{ff}_1}}} \quad \zeta_{\text{eff}_2} := \zeta_{0_2} \cdot e^{\frac{\gamma_{\text{comp2}} \cdot V_{\text{comp2}}}{V_{\text{ff}_2}}}$$

$$D_{\text{m_count}} := \frac{R \cdot T_{\text{TempIndex}}}{\zeta_{\text{eff_count}}} \quad D_{\text{m}} = \begin{pmatrix} 2.162 \times 10^{-9} \\ 2.606 \times 10^{-9} \end{pmatrix} \frac{\text{m}^2}{\text{s}}$$

11.1 MEK/TEGDME/PDMS 5wt%

count := 1..3

$$\text{comp1} := \text{MEK} \quad \text{comp2} := \text{TEGDME} \quad \text{comp3} := \text{PDMS} \quad V_{\text{comp}} := \begin{pmatrix} V_{\text{compressMEK}} \\ V_{\text{compressTEGDME}} \\ V_{\text{compressPDMS}} \end{pmatrix} \quad \text{mw} := \begin{pmatrix} \text{MW}_{\text{MEK}} \\ \text{MW}_{\text{TEGDME}} \\ \text{MW}_{\text{PDMS}} \end{pmatrix} \quad x := x_{\text{mt}}$$

$$\begin{pmatrix} \gamma_{\text{PDMS}} \\ \gamma_{\text{MEK}} \\ \gamma_{\text{DEK}} \\ \gamma_{\text{TEGDME}} \\ \gamma_{\text{PEGDME}} \end{pmatrix} := \begin{pmatrix} 0.69 \\ 0.69 \\ 0.69 \\ 0.69 \\ 0.69 \end{pmatrix} \quad \begin{pmatrix} \gamma_{\text{MEK}} \\ \gamma_{\text{DEK}} \\ \gamma_{\text{TEGDME}} \\ \gamma_{\text{PEGDME}} \end{pmatrix} := \begin{pmatrix} 0.75 \\ 0.7 \\ 0.65 \\ 0.625 \end{pmatrix} \quad \begin{pmatrix} \gamma_{\text{PDMS}} \\ \gamma_{\text{MEK}} \\ \gamma_{\text{DEK}} \\ \gamma_{\text{TEGDME}} \\ \gamma_{\text{PEGDME}} \end{pmatrix} := \begin{pmatrix} 0.7 \\ 0.7 \\ 0.7 \\ 0.7 \\ 0.7 \end{pmatrix} \quad \begin{pmatrix} \gamma_{\text{PDMS}} \\ \gamma_{\text{MEK}} \\ \gamma_{\text{DEK}} \\ \gamma_{\text{TEGDME}} \\ \gamma_{\text{PEGDME}} \end{pmatrix} := \begin{pmatrix} 1 \\ 1 \\ 1 \\ 1 \\ 1 \end{pmatrix} \quad \begin{pmatrix} \gamma_{\text{PDMS}} \\ \gamma_{\text{MEK}} \\ \gamma_{\text{DEK}} \\ \gamma_{\text{TEGDME}} \\ \gamma_{\text{PEGDME}} \end{pmatrix} := \begin{pmatrix} 0.5 \\ 0.5 \\ 0.5 \\ 0.5 \\ 0.5 \end{pmatrix} \quad \begin{pmatrix} \gamma_{\text{PDMS}} \\ \gamma_{\text{MEK}} \\ \gamma_{\text{DEK}} \\ \gamma_{\text{TEGDME}} \\ \gamma_{\text{PEGDME}} \end{pmatrix} := \begin{pmatrix} 0.7 \\ 0.75 \\ 0.65 \\ 0.675 \end{pmatrix} \quad \begin{pmatrix} \gamma_{\text{PDMS}} \\ \gamma_{\text{MEK}} \\ \gamma_{\text{DEK}} \\ \gamma_{\text{TEGDME}} \\ \gamma_{\text{PEGDME}} \end{pmatrix} := \begin{pmatrix} 0.75 \\ 0.75 \\ 0.725 \\ 0.675 \end{pmatrix}$$

$$d_{\text{count}} := 2 \sqrt[3]{\frac{V_{\text{compcount}}}{\frac{4}{3} \cdot \pi \cdot \text{Avog}}} \quad \rho_{\text{compcount}} := \frac{m_{\text{wcount}}}{V_{\text{compcount}}}$$

$$\sigma_{\text{composition, count}} := \frac{x_{\text{composition, count}} \cdot (V_{\text{compcount}})^{\frac{2}{3}}}{\sum_{\text{count}} x_{\text{composition, count}} \cdot (V_{\text{compcount}})^{\frac{2}{3}}}$$

$$V_{\text{freecomposition}} := x_{\text{composition, 1}} \cdot V_{\text{free, 1comp1}} + x_{\text{composition, 2}} \cdot V_{\text{free, 1comp2}} + x_{\text{composition, 3}} \cdot V_{\text{free, 1comp3}}$$

$$V_{\text{ffcomposition, count}} := \frac{\sigma_{\text{composition, count}}}{x_{\text{composition, count}}} \cdot V_{\text{freecomposition}}$$

$$\rho_{\text{mixcomposition}} := \sum_{\text{count}} x_{\text{composition, count}} \cdot \rho_{\text{compcount}}$$

$$\zeta_{0\text{composition, count}} := 2 \cdot \text{Avog} \cdot \sqrt{3 \cdot k_B \cdot T_{\text{TempIndex}} \cdot \rho_{\text{mixcomposition}} \cdot d_{\text{count}}}$$

$$\zeta_{\text{effcomposition, 1}} := \zeta_{0\text{composition, 1}} \cdot e^{\frac{\gamma_{\text{comp1}}}{V_{\text{ffcomposition, 1}}} \cdot \frac{V_{\text{comp1}}}{V_{\text{ffcomposition, 1}}}}$$

$$\zeta_{\text{effcomposition, 2}} := \zeta_{0\text{composition, 2}} \cdot e^{\frac{\gamma_{\text{comp2}}}{V_{\text{ffcomposition, 2}}} \cdot \frac{V_{\text{comp2}}}{V_{\text{ffcomposition, 2}}}}$$

$$\zeta_{\text{effcomposition, 3}} := \zeta_{0\text{composition, 3}} \cdot e^{\frac{\gamma_{\text{comp3}}}{V_{\text{ffcomposition, 3}}} \cdot \frac{V_{\text{comp3}}}{V_{\text{ffcomposition, 3}}}}$$

$$D_{\text{mtcomposition, count}} := \frac{R \cdot T_{\text{TempIndex}}}{\zeta_{\text{effcomposition, count}}}$$

$$D_{\text{mt}} = \begin{pmatrix} 1.983 \times 10^{-9} & 9.203 \times 10^{-10} & 1.982 \times 10^{-9} \\ 1.764 \times 10^{-9} & 7.961 \times 10^{-10} & 1.763 \times 10^{-9} \\ 1.537 \times 10^{-9} & 6.71 \times 10^{-10} & 1.536 \times 10^{-9} \end{pmatrix} \frac{\text{m}^2}{\text{s}}$$

11.2 MEK/PEGDME/PDMS

$$\begin{aligned} \text{comp1} &:= \text{MEK} \\ \text{comp2} &:= \text{PEGDME} \\ \text{comp3} &:= \text{PDMS} \end{aligned} \quad V_{\text{comp}} := \begin{pmatrix} V_{\text{compressMEK}} \\ V_{\text{compressPEGDME}} \\ V_{\text{compressPDMS}} \end{pmatrix} \quad m_{\text{w}} := \begin{pmatrix} MW_{\text{MEK}} \\ MW_{\text{PEGDME}} \\ MW_{\text{PDMS}} \end{pmatrix} \quad x := x_{\text{mp}}$$

$$d_{\text{count}} := 2 \sqrt[3]{\frac{V_{\text{compcount}}}{\frac{4}{3} \cdot \pi \cdot \text{Avog}}} \quad \rho_{\text{compcount}} := \frac{m_{\text{wcount}}}{V_{\text{compcount}}}$$

$$\sigma_{\text{composition, count}} := \frac{x_{\text{composition, count}} \cdot (V_{\text{compcount}})^{\frac{2}{3}}}{\sum_{\text{count}} x_{\text{composition, count}} \cdot (V_{\text{compcount}})^{\frac{2}{3}}}$$

$$V_{\text{freecomposition}} := x_{\text{composition, 1}} \cdot V_{\text{free, 1comp1}} + x_{\text{composition, 2}} \cdot V_{\text{free, 1comp2}} + x_{\text{composition, 3}} \cdot V_{\text{free, 1comp3}}$$

$$V_{\text{ffcomposition, count}} := \frac{\sigma_{\text{composition, count}}}{x_{\text{composition, count}}} \cdot V_{\text{freecomposition}}$$

$$\rho_{\text{mixcomposition}} := \sum_{\text{count}} x_{\text{composition, count}} \cdot \rho_{\text{compcount}}$$

$$\zeta_{0\text{composition, count}} := 2 \cdot \text{Avog} \cdot \sqrt{3 \cdot k_B \cdot T_{\text{TempIndex}} \cdot \rho_{\text{mixcomposition}} \cdot d_{\text{count}}}$$

$$\zeta_{\text{effcomposition, 1}} := \zeta_{0\text{composition, 1}} \cdot e^{\frac{\gamma_{\text{comp1}}}{V_{\text{ffcomposition, 1}}} \cdot \frac{V_{\text{comp1}}}{V_{\text{ffcomposition, 1}}}}$$

$$\zeta_{\text{effcomposition, 2}} := \zeta_{0\text{composition, 2}} \cdot e^{\frac{\gamma_{\text{comp2}}}{V_{\text{ffcomposition, 2}}} \cdot \frac{V_{\text{comp2}}}{V_{\text{ffcomposition, 2}}}}$$

$$\zeta_{\text{effcomposition, 3}} := \zeta_{0\text{composition, 3}} \cdot e^{\frac{\gamma_{\text{comp3}}}{V_{\text{ffcomposition, 3}}} \cdot \frac{V_{\text{comp3}}}{V_{\text{ffcomposition, 3}}}}$$

$$D_{\text{mpcomposition, count}} := \frac{R \cdot T_{\text{TempIndex}}}{\zeta_{\text{effcomposition, count}}}$$

11.3 DEK/TEGDME/PDMS

$$\begin{aligned} \text{comp1} &:= \text{DEK} \\ \text{comp2} &:= \text{TEGDME} \\ \text{comp3} &:= \text{PDMS} \end{aligned} \quad \text{Vcomp} := \begin{pmatrix} \text{VcompressDEK} \\ \text{VcompressTEGDME} \\ \text{VcompressPDMS} \end{pmatrix} \quad \text{mw} := \begin{pmatrix} \text{MWDEK} \\ \text{MWTEGDME} \\ \text{MWPDMS} \end{pmatrix} \quad x := x_{\text{dt}}$$

$$d_{\text{count}} := 2 \sqrt[3]{\frac{\text{Vcomp}_{\text{count}}}{\frac{4}{3} \cdot \pi \cdot \text{Avog}}} \quad \rho_{\text{compcount}} := \frac{\text{mw}_{\text{count}}}{\text{Vcomp}_{\text{count}}}$$

$$\sigma_{\text{composition, count}} := \frac{x_{\text{composition, count}} \cdot (\text{Vcomp}_{\text{count}})^{\frac{2}{3}}}{\sum_{\text{count}} x_{\text{composition, count}} \cdot (\text{Vcomp}_{\text{count}})^{\frac{2}{3}}} \quad \text{Vfree}_{\text{composition}} := x_{\text{composition, 1}} \cdot \text{Vfree}_{\text{icomp1}} + x_{\text{composition, 2}} \cdot \text{Vfree}_{\text{icomp2}} + x_{\text{composition, 3}} \cdot \text{Vfree}_{\text{icomp3}}$$

$$\text{Vff}_{\text{composition, count}} := \frac{\sigma_{\text{composition, count}}}{x_{\text{composition, count}}} \cdot \text{Vfree}_{\text{composition}} \quad \rho_{\text{mix}_{\text{composition}}} := \sum_{\text{count}} x_{\text{composition, count}} \cdot \rho_{\text{compcount}}$$

$$\zeta_{\text{0composition, count}} := 2 \cdot \text{Avog} \cdot \sqrt{3 \cdot k_{\text{B}} \cdot T_{\text{TempIndex}} \cdot \rho_{\text{mix}_{\text{composition}}} \cdot d_{\text{count}}}$$

$$\zeta_{\text{eff}_{\text{composition, 1}}} := \zeta_{\text{0composition, 1}} \cdot e^{\frac{\gamma_{\text{comp1}}}{\text{Vff}_{\text{composition, 1}}}} \quad \zeta_{\text{eff}_{\text{composition, 2}}} := \zeta_{\text{0composition, 2}} \cdot e^{\frac{\gamma_{\text{comp2}}}{\text{Vff}_{\text{composition, 2}}}} \quad \zeta_{\text{eff}_{\text{composition, 3}}} := \zeta_{\text{0composition, 3}} \cdot e^{\frac{\gamma_{\text{comp3}}}{\text{Vff}_{\text{composition, 3}}}}$$

$$D_{\text{dt}_{\text{composition, count}}} := \frac{R \cdot T_{\text{TempIndex}}}{\zeta_{\text{eff}_{\text{composition, count}}}}$$

11.4 DEK/PEGDME/PDMS

$$\begin{aligned} \text{comp1} &:= \text{DEK} \\ \text{comp2} &:= \text{PEGDME} \\ \text{comp3} &:= \text{PDMS} \end{aligned} \quad \text{Vcomp} := \begin{pmatrix} \text{VcompressDEK} \\ \text{VcompressPEGDME} \\ \text{VcompressPDMS} \end{pmatrix} \quad \text{mw} := \begin{pmatrix} \text{MWDEK} \\ \text{MWPEGDME} \\ \text{MWPDMS} \end{pmatrix} \quad x := x_{\text{dp}}$$

$$d_{\text{count}} := 2 \sqrt[3]{\frac{\text{Vcomp}_{\text{count}}}{\frac{4}{3} \cdot \pi \cdot \text{Avog}}} \quad \rho_{\text{compcount}} := \frac{\text{mw}_{\text{count}}}{\text{Vcomp}_{\text{count}}}$$

$$\sigma_{\text{composition, count}} := \frac{x_{\text{composition, count}} \cdot (\text{Vcomp}_{\text{count}})^{\frac{2}{3}}}{\sum_{\text{count}} x_{\text{composition, count}} \cdot (\text{Vcomp}_{\text{count}})^{\frac{2}{3}}} \quad \text{Vfree}_{\text{composition}} := x_{\text{composition, 1}} \cdot \text{Vfree}_{\text{icomp1}} + x_{\text{composition, 2}} \cdot \text{Vfree}_{\text{icomp2}} + x_{\text{composition, 3}} \cdot \text{Vfree}_{\text{icomp3}}$$

$$\text{Vff}_{\text{composition, count}} := \frac{\sigma_{\text{composition, count}}}{x_{\text{composition, count}}} \cdot \text{Vfree}_{\text{composition}} \quad \rho_{\text{mix}_{\text{composition}}} := \sum_{\text{count}} x_{\text{composition, count}} \cdot \rho_{\text{compcount}}$$

$$\zeta_{\text{0composition, count}} := 2 \cdot \text{Avog} \cdot \sqrt{3 \cdot k_{\text{B}} \cdot T_{\text{TempIndex}} \cdot \rho_{\text{mix}_{\text{composition}}} \cdot d_{\text{count}}}$$

$$\zeta_{\text{eff}_{\text{composition, 1}}} := \zeta_{\text{0composition, 1}} \cdot e^{\frac{\gamma_{\text{comp1}}}{\text{Vff}_{\text{composition, 1}}}} \quad \zeta_{\text{eff}_{\text{composition, 2}}} := \zeta_{\text{0composition, 2}} \cdot e^{\frac{\gamma_{\text{comp2}}}{\text{Vff}_{\text{composition, 2}}}} \quad \zeta_{\text{eff}_{\text{composition, 3}}} := \zeta_{\text{0composition, 3}} \cdot e^{\frac{\gamma_{\text{comp3}}}{\text{Vff}_{\text{composition, 3}}}}$$

$$D_{\text{dp}_{\text{composition, count}}} := \frac{R \cdot T_{\text{TempIndex}}}{\zeta_{\text{eff}_{\text{composition, count}}}}$$

$$D_mt = \begin{pmatrix} 1.983 \times 10^{-9} & 9.203 \times 10^{-10} & 1.982 \times 10^{-9} \\ 1.764 \times 10^{-9} & 7.961 \times 10^{-10} & 1.763 \times 10^{-9} \\ 1.537 \times 10^{-9} & 6.71 \times 10^{-10} & 1.536 \times 10^{-9} \end{pmatrix} \frac{m^2}{s}$$

$$D_mp = \begin{pmatrix} 1.93 \times 10^{-9} & 5.552 \times 10^{-10} & 1.928 \times 10^{-9} \\ 1.666 \times 10^{-9} & 4.512 \times 10^{-10} & 1.665 \times 10^{-9} \\ 1.431 \times 10^{-9} & 3.642 \times 10^{-10} & 1.43 \times 10^{-9} \end{pmatrix} \frac{m^2}{s}$$

$$D_dt = \begin{pmatrix} 1.87 \times 10^{-9} & 9.87 \times 10^{-10} & 2.101 \times 10^{-9} \\ 1.727 \times 10^{-9} & 8.977 \times 10^{-10} & 1.945 \times 10^{-9} \\ 1.57 \times 10^{-9} & 8.01 \times 10^{-10} & 1.774 \times 10^{-9} \end{pmatrix} \frac{m^2}{s}$$

$$D_dp = \begin{pmatrix} 1.83 \times 10^{-9} & 6.063 \times 10^{-10} & 2.058 \times 10^{-9} \\ 1.658 \times 10^{-9} & 5.301 \times 10^{-10} & 1.87 \times 10^{-9} \\ 1.479 \times 10^{-9} & 4.538 \times 10^{-10} & 1.675 \times 10^{-9} \end{pmatrix} \frac{m^2}{s}$$

stack(D_mt, D_mp, D_dt, D_dp) · 10⁹ =

	1	2	3
1	1.983	0.92	1.982
2	1.764	0.796	1.763
3	1.537	0.671	1.536
4	1.93	0.555	1.928
5	1.666	0.451	1.665
6	1.431	0.364	1.43
7	1.87	0.987	2.101
8	1.727	0.898	1.945
9	1.57	0.801	1.774
10	1.83	0.606	2.058
11	1.658	0.53	1.87
12	1.479	0.454	1.675

$\frac{m^2}{s}$

$$V_{PTemplIndex, PDMS} := V_{PTemplIndex, PDMS} \cdot I \quad \begin{pmatrix} \xi_{MEK} \\ \xi_{DEK} \\ \xi_{TEGDME} \\ \xi_{PEGDME} \end{pmatrix} := \begin{pmatrix} 1.193 \\ 1.209 \\ 0.770 \\ 0.950 \end{pmatrix}$$

12.1.1 MEK/TEGDME/PDMS 5wt% $\omega 1 := \omega_mt_{1,1}$ $\omega 2 := \omega_mt_{1,2}$ $\omega 3 := \omega_mt_{1,3}$

$$D_{mt_{1,1}} := D_{0_{MEK}} \cdot e^{-\frac{\omega 1 \cdot V_{ch_{MEK}} + \omega 2 \cdot V_{ch_{TEGDME}} \cdot \frac{\xi_{MEK}}{\xi_{TEGDME}} + \omega 3 \cdot V_{ch_{PDMS}} \cdot \frac{\xi_{MEK}}{\xi_{TEGDME}}}{\omega 1 \cdot f_{r_{TemplIndex, MEK}} \cdot V_{PTemplIndex, MEK} + \omega 2 \cdot f_{r_{TemplIndex, TEGDME}} \cdot V_{PTemplIndex, TEGDME} + \omega 3 \cdot f_{r_{TemplIndex, PDMS}} \cdot V_{PTemplIndex, PDMS}}} \quad \omega 1 = 0.516$$

$$D_{mt_{1,2}} := D_{0_{TEGDME}} \cdot e^{-\frac{\omega 1 \cdot V_{ch_{MEK}} \cdot \frac{\xi_{TEGDME}}{\xi_{MEK}} + \omega 2 \cdot V_{ch_{TEGDME}} + \omega 3 \cdot V_{ch_{PDMS}} \cdot \frac{\xi_{TEGDME}}{\xi_{MEK}}}{\omega 1 \cdot f_{r_{TemplIndex, MEK}} \cdot V_{PTemplIndex, MEK} + \omega 2 \cdot f_{r_{TemplIndex, TEGDME}} \cdot V_{PTemplIndex, TEGDME} + \omega 3 \cdot f_{r_{TemplIndex, PDMS}} \cdot V_{PTemplIndex, PDMS}}} \quad \omega 2 = 0.027$$

$$\omega 3 = 0.457$$

12.1.2 MEK/TEGDME/PDMS 10wt% $\omega 1 := \omega_mt_{2,1}$ $\omega 2 := \omega_mt_{2,2}$ $\omega 3 := \omega_mt_{2,3}$

$$D_{mt_{2,1}} := D_{0_{MEK}} \cdot e^{-\frac{\omega 1 \cdot V_{ch_{MEK}} + \omega 2 \cdot V_{ch_{TEGDME}} \cdot \frac{\xi_{MEK}}{\xi_{TEGDME}} + \omega 3 \cdot V_{ch_{PDMS}} \cdot \frac{\xi_{MEK}}{\xi_{TEGDME}}}{\omega 1 \cdot f_{r_{TemplIndex, MEK}} \cdot V_{PTemplIndex, MEK} + \omega 2 \cdot f_{r_{TemplIndex, TEGDME}} \cdot V_{PTemplIndex, TEGDME} + \omega 3 \cdot f_{r_{TemplIndex, PDMS}} \cdot V_{PTemplIndex, PDMS}}} \quad \omega 1 = 0.516$$

$$D_{mt_{2,2}} := D_{0_{TEGDME}} \cdot e^{-\frac{\omega 1 \cdot V_{ch_{MEK}} \cdot \frac{\xi_{TEGDME}}{\xi_{MEK}} + \omega 2 \cdot V_{ch_{TEGDME}} + \omega 3 \cdot V_{ch_{PDMS}} \cdot \frac{\xi_{TEGDME}}{\xi_{MEK}}}{\omega 1 \cdot f_{r_{TemplIndex, MEK}} \cdot V_{PTemplIndex, MEK} + \omega 2 \cdot f_{r_{TemplIndex, TEGDME}} \cdot V_{PTemplIndex, TEGDME} + \omega 3 \cdot f_{r_{TemplIndex, PDMS}} \cdot V_{PTemplIndex, PDMS}}} \quad \omega 2 = 0.027$$

$$\omega 3 = 0.457$$

12.3.3 DEK/TEGDME/PDMS 15wt%

$$\omega_1 := \omega_{dt_{3,1}} \quad \omega_2 := \omega_{dt_{3,2}} \quad \omega_3 := \omega_{dt_{3,3}}$$

$$Ddt_{3,1} := D0_{DEK} \cdot e^{-\left(\omega_1 V_{ch_{DEK}} + \omega_2 V_{ch_{TEGDME}} \frac{\xi_{DEK}}{\xi_{TEGDME}} + \omega_3 V_{ch_{PDMS}} \frac{\xi_{DEK}}{\xi_{TEGDME}} \right) \frac{\omega_1 f_{T_{TemplIndex, DEK}} V_{p_{TemplIndex, DEK}} + \omega_2 f_{T_{TemplIndex, TEGDME}} V_{p_{TemplIndex, TEGDME}} + \omega_3 f_{T_{TemplIndex, PDMS}} V_{p_{TemplIndex, PDMS}}}{\xi_{DEK}}}$$

$$Ddt_{3,2} := D0_{TEGDME} \cdot e^{-\left(\omega_1 V_{ch_{DEK}} \frac{\xi_{TEGDME}}{\xi_{DEK}} + \omega_2 V_{ch_{TEGDME}} + \omega_3 V_{ch_{PDMS}} \frac{\xi_{TEGDME}}{\xi_{TEGDME}} \right) \frac{\omega_1 f_{T_{TemplIndex, DEK}} V_{p_{TemplIndex, DEK}} + \omega_2 f_{T_{TemplIndex, TEGDME}} V_{p_{TemplIndex, TEGDME}} + \omega_3 f_{T_{TemplIndex, PDMS}} V_{p_{TemplIndex, PDMS}}}{\xi_{TEGDME}}}$$

12.4.1 DEK/PEGDME/PDMS 5wt%

$$\omega_1 := \omega_{dp_{1,1}} \quad \omega_2 := \omega_{dp_{1,2}} \quad \omega_3 := \omega_{dp_{1,3}}$$

$$Ddp_{1,1} := D0_{DEK} \cdot e^{-\left(\omega_1 V_{ch_{DEK}} + \omega_2 V_{ch_{PEGDME}} \frac{\xi_{DEK}}{\xi_{PEGDME}} + \omega_3 V_{ch_{PDMS}} \frac{\xi_{DEK}}{\xi_{DEK}} \right) \frac{\omega_1 f_{T_{TemplIndex, DEK}} V_{p_{TemplIndex, DEK}} + \omega_2 f_{T_{TemplIndex, PEGDME}} V_{p_{TemplIndex, PEGDME}} + \omega_3 f_{T_{TemplIndex, PDMS}} V_{p_{TemplIndex, PDMS}}}{\xi_{DEK}}}$$

$$Ddp_{1,2} := D0_{PEGDME} \cdot e^{-\left(\omega_1 V_{ch_{DEK}} \frac{\xi_{PEGDME}}{\xi_{DEK}} + \omega_2 V_{ch_{PEGDME}} + \omega_3 V_{ch_{PDMS}} \frac{\xi_{PEGDME}}{\xi_{PEGDME}} \right) \frac{\omega_1 f_{T_{TemplIndex, DEK}} V_{p_{TemplIndex, DEK}} + \omega_2 f_{T_{TemplIndex, PEGDME}} V_{p_{TemplIndex, PEGDME}} + \omega_3 f_{T_{TemplIndex, PDMS}} V_{p_{TemplIndex, PDMS}}}{\xi_{DEK}}}$$

12.4.2 DEK/PEGDME/PDMS 10wt%

$$\omega_1 := \omega_{dp_{2,1}} \quad \omega_2 := \omega_{dp_{2,2}} \quad \omega_3 := \omega_{dp_{2,3}}$$

$$Ddp_{2,1} := D0_{DEK} \cdot e^{-\left(\omega_1 V_{ch_{DEK}} + \omega_2 V_{ch_{PEGDME}} \frac{\xi_{DEK}}{\xi_{PEGDME}} + \omega_3 V_{ch_{PDMS}} \frac{\xi_{DEK}}{\xi_{DEK}} \right) \frac{\omega_1 f_{T_{TemplIndex, DEK}} V_{p_{TemplIndex, DEK}} + \omega_2 f_{T_{TemplIndex, PEGDME}} V_{p_{TemplIndex, PEGDME}} + \omega_3 f_{T_{TemplIndex, PDMS}} V_{p_{TemplIndex, PDMS}}}{\xi_{DEK}}}$$

$$Ddp_{2,2} := D0_{PEGDME} \cdot e^{-\left(\omega_1 V_{ch_{DEK}} \frac{\xi_{PEGDME}}{\xi_{DEK}} + \omega_2 V_{ch_{PEGDME}} + \omega_3 V_{ch_{PDMS}} \frac{\xi_{PEGDME}}{\xi_{PEGDME}} \right) \frac{\omega_1 f_{T_{TemplIndex, DEK}} V_{p_{TemplIndex, DEK}} + \omega_2 f_{T_{TemplIndex, PEGDME}} V_{p_{TemplIndex, PEGDME}} + \omega_3 f_{T_{TemplIndex, PDMS}} V_{p_{TemplIndex, PDMS}}}{\xi_{DEK}}}$$

12.4.3 DEK/PEGDME/PDMS 15wt%

$$\omega_1 := \omega_{dp_{3,1}} \quad \omega_2 := \omega_{dp_{3,2}} \quad \omega_3 := \omega_{dp_{3,3}}$$

$$Ddp_{3,1} := D0_{DEK} \cdot e^{-\left(\omega_1 V_{ch_{DEK}} + \omega_2 V_{ch_{PEGDME}} \frac{\xi_{DEK}}{\xi_{PEGDME}} + \omega_3 V_{ch_{PDMS}} \frac{\xi_{DEK}}{\xi_{DEK}} \right) \frac{\omega_1 f_{T_{TemplIndex, DEK}} V_{p_{TemplIndex, DEK}} + \omega_2 f_{T_{TemplIndex, PEGDME}} V_{p_{TemplIndex, PEGDME}} + \omega_3 f_{T_{TemplIndex, PDMS}} V_{p_{TemplIndex, PDMS}}}{\xi_{DEK}}}$$

$$Ddp_{3,2} := D0_{PEGDME} \cdot e^{-\left(\omega_1 V_{ch_{DEK}} \frac{\xi_{PEGDME}}{\xi_{DEK}} + \omega_2 V_{ch_{PEGDME}} + \omega_3 V_{ch_{PDMS}} \frac{\xi_{PEGDME}}{\xi_{PEGDME}} \right) \frac{\omega_1 f_{T_{TemplIndex, DEK}} V_{p_{TemplIndex, DEK}} + \omega_2 f_{T_{TemplIndex, PEGDME}} V_{p_{TemplIndex, PEGDME}} + \omega_3 f_{T_{TemplIndex, PDMS}} V_{p_{TemplIndex, PDMS}}}{\xi_{DEK}}}$$

$$Dmt = \begin{pmatrix} 2.141 \times 10^{-9} & 8.102 \times 10^{-10} \\ 1.972 \times 10^{-9} & 7.685 \times 10^{-10} \\ 1.832 \times 10^{-9} & 7.327 \times 10^{-10} \end{pmatrix} \frac{m^2}{s} \quad Dmp = \begin{pmatrix} 2.125 \times 10^{-9} & 6.055 \times 10^{-10} \\ 1.95 \times 10^{-9} & 5.653 \times 10^{-10} \\ 1.811 \times 10^{-9} & 5.33 \times 10^{-10} \end{pmatrix} \frac{m^2}{s}$$

$$Ddt = \begin{pmatrix} 1.953 \times 10^{-9} & 9.144 \times 10^{-10} \\ 1.779 \times 10^{-9} & 8.617 \times 10^{-10} \\ 1.623 \times 10^{-9} & 8.127 \times 10^{-10} \end{pmatrix} \frac{m^2}{s} \quad Ddp = \begin{pmatrix} 1.941 \times 10^{-9} & 7.035 \times 10^{-10} \\ 1.761 \times 10^{-9} & 6.518 \times 10^{-10} \\ 1.604 \times 10^{-9} & 6.055 \times 10^{-10} \end{pmatrix} \frac{m^2}{s}$$

$$\begin{pmatrix} \xi_{MEK} \\ \xi_{DEK} \\ \xi_{TEGDME} \\ \xi_{PEGDME} \end{pmatrix} = \begin{pmatrix} 1.193 \\ 1.209 \\ 0.77 \\ 0.95 \end{pmatrix}$$

$$stack(Dmt, Dmp, Ddt, Ddp) \cdot 10^9 =$$

	1	2
1	2.141	0.81
2	1.972	0.768
3	1.832	0.733
4	2.125	0.605
5	1.95	0.565
6	1.811	0.533
7	1.953	0.914
8	1.779	0.862
9	1.623	0.813
10	1.941	0.703
11	1.761	0.652
12	1.604	0.606

13.4.3 DEK/PEGDME/PDMS 15wt%

$$\omega_1 := \omega_{dp_{3,1}} \quad \omega_2 := \omega_{dp_{3,2}} \quad \omega_3 := \omega_{dp_{3,3}}$$

$$Ddp_{3,1} := D0_{DEK} \cdot e^{-\left(\frac{\omega_1 V_{ch_{DEK}} + \omega_2 V_{ch_{PEGDME}} \xi_{DEK}}{\xi_{PEGDME}} + \omega_3 V_{ch_{PDMS}} \xi_{DEK} \right) \frac{V_p}{V_p}} \cdot e^{-\omega_1 f_{T_{TemplIndex, DEK}} + \omega_2 f_{T_{TemplIndex, PEGDME}} + \omega_3 f_{T_{TemplIndex, PDMS}}}$$

$$Ddp_{3,2} := D0_{PEGDME} \cdot e^{-\left(\frac{\omega_1 V_{ch_{DEK}} \xi_{PEGDME}}{\xi_{DEK}} + \omega_2 V_{ch_{PEGDME}} + \omega_3 V_{ch_{PDMS}} \xi_{PEGDME} \right) \frac{V_p}{V_p}} \cdot e^{-\omega_1 f_{T_{TemplIndex, DEK}} + \omega_2 f_{T_{TemplIndex, PEGDME}} + \omega_3 f_{T_{TemplIndex, PDMS}}}$$

$$\begin{aligned} Dmt &= \begin{pmatrix} 2.078 \times 10^{-9} & 8.469 \times 10^{-10} \\ 1.866 \times 10^{-9} & 7.913 \times 10^{-10} \\ 1.686 \times 10^{-9} & 7.42 \times 10^{-10} \end{pmatrix} \frac{m^2}{s} & Dmp &= \begin{pmatrix} 2.065 \times 10^{-9} & 5.985 \times 10^{-10} \\ 1.845 \times 10^{-9} & 5.474 \times 10^{-10} \\ 1.665 \times 10^{-9} & 5.045 \times 10^{-10} \end{pmatrix} \frac{m^2}{s} \\ Ddt &= \begin{pmatrix} 1.998 \times 10^{-9} & 9.499 \times 10^{-10} \\ 1.796 \times 10^{-9} & 8.883 \times 10^{-10} \\ 1.614 \times 10^{-9} & 8.301 \times 10^{-10} \end{pmatrix} \frac{m^2}{s} & Ddp &= \begin{pmatrix} 1.994 \times 10^{-9} & 6.937 \times 10^{-10} \\ 1.791 \times 10^{-9} & 6.37 \times 10^{-10} \\ 1.607 \times 10^{-9} & 5.847 \times 10^{-10} \end{pmatrix} \frac{m^2}{s} \end{aligned}$$

$$\begin{pmatrix} \xi_{MEK} \\ \xi_{DEK} \\ \xi_{TEGDME} \\ \xi_{PEGDME} \end{pmatrix} = \begin{pmatrix} 0.806 \\ 0.807 \\ 0.51 \\ 0.64 \end{pmatrix}$$

	1	2
1	2.078	0.847
2	1.866	0.791
3	1.686	0.742
4	2.065	0.599
5	1.845	0.547
6	1.665	0.505
7	1.998	0.95
8	1.796	0.888
9	1.614	0.83
10	1.994	0.694
11	1.791	0.637
12	1.607	0.585

$$\text{stack}(Dmt, Dmp, Ddt, Ddp) \cdot 10^9 = \frac{m^2}{s}$$

A4.2 Estimation of the concentration of the permeants inside the membrane

Concentration inside the membrane

0) Units definition

$$R := 8.314 \frac{\text{kgm}^2}{\text{s}^2 \text{K mol}} \quad \text{mPa} := \frac{\text{Pa}}{1000} \quad \text{Avog} := 6.022 \cdot 10^{23} \frac{1}{\text{mol}} \quad k_B := 1.38 \cdot 10^{-23} \frac{\text{J}}{\text{K}}$$

$$\text{bar} := 100000 \cdot \text{Pa} \quad \text{kmol} := 1000 \cdot \text{mol} \quad \text{Avog} := 6.02214179 \cdot 10^{23} \cdot \text{mol}^{-1}$$

$$\text{ml} := 1 \cdot \text{cm}^3$$

1) Component list

Component Index

PDMS	:=	1
MEK		2
DEK		3
TEGDME		4
PEGDME		5
TEG		6

Ncompounds := 1 .. 6

j := Ncompounds

k := 2 .. 6 All except the polymer

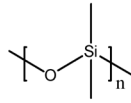
283.15	:=	K	1	1	K	Npoints := 1 .. 15
288.15			1	10		
293.15			2	15		
298.15			3	20		
303.15			4	25		
308.15			5	30		
313.15			6	35		
318.15			7	40		
323.15			8	45		
328.15			9	50		
333.15			10	55		
338.15			11	60		
343.15			12	65		
348.15			13	70		
353.15			14	75		
353.15	15	80				

T - 273.15K =

i := Npoints

2) Pure properties

2.1 PDMS



$$V_{p,PDMS} := 1.027 \cdot 10^{-3} \frac{\text{m}^3}{\text{kg}}$$

$$MW_{PDMS} := 74.1 \frac{\text{gm}}{\text{mol}}$$

$$V_{vdw,PDMS} := (16.6 + 5.25 + 2 \cdot 13.67) \frac{\text{cm}^3}{\text{mol}}$$

$$V_{vdw,PDMS} = 4.919 \times 10^{-5} \frac{\text{m}^3}{\text{mol}}$$

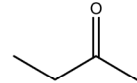
ρ1, PDMS	(0.974)
ρ2, PDMS	0.974
ρ3, PDMS	0.974
ρ4, PDMS	0.974
ρ5, PDMS	0.974
ρ6, PDMS	0.974
ρ7, PDMS	0.974
ρ8, PDMS	:= 0.974
ρ9, PDMS	0.974
ρ10, PDMS	0.974
ρ11, PDMS	0.974
ρ12, PDMS	0.974
ρ13, PDMS	0.974
ρ14, PDMS	(0.974)
ρ15, PDMS	(0.974)

$$V_{ch,PDMS} := 0.905 \frac{\text{cm}^3}{\text{gm}}$$

2.2 MEK

$$MW_{MEK} := 72.10692 \frac{\text{gm}}{\text{mol}}$$

$$V_{at0K,MEK} := 63.9 \frac{\text{cm}^3}{\text{mol}}$$



$$V_{c,MEK} := 267 \frac{\text{cm}^3}{\text{mol}}$$

<http://www.thermo.com/kdb/kdb/hcprop/showprop.php?cmpid=1192>

$$V_{vdw,MEK} := (2 \cdot 13.67 + 10 \cdot 23 + 11 \cdot 7) \frac{\text{cm}^3}{\text{mol}}$$

$$V_{vdw,MEK} = 4 \cdot 927 \times 10^{-5} \frac{\text{m}^3}{\text{mol}}$$

ρ1, MEK	(0.816)
ρ2, MEK	0.810
ρ3, MEK	0.805
ρ4, MEK	0.799
ρ5, MEK	0.794
ρ6, MEK	0.788
ρ7, MEK	0.783
ρ8, MEK	:= 0.777
ρ9, MEK	0.772
ρ10, MEK	0.766
ρ11, MEK	0.760
ρ12, MEK	0.754
ρ13, MEK	0.748
ρ14, MEK	0.742
ρ15, MEK	(0.736)

η1, MEK	(4.6762 × 10 ⁻⁴)
η2, MEK	4.4122 × 10 ⁻⁴
η3, MEK	4.1696 × 10 ⁻⁴
η4, MEK	3.9461 × 10 ⁻⁴
η5, MEK	3.7399 × 10 ⁻⁴
η6, MEK	3.5491 × 10 ⁻⁴
η7, MEK	3.3725 × 10 ⁻⁴
η8, MEK	:= 3.2085 × 10 ⁻⁴
η9, MEK	3.0562 × 10 ⁻⁴
η10, MEK	2.9143 × 10 ⁻⁴
η11, MEK	2.7821 × 10 ⁻⁴
η12, MEK	2.6586 × 10 ⁻⁴
η13, MEK	2.5432 × 10 ⁻⁴
η14, MEK	2.4351 × 10 ⁻⁴
η15, MEK	(2.3337 × 10 ⁻⁴)

	1
1	283.15
2	288.15
3	293.15
4	298.15
5	303.15
6	308.15
7	313.15
8	318.15
9	323.15
10	328.15
11	333.15
12	338.15
13	343.15
14	348.15
15	353.15

T = K

Appendix 4

2.3 DEK

$$MW_{\text{DEK}} := 86.1338 \frac{\text{gm}}{\text{mol}}$$

$$Vat0K_{\text{DEK}} := 78.4 \frac{\text{cm}^3}{\text{mol}}$$

c5h10o

$$5 \cdot 1.1 + 10 \cdot 6.7 + 5.9 = 78.4$$

$$Vc_{\text{DEK}} := 336 \frac{\text{cm}^3}{\text{mol}}$$

<http://www.chemic.org/kdb/kdb/hcprop/showprop.php?cmpid=1196>

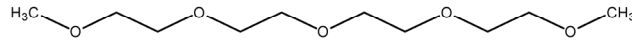
$$5 \cdot 0.77 + 10 \cdot 6.45 + 5.9 = 74.25$$

$$4 \cdot 0.77 + 8 \cdot 6.45 + 5.9 = 60.58$$

$$Vvdw_{\text{DEK}} := (2 \cdot 13.67 + 2 \cdot 10.23 + 11.7) \frac{\text{cm}^3}{\text{mol}}$$

$\begin{pmatrix} \rho_{1,\text{DEK}} \\ \rho_{2,\text{DEK}} \\ \rho_{3,\text{DEK}} \\ \rho_{4,\text{DEK}} \\ \rho_{5,\text{DEK}} \\ \rho_{6,\text{DEK}} \\ \rho_{7,\text{DEK}} \\ \rho_{8,\text{DEK}} \\ \rho_{9,\text{DEK}} \\ \rho_{10,\text{DEK}} \\ \rho_{11,\text{DEK}} \\ \rho_{12,\text{DEK}} \\ \rho_{13,\text{DEK}} \\ \rho_{14,\text{DEK}} \\ \rho_{15,\text{DEK}} \end{pmatrix} := \begin{pmatrix} 0.8241606 \\ 0.8192934 \\ 0.8143909 \\ 0.809452 \\ 0.8044755 \\ 0.7994602 \\ 0.7944049 \\ 0.7893084 \\ 0.7841691 \\ 0.7789856 \\ 0.7737564 \\ 0.7684799 \\ 0.7631542 \\ 0.7577776 \\ 0.7523481 \end{pmatrix} \frac{\text{gm}}{\text{cm}^3}$	$\begin{pmatrix} \eta_{1,\text{DEK}} \\ \eta_{2,\text{DEK}} \\ \eta_{3,\text{DEK}} \\ \eta_{4,\text{DEK}} \\ \eta_{5,\text{DEK}} \\ \eta_{6,\text{DEK}} \\ \eta_{7,\text{DEK}} \\ \eta_{8,\text{DEK}} \\ \eta_{9,\text{DEK}} \\ \eta_{10,\text{DEK}} \\ \eta_{11,\text{DEK}} \\ \eta_{12,\text{DEK}} \\ \eta_{13,\text{DEK}} \\ \eta_{14,\text{DEK}} \\ \eta_{15,\text{DEK}} \end{pmatrix} := \begin{pmatrix} 5.247 \times 10^{-4} \\ 4.953 \times 10^{-4} \\ 4.683 \times 10^{-4} \\ 4.435 \times 10^{-4} \\ 4.206 \times 10^{-4} \\ 3.995 \times 10^{-4} \\ 3.799 \times 10^{-4} \\ 3.617 \times 10^{-4} \\ 3.449 \times 10^{-4} \\ 3.292 \times 10^{-4} \\ 3.145 \times 10^{-4} \\ 3.009 \times 10^{-4} \\ 2.881 \times 10^{-4} \\ 2.762 \times 10^{-4} \\ 2.650 \times 10^{-4} \end{pmatrix} \text{Pa}\cdot\text{s}$
---	--

2.5 TEGDME



$$MW_{\text{TEGDME}} := 222.28168 \frac{\text{gm}}{\text{mol}}$$

$$Vat0K_{\text{TEGDME}} := 187.9 \frac{\text{cm}^3}{\text{mol}}$$

$$(2 \cdot 1.1 + 6 \cdot 6.7 + 5.9) + 4 \cdot (5.9 + 2 \cdot 1.1 + 4 \cdot 6.7) = 187.9$$

$$Vc_{\text{TEGDME}} := 691 \frac{\text{m}^3}{\text{kmol}}$$

$$Vvdw_{\text{TEGDME}} := [2 \cdot 13.67 + 5.25 + 4 \cdot (5.25 + 2 \cdot 10.23)] \frac{\text{cm}^3}{\text{mol}}$$

$\begin{pmatrix} \rho_{1,\text{TEGDME}} \\ \rho_{2,\text{TEGDME}} \\ \rho_{3,\text{TEGDME}} \\ \rho_{4,\text{TEGDME}} \\ \rho_{5,\text{TEGDME}} \\ \rho_{6,\text{TEGDME}} \\ \rho_{7,\text{TEGDME}} \\ \rho_{8,\text{TEGDME}} \\ \rho_{9,\text{TEGDME}} \\ \rho_{10,\text{TEGDME}} \\ \rho_{11,\text{TEGDME}} \\ \rho_{12,\text{TEGDME}} \\ \rho_{13,\text{TEGDME}} \\ \rho_{14,\text{TEGDME}} \\ \rho_{15,\text{TEGDME}} \end{pmatrix} := \begin{pmatrix} 1020 \\ 1016 \\ 1012 \\ 1007 \\ 1003 \\ 998.4 \\ 993.8 \\ 989.2 \\ 984.6 \\ 979.9 \\ 975.2 \\ 970.5 \\ 965.8 \\ 961.1 \\ 956.4 \end{pmatrix} \frac{\text{kg}}{\text{m}^3}$	$\begin{pmatrix} \eta_{1,\text{TEGDME}} \\ \eta_{2,\text{TEGDME}} \\ \eta_{3,\text{TEGDME}} \\ \eta_{4,\text{TEGDME}} \\ \eta_{5,\text{TEGDME}} \\ \eta_{6,\text{TEGDME}} \\ \eta_{7,\text{TEGDME}} \\ \eta_{8,\text{TEGDME}} \\ \eta_{9,\text{TEGDME}} \\ \eta_{10,\text{TEGDME}} \\ \eta_{11,\text{TEGDME}} \\ \eta_{12,\text{TEGDME}} \\ \eta_{13,\text{TEGDME}} \\ \eta_{14,\text{TEGDME}} \\ \eta_{15,\text{TEGDME}} \end{pmatrix} := \begin{pmatrix} 4.979 \times 10^{-3} \\ 4.361 \times 10^{-3} \\ 3.749 \times 10^{-3} \\ 3.348 \times 10^{-3} \\ 2.951 \times 10^{-3} \\ 2.673 \times 10^{-3} \\ 2.398 \times 10^{-3} \\ 2.201 \times 10^{-3} \\ 2.007 \times 10^{-3} \\ 1.848 \times 10^{-3} \\ 1.691 \times 10^{-3} \\ 1.569 \times 10^{-3} \\ 1.449 \times 10^{-3} \\ 1.352 \times 10^{-3} \\ 1.257 \times 10^{-3} \end{pmatrix} \text{Pa}\cdot\text{s}$
---	---

2.6 PEGDME 250

$$MW_{\text{PEGDME}} := 298.21 \frac{\text{gm}}{\text{mol}} \quad (2 \cdot 1.1 + 6 \cdot 6.7 + 5.9) + 5.723(5.9 + 2 \cdot 1.1 + 4 \cdot 6.7) = 248.033$$

$$V_{c,\text{PEGDME}} := \left(0.915 \frac{\text{m}^3}{\text{kmol}} \right)$$

$$V_{at0K,\text{PEGDME}} := 248.03 \frac{\text{cm}^3}{\text{mol}} \quad n = 5.723$$

ρ1, PEGDME	
ρ2, PEGDME	1044
ρ3, PEGDME	1040
ρ4, PEGDME	1036
ρ5, PEGDME	1031
ρ6, PEGDME	1026
ρ7, PEGDME	1022
ρ8, PEGDME	1017
ρ9, PEGDME	1013
ρ10, PEGDME	1008
ρ11, PEGDME	1004
ρ12, PEGDME	999.5
ρ13, PEGDME	995.1
ρ14, PEGDME	990.6
ρ15, PEGDME	981.7

η1, PEGDME	10.23 × 10 ⁻³
η2, PEGDME	8.843 × 10 ⁻³
η3, PEGDME	7.471 × 10 ⁻³
η4, PEGDME	6.552 × 10 ⁻³
η5, PEGDME	5.601 × 10 ⁻³
η6, PEGDME	4.980 × 10 ⁻³
η7, PEGDME	4.365 × 10 ⁻³
η8, PEGDME	3.927 × 10 ⁻³
η9, PEGDME	3.493 × 10 ⁻³
η10, PEGDME	3.180 × 10 ⁻³
η11, PEGDME	2.869 × 10 ⁻³
η12, PEGDME	2.618 × 10 ⁻³
η13, PEGDME	2.369 × 10 ⁻³
η14, PEGDME	2.212 × 10 ⁻³
η15, PEGDME	2.058 × 10 ⁻³

$$V_{vdw,\text{PEGDME}} := [2 \cdot 13.67 + 5.25 + 5.723(5.25 + 2 \cdot 10.23)] \frac{\text{cm}^3}{\text{mol}}$$

$$V_{vdw,\text{PEGDME}} = 1.797 \times 10^{-4} \frac{\text{m}^3}{\text{mol}}$$

$$0.0029 \frac{\text{m}^3}{\text{kg}} \cdot 194.23 \frac{\text{gm}}{\text{mol}} = 5.633 \times 10^{-4} \frac{\text{m}^3}{\text{mol}}$$

2.7 TEG

$$MW_{\text{TEG}} := 194.23 \frac{\text{gm}}{\text{mol}} \quad 1 \cdot \text{O} + 2 \cdot \text{H} + 4 \cdot (2 \cdot \text{C} + 2 \cdot \text{H} + 1 \cdot \text{O}) \quad 1 \cdot 5 + 2 \cdot 6.7 + 4 \cdot (2 \cdot 1.1 + 4 \cdot 6.7 + 1 \cdot 5) = 154.4 \quad \text{c8h18o5}$$

$$V_{c,\text{TEG}} := \left(5.633 \cdot 10^{-4} \frac{\text{m}^3}{\text{mol}} \right)$$

$$V_{at0K,\text{TEG}} := 154.4 \frac{\text{cm}^3}{\text{mol}}$$

$$V_{vdw,\text{TEG}} := 113.59 \frac{\text{cm}^3}{\text{mol}}$$

$$2 \cdot \text{OH} + 8 \cdot \text{CH}_2 + 3 \cdot \text{O}$$

$$2 \cdot 8 + 8 \cdot 10.23 + 3 \cdot 5.25 = 113.59$$

ρ1, TEG	
ρ2, TEG	1134
ρ3, TEG	1131
ρ4, TEG	1127
ρ5, TEG	1124
ρ6, TEG	1120
ρ7, TEG	1116
ρ8, TEG	1113
ρ9, TEG	1109
ρ10, TEG	1105
ρ11, TEG	1102
ρ12, TEG	1098
ρ13, TEG	1094
ρ14, TEG	1090
ρ15, TEG	1086
ρ15, TEG	1083

η1, TEG	
η2, TEG	0.1004
η3, TEG	0.0775
η4, TEG	0.05965
η5, TEG	0.04657
η6, TEG	0.03666
η7, TEG	0.02908
η8, TEG	0.02324
η9, TEG	0.01870
η10, TEG	0.01515
η11, TEG	0.01236
η12, TEG	0.01014
η13, TEG	0.008368
η14, TEG	0.006944
η15, TEG	0.005794
η15, TEG	0.004859

Appendix 4

1.1) MEK/TEGDME

$MT := 1$ $MPol := 2$ $TPol := 3$ $V_{mol1} := \frac{1}{\rho_{4,MEK}} \cdot MW_{MEK}$ $V_{mol2} := \frac{1}{\rho_{4,TEGDME}} \cdot MW_{TEGDME}$ $V_{mol3} := \frac{1}{\rho_{4,PDMS}} \cdot MW_{PDMS}$
 $RU3 := 100000$ $m := 1..16$

$$ap^{(1)} := \begin{pmatrix} 1 \\ 1 \\ 1 \\ 1 \\ 0.988 \\ 0.99 \\ 0.991 \\ 0.992 \\ 0.973 \\ 0.977 \\ 0.981 \\ 0.983 \\ 0.956 \\ 0.963 \\ 0.969 \\ 0.972 \end{pmatrix}$$

$$ap^{(2)} := \begin{pmatrix} 10^{-50} \\ 10^{-50} \\ 10^{-50} \\ 10^{-50} \\ 0.012 \\ 9.52 \times 10^{-3} \\ 8.23 \times 10^{-3} \\ 7.33 \times 10^{-3} \\ 0.025 \\ 0.021 \\ 0.018 \\ 0.016 \\ 0.041 \\ 0.035 \\ 0.029 \\ 0.026 \end{pmatrix}$$

$$\Delta P := \begin{pmatrix} 9 \\ 19.05 \\ 29.025 \\ 39.025 \\ 9.05 \\ 19 \\ 29 \\ 39 \\ 9.05 \\ 19.05 \\ 29 \\ 39 \\ 9 \\ 19 \\ 29 \\ 39 \end{pmatrix} \cdot \text{bar}$$

	1	2
1	1	0
2	1	0
3	1	0
4	1	0
5	0.988	0.012
6	0.99	9.52·10 ⁻³
7	0.991	8.23·10 ⁻³
8	0.992	7.33·10 ⁻³
9	0.973	0.025
10	0.977	0.021
11	0.981	0.018
12	0.983	0.016
13	0.956	0.041
14	0.963	0.035
15	0.969	0.029
16	0.972	0.026

$$ap = \begin{matrix} & \begin{matrix} 1 & 2 \end{matrix} \\ \begin{matrix} 1 \\ 2 \\ 3 \\ 4 \\ 5 \\ 6 \\ 7 \\ 8 \\ 9 \\ 10 \\ 11 \\ 12 \\ 13 \\ 14 \\ 15 \\ 16 \end{matrix} & \begin{matrix} 1 & 0 \\ 1 & 0 \\ 1 & 0 \\ 1 & 0 \\ 0.988 & 0.012 \\ 0.99 & 9.52 \cdot 10^{-3} \\ 0.991 & 8.23 \cdot 10^{-3} \\ 0.992 & 7.33 \cdot 10^{-3} \\ 0.973 & 0.025 \\ 0.977 & 0.021 \\ 0.981 & 0.018 \\ 0.983 & 0.016 \\ 0.956 & 0.041 \\ 0.963 & 0.035 \\ 0.969 & 0.029 \\ 0.972 & 0.026 \end{matrix} \end{matrix}$$

$$n := 1..3$$

$$ip_{m,1} := e^{\ln[ap^{(1)}]_m \cdot \frac{V_{mol1}}{R \cdot 298.15 \cdot K} \cdot \Delta P_m}$$

$$ip_{m,2} := e^{\ln[ap^{(2)}]_m \cdot \frac{V_{mol2}}{R \cdot 298.15 \cdot K} \cdot \Delta P_m}$$

$$\chi := \begin{pmatrix} 0.046 & 0.054 & 0.053 & 0.052 \\ 0.567 & 0.732 & 0.798 & 0.864 \\ 0.711 & 0.965 & 0.804 & 0.739 \end{pmatrix}$$

T=25°C, 0 wt%

m := 1

$$\chi_{m,n} := \chi_{n,1} \quad \begin{pmatrix} \phi_1 \\ \phi_2 \\ \phi_3 \end{pmatrix} := \begin{pmatrix} 0.4 \\ 0.2 \\ 0.4 \end{pmatrix}$$

Given

$$amp_{m,1} = e^{\ln(\phi_1) + (1-\phi_1) \cdot \left(\frac{V_{mol1}}{V_{mol2}} \right) \cdot \phi_2 - \left(\frac{V_{mol1}}{V_{mol3} \cdot RU3} \right) \cdot \phi_3 + (\chi_{m1} \cdot \phi_2 + \chi_{m2} \cdot \phi_3) \cdot (\phi_2 + \phi_3) - \chi_{m3} \cdot \left(\frac{V_{mol1}}{V_{mol2}} \right) \cdot \phi_2 \cdot \phi_3}$$

$$amp_{m,2} = e^{\ln(\phi_2) + (1-\phi_2) \cdot \left(\frac{V_{mol2}}{V_{mol1}} \right) \cdot \phi_1 - \left(\frac{V_{mol2}}{V_{mol3} \cdot RU3} \right) \cdot \phi_3 + (\chi_{m1} \cdot \phi_1 + \chi_{m3} \cdot \phi_3) \cdot (\phi_1 + \phi_3) - \chi_{m2} \cdot \left(\frac{V_{mol2}}{V_{mol1}} \right) \cdot \phi_1 \cdot \phi_3}$$

$$\phi_3 = 1 - \phi_1 - \phi_2$$

$$\begin{pmatrix} \phi_{1,1} \\ \phi_{m,2} \\ \phi_{m,3} \end{pmatrix} := \text{Find}(\phi_1, \phi_2, \phi_3)$$

$$\begin{pmatrix} \phi_{m,1} \\ \phi_{m,2} \\ \phi_{m,3} \end{pmatrix} = \begin{pmatrix} 0.551 \\ -1.301 \times 10^{-7} \\ 0.449 \end{pmatrix}$$

$$\phi_{2,n} := \phi_{1,n} \quad \phi_{3,n} := \phi_{1,n} \quad \phi_{4,n} := \phi_{1,n}$$

T=25°C, 5 wt%

m := 5

$$\chi_{m,n} := \chi_{n,2} \quad \begin{pmatrix} \phi_1 \\ \phi_2 \\ \phi_3 \end{pmatrix} := \begin{pmatrix} 0.6 \\ 0.2 \\ 0.4 \end{pmatrix}$$

Given

$$\text{amp}_{m,1} = e^{\ln(\phi_1)+(1-\phi_1)\left(\frac{V_{\text{mol1}}}{V_{\text{mol2}}}\right)\cdot\phi_2-\left(\frac{V_{\text{mol1}}}{V_{\text{mol3-RU3}}}\right)\cdot\phi_3+(\chi_{m_1}\cdot\phi_2+\chi_{m_2}\cdot\phi_3)\cdot(\phi_2+\phi_3)-\chi_{m_3}\left(\frac{V_{\text{mol1}}}{V_{\text{mol2}}}\right)\cdot\phi_2\cdot\phi_3}$$

$$\text{amp}_{m,2} = e^{\ln(\phi_2)+(1-\phi_2)\left(\frac{V_{\text{mol2}}}{V_{\text{mol1}}}\right)\cdot\phi_1-\left(\frac{V_{\text{mol2}}}{V_{\text{mol3-RU3}}}\right)\cdot\phi_3+\left(\chi_{m_1}\cdot\phi_1\frac{V_{\text{mol2}}}{V_{\text{mol1}}}+\chi_{m_3}\cdot\phi_3\right)\cdot(\phi_1+\phi_3)-\chi_{m_2}\left(\frac{V_{\text{mol2}}}{V_{\text{mol1}}}\right)\cdot\phi_1\cdot\phi_3}$$

$$\phi_3 = 1 - \phi_1 - \phi_2$$

$$\begin{pmatrix} \phi_{5,1} \\ \phi_{m,2} \\ \phi_{m,3} \end{pmatrix} := \text{Find}(\phi_1, \phi_2, \phi_3) \quad \begin{pmatrix} \phi_{m,1} \\ \phi_{m,2} \\ \phi_{m,3} \end{pmatrix} = \begin{pmatrix} 0.433 \\ 0.01 \\ 0.557 \end{pmatrix}$$

m := 6

$$\chi_{m,n} := \chi_{n,2} \quad \begin{pmatrix} \phi_1 \\ \phi_2 \\ \phi_3 \end{pmatrix} := \begin{pmatrix} 0.4 \\ 0.2 \\ 0.4 \end{pmatrix}$$

Given

$$\text{amp}_{m,1} = e^{\ln(\phi_1)+(1-\phi_1)\left(\frac{V_{\text{mol1}}}{V_{\text{mol2}}}\right)\cdot\phi_2-\left(\frac{V_{\text{mol1}}}{V_{\text{mol3-RU3}}}\right)\cdot\phi_3+(\chi_{m_1}\cdot\phi_2+\chi_{m_2}\cdot\phi_3)\cdot(\phi_2+\phi_3)-\chi_{m_3}\left(\frac{V_{\text{mol1}}}{V_{\text{mol2}}}\right)\cdot\phi_2\cdot\phi_3}$$

$$\text{amp}_{m,2} = e^{\ln(\phi_2)+(1-\phi_2)\left(\frac{V_{\text{mol2}}}{V_{\text{mol1}}}\right)\cdot\phi_1-\left(\frac{V_{\text{mol2}}}{V_{\text{mol3-RU3}}}\right)\cdot\phi_3+\left(\chi_{m_1}\cdot\phi_1\frac{V_{\text{mol2}}}{V_{\text{mol1}}}+\chi_{m_3}\cdot\phi_3\right)\cdot(\phi_1+\phi_3)-\chi_{m_2}\left(\frac{V_{\text{mol2}}}{V_{\text{mol1}}}\right)\cdot\phi_1\cdot\phi_3}$$

$$\phi_3 = 1 - \phi_1 - \phi_2$$

$$\begin{pmatrix} \phi_{6,1} \\ \phi_{m,2} \\ \phi_{m,3} \end{pmatrix} := \text{Find}(\phi_1, \phi_2, \phi_3) \quad \begin{pmatrix} \phi_{m,1} \\ \phi_{m,2} \\ \phi_{m,3} \end{pmatrix} = \begin{pmatrix} 0.371 \\ 5.842 \times 10^{-3} \\ 0.623 \end{pmatrix}$$

m := 7

$$\chi_{m,n} := \chi_{n,2} \quad \begin{pmatrix} \phi_1 \\ \phi_2 \\ \phi_3 \end{pmatrix} := \begin{pmatrix} 0.4 \\ 0.2 \\ 0.4 \end{pmatrix}$$

Given

$$\text{amp}_{m,1} = e^{\ln(\phi_1)+(1-\phi_1)\left(\frac{V_{\text{mol1}}}{V_{\text{mol2}}}\right)\cdot\phi_2-\left(\frac{V_{\text{mol1}}}{V_{\text{mol3-RU3}}}\right)\cdot\phi_3+(\chi_{m_1}\cdot\phi_2+\chi_{m_2}\cdot\phi_3)\cdot(\phi_2+\phi_3)-\chi_{m_3}\left(\frac{V_{\text{mol1}}}{V_{\text{mol2}}}\right)\cdot\phi_2\cdot\phi_3}$$

$$\text{amp}_{m,2} = e^{\ln(\phi_2)+(1-\phi_2)\left(\frac{V_{\text{mol2}}}{V_{\text{mol1}}}\right)\cdot\phi_1-\left(\frac{V_{\text{mol2}}}{V_{\text{mol3-RU3}}}\right)\cdot\phi_3+\left(\chi_{m_1}\cdot\phi_1\frac{V_{\text{mol2}}}{V_{\text{mol1}}}+\chi_{m_3}\cdot\phi_3\right)\cdot(\phi_1+\phi_3)-\chi_{m_2}\left(\frac{V_{\text{mol2}}}{V_{\text{mol1}}}\right)\cdot\phi_1\cdot\phi_3}$$

$$\phi_3 = 1 - \phi_1 - \phi_2$$

$$\begin{pmatrix} \phi_{7,1} \\ \phi_{m,2} \\ \phi_{m,3} \end{pmatrix} := \text{Find}(\phi_1, \phi_2, \phi_3) \quad \begin{pmatrix} \phi_{m,1} \\ \phi_{m,2} \\ \phi_{m,3} \end{pmatrix} = \begin{pmatrix} 0.33 \\ 3.936 \times 10^{-3} \\ 0.666 \end{pmatrix}$$

m := 8

$$\chi_{m,n} := \chi_{n,2} \quad \begin{pmatrix} \phi_1 \\ \phi_2 \\ \phi_3 \end{pmatrix} := \begin{pmatrix} 0.4 \\ 0.2 \\ 0.4 \end{pmatrix}$$

Given

$$\text{amp}_{m,1} = e^{\ln(\phi_1)+(1-\phi_1)\left(\frac{V_{\text{mol}1}}{V_{\text{mol}2}}\right)\cdot\phi_2-\left(\frac{V_{\text{mol}1}}{V_{\text{mol}3}\text{-RU}3}\right)\cdot\phi_3+(\chi_{m_1}\cdot\phi_2+\chi_{m_2}\cdot\phi_3)\cdot(\phi_2+\phi_3)-\chi_{m_3}\left(\frac{V_{\text{mol}1}}{V_{\text{mol}2}}\right)\cdot\phi_2\cdot\phi_3}$$

$$\text{amp}_{m,2} = e^{\ln(\phi_2)+(1-\phi_2)\left(\frac{V_{\text{mol}2}}{V_{\text{mol}1}}\right)\cdot\phi_1-\left(\frac{V_{\text{mol}2}}{V_{\text{mol}3}\text{-RU}3}\right)\cdot\phi_3+(\chi_{m_1}\cdot\phi_1\cdot\frac{V_{\text{mol}2}}{V_{\text{mol}1}}+\chi_{m_3}\cdot\phi_3)\cdot(\phi_1+\phi_3)-\chi_{m_2}\left(\frac{V_{\text{mol}2}}{V_{\text{mol}1}}\right)\cdot\phi_1\cdot\phi_3}$$

$$\phi_3 = 1 - \phi_1 - \phi_2$$

$$\begin{pmatrix} \phi_{8,1} \\ \phi_{m,2} \\ \phi_{m,3} \end{pmatrix} := \text{Find}(\phi_1, \phi_2, \phi_3) \quad \begin{pmatrix} \phi_{m,1} \\ \phi_{m,2} \\ \phi_{m,3} \end{pmatrix} = \begin{pmatrix} 0.299 \\ 2.832 \times 10^{-3} \\ 0.698 \end{pmatrix}$$

m := 9

$$\chi_{m,n} := \chi_{n,3} \quad \begin{pmatrix} \phi_1 \\ \phi_2 \\ \phi_3 \end{pmatrix} := \begin{pmatrix} 0.4 \\ 0.2 \\ 0.4 \end{pmatrix}$$

Given

$$\text{amp}_{m,1} = e^{\ln(\phi_1)+(1-\phi_1)\left(\frac{V_{\text{mol}1}}{V_{\text{mol}2}}\right)\cdot\phi_2-\left(\frac{V_{\text{mol}1}}{V_{\text{mol}3}\text{-RU}3}\right)\cdot\phi_3+(\chi_{m_1}\cdot\phi_2+\chi_{m_2}\cdot\phi_3)\cdot(\phi_2+\phi_3)-\chi_{m_3}\left(\frac{V_{\text{mol}1}}{V_{\text{mol}2}}\right)\cdot\phi_2\cdot\phi_3}$$

$$\text{amp}_{m,2} = e^{\ln(\phi_2)+(1-\phi_2)\left(\frac{V_{\text{mol}2}}{V_{\text{mol}1}}\right)\cdot\phi_1-\left(\frac{V_{\text{mol}2}}{V_{\text{mol}3}\text{-RU}3}\right)\cdot\phi_3+(\chi_{m_1}\cdot\phi_1\cdot\frac{V_{\text{mol}2}}{V_{\text{mol}1}}+\chi_{m_3}\cdot\phi_3)\cdot(\phi_1+\phi_3)-\chi_{m_2}\left(\frac{V_{\text{mol}2}}{V_{\text{mol}1}}\right)\cdot\phi_1\cdot\phi_3}$$

$$\phi_3 = 1 - \phi_1 - \phi_2$$

$$\begin{pmatrix} \phi_{9,1} \\ \phi_{m,2} \\ \phi_{m,3} \end{pmatrix} := \text{Find}(\phi_1, \phi_2, \phi_3) \quad \begin{pmatrix} \phi_{m,1} \\ \phi_{m,2} \\ \phi_{m,3} \end{pmatrix} = \begin{pmatrix} 0.384 \\ 0.021 \\ 0.595 \end{pmatrix}$$

m := 10

$$\chi_{m,n} := \chi_{n,3} \quad \begin{pmatrix} \phi_1 \\ \phi_2 \\ \phi_3 \end{pmatrix} := \begin{pmatrix} 0.4 \\ 0.2 \\ 0.4 \end{pmatrix}$$

Given

$$\text{amp}_{m,1} = e^{\ln(\phi_1)+(1-\phi_1)\left(\frac{V_{\text{mol}1}}{V_{\text{mol}2}}\right)\cdot\phi_2-\left(\frac{V_{\text{mol}1}}{V_{\text{mol}3}\text{-RU}3}\right)\cdot\phi_3+(\chi_{m_1}\cdot\phi_2+\chi_{m_2}\cdot\phi_3)\cdot(\phi_2+\phi_3)-\chi_{m_3}\left(\frac{V_{\text{mol}1}}{V_{\text{mol}2}}\right)\cdot\phi_2\cdot\phi_3}$$

$$\text{amp}_{m,2} = e^{\ln(\phi_2)+(1-\phi_2)\left(\frac{V_{\text{mol}2}}{V_{\text{mol}1}}\right)\cdot\phi_1-\left(\frac{V_{\text{mol}2}}{V_{\text{mol}3}\text{-RU}3}\right)\cdot\phi_3+(\chi_{m_1}\cdot\phi_1\cdot\frac{V_{\text{mol}2}}{V_{\text{mol}1}}+\chi_{m_3}\cdot\phi_3)\cdot(\phi_1+\phi_3)-\chi_{m_2}\left(\frac{V_{\text{mol}2}}{V_{\text{mol}1}}\right)\cdot\phi_1\cdot\phi_3}$$

$$\phi_3 = 1 - \phi_1 - \phi_2$$

$$\begin{pmatrix} \phi_{10,1} \\ \phi_{m,2} \\ \phi_{m,3} \end{pmatrix} := \text{Find}(\phi_1, \phi_2, \phi_3) \quad \begin{pmatrix} \phi_{m,1} \\ \phi_{m,2} \\ \phi_{m,3} \end{pmatrix} = \begin{pmatrix} 0.333 \\ 0.013 \\ 0.655 \end{pmatrix}$$

m := 11

$$\chi_{m,n} := \chi_{n,3} \quad \begin{pmatrix} \phi_1 \\ \phi_2 \\ \phi_3 \end{pmatrix} := \begin{pmatrix} 0.4 \\ 0.2 \\ 0.4 \end{pmatrix}$$

Given

$$\text{amp}_{m,1} = e^{\ln(\phi_1)+(1-\phi_1)\left(\frac{V_{\text{mol}1}}{V_{\text{mol}2}}\right)\cdot\phi_2-\left(\frac{V_{\text{mol}1}}{V_{\text{mol}3}\cdot\text{RU}3}\right)\cdot\phi_3+(\chi_{m_1}\cdot\phi_2+\chi_{m_2}\cdot\phi_3)\cdot(\phi_2+\phi_3)-\chi_{m_3}\left(\frac{V_{\text{mol}1}}{V_{\text{mol}2}}\right)\cdot\phi_2\cdot\phi_3}$$

$$\text{amp}_{m,2} = e^{\ln(\phi_2)+(1-\phi_2)\left(\frac{V_{\text{mol}2}}{V_{\text{mol}1}}\right)\cdot\phi_1-\left(\frac{V_{\text{mol}2}}{V_{\text{mol}3}\cdot\text{RU}3}\right)\cdot\phi_3+\left(\chi_{m_1}\cdot\phi_1\frac{V_{\text{mol}2}}{V_{\text{mol}1}}+\chi_{m_3}\cdot\phi_3\right)\cdot(\phi_1+\phi_3)-\chi_{m_2}\left(\frac{V_{\text{mol}2}}{V_{\text{mol}1}}\right)\cdot\phi_1\cdot\phi_3}$$

$$\phi_3 = 1 - \phi_1 - \phi_2$$

$$\begin{pmatrix} \phi_{11,1} \\ \phi_{m,2} \\ \phi_{m,3} \end{pmatrix} := \text{Find}(\phi_1, \phi_2, \phi_3) \quad \begin{pmatrix} \phi_{m,1} \\ \phi_{m,2} \\ \phi_{m,3} \end{pmatrix} = \begin{pmatrix} 0.299 \\ 8.895 \times 10^{-3} \\ 0.692 \end{pmatrix}$$

m := 12

$$\chi_{m,n} := \chi_{n,3} \quad \begin{pmatrix} \phi_1 \\ \phi_2 \\ \phi_3 \end{pmatrix} := \begin{pmatrix} 0.4 \\ 0.2 \\ 0.4 \end{pmatrix}$$

Given

$$\text{amp}_{m,1} = e^{\ln(\phi_1)+(1-\phi_1)\left(\frac{V_{\text{mol}1}}{V_{\text{mol}2}}\right)\cdot\phi_2-\left(\frac{V_{\text{mol}1}}{V_{\text{mol}3}\cdot\text{RU}3}\right)\cdot\phi_3+(\chi_{m_1}\cdot\phi_2+\chi_{m_2}\cdot\phi_3)\cdot(\phi_2+\phi_3)-\chi_{m_3}\left(\frac{V_{\text{mol}1}}{V_{\text{mol}2}}\right)\cdot\phi_2\cdot\phi_3}$$

$$\text{amp}_{m,2} = e^{\ln(\phi_2)+(1-\phi_2)\left(\frac{V_{\text{mol}2}}{V_{\text{mol}1}}\right)\cdot\phi_1-\left(\frac{V_{\text{mol}2}}{V_{\text{mol}3}\cdot\text{RU}3}\right)\cdot\phi_3+\left(\chi_{m_1}\cdot\phi_1\frac{V_{\text{mol}2}}{V_{\text{mol}1}}+\chi_{m_3}\cdot\phi_3\right)\cdot(\phi_1+\phi_3)-\chi_{m_2}\left(\frac{V_{\text{mol}2}}{V_{\text{mol}1}}\right)\cdot\phi_1\cdot\phi_3}$$

$$\phi_3 = 1 - \phi_1 - \phi_2$$

$$\begin{pmatrix} \phi_{12,1} \\ \phi_{m,2} \\ \phi_{m,3} \end{pmatrix} := \text{Find}(\phi_1, \phi_2, \phi_3) \quad \begin{pmatrix} \phi_{m,1} \\ \phi_{m,2} \\ \phi_{m,3} \end{pmatrix} = \begin{pmatrix} 0.272 \\ 6.473 \times 10^{-3} \\ 0.722 \end{pmatrix}$$

m := 13

$$\chi_{m,n} := \chi_{n,4} \quad \begin{pmatrix} \phi_1 \\ \phi_2 \\ \phi_3 \end{pmatrix} := \begin{pmatrix} 0.4 \\ 0.2 \\ 0.4 \end{pmatrix}$$

Given

$$\text{amp}_{m,1} = e^{\ln(\phi_1)+(1-\phi_1)\left(\frac{V_{\text{mol}1}}{V_{\text{mol}2}}\right)\cdot\phi_2-\left(\frac{V_{\text{mol}1}}{V_{\text{mol}3}\cdot\text{RU}3}\right)\cdot\phi_3+(\chi_{m_1}\cdot\phi_2+\chi_{m_2}\cdot\phi_3)\cdot(\phi_2+\phi_3)-\chi_{m_3}\left(\frac{V_{\text{mol}1}}{V_{\text{mol}2}}\right)\cdot\phi_2\cdot\phi_3}$$

$$\text{amp}_{m,2} = e^{\ln(\phi_2)+(1-\phi_2)\left(\frac{V_{\text{mol}2}}{V_{\text{mol}1}}\right)\cdot\phi_1-\left(\frac{V_{\text{mol}2}}{V_{\text{mol}3}\cdot\text{RU}3}\right)\cdot\phi_3+\left(\chi_{m_1}\cdot\phi_1\frac{V_{\text{mol}2}}{V_{\text{mol}1}}+\chi_{m_3}\cdot\phi_3\right)\cdot(\phi_1+\phi_3)-\chi_{m_2}\left(\frac{V_{\text{mol}2}}{V_{\text{mol}1}}\right)\cdot\phi_1\cdot\phi_3}$$

$$\phi_3 = 1 - \phi_1 - \phi_2$$

$$\begin{pmatrix} \phi_{13,1} \\ \phi_{m,2} \\ \phi_{m,3} \end{pmatrix} := \text{Find}(\phi_1, \phi_2, \phi_3) \quad \begin{pmatrix} \phi_{m,1} \\ \phi_{m,2} \\ \phi_{m,3} \end{pmatrix} = \begin{pmatrix} 0.341 \\ 0.032 \\ 0.627 \end{pmatrix}$$

m := 14

$$\chi_{m,n} := \chi_{n,4} \quad \begin{pmatrix} \phi_1 \\ \phi_2 \\ \phi_3 \end{pmatrix} := \begin{pmatrix} 0.4 \\ 0.2 \\ 0.4 \end{pmatrix}$$

Given

$$\text{amp}_{m,1} = e^{\ln(\phi_1)+(1-\phi_1)\left(\frac{V_{\text{mol}1}}{V_{\text{mol}2}}\right)\cdot\phi_2-\left(\frac{V_{\text{mol}1}}{V_{\text{mol}3}\cdot\text{RU}3}\right)\cdot\phi_3+(\chi_{m1}\cdot\phi_2+\chi_{m2}\cdot\phi_3)\cdot(\phi_2+\phi_3)-\chi_{m3}\left(\frac{V_{\text{mol}1}}{V_{\text{mol}2}}\right)\cdot\phi_2\cdot\phi_3}$$

$$\text{amp}_{m,2} = e^{\ln(\phi_2)+(1-\phi_2)\left(\frac{V_{\text{mol}2}}{V_{\text{mol}1}}\right)\cdot\phi_1-\left(\frac{V_{\text{mol}2}}{V_{\text{mol}3}\cdot\text{RU}3}\right)\cdot\phi_3+\left(\chi_{m1}\cdot\phi_1\frac{V_{\text{mol}2}}{V_{\text{mol}1}}+\chi_{m3}\cdot\phi_3\right)\cdot(\phi_1+\phi_3)-\chi_{m2}\left(\frac{V_{\text{mol}2}}{V_{\text{mol}1}}\right)\cdot\phi_1\cdot\phi_3}$$

$$\phi_3 = 1 - \phi_1 - \phi_2$$

$$\begin{pmatrix} \phi_{14,1} \\ \phi_{m,2} \\ \phi_{m,3} \end{pmatrix} := \text{Find}(\phi_1, \phi_2, \phi_3) \quad \begin{pmatrix} \phi_{m,1} \\ \phi_{m,2} \\ \phi_{m,3} \end{pmatrix} = \begin{pmatrix} 0.299 \\ 0.021 \\ 0.681 \end{pmatrix}$$

m := 15

$$\chi_{m,n} := \chi_{n,4} \quad \begin{pmatrix} \phi_1 \\ \phi_2 \\ \phi_3 \end{pmatrix} := \begin{pmatrix} 0.4 \\ 0.2 \\ 0.4 \end{pmatrix}$$

Given

$$\text{amp}_{m,1} = e^{\ln(\phi_1)+(1-\phi_1)\left(\frac{V_{\text{mol}1}}{V_{\text{mol}2}}\right)\cdot\phi_2-\left(\frac{V_{\text{mol}1}}{V_{\text{mol}3}\cdot\text{RU}3}\right)\cdot\phi_3+(\chi_{m1}\cdot\phi_2+\chi_{m2}\cdot\phi_3)\cdot(\phi_2+\phi_3)-\chi_{m3}\left(\frac{V_{\text{mol}1}}{V_{\text{mol}2}}\right)\cdot\phi_2\cdot\phi_3}$$

$$\text{amp}_{m,2} = e^{\ln(\phi_2)+(1-\phi_2)\left(\frac{V_{\text{mol}2}}{V_{\text{mol}1}}\right)\cdot\phi_1-\left(\frac{V_{\text{mol}2}}{V_{\text{mol}3}\cdot\text{RU}3}\right)\cdot\phi_3+\left(\chi_{m1}\cdot\phi_1\frac{V_{\text{mol}2}}{V_{\text{mol}1}}+\chi_{m3}\cdot\phi_3\right)\cdot(\phi_1+\phi_3)-\chi_{m2}\left(\frac{V_{\text{mol}2}}{V_{\text{mol}1}}\right)\cdot\phi_1\cdot\phi_3}$$

$$\phi_3 = 1 - \phi_1 - \phi_2$$

$$\begin{pmatrix} \phi_{15,1} \\ \phi_{m,2} \\ \phi_{m,3} \end{pmatrix} := \text{Find}(\phi_1, \phi_2, \phi_3) \quad \begin{pmatrix} \phi_{m,1} \\ \phi_{m,2} \\ \phi_{m,3} \end{pmatrix} = \begin{pmatrix} 0.269 \\ 0.014 \\ 0.717 \end{pmatrix}$$

m := 16

$$\chi_{m,n} := \chi_{n,4} \quad \begin{pmatrix} \phi_1 \\ \phi_2 \\ \phi_3 \end{pmatrix} := \begin{pmatrix} 0.4 \\ 0.2 \\ 0.4 \end{pmatrix}$$

Given

$$\text{amp}_{m,1} = e^{\ln(\phi_1)+(1-\phi_1)\left(\frac{V_{\text{mol}1}}{V_{\text{mol}2}}\right)\cdot\phi_2-\left(\frac{V_{\text{mol}1}}{V_{\text{mol}3}\cdot\text{RU}3}\right)\cdot\phi_3+(\chi_{m1}\cdot\phi_2+\chi_{m2}\cdot\phi_3)\cdot(\phi_2+\phi_3)-\chi_{m3}\left(\frac{V_{\text{mol}1}}{V_{\text{mol}2}}\right)\cdot\phi_2\cdot\phi_3}$$

$$\text{amp}_{m,2} = e^{\ln(\phi_2)+(1-\phi_2)\left(\frac{V_{\text{mol}2}}{V_{\text{mol}1}}\right)\cdot\phi_1-\left(\frac{V_{\text{mol}2}}{V_{\text{mol}3}\cdot\text{RU}3}\right)\cdot\phi_3+\left(\chi_{m1}\cdot\phi_1\frac{V_{\text{mol}2}}{V_{\text{mol}1}}+\chi_{m3}\cdot\phi_3\right)\cdot(\phi_1+\phi_3)-\chi_{m2}\left(\frac{V_{\text{mol}2}}{V_{\text{mol}1}}\right)\cdot\phi_1\cdot\phi_3}$$

$$\phi_3 = 1 - \phi_1 - \phi_2$$

$$\begin{pmatrix} \phi_{16,1} \\ \phi_{m,2} \\ \phi_{m,3} \end{pmatrix} := \text{Find}(\phi_1, \phi_2, \phi_3) \quad \begin{pmatrix} \phi_{m,1} \\ \phi_{m,2} \\ \phi_{m,3} \end{pmatrix} = \begin{pmatrix} 0.246 \\ 0.01 \\ 0.744 \end{pmatrix}$$

m := 1 .. 16

$$\text{xmp}_{m,1} := \frac{\frac{\phi_{m,1}}{V_{\text{mol}1}}}{\frac{\phi_{m,1}}{V_{\text{mol}1}} + \frac{\phi_{m,2}}{V_{\text{mol}2}} + \frac{\phi_{m,3}}{V_{\text{mol}3}} + \frac{\text{MW}_{\text{PDMS}}}{P_{4,\text{PDMS}}}} \quad \text{xmp}_{m,2} := \frac{\frac{\phi_{m,2}}{V_{\text{mol}2}}}{\frac{\phi_{m,1}}{V_{\text{mol}1}} + \frac{\phi_{m,2}}{V_{\text{mol}2}} + \frac{\phi_{m,3}}{V_{\text{mol}3}} + \frac{\text{MW}_{\text{PDMS}}}{P_{4,\text{PDMS}}}}$$

$$xmp_{m,3} := 1 - xmp_{m,1} - xmp_{m,2}$$

$$o := 1..4$$

$$xmf_{o,1} := 0.59 \quad xmf_{o,2} := 10^{-50} \quad xmf_{o,3} := 1 - xmf_{o,1}$$

$$o := 5..8$$

$$xmf_{o,1} := 0.532 \quad xmf_{o,2} := 0.009035 \quad xmf_{o,3} := 1 - xmf_{o,1} - xmf_{o,2}$$

$$o := 9..12$$

$$xmf_{o,1} := 0.468 \quad xmf_{o,2} := 0.017 \quad xmf_{o,3} := 1 - xmf_{o,1} - xmf_{o,2}$$

$$o := 13..16$$

$$xmf_{o,1} := 0.399 \quad xmf_{o,2} := 0.023 \quad xmf_{o,3} := 1 - xmf_{o,1} - xmf_{o,2}$$

$$x := \frac{xmf + xmp}{2}$$

$$\omega_{m,1} := \frac{x_{m,1} \cdot MW_{MEK}}{x_{m,1} \cdot MW_{MEK} + x_{m,2} \cdot MW_{TEGDME} + x_{m,3} \cdot MW_{PDMS}}$$

$$\omega_{m,2} := \frac{x_{m,2} \cdot MW_{TEGDME}}{x_{m,1} \cdot MW_{MEK} + x_{m,2} \cdot MW_{TEGDME} + x_{m,3} \cdot MW_{PDMS}}$$

$$\omega_{m,3} := \frac{x_{m,3} \cdot MW_{PDMS}}{x_{m,1} \cdot MW_{MEK} + x_{m,2} \cdot MW_{TEGDME} + x_{m,3} \cdot MW_{PDMS}}$$

$$CM_{m,n} := \frac{x_{m,n}}{x_{m,1} \cdot Vmol1 + x_{m,2} \cdot Vmol2 + x_{m,3} \cdot \frac{MW_{PDMS}}{\rho_{4,PDMS}}}$$

$$CMmf_{m,n} := \frac{xmf_{m,n}}{xmf_{m,1} \cdot Vmol1 + xmf_{m,2} \cdot Vmol2 + xmf_{m,3} \cdot \frac{MW_{PDMS}}{\rho_{4,PDMS}}}$$

$$CMmp_{m,n} := \frac{xmp_{m,n}}{xmp_{m,1} \cdot Vmol1 + xmp_{m,2} \cdot Vmol2 + xmp_{m,3} \cdot \frac{MW_{PDMS}}{\rho_{4,PDMS}}}$$

Appendix 4

	1	2	3
1	6548.6	-0	5376.2
2	6548.6	-0	5376.2
3	6548.6	-0	5376.2
4	6548.6	-0	5376.2
5	5542.5	76.7	6347.3
6	5212.8	67.3	6765.4
7	4995.3	63.3	7035.2
8	4832.6	61	7234.8
9	4885.6	147.5	6921
10	4612.5	131	7292.9
11	4434.9	122.3	7528.8
12	4293.3	117.2	7711.5
13	4242.4	208.4	7507.3
14	4016.8	184.6	7843.9
15	3861.9	169.8	8070.7
16	3739.5	162.2	8237.8

CM =

$\frac{\text{mol}}{\text{m}^3}$

	1	2	3
1	6.987·10 ³	0	4.856·10 ³
2	6.987·10 ³	0	4.856·10 ³
3	6.987·10 ³	0	4.856·10 ³
4	6.987·10 ³	0	4.856·10 ³
5	6.265·10 ³	106.391	5.405·10 ³
6	6.265·10 ³	106.391	5.405·10 ³
7	6.265·10 ³	106.391	5.405·10 ³
8	6.265·10 ³	106.391	5.405·10 ³
9	5.495·10 ³	199.605	6.047·10 ³
10	5.495·10 ³	199.605	6.047·10 ³
11	5.495·10 ³	199.605	6.047·10 ³
12	5.495·10 ³	199.605	6.047·10 ³
13	4.691·10 ³	270.403	6.795·10 ³
14	4.691·10 ³	270.403	6.795·10 ³
15	4.691·10 ³	270.403	6.795·10 ³
16	4.691·10 ³	270.403	6.795·10 ³

CMmf =

$\frac{\text{mol}}{\text{m}^3}$

	1	2	3
1	6.104·10 ³	-5.894·10 ⁻⁴	5.904·10 ³
2	6.104·10 ³	-5.894·10 ⁻⁴	5.904·10 ³
3	6.104·10 ³	-5.894·10 ⁻⁴	5.904·10 ³
4	6.104·10 ³	-5.894·10 ⁻⁴	5.904·10 ³
5	4.797·10 ³	45.929	7.321·10 ³
6	4.112·10 ³	26.467	8.19·10 ³
7	3.655·10 ³	17.831	8.756·10 ³
8	3.312·10 ³	12.831	9.178·10 ³
9	4.254·10 ³	93.432	7.827·10 ³
10	3.684·10 ³	58.839	8.603·10 ³
11	3.311·10 ³	40.298	9.1·10 ³
12	3.011·10 ³	29.326	9.488·10 ³
13	3.778·10 ³	144.21	8.244·10 ³
14	3.309·10 ³	94.445	8.945·10 ³
15	2.983·10 ³	63.041	9.423·10 ³
16	2.724·10 ³	46.744	9.777·10 ³

CMmp =

$\frac{\text{mol}}{\text{m}^3}$

	1	2	3
1	0.542	-7.472·10 ⁻⁸	0.458
2	0.542	-7.472·10 ⁻⁸	0.458
3	0.542	-7.472·10 ⁻⁸	0.458
4	0.542	-7.472·10 ⁻⁸	0.458
5	0.451	0.019	0.53
6	0.421	0.017	0.562
7	0.402	0.016	0.582
8	0.388	0.015	0.597
9	0.392	0.037	0.571
10	0.369	0.032	0.599
11	0.353	0.03	0.617
12	0.341	0.029	0.63
13	0.337	0.051	0.612
14	0.318	0.045	0.637
15	0.305	0.041	0.654
16	0.294	0.039	0.666

ω =

x =

	1	2	3
1	0.549	-2.454·10 ⁻⁸	0.451
2	0.549	-2.454·10 ⁻⁸	0.451
3	0.549	-2.454·10 ⁻⁸	0.451
4	0.549	-2.454·10 ⁻⁸	0.451
5	0.463	6.405·10 ⁻³	0.53
6	0.433	5.591·10 ⁻³	0.562
7	0.413	5.235·10 ⁻³	0.582
8	0.398	5.031·10 ⁻³	0.597
9	0.409	0.012	0.579
10	0.383	0.011	0.606
11	0.367	0.01	0.623
12	0.354	9.67·10 ⁻³	0.636
13	0.355	0.017	0.628
14	0.333	0.015	0.651
15	0.319	0.014	0.667
16	0.308	0.013	0.679

	1	2	3
1	0.551	-1.301·10 ⁻⁷	0.449
2	0.551	-1.301·10 ⁻⁷	0.449
3	0.551	-1.301·10 ⁻⁷	0.449
4	0.551	-1.301·10 ⁻⁷	0.449
5	0.433	0.01	0.557
6	0.371	5.842·10 ⁻³	0.623
7	0.33	3.936·10 ⁻³	0.666
8	0.299	2.832·10 ⁻³	0.698
9	0.384	0.021	0.595
10	0.333	0.013	0.655
11	0.299	8.895·10 ⁻³	0.692
12	0.272	6.473·10 ⁻³	0.722
13	0.341	0.032	0.627
14	0.299	0.021	0.681
15	0.269	0.014	0.717
16	0.246	0.01	0.744

φ =

	1	2	3
1	54.2	-7.5·10 ⁻⁶	45.8
2	54.2	-7.5·10 ⁻⁶	45.8
3	54.2	-7.5·10 ⁻⁶	45.8
4	54.2	-7.5·10 ⁻⁶	45.8
5	45.1	1.9	53
6	42.1	1.7	56.2
7	40.2	1.6	58.2
8	38.8	1.5	59.7
9	39.2	3.7	57.1
10	36.9	3.2	59.9
11	35.3	3	61.7
12	34.1	2.9	63
13	33.7	5.1	61.2
14	31.8	4.5	63.7
15	30.5	4.1	65.4
16	29.4	3.9	66.6

ω · 100 =

A4.3 Estimation of thermodynamic diffusion coefficients

Mutual diffusion coefficients

0) Units definition

$$R := 8.314 \frac{\text{kg m}^2}{\text{s}^2 \text{K mol}}$$

$$\text{mPa} := \frac{\text{Pa}}{1000}$$

$$\text{Avog} := 6.022 \cdot 10^{23} \frac{1}{\text{mol}}$$

$$k_B := 1.38 \cdot 10^{-23} \frac{\text{J}}{\text{K}}$$

$$\text{bar} := 100000 \cdot \text{Pa}$$

$$\text{kmol} := 1000 \cdot \text{mol}$$

$$\text{Avog} := 6.02214179 \cdot 10^{23} \cdot \text{mol}^{-1}$$

$$\text{ml} := 1 \cdot \text{cm}^3$$

1) Component list

Component Index

PDMS	:=	1
MEK		2
DEK		3
TEGDME		4
PEGDME		5
TEG		6

Ncompounds := 1..6

j := Ncompounds

k := 2..6 All except the polymer

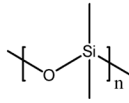
T :=	283.15	·K	T - 273.15K =	1	K	Npoints := 1..15
	288.15			10		
	293.15			15		
	298.15			20		
	303.15			25		
	308.15			30		
	313.15			35		
	318.15			40		
	323.15			45		
	328.15			50		
	333.15			55		
	338.15			60		
	343.15			65		
	348.15			70		
	353.15			75		
	80					

i := Npoints

Appendix 4

2) Pure properties

2.1 PDMS



$$V_{PDMS} := 1.027 \cdot 10^{-3} \frac{\text{m}^3}{\text{kg}}$$

$$MW_{PDMS} := 74.1 \frac{\text{gm}}{\text{mol}}$$

$$V_{vdw,PDMS} := (16.6 + 5.25 + 2 \cdot 13.67) \frac{\text{cm}^3}{\text{mol}}$$

$$V_{vdw,PDMS} = 4.919 \times 10^{-5} \frac{\text{m}^3}{\text{mol}}$$

ρ1, PDMS	(0.974)
ρ2, PDMS	0.974
ρ3, PDMS	0.974
ρ4, PDMS	0.974
ρ5, PDMS	0.974
ρ6, PDMS	0.974
ρ7, PDMS	0.974
ρ8, PDMS	:= 0.974 $\frac{\text{gm}}{\text{cm}^3}$
ρ9, PDMS	0.974
ρ10, PDMS	0.974
ρ11, PDMS	0.974
ρ12, PDMS	0.974
ρ13, PDMS	0.974
ρ14, PDMS	(0.974)
ρ15, PDMS	

$$V_{ch,PDMS} := 0.905 \frac{\text{cm}^3}{\text{gm}}$$

2.2 MEK

$$MW_{MEK} := 72.10692 \frac{\text{gm}}{\text{mol}}$$

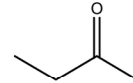
$$V_{at0K,MEK} := 63.9 \frac{\text{cm}^3}{\text{mol}}$$

$$V_{c,MEK} := 267 \frac{\text{cm}^3}{\text{mol}}$$

<http://www.thermo.com/kdb/kdb/hcprop/showprop?cmpid=1192>

$$V_{vdw,MEK} := (2 \cdot 13.67 + 10.23 + 11.7) \frac{\text{cm}^3}{\text{mol}}$$

$$V_{vdw,MEK} = 4.927 \times 10^{-5} \frac{\text{m}^3}{\text{mol}}$$



ρ1, MEK	(0.816)
ρ2, MEK	0.810
ρ3, MEK	0.805
ρ4, MEK	0.799
ρ5, MEK	0.794
ρ6, MEK	0.788
ρ7, MEK	0.783
ρ8, MEK	:= 0.777 $\frac{\text{gm}}{\text{cm}^3}$
ρ9, MEK	0.772
ρ10, MEK	0.766
ρ11, MEK	0.760
ρ12, MEK	0.754
ρ13, MEK	0.748
ρ14, MEK	0.742
ρ15, MEK	(0.736)

η1, MEK	(4.6762 × 10 ⁻⁴)
η2, MEK	4.4122 × 10 ⁻⁴
η3, MEK	4.1696 × 10 ⁻⁴
η4, MEK	3.9461 × 10 ⁻⁴
η5, MEK	3.7399 × 10 ⁻⁴
η6, MEK	3.5491 × 10 ⁻⁴
η7, MEK	3.3725 × 10 ⁻⁴
η8, MEK	:= 3.2085 × 10 ⁻⁴ .Pa·s
η9, MEK	3.0562 × 10 ⁻⁴
η10, MEK	2.9143 × 10 ⁻⁴
η11, MEK	2.7821 × 10 ⁻⁴
η12, MEK	2.6586 × 10 ⁻⁴
η13, MEK	2.5432 × 10 ⁻⁴
η14, MEK	2.4351 × 10 ⁻⁴
η15, MEK	(2.3337 × 10 ⁻⁴)

	1
1	283.15
2	288.15
3	293.15
4	298.15
5	303.15
6	308.15
7	313.15
8	318.15
9	323.15
10	328.15
11	333.15
12	338.15
13	343.15
14	348.15
15	353.15

T = K

2.3 DEK

$$MW_{DEK} := 86.1338 \frac{\text{gm}}{\text{mol}} \quad \text{Vat0K}_{DEK} := 78.4 \frac{\text{cm}^3}{\text{mol}} \quad \text{c5h10o} \quad 5 \cdot 1.1 + 10 \cdot 6.7 + 5.9 = 78.4$$

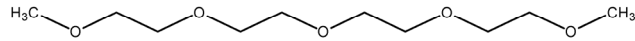
$$Vc_{DEK} := 336 \frac{\text{cm}^3}{\text{mol}} \quad \text{http://www.thermo.com/kdb/kdb/hcprop/showprop.php?cmpid=1196} \quad 5 \cdot 0.77 + 10 \cdot 6.45 + 5.9 = 74.25$$

$$Vvdw_{DEK} := (2 \cdot 13.67 + 2 \cdot 10.23 + 11.7) \frac{\text{cm}^3}{\text{mol}} \quad 4 \cdot 0.77 + 8 \cdot 6.45 + 5.9 = 60.58$$

$\rho_{1,DEK}$		$\eta_{1,DEK}$	5.247×10^{-4}
$\rho_{2,DEK}$	0.8241606	$\eta_{2,DEK}$	4.953×10^{-4}
$\rho_{3,DEK}$	0.8192934	$\eta_{3,DEK}$	4.683×10^{-4}
$\rho_{4,DEK}$	0.8143909	$\eta_{4,DEK}$	4.435×10^{-4}
$\rho_{5,DEK}$	0.809452	$\eta_{5,DEK}$	4.206×10^{-4}
$\rho_{6,DEK}$	0.8044755	$\eta_{6,DEK}$	3.995×10^{-4}
$\rho_{7,DEK}$	0.7994602	$\eta_{7,DEK}$	3.799×10^{-4}
$\rho_{8,DEK}$	0.7944049	$\eta_{8,DEK}$	3.617×10^{-4}
$\rho_{9,DEK}$	0.7893084	$\eta_{9,DEK}$	3.449×10^{-4}
$\rho_{10,DEK}$	0.7841691	$\eta_{10,DEK}$	3.292×10^{-4}
$\rho_{11,DEK}$	0.7789856	$\eta_{11,DEK}$	3.145×10^{-4}
$\rho_{12,DEK}$	0.7737564	$\eta_{12,DEK}$	3.009×10^{-4}
$\rho_{13,DEK}$	0.7684799	$\eta_{13,DEK}$	2.881×10^{-4}
$\rho_{14,DEK}$	0.7631542	$\eta_{14,DEK}$	2.762×10^{-4}
$\rho_{15,DEK}$	0.7577776	$\eta_{15,DEK}$	2.650×10^{-4}
$\rho_{15,DEK}$	0.7523481		

$\frac{\text{gm}}{\text{cm}^3}$ $\text{Pa}\cdot\text{s}$

2.5 TEGDME



$$MW_{TEGDME} := 222.28168 \frac{\text{gm}}{\text{mol}} \quad \text{Vat0K}_{TEGDME} := 187.9 \frac{\text{cm}^3}{\text{mol}} \quad (2 \cdot 1.1 + 6 \cdot 6.7 + 5.9) + 4 \cdot (5.9 + 2 \cdot 1.1 + 4 \cdot 6.7) = 187.9$$

$$Vc_{TEGDME} := 0.691 \frac{\text{m}^3}{\text{kmol}} \quad Vvdw_{TEGDME} := [2 \cdot 13.67 + 5.25 + 4 \cdot (5.25 + 2 \cdot 10.23)] \frac{\text{cm}^3}{\text{mol}}$$

$\rho_{1,TEGDME}$		$\eta_{1,TEGDME}$	4.979×10^{-3}
$\rho_{2,TEGDME}$	1020	$\eta_{2,TEGDME}$	4.361×10^{-3}
$\rho_{3,TEGDME}$	1016	$\eta_{3,TEGDME}$	3.749×10^{-3}
$\rho_{4,TEGDME}$	1012	$\eta_{4,TEGDME}$	3.348×10^{-3}
$\rho_{5,TEGDME}$	1007	$\eta_{5,TEGDME}$	2.951×10^{-3}
$\rho_{6,TEGDME}$	1003	$\eta_{6,TEGDME}$	2.673×10^{-3}
$\rho_{7,TEGDME}$	998.4	$\eta_{7,TEGDME}$	2.398×10^{-3}
$\rho_{8,TEGDME}$	993.8	$\eta_{8,TEGDME}$	2.201×10^{-3}
$\rho_{9,TEGDME}$	989.2	$\eta_{9,TEGDME}$	2.007×10^{-3}
$\rho_{10,TEGDME}$	984.6	$\eta_{10,TEGDME}$	1.848×10^{-3}
$\rho_{11,TEGDME}$	979.9	$\eta_{11,TEGDME}$	1.691×10^{-3}
$\rho_{12,TEGDME}$	975.2	$\eta_{12,TEGDME}$	1.569×10^{-3}
$\rho_{13,TEGDME}$	970.5	$\eta_{13,TEGDME}$	1.449×10^{-3}
$\rho_{14,TEGDME}$	965.8	$\eta_{14,TEGDME}$	1.352×10^{-3}
$\rho_{15,TEGDME}$	961.1	$\eta_{15,TEGDME}$	1.257×10^{-3}
$\rho_{15,TEGDME}$	956.4		

$\frac{\text{kg}}{\text{m}^3}$ $\text{Pa}\cdot\text{s}$

Appendix 4

2.6 PEGDME 250

$$MW_{\text{PEGDME}} := 298.21 \cdot \frac{\text{gm}}{\text{mol}} \quad (2 \cdot 1.1 + 6 \cdot 6.7 + 5.9) + 5.723 \cdot (5.9 + 2 \cdot 1.1 + 4 \cdot 6.7) = 248.033$$

$$V_{c,\text{PEGDME}} := \left(0.915 \cdot \frac{\text{m}^3}{\text{kmol}} \right) \quad V_{at0K,\text{PEGDME}} := 248.03 \cdot \frac{\text{cm}^3}{\text{mol}} \quad n = 5.723$$

$\rho_{1,\text{PEGDME}}$	$:= \begin{pmatrix} 1044 \\ 1040 \\ 1036 \\ 1031 \\ 1026 \\ 1022 \\ 1017 \\ 1013 \\ 1008 \\ 1004 \\ 999.5 \\ 995.1 \\ 990.6 \\ 986.2 \\ 981.7 \end{pmatrix} \cdot \frac{\text{kg}}{\text{m}^3}$	$\eta_{1,\text{PEGDME}}$	$:= \begin{pmatrix} 10.23 \times 10^{-3} \\ 8.843 \times 10^{-3} \\ 7.471 \times 10^{-3} \\ 6.532 \times 10^{-3} \\ 5.601 \times 10^{-3} \\ 4.980 \times 10^{-3} \\ 4.365 \times 10^{-3} \\ 3.927 \times 10^{-3} \\ 3.493 \times 10^{-3} \\ 3.180 \times 10^{-3} \\ 2.869 \times 10^{-3} \\ 2.618 \times 10^{-3} \\ 2.369 \times 10^{-3} \\ 2.212 \times 10^{-3} \\ 2.058 \times 10^{-3} \end{pmatrix} \text{ (Pa}\cdot\text{s)}$
$\rho_{2,\text{PEGDME}}$		$\eta_{2,\text{PEGDME}}$	
$\rho_{3,\text{PEGDME}}$		$\eta_{3,\text{PEGDME}}$	
$\rho_{4,\text{PEGDME}}$		$\eta_{4,\text{PEGDME}}$	
$\rho_{5,\text{PEGDME}}$		$\eta_{5,\text{PEGDME}}$	
$\rho_{6,\text{PEGDME}}$		$\eta_{6,\text{PEGDME}}$	
$\rho_{7,\text{PEGDME}}$		$\eta_{7,\text{PEGDME}}$	
$\rho_{8,\text{PEGDME}}$		$\eta_{8,\text{PEGDME}}$	
$\rho_{9,\text{PEGDME}}$		$\eta_{9,\text{PEGDME}}$	
$\rho_{10,\text{PEGDME}}$		$\eta_{10,\text{PEGDME}}$	
$\rho_{11,\text{PEGDME}}$		$\eta_{11,\text{PEGDME}}$	
$\rho_{12,\text{PEGDME}}$		$\eta_{12,\text{PEGDME}}$	
$\rho_{13,\text{PEGDME}}$		$\eta_{13,\text{PEGDME}}$	
$\rho_{14,\text{PEGDME}}$		$\eta_{14,\text{PEGDME}}$	
$\rho_{15,\text{PEGDME}}$		$\eta_{15,\text{PEGDME}}$	

$$V_{vdw,\text{PEGDME}} := [2 \cdot 13.67 + 5.25 + 5.723 \cdot (5.25 + 2 \cdot 10.23)] \cdot \frac{\text{cm}^3}{\text{mol}}$$

$$V_{vdw,\text{PEGDME}} = 1.797 \times 10^{-4} \frac{\text{m}^3}{\text{mol}}$$

$$0.0029 \cdot \frac{\text{m}^3}{\text{kg}} \cdot 194.23 \cdot \frac{\text{gm}}{\text{mol}} = 5.633 \times 10^{-4} \frac{\text{m}^3}{\text{mol}}$$

2.7 TEG

$$MW_{\text{TEG}} := 194.23 \cdot \frac{\text{gm}}{\text{mol}} \quad 1 \cdot \text{O} + 2 \cdot \text{H} + 4 \cdot (2 \cdot \text{C} + 2 \cdot \text{H} + 1 \cdot \text{O}) \quad 1 \cdot 5 + 2 \cdot 6.7 + 4 \cdot (2 \cdot 1.1 + 4 \cdot 6.7 + 1 \cdot 5) = 154.4 \quad c8h18o5$$

$$V_{c,\text{TEG}} := \left(5.633 \cdot 10^{-4} \cdot \frac{\text{m}^3}{\text{mol}} \right) \quad V_{at0K,\text{TEG}} := 154.4 \cdot \frac{\text{cm}^3}{\text{mol}} \quad V_{vdw,\text{TEG}} := 113.59 \cdot \frac{\text{cm}^3}{\text{mol}}$$

$\rho_{1,\text{TEG}}$	$:= \begin{pmatrix} 1134 \\ 1131 \\ 1127 \\ 1124 \\ 1120 \\ 1116 \\ 1113 \\ 1109 \\ 1105 \\ 1102 \\ 1098 \\ 1094 \\ 1090 \\ 1086 \\ 1083 \end{pmatrix} \cdot \frac{\text{kg}}{\text{m}^3}$	$\eta_{1,\text{TEG}}$	$:= \begin{pmatrix} 0.1004 \\ 0.0775 \\ 0.05965 \\ 0.04657 \\ 0.03666 \\ 0.02908 \\ 0.02324 \\ 0.01870 \\ 0.01515 \\ 0.01236 \\ 0.01014 \\ 0.008368 \\ 0.006944 \\ 0.005794 \\ 0.004859 \end{pmatrix} \text{ (Pa}\cdot\text{s)}$
$\rho_{2,\text{TEG}}$		$\eta_{2,\text{TEG}}$	
$\rho_{3,\text{TEG}}$		$\eta_{3,\text{TEG}}$	
$\rho_{4,\text{TEG}}$		$\eta_{4,\text{TEG}}$	
$\rho_{5,\text{TEG}}$		$\eta_{5,\text{TEG}}$	
$\rho_{6,\text{TEG}}$		$\eta_{6,\text{TEG}}$	
$\rho_{7,\text{TEG}}$		$\eta_{7,\text{TEG}}$	
$\rho_{8,\text{TEG}}$		$\eta_{8,\text{TEG}}$	
$\rho_{9,\text{TEG}}$		$\eta_{9,\text{TEG}}$	
$\rho_{10,\text{TEG}}$		$\eta_{10,\text{TEG}}$	
$\rho_{11,\text{TEG}}$		$\eta_{11,\text{TEG}}$	
$\rho_{12,\text{TEG}}$		$\eta_{12,\text{TEG}}$	
$\rho_{13,\text{TEG}}$		$\eta_{13,\text{TEG}}$	
$\rho_{14,\text{TEG}}$		$\eta_{14,\text{TEG}}$	
$\rho_{15,\text{TEG}}$		$\eta_{15,\text{TEG}}$	

$$2 \cdot \text{OH} + 8 \cdot \text{CH}_2 + 3 \cdot \text{O}$$

$$2 \cdot 8 + 8 \cdot 10.23 + 3 \cdot 5.25 = 113.59$$

$$V_{ch,k} := \frac{V_{at0K,k}}{MW_k} \quad V_{p,i,j} := \frac{1}{\rho_{i,j}}$$

$$\text{TempIndex} := 4$$

$$D_{t_P_5} := 2.33 \cdot 10^{-9} \frac{\text{m}^2}{\text{s}} \quad D_{t_P_10} := 2.09 \cdot 10^{-9} \frac{\text{m}^2}{\text{s}} \quad D_{t_P_15} := 1.837 \cdot 10^{-9} \frac{\text{m}^2}{\text{s}}$$

$$D_{t_P_5} := 1.982 \cdot 10^{-9} \frac{\text{m}^2}{\text{s}} \quad D_{t_P_10} := 1.763 \cdot 10^{-9} \frac{\text{m}^2}{\text{s}} \quad D_{t_P_15} := 1.536 \cdot 10^{-9} \frac{\text{m}^2}{\text{s}}$$

$$f_T := \begin{pmatrix} 0.18351 & 0.15193 & 0.1605 & 0.18505 & 0.14637 & 0.05424 \\ 0.18804 & 0.15303 & 0.16195 & 0.19072 & 0.1503 & 0.05502 \\ 0.19258 & 0.1543 & 0.16336 & 0.19635 & 0.15419 & 0.05575 \\ 0.19712 & 0.15534 & 0.16474 & 0.20172 & 0.15789 & 0.05652 \\ 0.20166 & 0.15654 & 0.16609 & 0.20723 & 0.16154 & 0.05723 \\ 0.2062 & 0.15752 & 0.16739 & 0.21256 & 0.16532 & 0.05794 \\ 0.21074 & 0.15867 & 0.16866 & 0.21784 & 0.1689 & 0.05869 \\ 0.21528 & 0.15958 & 0.16989 & 0.22306 & 0.1726 & 0.05939 \\ 0.21982 & 0.16067 & 0.17108 & 0.22822 & 0.17609 & 0.06008 \\ 0.22435 & 0.16153 & 0.17224 & 0.2333 & 0.17972 & 0.06082 \\ 0.22889 & 0.16234 & 0.17335 & 0.23832 & 0.18323 & 0.06149 \\ 0.23343 & 0.16313 & 0.17441 & 0.24329 & 0.18671 & 0.06216 \\ 0.23797 & 0.16388 & 0.17544 & 0.24819 & 0.19014 & 0.06283 \\ 0.24251 & 0.1646 & 0.17643 & 0.25303 & 0.19354 & 0.06348 \\ 0.24705 & 0.16529 & 0.17736 & 0.25782 & 0.19689 & 0.06419 \end{pmatrix}$$

$$D_0 := \begin{pmatrix} 0 \\ 3.097 \times 10^{-7} \\ 2.498 \times 10^{-7} \\ 2.009 \times 10^{-8} \\ 3.199 \times 10^{-8} \\ 1.731 \times 10^{-4} \end{pmatrix} \frac{\text{m}^2}{\text{s}}$$

$$\begin{pmatrix} \xi_{\text{MEK}} \\ \xi_{\text{DEK}} \\ \xi_{\text{TEGDME}} \\ \xi_{\text{PEGDME}} \end{pmatrix} := \begin{pmatrix} 0.806 \\ 0.807 \\ 0.510 \\ 0.640 \end{pmatrix} \quad V_{p_TempIndex, PDMS} := V_{p_TempIndex, PDMS} \cdot 0.643$$

$$\omega := \begin{pmatrix} 0.542 & -7.47 \times 10^{-8} & 0.458 \\ 0.542 & -7.47 \times 10^{-8} & 0.458 \\ 0.542 & -7.47 \times 10^{-8} & 0.458 \\ 0.542 & -7.47 \times 10^{-8} & 0.458 \\ 0.451 & 0.019 & 0.53 \\ 0.421 & 0.017 & 0.562 \\ 0.402 & 0.016 & 0.582 \\ 0.388 & 0.015 & 0.597 \\ 0.392 & 0.037 & 0.571 \\ 0.369 & 0.032 & 0.599 \\ 0.353 & 0.03 & 0.617 \\ 0.341 & 0.029 & 0.63 \\ 0.337 & 0.051 & 0.612 \\ 0.318 & 0.045 & 0.637 \\ 0.305 & 0.041 & 0.654 \\ 0.294 & 0.039 & 0.666 \end{pmatrix}$$

$$p := 1 \dots 16 \quad n := 1 \dots 3$$

$$q := 5 \dots 16 \quad r := 1 \dots 4$$

$$x := \begin{pmatrix} 0.549 & -2.45 \times 10^{-8} & 0.451 \\ 0.549 & -2.45 \times 10^{-8} & 0.451 \\ 0.549 & -2.45 \times 10^{-8} & 0.451 \\ 0.549 & -2.45 \times 10^{-8} & 0.451 \\ 0.463 & 6.41 \times 10^{-3} & 0.53 \\ 0.433 & 5.59 \times 10^{-3} & 0.562 \\ 0.413 & 5.24 \times 10^{-3} & 0.582 \\ 0.398 & 5.03 \times 10^{-3} & 0.597 \\ 0.409 & 0.012 & 0.579 \\ 0.383 & 0.011 & 0.606 \\ 0.367 & 0.01 & 0.623 \\ 0.354 & 9.67 \times 10^{-3} & 0.636 \\ 0.355 & 0.017 & 0.628 \\ 0.333 & 0.015 & 0.651 \\ 0.319 & 0.014 & 0.667 \\ 0.308 & 0.013 & 0.679 \end{pmatrix}$$

$$D_{mt_p,1} := D_{0_MEK} \cdot e^{\omega_{p,1} \cdot \hat{r}_{TempIndex, MEK} \cdot V_{PTempIndex, MEK} + \omega_{p,2} \cdot \hat{r}_{TempIndex, TEGDME} \cdot V_{PTempIndex, TEGDME} + \omega_{p,3} \cdot \hat{r}_{TempIndex, PDMS} \cdot V_{PTempIndex, PDMS}} \cdot \left(\omega_{p,1} \cdot V_{chMEK} + \omega_{p,2} \cdot V_{chTEGDME} \cdot \frac{\xi_{MEK}}{\xi_{TEGDME}} + \omega_{p,3} \cdot V_{chPDMS} \cdot \xi_{MEK} \right)$$

$$D_{mt_p,2} := D_{0_TEGDME} \cdot e^{\omega_{p,1} \cdot \hat{r}_{TempIndex, MEK} \cdot V_{PTempIndex, MEK} + \omega_{p,2} \cdot \hat{r}_{TempIndex, TEGDME} \cdot V_{PTempIndex, TEGDME} + \omega_{p,3} \cdot \hat{r}_{TempIndex, PDMS} \cdot V_{PTempIndex, PDMS}} \cdot \left(\omega_{p,1} \cdot V_{chMEK} \cdot \frac{\xi_{TEGDME}}{\xi_{MEK}} + \omega_{p,2} \cdot V_{chTEGDME} + \omega_{p,3} \cdot V_{chPDMS} \cdot \xi_{TEGDME} \right)$$

Appendix 4

$$o := 1..4$$

$$Dmt_{o,3} := 2.554 \cdot 10^{-9} \cdot \frac{m^2}{s} \quad Dmt_{o,2} := 0 \cdot \frac{m^2}{s}$$

$$o := 5..8$$

$$Dmt_{o,3} := Dt_P_5$$

$$o := 9..12$$

$$Dmt_{o,3} := Dt_P_10$$

$$o := 13..16$$

$$Dmt_{o,3} := Dt_P_15$$

	1	2	3
1	2.224·10 ⁻⁹	0	2.554·10 ⁻⁹
2	2.224·10 ⁻⁹	0	2.554·10 ⁻⁹
3	2.224·10 ⁻⁹	0	2.554·10 ⁻⁹
4	2.224·10 ⁻⁹	0	2.554·10 ⁻⁹
5	1.969·10 ⁻⁹	8.184·10 ⁻¹⁰	1.982·10 ⁻⁹
6	1.913·10 ⁻⁹	8.036·10 ⁻¹⁰	1.982·10 ⁻⁹
7	1.877·10 ⁻⁹	7.94·10 ⁻¹⁰	1.982·10 ⁻⁹
8	1.851·10 ⁻⁹	7.871·10 ⁻¹⁰	1.982·10 ⁻⁹
9	1.796·10 ⁻⁹	7.723·10 ⁻¹⁰	1.763·10 ⁻⁹
10	1.764·10 ⁻⁹	7.636·10 ⁻¹⁰	1.763·10 ⁻⁹
11	1.738·10 ⁻⁹	7.564·10 ⁻¹⁰	1.763·10 ⁻⁹
12	1.717·10 ⁻⁹	7.506·10 ⁻¹⁰	1.763·10 ⁻⁹
13	1.652·10 ⁻⁹	7.324·10 ⁻¹⁰	1.536·10 ⁻⁹
14	1.631·10 ⁻⁹	7.265·10 ⁻¹⁰	1.536·10 ⁻⁹
15	1.616·10 ⁻⁹	7.223·10 ⁻¹⁰	1.536·10 ⁻⁹
16	1.6·10 ⁻⁹	7.179·10 ⁻¹⁰	1.536·10 ⁻⁹

$$Dmt = \frac{m^2}{s}$$

$$\zeta_{\text{eff},q,n} := \frac{R \cdot T_{\text{TempIndex}}}{Dmt_{q,n}}$$

$$\zeta_{\text{eff},r,1} := \frac{R \cdot T_{\text{TempIndex}}}{Dmt_{r,1}} \quad \zeta_{\text{eff},r,2} := 0 \cdot \frac{kg}{s \cdot mol} \quad \zeta_{\text{eff},r,3} := \frac{R \cdot T_{\text{TempIndex}}}{Dmt_{r,3}}$$

$$\zeta_{p,1} := \frac{\zeta_{\text{eff},p,1} \cdot \zeta_{\text{eff},p,3}}{x_{p,1} \cdot \zeta_{\text{eff},p,1} + x_{p,2} \cdot \zeta_{\text{eff},p,2} + x_{p,3} \cdot \zeta_{\text{eff},p,3}}$$

$$\zeta_{p,2} := \frac{\zeta_{\text{eff},p,2} \cdot \zeta_{\text{eff},p,3}}{x_{p,1} \cdot \zeta_{\text{eff},p,1} + x_{p,2} \cdot \zeta_{\text{eff},p,2} + x_{p,3} \cdot \zeta_{\text{eff},p,3}}$$

$$D_{p,1} := \frac{R \cdot T_{\text{TempIndex}}}{\zeta_{p,1}} \quad D_{q,2} := \frac{R \cdot T_{\text{TempIndex}}}{\zeta_{q,2}} \quad D_{r,2} := 0$$

	1	2
1	2.40501·10 ⁻⁹	0
2	2.40501·10 ⁻⁹	0
3	2.40501·10 ⁻⁹	0
4	2.40501·10 ⁻⁹	0
5	1.99154·10 ⁻⁹	8.27931·10 ⁻¹⁰
6	1.95956·10 ⁻⁹	8.23274·10 ⁻¹⁰
7	1.93539·10 ⁻⁹	8.18816·10 ⁻¹⁰
8	1.91737·10 ⁻⁹	8.15308·10 ⁻¹⁰
9	1.8103·10 ⁻⁹	7.78326·10 ⁻¹⁰
10	1.78932·10 ⁻⁹	7.74363·10 ⁻¹⁰
11	1.77048·10 ⁻⁹	7.70432·10 ⁻¹⁰
12	1.75528·10 ⁻⁹	7.67238·10 ⁻¹⁰
13	1.64155·10 ⁻⁹	7.27829·10 ⁻¹⁰
14	1.62482·10 ⁻⁹	7.23826·10 ⁻¹⁰
15	1.61591·10 ⁻⁹	7.22275·10 ⁻¹⁰
16	1.60422·10 ⁻⁹	7.19607·10 ⁻¹⁰

$$D = \frac{m^2}{s}$$